Heft 32
No. 32

Schriftenreihe Baustoffe und Massivbau
Structural Materials and Engineering Series

UNIKASSEL
VERSITÄT

Ultra-High Performance Concrete and High Performance Construction Materials

Proceedings of HiPerMat 2020
5th International Symposium on
Ultra-High Performance Concrete and
High Performance Construction Materials
Kassel, March 11–13, 2020

Edited by
B. Middendorf
E. Fehling
A. Wetzel

kassel university press

Schriftenreihe Baustoffe und Massivbau
Structural Materials and Engineering Series

Heft 32
No. 32

Ultra-High Performance Concrete and High Performance Construction Materials

Proceedings of HiPerMat 2020
5th International Symposium on
Ultra-High Performance Concrete and
High Performance Construction Materials
Kassel, March 11-13, 2020

Edited by
B. Middendorf
E. Fehling
A. Wetzel

kassel university press

Bibliografische Information Der Deutschen Nationalbibliothek
Die Deutsche Nationalbibliothek verzeichnet diese Publikation in der Deutschen Nationalbibliografie; detaillierte bibliografische Daten sind im Internet über http://dnb.d-nb.de abrufbar

ISBN: 978-3-7376-0828-2 (print)
ISBN: 978-3-7376-0829-9 (e-book)
DOI: 10.17170/kobra-202002271026

Herausgeber

Prof. Dr. rer. nat. Bernhard Middendorf
Universität Kassel
Fachbereich Bauingenieur- und Umweltingenieurwesen
Institut für Konstruktiven Ingenieurbau
Fachgebiet Werkstoffe des Bauwesens und Bauchemie
Mönchebergstraße 7
D-34125 Kassel
Tel. +49 (561) 804 2601
Fax +49 (561) 804 2662
baustk@uni-kassel.de
www.uni-kassel.de/fb14bau/institute/iki/werkstoffe-des-bauwesens-und-bauchemie/

Prof. Dr.-Ing. Ekkehard Fehling
Universität Kassel
Fachbereich Bauingenieur- und Umweltingenieurwesen
Institut für Konstruktiven Ingenieurbau
Fachgebiet Massivbau
Kurt-Wolters-Str. 3
D-34125 Kassel
Tel. +49 (561) 804 2608
Fax +49 (561) 804 2803
bauing.massivbau@uni-kassel.de
www.uni-kassel.de/fb14bau/institute/iki/massivbau/

Printed in Germany

Introduction

The ongoing development of construction materials, more precise analytical methods, and viewpoints from other disciplines enhanced their influence on construction and material sciences in the last years. Consequently, the knowledge about high performance materials and the possibilities for architects and structural engineers have leapt ahead significantly and will increase in the future. UHPC is one of the products that arose from this synthesis of interests, as there are new opportunities for innovative architectural designs, conductive concrete elements, photocatalytic cleaning of surfaces, self-healing potential of building blocks, smart construction materials, or new binders, to name a few. UHPC in particular has recently come to fruition as the worldwide efforts for standardisation will soon allow the regular application of this innovative material. Its widespread use will permit the design of sustainable concrete structures such as wide-span bridges, filigree shells, and high-rise towers and opportunities for spectacular architectural designs.

Every four years since 2004, we and our retired colleague Prof. Michael Schmidt provided a forum for the exchange of knowledge around UHPC and other advances in construction material science for the scientific and civil engineering community. Since then, we have decided to introduce these symposia as HiPerMat, referring to High Performance Materials in construction, their development, and their application with a more general scope.

With HiPerMat 5 on March 11-13, 2020 the 5th International Symposium on Ultra-High Performance Concrete and High Performance Construction Materials documents the actual state of development of application in the fields of:

- Material Science and Development
- Composite Concrete Materials
- Strength and Deformation behaviour of UHPC
- Durability and Sustainability of UHPC
- Design and Construction with UHPC
- Structural Modelling and Optimisation
- Lightweight Concrete Structures
- High-Precision Manufacturing for Pre-Fabrication
- Nanotechnology for Construction Materials
- Innovative Applications
- Smart Construction Materials

This volume contains the short versions (two pages) of all contributions that have been accepted for publication at HiPerMat 5.

Kassel, in February of 2020

Prof. Dr. rer. nat. Bernhard Middendorf

Prof. Dr.-Ing. Ekkehard Fehling

We thank our supporters:

Participants of the technical exhibition I:

EIRICH

Maschinenfabrik Gustav Eirich GmbH & Co. KG
Walldürner Str. 50
74736 Hardheim
Germany
www.eirich.com

BECKMAN COULTER

Beckman Coulter GmbH
Europark Fichtenhain B 13
47807 Krefeld
Germany
www.beckman.com

Participants of the technical exhibition II:

Aalborg Portland A/S
Postboks 165, 9100 Aalborg
Rørdalsvej 44, 9220 Aalborg Øst
Denmark
www.aalborgportland.dk

Saint-Gobain SEVA
43 Rue du Pont de Fer – BP 10176
71105 Chalon-sur-Saône CEDEX
France
http://www.fibraflex.fr/en

KrampeHarex GmbH & Co. KG
Pferdekamp 6-8
59075 Hamm
Germany
www.krampeharex.com

Omya International AG
Marketing Communications
P.O. Box 335
4665 Oftringen
Switzerland
www.omya.com

Prefabricados Formex S.L.
Calle Rodanes s/n
46191 Vilamarxant, Valencia
Spain
www.preffor.com/en/

EFFIX® PLUS

Der Compound für ultrahochfeste Betone (UHPC)

- Vielseitige Einsatz- und Gestaltungsmöglichkeiten
- Außerordentlich hohe Druck- und Biegezugfestigkeit
- Sehr hohe Dauerhaftigkeit durch dichtes Gefüge sowie hohe Festigkeit
- Leichter Einbau durch hohe Fließfähigkeit

Stark, dauerhaft, wirtschaftlich: Ultrahochfeste Betone auf Basis des EFFIX® PLUS Compounds eignen sich für hoch beanspruchte Bauteile und filigrane, belastbare Fertigteilkonstruktionen.

www.heidelbergcement.de/effix-plus

www.heidelbergcement.de

HEIDELBERGCEMENT

ECHT. STARK. GRÜN.

AALBORG EXTREME™

LIGHT 120

HIGH-PERFORMANCE CONCRETE

AALBORG INWHITE™ SOLUTION

Premixed High-Performance Concrete

AALBORG EXTREME™ LIGHT 120 is a shrinkage reduced, ready-to-use, self-compacting High-Performance Concrete for the manufacturing of thin/slim concrete products with high aesthetic, mechanical and durability performance.

Main Applications

- **Light weight high strength panels:** façades, cladding, sun-screens, ornamental elements
- **Artistic and ornamental elements made in concrete**
- **Wet cast tiles**
- **Gardening / street architectural elements**

cementirgroup
CALTAGIRONE GROUP

Aalborg Portland Belgium www.aalborgportland.be **Yves Terneu** Mobile: +32 471 955 129 Email: yves.terneu@aalborgportland.com

Unlocking crystallographic information in your lab.

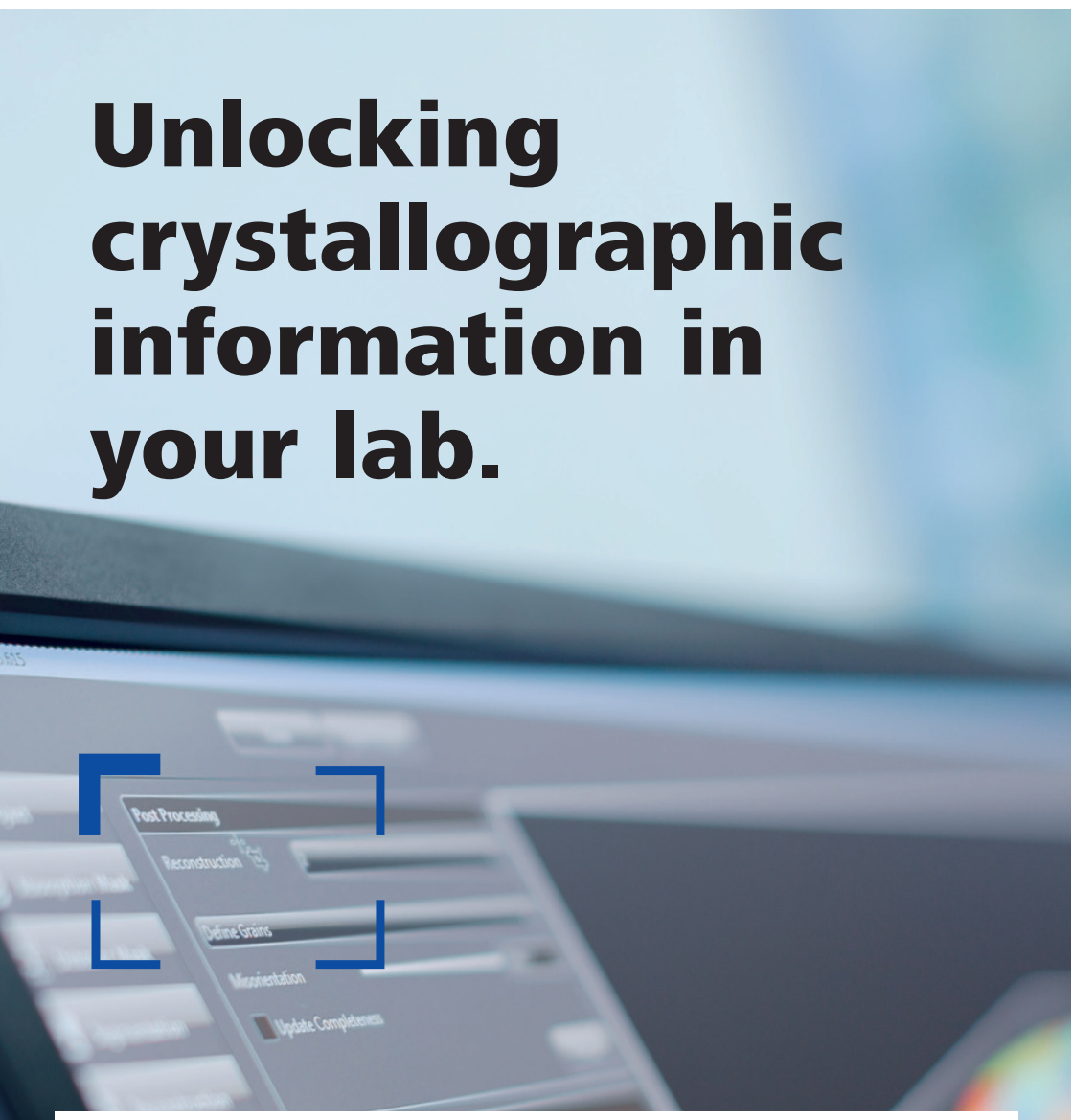

ZEISS Xradia 620 Versa with LabDCT

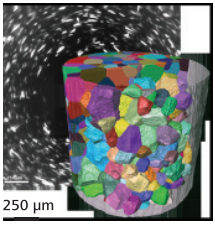

Extend the performance of your Xradia 620 Versa X-ray microscope with LabDCT. Achieve direct visualization of 3D crystallographic grain orientation in your lab. This unique technology enables non-destructive mapping of orientation and microstructure in 3D and 4D. LabDCT opens up a new dimension in the characterization of metal alloys and polycrystalline materials.

www.zeiss.com/620-versa

ZEISS

Seeing beyond

Scientific Committee for HiPerMat 2020

Chairs

Prof. Bernhard Middendorf
Prof. Ekkehard Fehling

Members in Alphabetical Order

Prof. Tess Ahlborn	Michigan Tech Transportation Institute, US
Prof. Thomas Bier	TU Bergakademie Freiberg, DE
Prof. Eugen Brühwiler	Ecole Polytechnique Fédérale de Lausanne, CH
Prof. Manfred Curbach	TU Dresden, DE
Prof. Marco di Prisco	Politecnico di Milano, IT
Prof. Ekkehard Fehling	Universität Kassel, DE
Prof. Oliver Fischer	TU München, DE
Prof. Robert Flatt	ETH Zürich, CH
Prof. Pietro Gambarova	Politecnico di Milano, IT
Dr. Benjamin A. Graybeal	Federal Highway Administration, US
Prof. Petr Hajek	Prague Technical University, CZ
Prof. Josef Hegger	RWTH Aachen University, DE
Prof. Detlef Heinz	TU München, DE
Prof. Shiho Kawashima	Columbia University, US
Dr. Byung-Suk Kim	KICT, KR
Steve Kosmatka	Portland Cement Association, US
Prof. Torsten Leutbecher	Universität Siegen, DE
Prof. Ludger Lohaus	Leibniz Universität Hannover, DE
Prof. Fernando Martirena	Universidad "Marta Abreu", CU
Prof. Victor Mechtcherine	TU Dresden, DE
Prof. Bernhard Middendorf	Universität Kassel, DE
Prof. Harald Müller	Karlsruher Institut für Technologie, DE
Prof. Markus Nöldgen	TH Köln, DE
Prof. Rafael Pileggi	CICS, BR
Prof. Michael Schmidt	Universität Kassel, DE
Prof. Caijun Shi	Hunan University, CN
Alain Simon	Eiffage TP, FR
Prof. N.B. Singh	Sharda University, IN
Prof. Dietmar Stephan	TU Berlin, DE
Dr. François Toutlemonde	IFSTTAR, FR
Prof. Jan Vitek	Prague Technical University, CZ
Prof. Yen Lei Voo	Dura Technology, MY
Prof. Kay Wille	University of Connecticut, US

Organising Committee

Dr. Alexander Wetzel	Dr. Jenny Thiemicke
Dr. Viola Koch	Tim Schade
Maximilian Schleiting	Johannes Arend
Cristin Umbach	Daniela Göbel
Niels Wiemer	Richard Kolbe
Anna-Katharina Reim	Alexandra Jung

Table of content

Influence of fine recycled concrete aggregates on the design and durability properties of UHPC

Louise Andersson[1], Nelson Silva[2]
1: RISE Research Institute of Sweden, Built Environment, Sweden
2: SIKA, Sweden

1 Background

From a technological and social perspective, ultra high performance concrete (UHPC) is a material with a number of advantages: increased productivity, superior mechanical and durability properties, improved work environment and architectural flexibility. The use of UHPC is yet limited due to the high costs and environmental impact. To increase the application of UHPCs, cost-effective manufacturing techniques, commonly available materials and methods must be possible to employ. Furthermore, also the use of recycled concrete should be considered.

In the EU-27, the annual production of concrete is estimated to be around 1350 Mt of which 250 Mt are precast. It is estimated that concrete represents 60-70% of the total construction and demolition waste (CDW) generated. Among the total CDW recovered, recycled aggregates account for 6-8% of aggregates used in Europe [1]. As the usage of UHPCs increases, so does the necessity to utilize recycled aggregates as replacement for special grade sands. This is especially interesting for the precast industry where the quality of the rubble material is more homogeneous.

The present study analyses the influence of fine recycled concrete aggregates (FRCA) on the rheological, shrinkage and mechanical properties of UHPC made with FRCA in the range of 0-4 mm from concrete railway sleepers.

2 Method

The aim was to examine the effect of increased replacement of natural crushed aggregates by FRCA, 0-4 mm, up to 100%. The examined proportions were 0%, 25%, 50%, 75% and 100% FRCA replacement by volume. The natural crushed aggregates (NCA) were sieved and proportioned to fit the sieving curve of the FRCA. The base recipe to create an UHPC has a cement content (CEM I) of 600 kg/m^3 as well as fly ash as a supplementary cementitious material. In the fresh state, the recipes were compared with regards to their workability as well as heat of hydration (isothermal calorimetry) and compressive and flexural strength in hardened state. The compressive strengths were tested at the ages of 1, 7, 14, 21, 28 & 56 days while the flexural strengths was tested at 7 and 28 days. Water absorption tests of all samples were also conducted with 28 days mature samples. Shrinkage tests were performed during a six months period. All tests reported are an average of at least 3 samples. The standard deviations within a recipe were within in a 5% difference but usually lower. The results will be shown in full at the conference.

3 Results

With an increase of FRCA, the flow spread decreased up to 16% (100% replacement). The compressive strength had an increase with up to 10% with increased FRCA content, while the flexural strength decreased between 35-40% with FRCA replacement of 50% and higher. The shrinkage increased with the increased FRCA content except for 25% replacement that had the lowest shrinkage. For water absorption there was a minor increase from the reference (0%

FRCA) to 25-75% FRCA. The 100% replacement however had a big relative increase in water absorption in comparison to the rest.

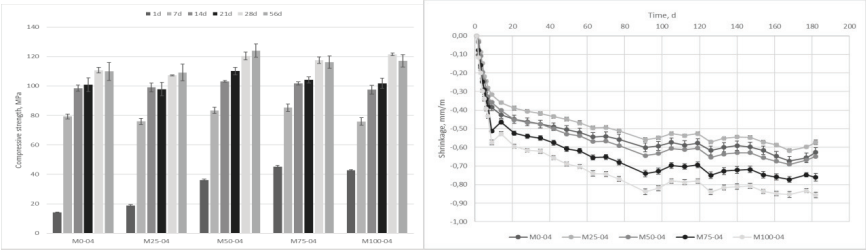

Figure 1 & 2: (left) compressive strength; (right) drying shrinkage.

It is well known that RCAs have a higher water absorption in comparison to NCR which is in line with the effect the RCA had on the flowability in the fresh state. This water absorption also means that the effective water cement ratio is a bit lower for UHPC with RCA, unless they are pre-wetted, which can be seen in the slight increase in compressive strength. The effects are more prominent with 50% replacement and higher. The large decrease in flexural strength with 50% replacement and higher are most likely related to micro-cracking, which has a more prominent effect on flexural than compression.

4 Discussion

It is possible to create UHPC with FRCA, even up to 100% replacement. Up to 25% FRCA replacement there are few differences in comparison to 0% replacement in the hardened state, while there is an effect in the fresh state due to water absorption of the FRCA. When the replacement reaches 50% and higher, the effects are both good and bad. There is an increase in compressive strength but the shrinkage, water absorption and flexural strength shows the drawbacks of the FRCA. But these are well known, and some can be compensated for or used in structures where they are less important.

5 Acknowledgement

The authors would like to thank for the financial support of RISE CBI Betonginstitutet's industrial consortium of Cementa, Färdig Betong, Abetong, Strängbetong, Betongindustri and Swerock and the fruitful discussions with the reference group of the consortium.

References

[1] WBCSD(2009), Concrete recycling: the cement sustainability initiative, http://www.wbcsdcement.org/pdf/CSIRecyclingConcrete-FullReport.pdf.

Influence of maximum aggregate size and distribution modulus on UHPC matrix properties

Dhanendra Kumar[1], Ketan Ragalwar[2], William F. Heard[3], Brett A. Williams[3], Ravi Ranade[1]
1: Department of Civil, Structural and Environmental Engineering (CSEE), University at Buffalo, USA
2: Schnabel Engineering, Clifton Park, NY, USA
3: Engineer Research and Development Center, US Army Corps of Engineers, Vicksburg, MS, USA

1 Introduction

Dense particle packing is a key principle for achieving high compressive strength in ultra-high performance concrete (UHPC) [1-2]. Particle-packing models, such as the modified Andreasen and Andersen (A&A) model, are typically used in the design of UHPC for systematically achieving dense particle packing [3]. The key parameter in the A&A model is the distribution modulus (q), which governs the curvature of the target particle size distribution (P_{tar}) and the aggregate/paste (or coarse/fine) ratio. Researchers have typically selected the value of q from a narrow range of 0.22 to 0.25 for designing UHPC without considering the maximum aggregate size (D_{max}) [1,3]. However, as the P_{tar} also depends on D_{max} in the modified A&A model [4], the value of q for achieving the target combination of rheological and mechanical properties of a UHPC should depend on D_{max}. This study aims to experimentally determine the influence of D_{max} and q and their interaction on the rheological and mechanical properties of a UHPC.

2 Experimental Program

The UHPC matrices utilized ASTM Type I/II cement, microsilica, fine silica powder, washed manufactured sand, and polycarboxylate ether-based high range water reducing admixture (HRWRA). The sand from the same source was sieved to achieve different maximum aggregate sizes to eliminate the effects of particle morphology and texture. A combination of central composite design (CCD) of experiments and modified A&A model was used to determine the mixture proportions (details in [1]). The two factors varied in the CCD were (a) D_{max} of 0.72 to 3.28 mm, and (b) q of 0.10 to 0.25. The water/binder and HRWRA/binder weight ratios were kept constant at 22.5% and 2.7%, respectively.

The flow (without drops) and the air content of each mixture were determined according to ASTM C1437 and C231, respectively. Six 51 mm cubes were cast to characterize the compressive strength of each mixture. The cubes were demolded after 48 hours of casting and cured under water after demolding for next 24 hours at room temperature. The cubes were then cured under water at 90°C for 72 hours followed by air curing at 90°C for the next 48 hours. The cubes were tested at an age of 8 days according to ASTM C109.

3 Results and Discussion

The effects of the two factors, i.e. D_{max} and q, on the *workability*, *air content*, and *compressive strength* are presented in Figure 1. The contour plots were obtained using second order regression models.

The workability (flow) decreased with increase in D_{max}, especially for q > 0.15, due to greater resistance to flow offered by larger aggregate particles. Greater q implied higher aggregates/paste volumetric ratio, and therefore, lesser paste was available to lubricate the aggregate particles, which reduced the workability. A significant interaction was observed between D_{max} and q, and the influence of D_{max} on workability became more prominent with increase in q.

The air content of the UHPC increased with D_{max} indicating lower packing density. The reduced workability with increase in D_{max} also led to more entrapped air. The value of q did not

influence the air content (or packing density) for $D_{max} \leq 2$ mm. For $D_{max} > 2$ mm, the air content increased or the packing density decreased with increase in q.

The compressive strength of the UHPC decreased with increases in D_{max} and q. The particle packing density and the interfacial transition zone (ITZ) between aggregate and cement paste were the major factors governing the compressive strength of the UHPC. An interaction between D_{max} and q was also observed. The effect of D_{max} diminished at greater values of q, and the effect of q diminished at greater values of D_{max}. Both of these interaction effects could be explained by the influence of increasing total surface area of the ITZ (due to increasing q) and increasing size of the ITZ of an individual aggregate (due to increasing D_{max}).

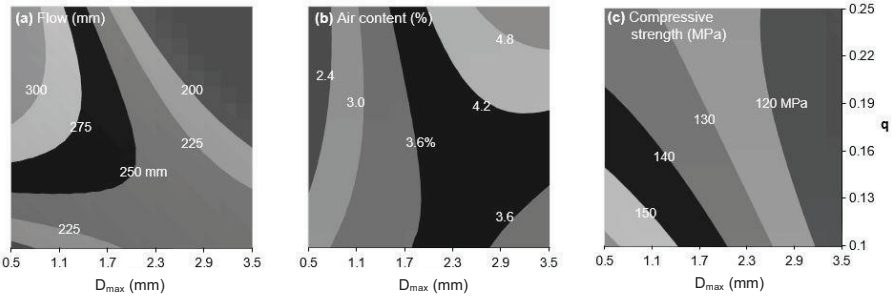

Figure 1: Effect of D_{max} and q on (a) flow (mm), (b) air content (%), and (c) compressive strength (MPa).

4 Conclusions

This study experimentally investigated the influence of maximum aggregate size (D_{max}) and distribution modulus (q) of the composite particle distribution on the UHPC properties. For the materials and the range of factors considered in this study, the optimum values of D_{max} and q are 0.7 mm and 0.16, respectively. Although a lower q improves the compressive strength, it also reduces the flow. In the future, this study will be extended to understand the influence of the two factors on viscosity which is essential for fiber dispersion, void size distribution, and the fracture toughness of the UHPC.

Acknowledgements

The tests described and the resulting data presented herein, unless otherwise noted, are based upon work supported by the US Army ERDC under PE 622144, Project BL9 'Protection from Advanced Weapons Effects Technology', Task 'Defeat of Complex Attack'. Permission was granted by the Director, Geotechnical and Structures Laboratory to publish this information.

References

[1] Ragalwar, K.; Prieto, V.; Fakhri, H.; Heard, W. F.; Williams, B. A.; Ranade, R.: Systematic development of environmentally sustainable UHPC. Proc. HiPerMat, Kassel 2016.

[2] Geisenhanslüke, C.; Schmidt, M.: Methods for modelling and calculation of high density packing for cement and fillers in UHPC. Proc. International Symposium on UHPC, Kassel 2004.

[3] Yu, R.; Spiesz, P.; Brouwers, H.: Development of UHPFRC: Towards an efficient utilization of binders and fibres, *Construction and Building Materials* 79, pp. 273-282, 2015.

[4] Brouwers, H.: Particle-size distribution and packing fraction of geometric random packings, *Physical Review E* 74 (3), 2006.

Optimization of coarse aggregate UHPC composition for UHPC-filled steel tubes / hollow precast concrete columns

Kim Huy Hoang, Michael Huss, Goran Vojvodic, Nguyen Viet Tue
Institute of Structural Concrete, Faculty of Civil Engineering, Graz University of Technology, Austria

1 Introduction

Ultra-high performance concrete (UHPC)-filled steel tubes / hollow precast concrete columns are most advantageous for the columns of a high-rise building or bridge piers subjected to the extensive compressive loading. Self-compacting UHPC with a minimum characteristic compressive strength of 150 MPa and low / no autogenous shrinkage is of great interest [1]. Besides, a robust UHPC having a simple composition compatible with the existing production chain is significant for concrete producers and contractors.

The Institute of Structural Concrete, Graz University of Technology (IBB-TUGraz) successfully developed a practical approach to optimizing mix design for UHPC [2].

The proposed approach allows formulating several self-compacting coarse grain UHPCs. This contribution presents the mix design and properties assessment of the developed coarse grain UHPCs.

2 Concrete composition optimization approach

The proposed mix design approach, as illustrated in Figure 1, is a stepwise optimization procedure considering the compatibilities of superplasticizer, cement, inert/reactive powders and the compatibilities of different grading aggregates for improvement of the packing density, self-flowability and strength of concrete. Superplasticizer-Water (SP-Water) Solution Demand Test is a newly developed method for measuring real packing density of cement, inert/reactive powders and optimizing cementitious paste component.

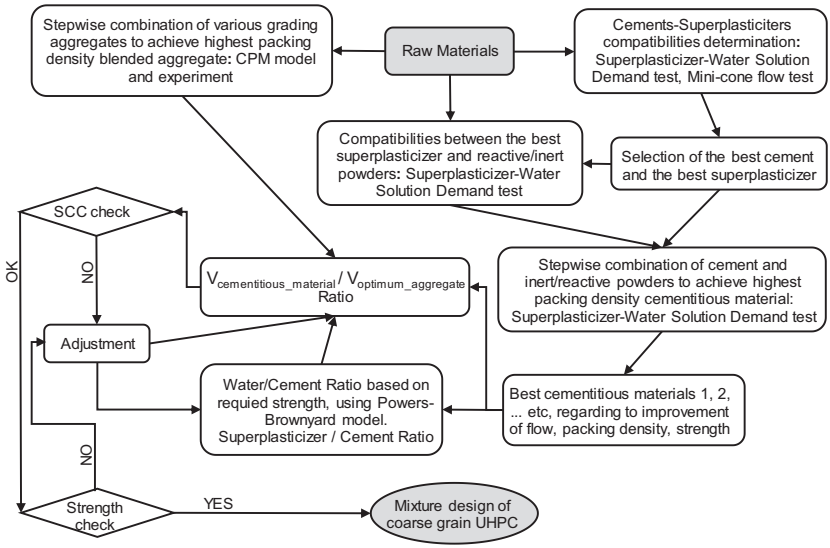

Figure 1: Flow chart for the optimization of coarse grain UHPC according to the proposed approach.

3 Experimental results and discussions

The results of the study confirmed that SP-Water Solution Demand Test is a valuable method for formulating a low-cost sustainable binder. Additionally, an optimal packing density of blended aggregate is significant to obtain a fine self-compacting coarse grain UHPC with low cementitious paste. Furthermore, binder consisting of low cement and high slag (GGBFS) volume is functional to improve the autogenous shrinkages of UHPCs, as seen in Table 1.

Table 1: The optimal UHPCs in comparison with the control mixtures: compositions and properties.

Materials		**Control 1 1mm**	**Control 2 8mm**	**Opt.Mix1 12mm**	**Opt.Mix2 16mm**	**Opt.Mix3 12mm**	**Opt.Mix4 12mm**
Cem I 52.5N	kg/m^3	720	640	580	580	460	460
Silica fume	kg/m^3	72	64	58	58	46	46
Quartz powder	kg/m^3	288	256	--	--	--	--
Slag (GGBFS)	kg/m^3	--	--	261	261	552	552
Superplasticizer	kg/m^3	21.6	19.2	18.6	18.6	16.1	14.3
Chemical Admixture	kg/m^3	--	--	--	--		4.6
Water	kg/m^3	172	153	150	149	154.3	151
Quartz Sand 0.1-1mm	kg/m^3	1138	741	512	412	451	456
Basalt 2-4mm	kg/m^3	--	290	415	426	364	368
Basalt 4-8mm	kg/m^3	--	387	--	--	--	
Basalt 8-12mm	kg/m^3	--	--	567	365	498	503
Basalt 8-16mm	kg/m^3	--	--	--	350	--	--
Properties							
Slump-flow [EN12350-8]	mm	800	805	800	780	800	800
Comp. Strength, 20°C-65%RH, cube 100mm: 28 days and (90 days)	MPa	193 (--)	191 (--)	178 (188)	175 (185)	178 (185)	178 (189)
Autogenous Shrinkage, 28 days	‰	-0.650	-0.480	-0.300	-0.300	-0.100	+0.025

4 Conclusions

In this study the stepwise optimization approach for HPC/UHPC mix-design developed by IBB-TU Graz was employed, thereby establishing the most compatible materials for UHPC mix design and optimizing the components of cementitious materials, of blended aggregates as well as the whole concrete mixture. The manageable component and excellent properties of the developed UHPCs demonstrate the effectiveness of the proposed mix design approach. The UHPCs with a slump-flow of 75-80 cm, high segregation resistance, compressive strength of 180-190 MPa and a low / no autogenous shrinkage of -0.300‰ to +0.025‰ well satisfy the target concrete properties of the study.

The influence of polypropylene fibres with a dosage of 1.5-2 kg/m^3_concrete on the fire resistance of the developed UHPCs is of interest. The investigation is ongoing.

References

[1] Vojvodic, G.; Hadl, P.; Hoang, K. H.; and Tue, N. V.: Substitution of steel components by ultra-high performance fibre reinforced concrete. In: Proceedings of the Sixth International Conference on Structural Engineering, Mechanics and Computation, South Africa, 2016.

[2] Hoang, K., H.: A Systematic Mix Design Approach for UHPFRC, Dissertation, Graz University of Technology, 2017.

[3] de Larrard, F.: Concrete Mixture Proportioning – A Scientific Approach, E & FN SPON, 1999.

Development and testing of High / Ultra-High Early Strength Concrete

Bijaya Rai, Kay Wille
Department of Civil and Environmental Engineering, University of Connecticut, Storrs, Connecticut, United States

Abstract

Accelerated Bridge Construction (ABC) is a widely used and popular technology especially in areas of heavy traffic with the need of minimal traffic disruption, which gives rise to the necessity for the use of high early strength (HES) concrete to connect prefabricated elements and thus facilitate ABC. In this research emphasis is being placed on enhancing the early age strength development of concrete with improved durability properties, volume stability and robustness using non-proprietary materials and local available constituents.

1 Introduction

Several mixture methodologies exist to produce HES concrete such as i) reduction of the water to cementitious ratio (w/c) in combination with the use of high range water reducer, ii) use of higher finely gound cement, iii) use of tailored supplemental materials, iv) use of nano-sized pozzolanic material, v) tailored tailored curing, and vi) use of accelerating admixtures [1,2]. The use of higher finely ground cement such as Portland Cement Type III as per ASTM C 150 [1-3] accelerates the hydration due to increase in surface area. Supplementary cementitious materials such as class C fly ash has shown higher rate of reaction at early ages than concrete containing class F fly ash [3]. Due to the high surface area of nano-sized pozzolanic material like nano silica (NS) [4-6] accelerated pozzolanic reaction can be achieved and the filler effect of NS can potentially increase the strength of concrete and enhance other durability properties [7]. Accelerating admixture, such as calcium chloride is used to accelerate the rate of hydration and strength its dosage is limited to 2% by mass of cement [8]. Besides these, Federal Highway Report suggests that ultra high performance concrete (UHPC) to be used for closure pour connections as it has high bond strength and durability properties due to very high packing density, relatively high binder ratio and low water to cementitious (w/c) ratio [9-10].

2 Methods

*Table 1: Mix 6 (reference mix) description [11]**

Cement, lb/yd^3	Flyash, lb/yd^3	Sand, lb/yd^3	Water, lb/yd^3	Superplasticizer, fl.oz.
1190	210	1043	398	171

**The above table provides the mixture proportion for mortar mix as this is the first step of research.*

Compressive strength at 24h

In the first step of this research mortar cubes have been cast, using 0.5%, 2%, and 3% of NS in replacement for cementitious material. The average compressive strengths at 24h using different amounts of NS are summarized in figure 1.

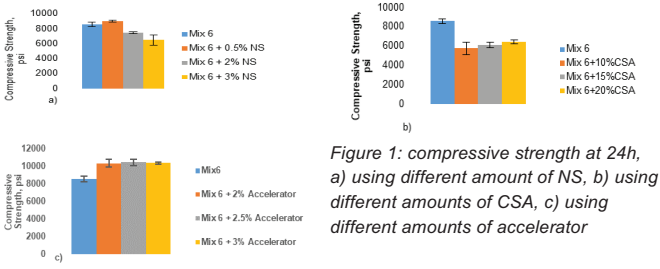

Figure 1: compressive strength at 24h, a) using different amount of NS, b) using different amounts of CSA, c) using different amounts of accelerator

Air Void Characterization

Since the the amount of air void can significantly influence the compressive strength, it is important to link the amount of air with the tested compressive strength at different ages of concrete. First, the mortar cubes were cut using a blade saw and then polished with grinding pad sizes of 63 µm, 15.3 µm and 4.5µm. Second, the sample is dried for 15 minutes, painted with black ink and again, dried for 15 minutes before applying white barium sulphate to highlight the accessible air voids (fig. 2a), following by binary imaging (fig. 2b) and linking the air void content to the compressive strength (fig. 2c). This will allow to compare compressive strengths at similar air void contents.

a) b) c)

Figure 2: a) sample preparation, b) air void area and c) compressive strength vs air void %

The air void analysis in UHPC samples seems easier than in regular concrete because of it's uniformity in the texture and because of absence of grey sand and aggregate particles, light reflection is better with only two colors; black and white. This could be the reason that standard deviation for the determination of air void percentage is smaller in case of UHPC samples. Later in the research, this technique for finding the air voids can be verified by using air meter in the fresh concrete samples.

3 Conclusions

The first phase of research has been completed. The concrete with accelerating admixture is showing promising results to further enhance the early age strength of existing HES concretes.

References

[1] Johansen, V., P.C. Taylor, and P.D. Tennis, Effect of cement characteristics on concrete properties. Engineering bulletin ; 226.02. 2006, Skokie, Ill.: Portland Cement Association.

[2] Kosmatka, S.H., M.L. Wilson, and P.C. Association, Design and control of concrete mixtures. 1st printing ed. 2016, Skokie, Illinois: Portland Cement Association.

[3] Neville, A.M., Properties of concrete. 1996: John Wiley & Sons.

[4] Mohamed, A.E.-H., Khaled A., Effect of Using Different Types of Nano Materials on Mechanical Properties of High Strength Concrete. Construction and Building Materials, 2015.

[5] Min Liu, H.T., Xingyang He, Effects of nano-SiO2 on early strength and microstructure of steam-cured high volume fly ash cement system. Construction and Building Materials, 2019.

[6] Mohamed, A.M., Influence of Nano Materials on Flexural Behavior and Compressive Strength of Concrete. HBRC Journal, 2016. 12(2): p. 212-225.

[7] Du, H.L., Xuemei; Du, Suhuan, Durability Performance of Concrete with Nano Silica. Construction and Building Materials, 2014. 73:705-712.

[8] Palla, R.K., S.R.; Mishra, G.; Sharma, U.; Singh, L.P, High Strength Sustainable Concrete Using Silica Nanoparticles. Construction and Building Materials, 2017. 138: p. 285-295.

[9] "Properties and Behaviors of UHPC-Class Materials". March 2018. FHWA-HRT-18-036

[10] Graybeal, B., " Design and Construction of Field Cast UHPC Connections". FHWA-HRT-14-084

[11] S. Brena, S. Civjan, S. Castine and G. Ramos, "Development of High Early Strength Concrete for Accelerated Bridge Construction Closure Pour Connections", NETCR No.13-1, Aug.15, 2018.

Experimental investigations on the shear bearing capacity of UHPFRC beams with compact cross-section

Kevin Metje, Torsten Leutbecher
Chair of Structural Concrete, Department of Civil Engineering, University of Siegen, Germany

1 Introduction

Up to now, extensive test series on the shear bearing behaviour of UHPFRC beams have been carried out [1-6]. Various cross-sectional dimensions, fibre volume fractions, and prestressing were investigated focusing on I-shaped cross-section. As the shear bearing mechanisms significantly differ for beams with compact cross-section, the findings on beams with I-shaped cross-section may, however, not be generally applicable.

In the present study, a series of shear tests on UHPFRC beams with compact cross-section, different fibre volume fractions, and prestressing was performed, in order to examine the influences on the formation of the critical shear crack as well as on the shear bearing capacity.

2 Experimental programme

Varying the fibre volume fraction (0 %, 1 % or 2 %) and the prestressing of the tendons (0 MPa, 720 MPa or 1440 MPa) resulted in a total of nine specimen configurations with one specimen each. The specimen's geometry as well as the arrangement of reinforcement and prestressing tendons are shown in Fig. 1. The total length of the beams was 3,000 mm to enable at least two shear tests per specimen. The three-point tests were performed displacement controlled with shear span-to-depth ratios *a/d* between 3.5 and 5.5. Displacements including crack widths were measured by digital image correlation (DIC).

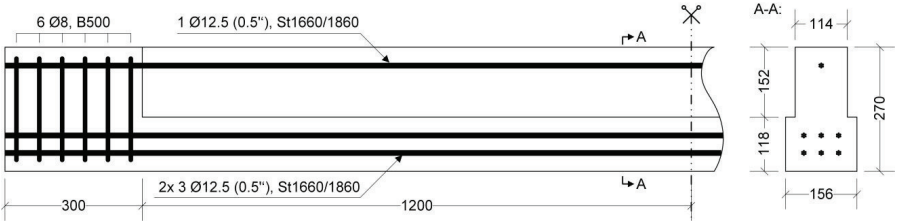

Figure 1: Specimen's geometry and arrangement of reinforcement and prestressing tendons.

Before manufacturing the beams, a measuring system was installed for recording the specimen's deformation due to shrinkage and creep in order to derive the loss of prestress.

A concrete mixture with a maximum aggregate size of 8 mm was used. The smooth and straight steel fibres had a length-to-diameter ratio of 20 mm/0.40 mm. The average 28-day cube compressive strength of the concrete was 154 MPa, 164 MPa, and 168 MPa for fibre volume fractions of 0 %, 1 %, and 2 %, respectively. The residual flexural tensile strength, which was obtained in three-point tests on accompanyingly fabricated notched beams, showed mean values of 11.1 MPa and 17.6 MPa for fibre volume fractions of 1 % and 2 %, respectively.

3 Test results

Figure 2 shows the load-displacement curves of selected tests, which failed in shear after formation of the critical shear crack. A DIC image of a typical crack pattern is depicted in Fig. 3.

Due to the specimens' compact cross-section, the critical shear crack developed from a flexural crack in all tests, irrespective of the fibre volume fraction or prestressing. This behaviour differs from beams with I-shaped cross-section where the shear crack starts at the thin web.

The critical shear crack was inclined by 21 to 35 degrees with respect to the longitudinal axis of the beam.

The specimens without fibres showed a brittle failure, while the fibre reinforced specimens showed some higher deformation capacity. The shear bearing capacity of the specimen without fibres and without prestressing (0 %; 0 MPa) was the smallest (63 kN). As expected, the ultimate shear load increased with increasing fibre volume fraction and/or prestressing resulting in a shear bearing capacity of 218 kN for the specimen with 1 % of fibres and tendons prestressed to 1440 MPa.

For the fibre reinforced specimens with the highest level of prestressing it was difficult to provoke a shear failure before flexural failure, however, an initiating shear crack could be observed via DIC in all cases. The specimens showing this behaviour will be further evaluated.

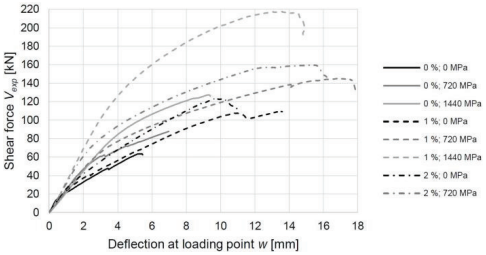

Figure 2: Load-displacement curves of selected tests.

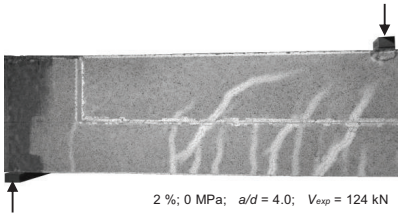

Figure 3: Crack pattern measured by DIC.

4 Conclusions and outlook

Based on the current evaluation the following conclusions may be drawn:

- For the specimens without fibres the inclination of the critical shear crack decreases with increase of prestressing. The fibre reinforced specimens show no clear trend in this respect.
- The increase in shear bearing capacity between the specimens with 1 % and 2 % of fibres is less than proportional to the increase of the associated residual flexural tensile strengths.
- The shear bearing capacities of the specimens without fibres is well predicted by Eq. (6.2.a) in Eurocode 2.

In the next step, fibre distribution and orientation will be examined by optoanalytic method in order to identify the actual residual tensile strength contributing in the critical shear crack. This may help to perform parameter studies by FEA investigating the influence of various parameters on the shear crack propagation as well as on the shear bearing capacity.

References

[1] Graybeal, B.A.: Structural Behavior of Ultra-High Performance Concrete Prestressed I-Girders. Report FHWA-HRT-06-115, US Dep. of Transp., FHWA, McLean, Virginia, USA, 2006.

[2] Voo, J.Y.L.; Foster, S.J.; Gilbert, R.I.: Shear Strength of Fiber Reinforced Reactive Powder Concrete Prestressed Girders without Stirrups. *J. Adv. Concr. Technol.* 4 (1), pp. 123-132, 2006.

[3] Voo, J.Y.L.; Poon, W.K.; Foster, S.J.: Shear Strength of Steel Fiber-Reinforced Ultrahigh-Performance Concrete Beams without Stirrups. *J. Struct. Eng.* 136 (11), pp. 1393-1400, 2010.

[4] Bertram, G.: Experimentelle Untersuchungen zum Querkrafttragverhalten von Spannbetonträgern aus UHPC mit und ohne Stegöffnungen. *Bauingenieur* 90 (7), pp. 444-455, 2015.

[5] Thiemicke, J.; Fehling, E.: Proposed Model to Predict the Shear Bearing Capacity of UHPC-Beams with Combined Reinforcement. Proc. 4th International Symposium on Ultra-High Performance Concrete and High Performance Construction Materials, Kassel 2016.

[6] Schramm, N.; Fischer, O.: Querkraftversuche an profilierten Spannbetonträgern aus UHPFRC. *Beton- und Stahlbetonbau* 114 (9), pp. 641-652, 2019.

Shear strength of Ultra-High Performance Fibre Reinforced Concrete dry and epoxy joints for segmental girders

Balamurugan A. Gopal[1], Milad Hafezolghorani[1,2], Yen Lei Voo[2,3], Farzad Hejazi[1]
1: Department of Civil Engineering, Universiti Putra Malaysia, Selangor, Malaysia
2: DURA Technology Sdn Bhd, Malaysia
3: School of Civil and Environmental Engineering, University of New South Wales, Australia

1 Abstract

This paper presents the experimental studies on the ultimate shear capacity ($V_{j,u}$) of typical joints used in ultra-high performance fibre reinforced concrete (UHPFRC) precast segmental bridge girder (PSBG). Twelve (12) pilot-scale shear key joints UHPFRC specimens (i.e. six (6) with dry keyed joints and six (6) with epoxied keyed joints) were tested experimentally to failure with three parameters namely, (i) number of shear keys, (ii) confining stresses, and (iii) the type of joint (dry or epoxy). Enabling shear was used in the test setup and applied across the shear plane with negligible moment. The experimental results show the shear capacity of the UHPFRC key joints increased with increasing confining pressure, number of shear keys and the epoxy layers applied on joints. A new design plastic shear joint model (PSJM) derived from the failure criterion of Mohr's circle theory is presented herein and the model was used to calibrate against the tested specimens. The new PSJM compared well with the experimental results for both the dry and epoxy keyed joints at both stages (first crack and the ultimate shear capacity loads). The excellent agreement between the PSJM results and experimental data demonstrated the reliability of the present design plastic shear joint model.

2 Introduction

The precast concrete segmental joints can be constructed and erected either using an epoxy layer between the segments or in a dry condition; and the capacity of the joints increases by applying epoxy layers [1-4]. While considerable researches [5-8] have been undertaken to investigate the behavior of conventional precast concrete segmental bridges with dry and epoxy joints, few researchers [4,9] have attempted to evaluate shear behaviour of UHPFRC keyed dry joints. However, more importantly, no research has been carried out to assess the shear capacity of UHPFRC keyed epoxy joints. To address these issues, this paper presents new design models for UHPFRC girders with dry and epoxy joints. Validation of the proposed design provision models is accomplished by conducting a comparison study between the estimated shear load values from the new design provision models and the experimental data.

3 Experimental Results and Observations

From the experimental tests, shear behaviour and shear capacity of the joints were reported. Three important shear load capacities were monitored and recorded through shear load-displacement. $V_{j,cr,exp}$ is the experimental shear load capacity at which the first shear crack occurred at the lower shear key face of the male key component. The term $V_{j,u,exp}$ is the ultimate shear load capacity of the shear keyed joints. The term $V_{j,fric,exp}$ is the residual frictional shear load capacity on the contact surface after the shear keys sheared off completely. μ is the ratio of residual frictional shear load ($V_{j,fric,exp}$) to the initially applied normal force across the joint (P_i). From experimental results, it can be concluded that the failure shear loads at first crack ($V_{j,cr,exp}$) and ultimate ($V_{j,u,exp}$) are higher with an increasing number of keys, at higher confining pressure and with an epoxy layer on UHPFRC keyed joints. Moreover, the cohesive effect of the epoxy layer also allowed the epoxy keyed joint specimen to displace before these specimens fully

detached. However, $V_{j,fric,exp}$ and the μ of the dry joint specimens indicated a higher amount in comparison with the epoxy keyed joint specimens. This would occur due to the presence of the epoxy powder layer between the UHPFRC surfaces after failure, having a lubricating effect.

4 Development of a New Design Plastic Shear Joint Model (PSJM)

To develop new design shear models for UHPFRC keyed joints, the principle of Mohr's circle was utilized in this paper. Moreover, as reported by pervious researchers [4] UHPFRC can be treated as a perfectly plastic material and plasticity method can applied for this concrete. Hence, new PSJMs were developed for UHPFRC dry and epoxy keyed joints at first crack and ultimate. To assess the reliability of the proposed PSJMs, a comparison study between the experimental results and the calculated values from proposed models was conducted in this study. Comparisons were made on the $V_{j,cr,exp}$ and $V_{j,u,exp}$ stages on the both keyed joints (dry and epoxy). As observed, the shear capacity loads calculated from the new PSJMs shown a good agreement with the experimental results. The theo/exp ratio of all the comparisons are recorded below 1.0 which, leading to a safe design. The corresponding coefficient of variations (COV) of the four groups of specimens (dry and epoxy joints at first crack and ultimate states) are less than 10%. It indicates, an excellent level of consistency of failure shear loads ($V_{j,cr,exp}$ and $V_{j,u,exp}$) which are estimated from the new UHPFRC design PSJMs.

5 Conclusions

The new PSJM compared well with the experimental results for both the dry and epoxy keyed joints at both stages (first crack and the ultimate shear capacity loads). The mean and the coefficient of variation (COV) values of the theory/experimental ratio for dry keyed joints were 0.87 and 7.7% at the first crack and 0.72 and 6.7% at the ultimate shear load stage. Meanwhile, the mean and the coefficient of variation (COV) values for epoxy keyed joints were 0.95 and 5.3% at the first crack and 0.87 and 6.1% at the ultimate state. From the findings and observations from this study, it is envisaged that this study and the design PSJMs will provide an essential contribution and resource to the development of UHPFRC bridge girder guidelines and the standard codes in future particularly in the area of UHPFRC keyed joints design.

References

[1] Rombach, G. A.; Specker, A.: Segmentbrücken. Beton-Kalender, Teil 1, Verlag Ernst und Sohn. Berlin, Germany, pp. 177–211, 2004.

[2] Buyukozturk, O.; Bakhoum, M. M.; Michael Beattie, S.: Shear behavior of joints in precast concrete segmental bridges. *Journal of Structural Engineering* 116 (12), pp. 380–401, 1990.

[3] Bu, Z. Y.; Wu, W. Y.: Inter shear transfer of unbonded prestressing precast segmental bridge column dry joints. *Engineering Structures* 154 (June), pp. 52–65, 2018.

[4] Voo, Y. L.; Foster, S. J.; and Voo, C. C.: Ultrahigh-Performance Concrete Segmental Bridge Technology: Toward Sustainable Bridge Construction. *Journal of Bridge Engineering* 20 (8), p. B5014001, 2014.

[5] Shamass, R.; Zhou, X.; Wu, Z.: Numerical analysis of shear-off failure of keyed epoxied joints in precast concrete segmental bridges. *Journal of Bridge Engineering* 22 (1), p. 4016108, 2016.

[6] Alcalde, M.; Cifuentes, H.; Medina, F.: Influence of the number of keys on the shear strength of post-tensioned dry joints. *Materiales de Construcción*, 63 (10), pp. 297–307, 2013.

[7] Zhou, X.; Mickleborough, N.; Li, Z.: Shear strength of joints in precast concrete segmental bridges. *ACI structural journal* 102 (1), p. 3, 2005.

[8] Han, Q.; Zhou, Y.; Ou, Y., et al.: Seismic behavior of reinforced concrete sacrificial exterior shear keys of highway bridges. *Engineering Structures* 139, pp. 59–70,2017.

[9] Jang, H. O.; Lee, H. S.; Cho, K., et al.: Experimental study on shear performance of plain construction joints integrated with ultra-high performance concrete (UHPC). *Construction and Building Materials* 152, pp. 16–23, 2017.

Behavior of RC columns confined with UHPC

Yuliarti Kusumawardaningsih[1,2], Ekkehard Fehling[1]
1: Institute of Structural Engineering, Department of Concrete Structures, University of Kassel, Germany
2: Department of Civil Engineering, Faculty of Engineering, Universitas Negeri Semarang, Indonesia

1 Introduction

Many of currently existing buildings are built by using reinforced concrete (RC) structures, wherein normal strength concrete (NSC) is utilized. NSC has been used widely as a construction material, regards on its characteristics (i.e. strength, durability, resistance, shape versatility, low maintenance, and cheap price). Besides having a significant self weight, the NSC has limitations such as limited capacity to resist high compression loadings. Addressing to this limitation, a variety of research and studies have been conducted. In this study, a method of upgrading the strength capacity of RC structures by confining/ jacketing of columns is selected. The method is chosen as it is able to increase columns' stiffness, axial force and bending capacity, besides of its easy handling application [1]. The option to use Ultra High Performance Concrete (UHPC) as a confining material is taken, as this material gives benefit in limiting the thickness of the confinement, in addition of its superior properties [2,3]. In this paper, the behavior of RC columns confined with UHPC subjected to concentric and eccentric loadings are investigated. The results demonstrate that fibre reinforced UHPC confinement leads to the enhancement/ increase of stress, load carrying capacities and post-peak response.

2 Experimental investigation

Twelve short columns with a height of 750 mm were constructed. The RC columns were made from concrete C30/37 (200 x 200 mm^2), with a concrete cover thickness of 25 mm. 4∅12 mm deformed steel bars BSt500S(A) were used as longitudinal reinforcements (with an extra length of 20 mm for attachment to the test setup), while ∅8 mm stirrups have been used. Columns were subjected to 3 loading configurations: concentric loading (e = 0 mm) and eccentric loadings (e = 35 and 70 mm). The UHPC mixture formula, M3Q_210, was developed by the Material Testing Institution (Amtliche Materialprüfanstalt für das Bauwesen/ AMPA) at University of Kassel. One NSC column was left as control specimen (reference) for each loading configuration. The remaining 9 NSC columns were confined by UHPC having different percentages of fiber in volume (0, 1 and 2 vol.-% fiber), with a confinement thickness of 21 mm. Steel fibers having a length of 10 mm and a diameter of 0.2 mm were used for the UHPC mixture. Columns were tested at the age of about 28 days.

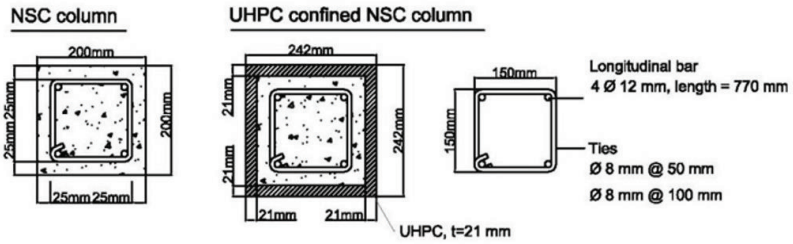

Figure 1: Columns' cross section.

3 Results and discussion

Load-deformation and stress-strain behaviours

The concentric loading of the columns resulted in the highest columns' load bearing and deformation deformation capacities. The bigger the eccentricity applied to the loading, the less strong the columns will be. This conclusion holds true for all columns, namely columns NSC (C), columns NSC + UHPC 0% (CF0), columns NSC + UHPFRC 1% (CF1) and columns NSC + UHPFRC 2% (CF2).

Fiber influence

Increasing the steel fiber volumetric percentage to the UHPFRC mixture will increase the load bearing capacities of the columns confined with UHPC/ UHPFRC. Compared to the load bearing capacities of columns C, the measured increase is as following: for concentric loading for column CF1 322% and column CF2 353%. For the case of excentric loading (e = 35 mm) for column CF1 320% and column CF2 383%. For excentric loading (e = 70 mm), for column CF1 321% and column CF2 351%. The deformation capacities of the columns also increase. The columns´ behavior due to fibers added to the UHPC is characterized by strain softening (descending branch) after reaching the maximum load, which appears to depend on the fibers' amount and orientation that is influencing the behavior of crack opening in UHPFRC. These observations are in line with the behavior of UHPC/ UHPFRC from other investigations.

Failure modes

Column CF2 shows the most ductile failure behavior, followed by column CF1. As expected, column CF0 shows the most brittle failure behavior. Failure of columns is marked by spalling of concrete cover/ confinement, which can be noticed by hearing a snapping sound due to the failure of the UHPC confinement. The general failure is brittle, except to UHPFRC with the highest fiber dosage, where failure tends to be more ductile due to the existence of a large amount of fibers.

4 Conclusion

RC columns confined with UHPC may sustain higher maximum loads, thus being able to sustain larger vertical deformation and strain; compared to the unconfined RC columns. The addition of fibers into UHPC delays the spalling of the UHPC confinement.

Acknowledgements

The work was conducted by Yuliarti Kusumawardaningsih under the supervision of Prof. Dr.-Ing. Ekkehard Fehling. The first author gratefully acknowledges all financial assistances provided by the Indonesian Directorate General of Higher Education, Universitas Negeri Semarang and the University of Kassel. The authors thank the assistance of colleagues, technical staff members and students in the study.

References

[1] Kusumawardaningsih, Y.; Hadi, M.N.S.: Comparative Behaviour of Hollow Columns Confined with FRP Composites, Composites Structures, Vol. 93, pp. 198-205, 2010.

[2] Fehling, E. et al.: Ultra High Performance Concrete (UHPC): Research, Development and Application in Europe, UHPC - 10 Years of Research and Development, Structural Materials and Engineering Series, Kassel University Press, No. 7, Kassel, 2007.

[3] Kusumawardaningsih, Y.; Fehling, E.; Hardjasaputra. H; Al-Ani. Y; Aboubakr. A.A.M.: Axial Tensile Strengths of UHPC and UHPFRC, IOP Conf. Ser.: Materials Science and Engineering, 2019.

Robustness of centrically loaded UHPC-columns

Henrik Matz, Martin Empelmann
Institute of Building Materials, Concrete Construction and Fire Safety, Division of Concrete Constructions,
Technische Universität Braunschweig, Germany

1 Introduction

A robust design of columns is essential to reduce economic, environmental and human damage after failure of structures. Robust columns should exhibit a non-brittle compression failure with sufficient prior notice announced by large deformations or primary concrete spalling. The trend toward exploiting the maximum load bearing capacity of columns coupled with application of more brittle material such as UHPC makes the quantification of the robustness of UHPC-columns essential. A quantification method can be based on the ratio of the ultimate load and the post-cracking load at a defined strain or deformation [1].

To quantify the decisive influences on the robustness, a numerical model is presented in this paper, which can simulate both the ultimate load and the post-cracking behaviour of UHPC-columns. On this basis, an efficient rheological model is introduced for a practical determination of the robustness of UHPC-columns and a theoretical parametric study has been conducted.

2 Numerical Investigations

FE Model

The FE model shown in Fig. 1 (a) was developed with the FE program DIANA FEA [2]. Due to the multiaxial stress conditions inside the column, a three-dimensional model with twenty-node isoparametric CHX60 elements was chosen. The longitudinal bars and stirrups were modelled as embedded reinforcements. While a simple ideal elastic-plastic material behaviour was assigned to the reinforcement, the Drucker-Prager model with tension cutoff was used to model the UHPC.

The numerical simulations were deformation controlled with an axial, vertical displacement of 0.005 mm/step at the top of the column.

Validation

The FE model was validated with a number of tested columns of a database. Fig. 1 (b) shows the validation by the example of the HPC-column VK3 with a compressive strength of f_{cm} = 90.9 N/mm² (4ϕ28; ϕ8/4.1) and the UHPC-column S6 with f_{cm} = 149.0 N/mm² (4ϕ28; ϕ8/12) [3]. It becomes apparent that both the ultimate load and the post-cracking behaviour can be recalculated in a sufficient manner.

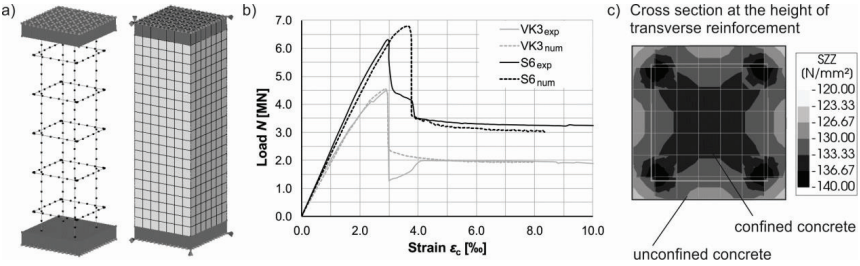

Figure 1: FE model (a), Validation by means of HPC- and UHPC-columns (b), Contour plot of σ_{ZZ} stresses (c).

The numerical investigations have shown that the load-strain curve of UHPC-columns is determined by three load bearing parts – longitudinal reinforcement, unconfined concrete cover

and confined concrete core. Fig. 1 (c) shows the compressive stresses σ_{ZZ} in the cross section of the UHPC-column S6 and reveals that the confined concrete core stands higher compressive stresses than the unconfined concrete cover.

3 Theoretical Investigations

Rheological Model

A rheological model has been developed in order to enable a practical assessment of the robustness of UHPC-columns [4]. The rheological model is shown in Fig. 2 (a) and consists of three springs, each describing one of the above mentioned load bearing parts. The three load-strain relationships are summed up (Eq. (1)) and result in the load-strain curve of the column.

$$N(\varepsilon) = N_{s,l}(\varepsilon) + N_{c,c}(\varepsilon) + N_{c,cc}(\varepsilon) \quad (1)$$

The rheological model was validated with experimental and numerical load-strain curves of HPC- and UHPC-columns.

Parametric Study

In order to quantify decisive influences on the robustness of UHPC-columns, a paramatric study was carried out using the rheological model. Fig. 2 (b) shows the influence of spacing of transverse reinforcement s_{transl} using the example of the UHPC-column S6. By adjusting the spacing s_{transl} from 8.0 cm to 2.0 cm, it is possible to increase the post-cracking load by over 50 %.

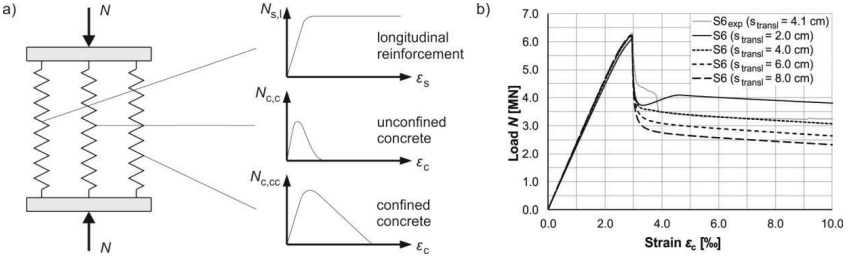

Figure 2: Rheological model (a), Variation of spacing of transverse reinforcement for UHPC-column S6 (b).

4 Conclusions

The rheological model derived from the validated FE model is able to simulate the load bearing and post-cracking behaviour of HPC- and UHPC-columns in a practical manner and enables a simple assessment of the robustness of centrically loaded columns. A parametric study on the influence of decisive column parameters suggests extended recommendations for the structural design of HPC- and UHPC-columns (minimum amount of longitudinal reinforcement, minimum number of bars, maximum spacing of transverse reinforcement, maximum spacing of longitudinal bars) to assure a robust behaviour.

References

[1] Empelmann, M.; Oettel, V.: Weiterentwicklung von Bemessungs- und Konstruktionsregeln bei großen Stabdurchmessern (>Ø32 mm, B500) – Tragverhalten von Druckgliedern. Schlussbericht zum AiF Forschungsvorhaben 16992 N, 2015.

[2] DIANA FEA BV: DIANA Version 10.2 [Software]. November 2018, https://www.dianafea.com [Access on: 15.08.2019].

[3] Steven, G.; Empelmann, M.: Gedrungene Stützen aus UHPFRC mit hochfester Längsbewehrung. *Beton- und Stahlbetonbau* 109 (5), p. 344-354, 2014.

[4] Empelmann, M.; Matz, H.: Robustheit gedrungener Stahlbetonstützen. Beton- und Stahlbetonbau 114 (11), p. 837-846, 2019.

Prestressing of carbon fiber reinforced concrete

Mathias Hammerl, Benjamin Kromoser
Research Group for Resource-Efficient Structural Engineering at the Institute of Structural Engineering, Department of Civil Engineering and Natural Hazards, University of Natural Resources and Life Sciences, Austria

1 Introduction

Motivation

The concrete industry is responsible for about 8 % of the worldwide CO^2-emissions. Therefore, the aim of the researchers is to reduce the demand of natural resources in the building industry by building lightweight structures with high performance materials such as carbon fiber reinforced polymers (CFRP's) and ultra-high-performance-concrete (UHPC).

Research approach

By using high performance materials with their advantages of high durability, high tensile strength of the reinforcement, and high compressive strength of the concrete light and thin-walled structures can be built.

These filigree structures lead to lower stiffness and therefore higher deflections. To improve the serviceability of these structures the authors approach is to prestress the CFRP reinforced concrete structures. The positive effect of prestressing has already been shown in previous investigations [1].

2 Experimental investigation

The main objective of the experiments was to determine the influence of different prestressing forces to structures with ultra-high-performance-fiber-reinforced concrete (UHPFRC) reinforced with a carbon lamella having a thickness of 1.4 mm and a width of 30 mm. Epoxy adhesive with filler was used to glue the lamella into the load introduction implants (end anchorages). All specimens had a rectangular cross section with a height of 200 mm and a width of 30 mm. This geometry was chosen to reduce interferences in the load-bearing behaviour of the beams due to geometrical discontinuities of the cross section. In all the tests, the load was applied in a displacement-controlled manner, with a load rate of 0.8 mm/min. The test setup as described can be seen in Figure 1.

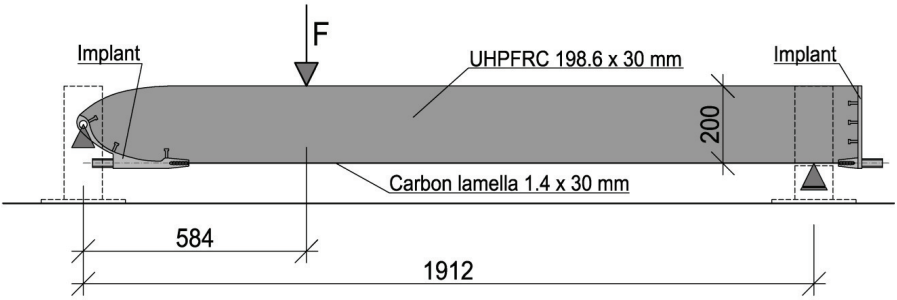

Figure 1: Test setup.

The compressive strength of the used UHPFRC was evaluated with 197 MPa, the flexural bending strength is 34.5 MPa, and the Young's modulus is 49,000 MPa. The material properties of the used reinforcement, S&P C-Laminate HM (200/2000) according to the data sheet are a

tensile strength of 2,800 MPa, a Young's modulus of 205,000 MPa, and an elongation at break of 13.5 % [2].

3 Results

In Figure 2 the load-displacement curves of the tests are shown. The difference between prestressed and non-prestressed specimen can clearly be seen by considering the cracked and non-cracked areas of the curves. While the first crack in specimen 1 occurred at a load of about 8 kN the first cracks in specimen 2 and 3 occurred at about 15 and 20 kN. This clearly shows the positive influence of prestressing. The maximum loads of specimen 1 to 3 were 19.9 kN, 23.8kN, and 29.8 kN. The failure of specimen 1 occurred due to debonding between carbon lamella and concrete. Specimen 2 and 3 failed at the anchorage, when the carbon lamella was pulled out of the implant.

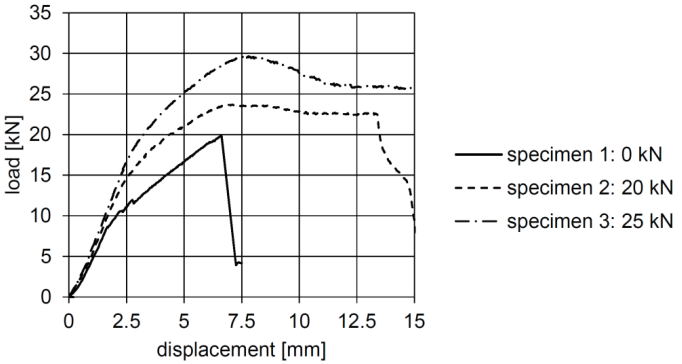

Figure 2: Load-displacement behaviour of the specimens with different prestressing forces of 0, 20, and 25 kN

4 Conclusions and outlook

By comparison of the load-displacement curves of the three specimens the positive effect of prestressing can be seen. Besides improving the serviceability of the structure by increasing the load when the first crack occurred, also the ultimate load was enhanced.

Due to the promising results of this preelimination further tests will be conducted to investigate the load-bearing behaviour of prestressed UHPC beams reinforced with carbon rods and textile reinforcement.

5 Acknowledgements

The authors would like to thank the Austrian Research Promotion Agency (FFG) for their financial support in the FFG research project "prestressed slab elements made of carbon fiber reinforced UHPC" ("Vorgespannte Deckenelemente aus carbonbewehrtem UHPC").

References

[1] Kromoser, B.; Preinstorfer, P.; Kollegger, J.: Building lightweight structures with carbon-fiber-reinforced polymer-reinforced ultra-high-performance concrete: Research approach, construction material, and conceptual design of three building components. *Structural Concrete*, p.1-15, 2018.

[2] S&P Handels GmbH: *URL: https://www.sp-reinforcement.at/de-AT/produkte/cfk-lamellen/sp-c-laminate-oberflachig-geklebt-oder-eingeschlitzt* (accessed 09/18/2019).

Performance increase of textile-reinforced concrete due to structured cross sections

Markus Beßling, Carmen Ochmann, Sven Wirtz, Katharina Zwanzig, Jeanette Orlowsky
Department of Building Materials, TU Dortmund University, Germany

1 Motivation

When Textile-Reinforced Concretes are used, the conventional steel reinforcement is replaced by technical textiles consisting of glass or carbon fibres. The thin-walled design of textile-reinforced concrete (TRC) elements with high load-bearing capacity provide great advantages concerning weight reduction, material saving and creating additional space. The disadvantage of this thin-walled design is the missing concrete cross section for the compression zone i.e. under bending tensile loads. One practical solution for this conflict of interests are structured cross sections build out of TRC. The dimensioning of these cross sections can be adjusted to the respected loads. This approach is primarily limited by manufacturing costs of TRC elements.
This contribution describes the development, testing and evaluation of three differently structured cross sections made of TRC Motivation for this work is the development of noise protection walls which have a load bearing structure out of TRC elements instead of steel reinforced concrete [1]. Using optimized TRC elements instead of steel reinforced concrete can reduce the weight about a factor of three.

2 Investigations and results

Development and testing of structured cross sections out of TRC
Hollow cross sections are a sensible solution for carrying symmetric loads i. e. wind loads. To create the internal voids, three different types of internal formwork are used. The first system (a) uses mineral foam plates, functioning as a lost formwork. This results in a carrying structure of a sandwich element and a hollow cross section. In case of methods b and c, compressed air filled tubes and a mechanically expendable wooden formwork are utilised The following picture 1 shows the three different manufacturing methods.

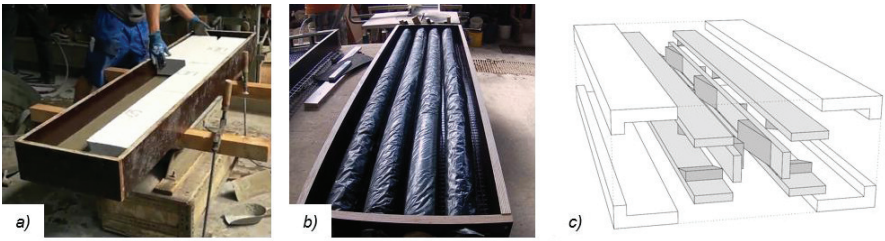

Figure 1: manufacturing methods of the hollow cross sections, a) mineral foam core, b) compressed air filled tubes, c) mechanically expendable wooden formwork

All samples are made with the same concrete mixture. It is characterized by the strength class C50/60 and a maximum grain size D= 2mm. As reinforcement carbon textiles were chosen.
The mineral foam core allows to laminate the lower TRC plate, while the shear bar has to be poured. By this it is necessary to prevent the floating of the lightweight core. Cracking of the mineral foam core due to the shrinkage of the fine grained concrete layer was observed.

Both systems for inner formwork save time in concreting because of pouring concrete in one step. The pouring process also results in a floating of the inner formwork. Due to this, distance holders in the upper TRC plate are necessary in both systems. While the wooden box is a relatively rigid system, the air filled tubes has to be improved. Using an emulsion of sand and water the density of the tubes can be approximated to the one of concrete. This results in a lower deflection of the tubes.

Test results

Each manufacturing method was used to produce three specimens. The cross sections got different shear bar geometries. To evaluate the load bearing capacity of the specimens 4 – point bending tests with support distances of 160 cm and 180 cm were performed. By this the element weights were determined. The results of the most suitable cross sections are summed up in table 1. The reduction of weight is calculated compared to a full cross section with the same height. All specimens showed shear cracks as failure mode.

Table 1: comparison of the load capacity and weight reduction of the three cross sections

	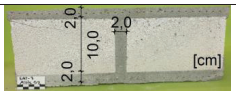		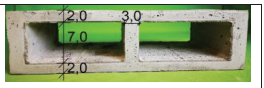
Mmax [kNm/m]	*11.0*	*18.2*	*21.2*
weight reduction [%]	*65*	*35*	*50*

3 Conclusions

In general, it is possible to produce hollow cross sections using the described methods. All of them reduce the element weight greatly while generating a sustainable load bearing capacity. The sandwich element needs to be strengthened with concrete shear bars to gain a tolerable load capacity since the mineral foam core itself is not sustainable enough. Furthermore, an effortful follow-up-treatment is necessary in order to limit the shrinking of the concrete. Using distance holders clearly reduces the floating of both inner formworks. The mechanically expandable inner formwork enables a higher position stability of the inner formwork. Therefore, the production of longer elements, compared to the system with compressed air-filled tubes, is possible. Whereas the advantage of the air tubes is to produce various cavity shapes arranging the tubes in different ways. In a next step the manufacturing methods will be tested in cooperation with the project partner Eudur to optimize the manufacturability of the components in a large scale.

Acknowledgements

This work was performed as part of a project funded by the FEDERAL MINISTRY FOR ECONOMIC AFFAIRS AND ENERGY – project number ZF4586101KI8.

References

[1] Beßling, M., Antons, U., Orlowsky, J. (2017): Potentials of Textile Reinforced Concrete for Lightweight Noise Protection Walls. In: High Tech Concrete: Where Technology and Engineering Meet, Hordijk, D.A., Luković, M. (Eds.), Springer International Publishing, Cham, pp. 2538–2545.

HPC and FRP textile reinforced HPC enhanced with self-sensing properties

Jan Suchorzewski, Miguel Prieto, Urs Mueller
RISE Research Institutes of Sweden, Infrastructure and Concrete Technology, Material Design, Borås, Sweden,

1 Introduction

Within EU project LightCoce (Building an Ecosystem for the upscaling of lightweight multi-functional concrete and ceramic materials and structures), RISE will be running a Pilot Line to allow the design and development of materials and elements of Cellular Lightweight Concrete (CLC) and/or lightweight composite elements with improved functionalities. For this purpose, a test case of a composite CLC/HPC sound-wall element with sound-absorbing, improved durability, self-sensing, and self-cleaning properties will be developed and upscaled. The structural performance and integrity of the sound-wall element will rely on an HPC shell strengthened with FRP textile reinforcement. For this aim, HPC was enhanced starting from a mix design developed in an EU project SESBE. The HPC mix has been upgraded for lowering the overall costs and improving its workability.

2 Self-sensing in concrete

One of the novel concrete functionalities explored in our project is the self-sensing ability gained with the addition of nanoparticles with high conductivity [1]. The recent development of the graphene production process brought novel, economically competitive material called multi-walled carbon nanotubes (MWCNTs), which have super-high-strength (1'000 MPa) and is a perfect electrical conductor. The addition of a small amount of MWCNTs decreases concretes overall electrical resistance enabling material internal structure condition monitoring [2]. A small current must be delivered to analyze the element and the voltage is measured in chosen points of structure (Fig.1). In this way, changes in material resistance are registered over time indicating stress level (Fig.2), cracking or other kinds of damage.

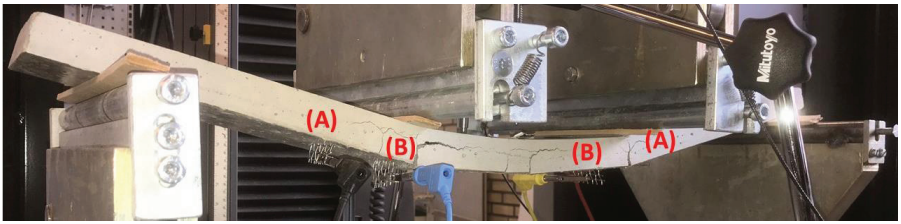

Figure 1: The test setup for resistivity measurements (A) DC current from a power supply (measuring voltage), (B) measuring current.

3 Experimental campaign

A test campaign with different amounts of MWCNT was performed to investigate their effect on mechanical and self-sensing properties. For the investigation of self-sensing several specimens (cubes 100x100x100 mm) and low thickness panels (40x100x700 mm) reinforced with two types of textile FRP (carbon and glass fibers) with different amounts of MWCNT were cast and tested. The textile-reinforced panels were tested (1) in elastic phase under cyclic load, (2) under static continuous deformation or (3) under cyclic load after cracking. Resistivity changes during

tests were recorded and compared with the registered load-displacement curves. The FRP reinforcement forced intensive cracking with multiple discrete cracks, which were monitored throughout all the test duration. The test campaign outcomes will help to understand the effect of the amount of MWCNT on strength and self-sensing properties in HPC.

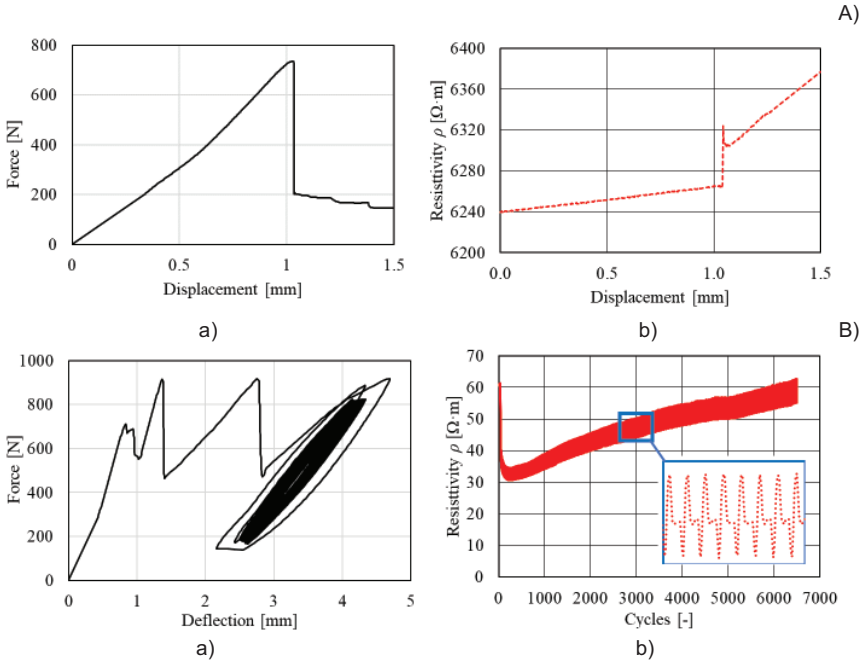

Figure 2: The self-sensing of concrete with the addition of 0.10% MWCNT for panels reinforced with A) GFRP under static loading and B) CFRP under cyclic loading with a) force-displacement curves and b) resistivity to displacement or number of cycles.

4 Conclusions

In our research, we present a novel method for structural health monitoring with no additional sensors. With this method, we were able to measure stresses in uniaxial compression and detect multiple cracks in bending. Moreover, concrete material degradation in cyclic loading (fatigue) could also be observed due to the increase of resistivity. Self-sensing could be used as an inexpensive and easy alternative for monitoring in combination with other methods used nowadays.

References

[1] Konsta-Gdoutos, M.S.; Aza, C.A.: Self-sensing nanotube (CNT) and nanofiber (CNF) cementitious composites for real-time damage assessment in smart structures. *Cement&Concrete Composites* 53 pp. 162-169, 2014.

[2] Danoglidis, P.A.; Konsta-Gdoutois, M.S.; Gdoutos, E.E; Shah, S.P.: Strength, energy absorption capability and self-sensing properties of multifunctional carbon nanotube reinforced mortars. *Construction and Building Materials* 120, pp. 265-274, 2016.

Experimental investigation on the drying shrinkage of structural lightweight aggregate concrete

Mohamed Abd Elrahman [1], Mohamed El Madawy [1], Sang-Yeop Chung [2], Pawel Sikora [3,4], Dietmar Stephan [3]
1: Structural Engineering Department, Mansoura University, Egypt
2: Department of Civil and Environmental Engineering, Sejong University, Republic of Korea
3: Building Materials and Construction Chemistry, Technische Universität Berlin, Germany
4: Faculty of Civil Engineering and Architecture, West Pomeranian University of Technology Szczecin, Poland

1 Introduction

Lightweight concrete (LWC) is a material with low density, excellent thermal insulation properties, and reasonable mechanical properties. However, due to replacing normal-weight aggregates with less rigid porous aggregates, LWC suffers high drying shrinkage and micro-cracking. The influence of mineral admixtures on the shrinkage of LWC was studied by Cheng et al. [1]. Grabois et al. [3] found that with increasing lightweight aggregate content compared tom normal-weight aggregate, the shrinkage significantly increases. Chen et al. [2] studied the influence of different types of fibers on mechanical properties and shrinkage of LWC. Results showed that steel, carbon and polypropylene fibers reduced the shrinkage of LWC effectively, while a study by Kayali et al. proves the important role of fibers in improving the tensile strength and reducing the shrinkage of LWC [4].

2 Materials and tests

This investigation studies the shrinkage behavior of lightweight concrete with a dry density of 800 ± 50 kg/m³. The influence of silica fume and fly ash on mechanical properties and shrinkage was investigated. The effect of two types of polypropylene (PP, density 0.91 g/cm³) fibers; 12 and 6 mm (0.031 mm diameter) on LWC characteristics were examined. Six different mixes have been prepared and tested (Table 1). Dry density, compressive and flexural strength, and drying shrinkage were measured. Chemical admixtures were adopted to produce stable LWC mixes with consistency class of F3/F4 (acc. to EN 206-1). As a lightweight aggregate, expanded glass (Liaver®) was used. Drying shrinkage has been measured as specified in DIN 52450 using the Graf-Kaufmann method.

Table 1: Composition of LWC mixes

Mix	Liaver	Cement	Silica fume	Fly ash	Water	Short fibers	Long fibers
			[kg/mix]			[vol.-%]	
Ref	275	410	50	-	240	-	-
C S	275	410	50	-	240	0.2	-
C L	275	410	50	-	240	-	0.4
C F	275	410	-	50	240	-	-
C FS	275	410	-	50	240	0.2	-
C FL	275	410	-	50	240	-	0.4

3 Results and Discussion

The experimental results showed that all LWC mixes have dry densities in the range of 750 - 850 kg/m³ as planned. Compressive strength is correlated directly to the dry density of LWC (Fig. 1a). Similarly, the thermal conductivity of lightweight concrete is proportioned directly to the dry density of concrete. However, flexural strength depends mainly on the PP fiber type and dry density. It is clear that addition of short fibers is more effective in improving the flexural strength of concrete (Fig. 1b). On the other hand, the addition of PP fibers has a negative influence on compressive strength but does not have any direct effect on thermal conductivity. The experimental results of drying shrinkage at different ages are presented in Fig. 1c. It is clear that in all mixes shrinkage is increasing with age. The addition of PP fibers reduces the shrinkage significantly. Both short and long fibers have similar effects on drying shrinkage. On the other hand, fly ash is more effective in hindering the micro-cracking and reducing the shrinkage compared with silica fume which increases the shrinkage at all replacement levels as

concluded by Nadesan et al. [5]. The addition of fly ash reduces the shrinkage by about 35% compared to control mix with silica fume. However, combination of fly ash and PP fibers resulted in significant reduction in shrinkage by about 70% after 28 days of curing.

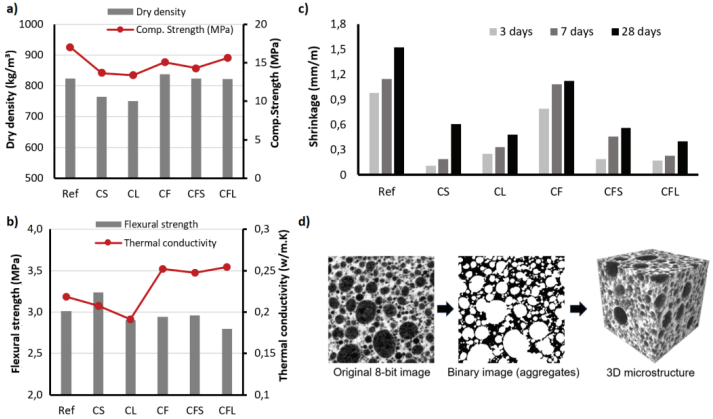

Figure 1: Dry density and compressive strength (a), flexural strength, and thermal conductivity (b), shrinkage (c) and micro-CT imaging process for lightweight aggregate concrete (d).

Concrete microstructure

X-ray micro-CT was applied to examine the microstructure characteristics of LWC specimens non-destructively. Fig. 1d presents the imaging process for classifying pores, aggregates, and solid matrix examination in order to obtain the material characteristics of higher accuracy. In this procedure, the original 8-bit image described in grayscale (Fig. 1d) was converted to the binary image, as shown in the 2nd image. The 3D image was then obtained by stacking a series of binary images, and the detailed pore size distribution of the specimen was evaluated.

The obtained results from the micro-CT data showed that the general trends of the wall-thickness and the pore structures are affected by its constituents. In particular, in each set of the specimens with silica fume and fly ash, the porosity and the wall thickness level within the specimen is almost the same regardless of the use of the fibers. However, as shown in Figs. 1a-1c, the material properties are enhanced by following the use of the fibers, and this result confirmed the effectiveness of the fibers to improve the material properties.

4 Conclusions

This investigation studied the influences of supplementary materials and polypropylene type fibers on mechanical properties as well as shrinkage of lightweight concrete. The experimental results indicated that polypropylene fibers significantly reduces the drying shrinkage. In addition, mixes prepared with silica fume suffer higher shrinkage compared to fly ash mixes. Moreover, X-ray micro-CT can be used to characterize the microstructure of lightweight concrete.

References

[1] Cheng, S., Shui, Z., et al.: Properties, microstructure and hydration products of lightweight aggregate concrete with metakaolin and slag addition, Construction and Building Materials 127 (2016) 59-67.

[2] Chen, B., Liu, J.: Contribution of hybrid fibers on the properties of the high-strength lightweight concrete having good workability, Cement and Concrete Research 35 (2005) 913-917.

[3] Grabois, T., Cordeiro, G., Filho, R.: Fresh and hardened-state properties of self-compacting lightweight concrete reinforced with steel fibers, Construction and Building Materials 104 (2016) 284-292.

[4] Kayali, O., Haque, M., Zhu, B.: Drying shrinkage of fibre-reinforced lightweight aggregate concrete containing fly ash, Cement and Concrete Research 29 (1999) 1835-1840.

[5] Nadesan, M., Dinakar, P.: Influence of type of binder on high performance sintered fly ash lightweight aggregate concrete, Construction and Building Materials 176 (2018) 665-675.

Ultra-High Performance Lightweight Concrete (UHPLC) – compressive strength and fracture behaviour

Cristin Umbach, Alexander Wetzel, Bernhard Middendorf
1: Institute of Structural Engineering, University of Kassel, Germany

1 Introduction

Lightweight concretes offer many advantages in the design and construction of structures. For lightweight concretes according to the German Standard DIN EN 206-1 [1], this is done by using lightweight aggregates with a raw density ≤ 2.0 g/cm³. The coarse aggregates are volumetrically replaced by lightweight aggregates such as perlite, expanded glass or expanded clay. The cement stone around the coarse aggregate remains closed, therefore the concretes are classified as structural lightweight concretes. The bulk density of these concretes can range between 800 – 2000 kg/m³. Structural lightweight concretes are regulated according to German Standard DIN EN 206-1 [1] up to a compressive strength of 80 N/mm². The standard defines concretes with a compressive strength of 60 MPa and above as high-strength structural lightweight concrete. Therefore, the concrete developed in these here presented investigations can be described as ultra-high performance lightweight concrete (UHPLC) due to a compressive strength of 100 MPa and above.

2 Material development

In this approach the concept of structural lightweight concrete was transferred to an ultra-high performance concrete (UHPC). For this purpose, the mix design of the fine-grained mixture M3Q [2] was modified. Therefore, volumetric parts of the fine aggregate were replaced by expanded glass or clay. The lightweight aggregates used had a maximum grain size of 2 mm. In a second step, the particle size distribution of the lightweight aggregates was measured and a packing density optimization was done.

It is reasonable to correlate the compressive strength of lightweight concretes with the bulk density. Therefore, the results of the concrete mixes are shown in a strength-density diagram (figure 1, left). The standard area for lightweight concrete was designed according to Thienel [3].

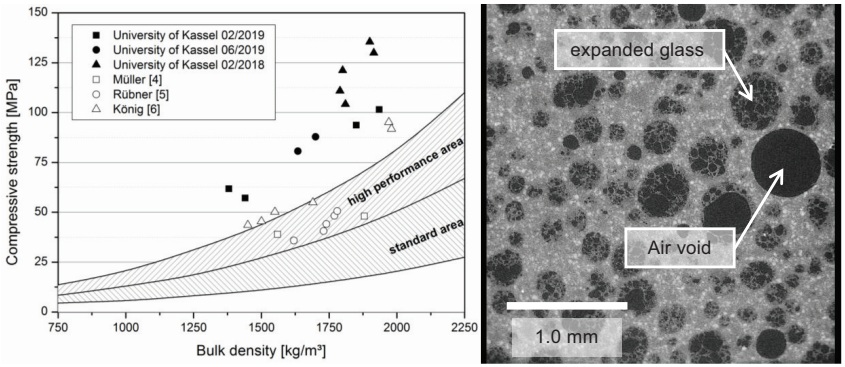

Figure 1: Strength-density diagram for different structural lightweight concretes (left). µ-CT image of the material structure (right).

The results show that the formulations developed by the University of Kassel are significantly better than the area specified in the literature for high-performance lightweight concrete. For additional classification, further results from publications were included in the diagram and show that it is possible to increase the compressive strength up to 50 MPa compared to [3].

Different imaging techniques were used to see the embedding and distribution of the light aggregate in cement stone. One method was a scan with a high-resolution computer tomograph (µ-CT). Figure 1, right shows a sectional image of a mix design with expanded glass and a resolution of 1.49 µm.

3 Fracture behaviour of UHPLC

The modification of the microstructure by the reduced stiffness and strength of the lightweight aggregates leads to a changed load-bearing and deformation behaviour of these concretes. In particular, crack development and crack interlocking are altered by the lightweight aggregates and cause a lower load-bearing capacity [7]. To describe the failure model, a distinction is made between state I, linear-elastic area (before the first visible crack) and state II, cracked component. For lightweight concretes, the German Standard DIN EN 1992-1-1 [8] specifies factors for reducing the strength depending on the bulk density. In the case of structural lightweight concretes, it is assumed that no appreciable load dissipation is possible in the cracked state (state II). This leads to a drastic reduction of the characteristic compressive strength.

The fracture behaviour of structural lightweight concrete can be investigated with in situ loading in 3D analyses (µ-CT). The focus is on the examination of state II and which failure form occurs. In this way, the design principles shall be questioned and new approaches for UHPLC can be generated.

4 Conclusions and outlook

With the UHPLC a new class of material could be developed. In order to be able to use the material safely, investigations still have to be carried out. These include further tests on the durability, load-bearing and deformation behaviour of the material.

References

[1] EN 206-1:2013 Concrete – Specification, performance, production and conformity. German version.

[2] Schmidt, M.; Fehling, E.; Fröhlich, S.;Thiemicke, J.: Sustainable Building with Ultra-High Performance Concrete. Structural Materials and Engineering Series – No. 22. kassel university press, Kassel, 2014.

[3] Thienel, K.-Ch.: Materialtechnologiesche Eigenschaften der Leichtbetone aus Blähton. Festschrift Prof. Dr.-Ing. F. S. Rostásy. S. 203-210, Wilhelm Ernst & Sohn Verlag, 1997.

[4] Müller, H. S.; Heist, M.; Mechtcherine, V.: Selbstverdichtender Hochleistungs-Leichtbeton. Beton- und Stahlbetonbau, Heft 6, S. 326 -333, 2002.

[5] Rübner, K.; Schnell, A.; Haamkens, F. et. al.: Leichtbeton aus Aufbaukörnung. Chemie Ingenieur Technik No. 8, S.1792 – 1797, 2012.

[6] König, G.; Dehn, F.; Hegger, J. et al.: Der Einfluss der Rissreibung auf die Querkrafttrag-fähigkeit – Erkenntnisse aus experimentellen Untersuchungen an Bauteilen aus Leichtbeton und hochfestem Beton. Beton- und Stahlbetonbau, Heft 10 (95), S.584 – 591, 2000.

[7] Zilch, K.; Zehetmaier, G.: Bemessung im konstruktiven Betonbau. Nach DIN 1045-1 (Fassung 2008) und EN 1992-1-1 (Eurocode 2). Springer-Verlag, Berlin/Heidelberg, 2006.

[8] EN 1992-1-1: Eurocode 2: Design of concrete structures - Part 1-1: General rules and rules for buildings. German version.

Effect of the mixing procedure on rheological properties and flocculation of cementitious suspensions

Mareike Thiedeitz[1], Inka Dreßler[2], Thomas Kränkel[1], Dirk Lowke[2], Christoph Gehlen[1]

1: Centre for Building Materials (cbm), Technical University of Munich, Germany
2: Institute of Building Materials, Concrete Construction & Fire Safety, Technische Universität Braunschweig, Germany

1 Introduction

The rheology of cementitious suspensions is dependent on various factors like solid content, particle size distribution and chemical composition. Moreover, the rheological parameters are reliant on shear history, which affects the formation of the particle network and thus the interparticle forces as the origin of yield stress and viscosity.

To investigate the effect of shear time on the apparent state of flocculation and rheological performance, tests were conducted regarding the effect of the mixing time on the apparent particle size distribution using Focused Beam Reflectance Measurement (FBRM) and compared to actual measured rheological parameters in a rheometer.

1.1 Rheological background

Cement paste is a two-phase colloidal Non-Newtonian suspension whose rheological parameters yield stress and viscosity are highly dependent on the shear history applied to it: Agglomerates in the particle network are broken due to applied shear, mixing time and intensity. The structural breakdown changes the effective apparent granulometry of the interparticle network consisting of the apparent specific surface area and the size distribution of the agglomerates [1, 2]. Equilibrium is reached, when the applied shear is not powerful enough to further break the agglomerates.

1.2 Focused Beam Reflectance Measurement (FBRM) for the in situ investigation of agglomerate size distributions

FBRM is an in-situ technique for the characterization of the apparent chord length distribution of flocculated agglomerates in highly packed suspensions. A laser beam is focused through a rotating lens to a circular moving point nearby the instrument's opening window. If an agglomerate is hit by this focus point, light is scattered back and registered by a detector. The tangential velocity of the beam and its speed are expected to be significantly larger than the agglomerate's velocity. Therefore, the median chord length d_{50} of the agglomerate can be calculated from the scattering time, rotation speed and speed of light. The chord length distribution is directly linked to the agglomerate diameter distribution [3].

2 Materials and methods

Two cement paste series using OPC 42.5 R and demineralized water with a solid content of 0.45 were prepared according to DIN EN 196:1 und subsequently investigated. Series one was tested without superplasticizer (0.45), series two contained a PCE-based superplasticizer with an adjusted amount for a mini slump flow of 250 ± 5 mm four min after water addition (0.45_SP). Preshear times of 30, 90, 150 and 300 s were applied to the pastes. Then the rheological and FBRM measurements were started 15 min after water addition. For each series the average value of two repetitions was calculated. The detailed experimental procedure can be seen in [4].

3 Results and conclusions

Table 1 shows the results of the FBRM (median chord length) and rheological measurements (slump flow (SF), yield stress (τ_0) and viscosity (μ)).

Table 1: Average slump flow (SF), yield stress (τ_0) and viscosity (μ) of the cement pastes 0.45 and 0.45_SP

Preshear time [s]	0.45				0.45_SP			
	d_{50} [μm]	SF [mm]	τ_0 [Pa]	μ [Pas]	d_{50} [μm]	SF [mm]	τ_0 [Pa]	μ [Pas]
30	90.65	151.0	62.5	0.79	91.25	239.0	13.3	0.48
90	93.21	158.0	58.8	0.75	78.71	251.0	13.2	0.37
150	-	173.0	54.1	0.55	-	260.0	12.8	0.31
300	88.28	182.5	48.4	0.48	80.04	261.5	11.9	0.27

Increasing the preshear time results in a reduction of the agglomerate sizes in the particle network which can be seen in *Fig. 1*. This reduction is more pronounced and proceeds faster in a system with superplasticizer. The breakage of agglomerates sizes meanwhile leads to a decrease in both viscosity and yield stress (*Fig. 2* and *Fig. 3*). The decrease in yield stress also correlates to the increase in slump flow with increasing preshear time (*Fig. 3*)

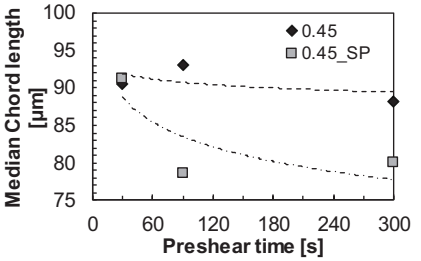

Fig. 1 Effect of preshear time on median chord length

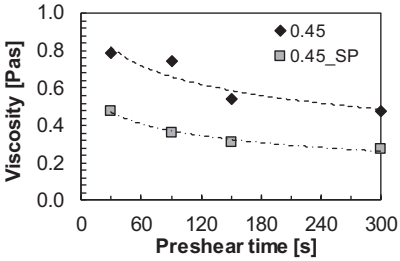

Fig. 2 Effect of preshear time on viscosity

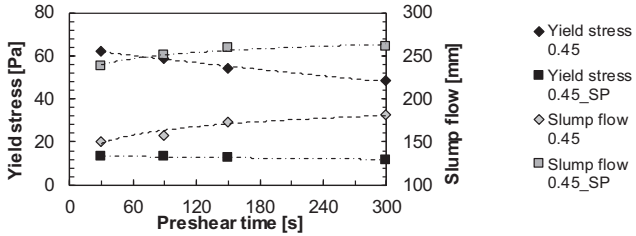

Fig. 3 Effect of preshear time on yield stress and slump flow

Through the combination of FBRM and rheological measurements it could be shown that the apparent agglomerate size affects both the paste yield stress and viscosity. These preliminary findings are to be deepened in future research.

These studies were funded by the Deutsche Forschungsgemeinschaft (DFG, German Research Foundation) – Project number TUM: 387065993; project number TUBS: 387066140.

References

[1] Roussel, N. et al.: *Steady state flow of cement suspensions*; In: *CCR* 40 (2010), Nr. 1, S. 77–84

[2] Genovese, D. B.: *Shear rheology of hard-sphere, dispersed, and aggregated suspensions, and filler-matrix composites*. In: *Adv.in colloid and interface science* 171-172 (2012), S. 1–16

[3] Krauss, H. et al.: *Experimentelle Bestimmung der Zusammenhänge zwischen rheol. Eigenschaften von feststoffreichen Suspensionen und deren Mikrostruktur*. In: *Chem Ing Tec* 90 (2018), Nr. 6, S. 881–887

[4] Thiedeitz, M. et al..: Effect of the mixing time on rheological parameters of cement pastes. In: *Rheologische Messungen an Baustoffen 2019*, S. 14–25

Hydration and flow characteristics of Ultra-High Performance Concrete with sodium silicate

Ji-Seul Park, Sung-Gul Hong
Department of Architecture & Architectural Engineering, Seoul National University, Korea

1 Introduction

In recent years, significant advance has been made in the 3D printing technology in construction and the use of building materials as the extrudable filaments. However, more general applications of 3D printing in construction require establishing reliability of printed structure by securing adequate mechanical performances.

Recent studies have investigated potential mixtures for 3D concrete printing, such as ordinary Portland cement, calcium sulfoaluminate cement, and self-compacting concrete [1]. However, there has been little discussion on using ultra high strength or ultra-high-performance concrete (UHPC) as 3D printing materials to overcome the limitation on the mechanical strength. Recent research has established that UHPC features outstanding strength, flowability, and durability, and the admixtures used in UHPC are also well-documented by extensive investigations. The high fluidity of UHPC is expected to be suitable for the early stage of the 3D printing process such as pumping and extrusion.

In this study, the compositional ingredients were based on the mixture of UHPC, generally does not include coarse aggregates. To estimate the suitability of UHPC for 3D printing, rheological properties were investigated using the flow table test, the ultrasonic pulse velocities (UPV) with admixture of sodium silicate solution (i.e., waterglass). Additionally, the effect of admixture on early age hydration was measured using an isothermal calorimeter.

2 Materials

The mix proportions are presented in Table 1. The sodium silicate solution (28-30 wt.% SiO_2, 9-10 wt.% Na_2O, pH 11-12 was chosen to facilitate mixing of the materials as accelerators. The waterglass (WG) was added immediately, or it was delayed after 10, 20, and 30 min after contact of water and dry mix.

Table 1: Mix proportions of samples with different dosage of sodium silicate (kg/m3).

Mixture	Water	WPC	Silica fume	Quartz powder	Micro sand	Super-plasticizer	Sodium silicate
UHPC	185	741	185	259	815	30	0
WG1	185 (203.52)[a]	741	185	259	815	30	23.15 (9.26)[b]
WG3	185 (240.56)[a]	741	185	259	815	30	69.45 (27.8)[b]

[a] *The value indicates the total amount of water including the amount of water in the sodium silicate solution.*
[b] *The value indicates the solid content of sodium silicate.*

3 Results and discussion

Hydration reaction at early ages

With increasing dosage of WG, the onset of acceleration period was shifted to earlier time, as shown in Fig. 1. The delayed additions enhanced the accelerating effect than direct additions did; however, there was no significant difference in terms of the delayed addition time.

Ultrasonic pulse velocity developments at early ages

In the current study, the 1500 m/s threshold was considered the indicator of initial setting time [2]. The higher the dosage of WG, the faster the initial setting time. In terms of the time of WG addition, no noticeable difference or apparent trend was among the samples.

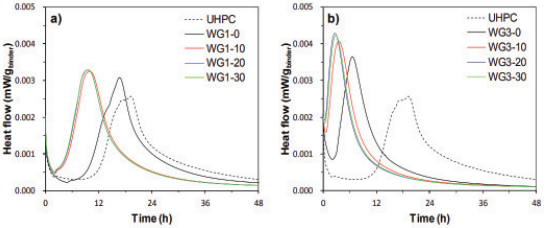

Figure 1: Heat flow of (a) WG1 and (b) WG3 groups compared with UHPC.

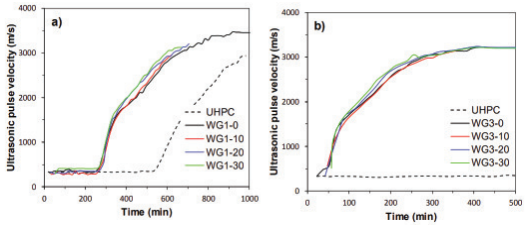

Figure 2. Influence of WG dosage and addition time on the evolution of ultrasonic pulse velocity of (a) WG1 and (b) WG3 compared to UHPC.

Flow table test

UHPC secured high fluidity due to the high dosage of SP and the increasing WG dosage and an increase of addition time led to a decrease in fluidity, as shown in Fig. 3.

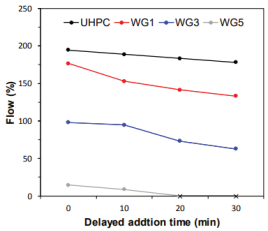

Figure 3. Fluidity of UHPC with different WG dosage and addition time.

4 Conclusions

This study presented the applicability of UHPC on 3D printing construction by controlling the rheological and hydration properties through a time-controlled dosage of WG. The increase in dosage and time of delayed addition of waterglass resulted in a decrease in induction period of UHPC. As a result, the significant decreases in the flow and the initial setting time suitable for 3D printing application, were achieved. The results suggested that the superior mechanical properties and the high fluidity of UHPC can be utilizable in 3D printing by the delayed addition of 3% waterglass and by applying sufficient shearing before deposition.

References

[1] Marchon, D., Kawashima, S., Bessaies-Bey H., Mantellato S., Ng S.: Hydration and rheology control of concrete for digital fabrication: Potential admixtures and cement chemistry. *Cement and Concrete Research* 112, pp. 96-110, 2018.

[2] Trtnik, G.; Turk, G.; Kavčič, F.; Bosiljkov, V.B.J.C.: Possibilities of using the ultrasonic wave transmission method to estimate initial setting time of cement paste. Cement and Concrete Research 38, pp.1336-1342, 2008.

Effect of chemical admixtures and addition times on rheology of Ultra-High Performance Concrete

Megan S. Voss, Dr. Kyle A. Riding, Raid S. Alrashidi
Department of Civil and Coastal Engineering, University of Florida, United States

1 Background

Ultra-High Performance Concrete's (UHPC's) compressive strength, tensile ductility, and excellent durability make it a desirable construction material for structures under high loads, unpredictable loads, or harsh environmental conditions. UHPC achieves these qualities in part due to its low water-to-cementitious materials ratio (w/cm). This ratio is usually below 0.25. In order to keep the mix workable, UHPC typically uses a very high amount of HRWRA (superplasticizer). Previous work has shown that the rheological properties of concrete are affected not only by the amount of water or admixture used, but also by the timing of addition. Several researchers suggest that delaying the addition of part of the water and admixtures can result in a more workable mix [1,2,3]. In concretes like UHPC with low w/cm, it has been found that a polyethylene glycol (PEG) used in conjunction with a superplasticizer can help disperse cement particles, thus making the mixture more fluid. Lange and Plank used a PEG with a molecular weight of 2000 (PEG-2000) to increase the spread flow of a cement paste with a w/cm of 0.30 [4]. The mechanism by which PEG assists in concrete flowability differs from that of a superplasticizer in that it does not adsorb on to the surface of the cement particles. Instead, it acts as a lubricant between the particles [4].

2 Research

Methods and Materials

A UHPC mix was developed using materials available in Florida, United States. Type IL cement was used because it is the most popular cement used in the state. Fly ash and silica fume were used as supplementary cementitious materials. A fine mason sand was used for aggregate, and a commercial superplasticizer was used. For some mixes, one of four PEGs, each with a different molecular weight, was used in addition to the superplasticizer. PEGs were dosed with respect to percentage of cementitious content, in amounts ranging from 0.2% to 1% by mass.

The UHPC was mixed in small batches of roughly 10 Litres each. A rheometer with torque-measurement capabilities was used to mix the concrete at a high speed while also measuring the power required to mix the material. This allowed the researchers to compare how the total mixing energy as well as peak mixing energy was affected by different admixtures and liquid addition times. The mixing sequence was as follows: 2 minutes of blending the dry ingredients together at slow speeds, followed by the first liquid addition. For the control mix, the first liquid addition contained 70% of the water as well as 100% of the superplasticizer. Three minutes after the first liquid addition, the second liquid addition was added to the mixture. For the control mix, this included the remaining 30% of water. This second addition was followed by nine more minutes of mixing. After mixing was completed, the flow measurement of the material was taken using the flow cone and table specified in ASTM C230 [5]. In accordance with the testing provisions for UHPC as defined in ASTM C1856, the flow table was not dropped before the measurement was taken [6]. After 10 minutes, a second flow measurement was taken to check slump retention. Paste samples were placed in an isothermal calorimeter soon after mixing was completed to record the heat released (and indirectly, the extent of the reaction) over time.

Results

The PEGs used in conjunction with the ADVA 600 superplasticizer had drastically different effects on the workability of the concrete, depending on the molecular weight of the PEG. Table 1 gives the flow results for each admixture. Because the flow cone had a base of 100mm, a mix with a flow radius of 100mm would be considered to have no flow at all.

Table 1: Flow Results from Different PEGs

Admixture Used	Flow Radius (mm)
Control (superplasticizer only)	215
PEG 400	120
PEG 1000	240
PEG 2000	220
PEG 8000	195

The effect of the order of addition for admixtures and water were also studied. Results were compared between mixes that had all the water and admixture added at the beginning of the mixing sequence to those with some water and possibly admixtures delayed. The mixes with all liquids added in the beginning showed reduced flow diameter and an increase in the maximum mixing energy required. Whether or not the PEG was delayed, did not make a difference in either mixing energy or flow diameter.

The isothermal calorimetry results showed that all of the PEGs used caused a delay in hydration. This delay ranged from about 1-5 hours, with larger doses of PEG causing longer hydration delays.

3 Conclusions

Polyethylene glycol (PEG) can have a substantial effect on the rheological properties of a concrete mixture. While it does cause a delay in hydration, some PEGs were able to improve the workability of UHPC with a low w/cm. More research into the different PEGs used is needed to see whether physical properties such as molecular weight or size are the reason that each PEG affects the mix differently. Delaying the addition of some of the mixing water improved concrete workability and decreased the peak mixing energy demand, but altering the time of addition for the PEG did not affect rheology.

References

[1] Shihada, S.; Arafa, M.: Effects of silica fume, ultrafine and mixing sequences on properties of ultra high performance concrete. Asian Journal of Materials Science 2 (3) (2010) 137-146.

[2] Hsu, K.; Chiu, J.; Chen, S.; Tseng, Y.: Effect of addition time of a superplasticizer on cement adsorption and on concrete workability. Cement and Concrete Composites 21 (5) (1999) 425-430.

[3] Ferdosian, I.; Camões, A.: Effective low-energy mixing procedure to develop high-fluidity cementitious pastes. Matéria 21 (1) (2016) 11-17.

[4] Lange, A.; Plank, J.: Contribution of non-adsorbing polymers to cement dispersion. Cement and Concrete Research 79 (2016) 131-136.

[5] ASTM C230-14, Standard Specification for Flow Table for Use in Tests of Hydraulic Cement. ASTM International. October 1, 2014.

[6] ASTM C1856, Standard Practice for Fabricating and Testing Specimens of Ultra-High Performance Concrete. ASTM International. May 15, 2017.

Flowable concrete during compaction – effect of external vibration on the evolution of yield stress and viscosity and the resulting deaeration and segregation behaviour

Thomas Kränkel, Daniel Weger, Christoph Gehlen
Center for Building Materials, Chair for Materials Science and Testing, Technical University of Munich, Germany

1 Motivation and Aim

Flowable concrete represents the link between Self Compacting Concrete (SCC) and conventional vibrating concrete. They exhibit outstanding workability but have to be slightly compacted to ensure sufficient deaeration. However, a too intense compaction may cause segregation of the coarse aggregate and thus impaired durability. Numerous studies have been carried out to rheologically characterize flowable concretes. However, only a few [1-4] were performed with simultaneous external compaction. Nevertheless, to ensure adequate deaeration and sufficient robustness against segregation, it is necessary to know the rheological properties during compaction. For this aim, rotational vane rheometer, deaeration and segregation tests during compaction were performed.

2 Materials and Methods

Materials and Mix Design

OPC 42.5 N, fly ash, naturally rounded sand 0/4 mm, coarse aggregate 4/16 mm and PCE-based superplasticizer (SP) were used. For variation of the (uncompacted) plastic viscosity μ, a 1st series of concretes (μ^-, $\mu°$, $\mu+$) was differed in its water to binder ratio *w/b* and thus relative solid concentration (direct effect on μ), but constant paste volume, binder composition and grading curve of the aggregate. The SP content was adjusted to reach a comparable dynamic yield stress ($\tau_{0D}°$). Furthermore, a 2nd series based on mix design of $\mu°$ but with a variation of the SP content and thus the initial dynamic yield stress (τ_{0D}^-, $\tau_{0D}°$, τ_{0D}^+) was investigated.

Compaction

The compaction work W was determined by assuming a harmonic sinusoid of the vibration table. The compaction scenarios represented the range from under-compaction (W~300 J), over usual compaction for flowable concrete (W~2,500 J) to over-compaction with concrete segregation (W~8,000 J).

Test Procedure

The test procedure began 19 min after water addition (after 30 s of remixing the concrete). The rheological investigations were carried out in a 4-bladed rotational vane-in-cup concrete rheometer with a speed-controlled step profile (8 steps, 8 s each, rotation speed stepwise reduced from 0.5 rps to 0.03 rps). The dynamic yield stress τ_{0D} and plastic viscosity μ were determined under the assumption of Bingham's law. For measurements during compaction, the cup of the rheometer was rigidly fixed to a vibrating table and thus the concrete inside could be compacted, while the vane paddle was decoupled from the vibration. The air void content was determined based on EN 12350-7 and the coarse aggregate segregation by cylinder segregation test [5] both without and with a successive increase in compaction by increasing either frequency or duration of the vibration table.

3 Results and Discussion

Figure 1 exemplarily shows the development of τ_{0D} (left) and μ (right) under the effect of W for varying μ^+, $\mu°$ and μ^- but with comparable $\tau_{0D}°$. Compaction reduces both τ_{0D} and μ of all tested

concretes. The reduction in τ_{0D} was linked to the initial concrete viscosity: for the high viscous concrete μ^+, even low compaction led to a significant reduction in τ_{0D}, whereas just a slight decrease could be observed for concrete μ^-, Figure 1 (left). Even a light compaction was sufficient to reduce μ of all investigated concretes by 30 to 50%, see Figure 1 (right).

The effect of W on the concretes with varying τ_{0D} but constant $\mu°$ showed comparable results to the behaviour of $\tau_{0D}°/\mu°$ in Figure 1. The development of μ under compaction proved to be largely independent of the initial τ_{0D}. Thus, the behaviour for $\tau_{0D}°/\mu°$ shown in Figure 1 (right) can also be assumed as representative for $\tau_{0D}^-/\mu°$ as well as $\tau_{0D}^+/\mu°$.

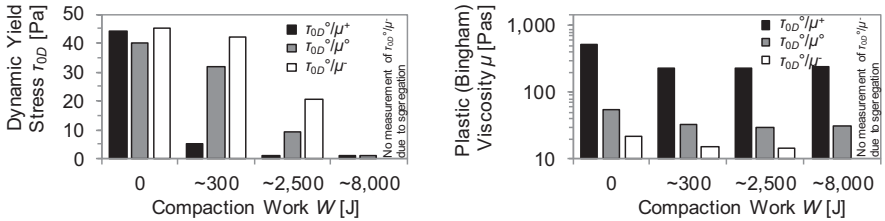

Figure 1: Evolution of dynamic yield stress (left) and plastic viscosity (right) of concretes μ^-, $\mu°$ and μ^+ with yield stress $\tau_{0D}°$ as function of the compaction work W

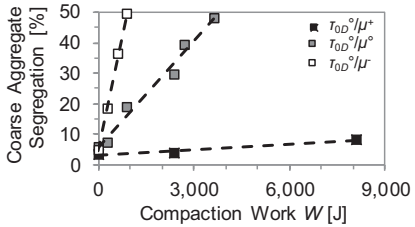

Figure 2: Segregation of concretes μ^+, $\mu°$ and μ^- with yield stress $\tau_{0D}°$ as a function of compaction work W

Figure 2 shows the segregation behaviour of concretes μ^+, $\mu°$ *and* μ^- with yield stress $\tau_{0D}°$ as a function of W. The low viscos concrete μ^- segregates significantly even at low W. With increasing viscosity, segregation is less affected by the compaction because high viscos concretes also exhibit high viscosity during compaction, which counteracts segregation. As expected, the robustness increased as well with increasing initial yield stress. Furthermore, the reduction of the initial viscosity led to improved deaeration behaviour, since the low viscous concretes had the lowest viscosity even during compaction.

4 Conclusions

The rheological, deaeration und segregation behaviour of flowable concretes with varied yield stress or viscosity were investigated in dependency of compaction intensity. It was found that yield stress and viscosity were reduced during compaction and that the magnitude of that reduction is directly linked to compaction intensity. Furthermore, concretes with high initial (not compacted) yield stress or viscosity showed also high values during compaction. This explains that highly viscous concretes showed higher robustness, but also a deteriorated deaeration.

5 References

[1] Petrou, M. F. et al.: A unique experimental method for monitoring aggregate settlement in concrete. Cement and Concrete Research 30 (2000) 5, p. 809-816

[2] Safawi, M. I.; Iwaki, I.; Miura, T.: The segregation tendency in the vibration of high fluidity concrete. Cement and Concrete Research 34 (2004) 2, p. 219-226

[3] Safawi, M. I.; Iwaki, I.; Miura, T.: A study on the applicability of vibration in fresh high fluidity concrete. Cement and Concrete Research 35 (2005) 9, p. 1834-1845

[4] Kränkel, T.; Lowke, D.; Rosa, S.O.; Gehlen, C.: Deaeration and segregation tendencies of highly flowable concrete owing to vibration. In: International Conference ACCTA, 2013

[5] Deutscher Ausschuss für Stahlbetonbau: Richtlinie Selbstverdichtender Beton (German), 2003

Direct tensile testing of Ultra-High Performance Fibre Reinforced Concrete

William Wilson[1,2], Tomas O'Flaherty[1,3]

1: Department of Civil Engineering & Construction, Institute of Technology Sligo, Republic of Ireland
2: Roadstone Ltd, Dublin, Republic of Ireland
3. Centre for Environmental Research Innovation and Sustainability, Institute of Technology Sligo, Republic of Ireland

1 Introduction

An advantage of ultra high performance fibre reinforced concrete (UHPFRC) over conventional strength concretes is that its mechanical properties include a tensile capacity greater than 10MPa, and significant ductility continues to develop even after cracking has occurred [1]. To encourage the industry to further exploit the structural advantages of UHPFRC it is necessary to accurately evaluate and demonstrate its significantly improved tensile behaviour in comparison to conventional concretes. This paper describes an experimental test method that was developed to determine the stress-strain behaviour of UHPFRC in direct tension.

2 Methodology

Tests in which the concrete specimen is pulled apart by a uniaxial load is the best method to determine the concrete tensile capacity as there are no additional stresses induced in the specimen. However, there is no standard method available for direct tension testing of concrete and issues commonly arise around the gripping mechanism, which can introduce significant stress concentrations that can cause premature failure.

Direct tensile dogbone specimens with circular cross sections were developed to ensure that fracture occurred away from the grips and stress concentrations at changes in cross-section were minimised. The diameter of the cross section of the specimen was gradually reduced from 120mm at the grips to 55mm at the centre of the specimen using a curved profile, as shown in Figure 1 (a). When gripping the concrete specimens, the main objective is to increase the friction at the concrete-steel interface, without inducing secondary stresses into the concrete specimen. Direct compression contact between the concrete specimen and the steel grips was used in this research, Figure 1(b). Numerical and experimental trials verified that no stress concentrations occurred at the gripping locations. A Tinius Olsen Hounsfield frame with displacement controlled loading was used for the direct tensile tests, as shown in Figure 1 (c).

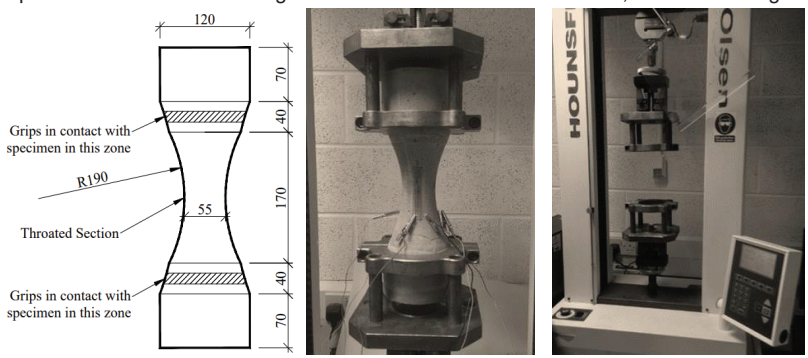

Figure 1: Details of (a) the dogbone specimen, (b) grips and strain gauge arrangement, and (c) testing frame.

Strain gauges were used to record the stress-strain relationship. Three strain gauges were attached to each specimen at 120º to each other around the circumference of the midsection of

the specimen, as shown in Figure 1 (b). By correctly aligning the specimen in the pre-load phase of testing and demonstrating that the strain recorded by each of the gauges was comparable in the pre-cracking stage, uniaxial behaviour was ensured. Preliminary test results and previous literature [2 - 4] illustrated that the most suitable loading rate was 0.4mm/min.

Mix Design

Table 1 presents the mix proportions of the mixes investigated. Particle size distribution curves of the individual constituents were used in conjunction with the modified Andreasen and Andersen model [5] to design the mixes investigated in this research. The steel fibres used were Dramix OL 13/.20 with a length of 13mm, a diameter of 0.20mm, and a tensile strength of 2600MPa. The steel fibre dosages used were 0%, 1%, 2%, 3% and 4% by volume of concrete.

Table 1: Mix proportion of UHPFRC by weight ratio.

Material	CEM I	MicroSilica	Sand	Water	Admixture
Ratio to CEM I by Weight	1.00	0.25	1.26	0.22	0.05

3 Results

Table 2 presents the average of three specimens first crack and peak direct tensile stress results for each fibre dosage. Failure occurred in the 0% and 1% fibre mixes due to the rapid propagation of a single crack. After first crack in the 2%, 3% and 4% fibre specimens, strain hardening resulted in an increase in post-cracking capacity with an increase in fibre dosage resulting in an increase in the post-cracking stress. This strain hardening behaviour differentiates UHPFRC from other lower strength concretes. The formation of multiple microcracks was evident and failure occurred due to fibre pullout with one or more microcracks expanding to form a macrocrack.

Table 2: Average dogbone specimen direct tensile first crack and peak stresses

Fibre Dosage	0%	1%	2%	3%	4%
First Crack Stress (MPa)	10.5	10.5	10.5	10.8	11.4
Peak Stress (MPa)	10.5	10.8	11.6	12.4	13.4

4 Conclusions

The primary advantage of the direct tension dogbone specimens is its circular cross-section and curved throated midsection that removed potential stress concentrations at sudden changes in cross-section. The tensile stress-strain behaviour was recorded using three strain gauges equally spaced around the circumference of the throated section of the specimens to ensure uniaxial load was applied. Fibre dosages of 2% and higher exhibited strain hardening and residual strength after first crack formation, which was a result of the fibres in the matrix bridging the first cracks and redistributing the stress released through microcracking.

References

[1] Richard, P.; Cheyrezy, M.: Composition of reactive powder concretes, Cem. Concr. Res., vol. 25, no. 7, pp. 1501–1511, 1995.

[2] Phillips, D.V.; Binsheng, Z.: Direct tension tests on notched and un-notched plain concrete specimens, Mag. Concr. Res., vol. 45, no. 162, pp. 25–35, 1993.

[3] Hassan, A.M.T.; Jones, S.W.; Mahmud, G.H.: Experimental test methods to determine the uniaxial tensile and compressive behaviour of ultra high performance fibre reinforced concrete (UHPFRC), Constr. Build. Mater., vol. 37, pp. 874–882, 2012.

[4] Park, S.H.; Kim, D.J.; Ryu, G.S.; Koh, K.T.: Tensile behavior of Ultra High Performance Hybrid Fiber Reinforced Concrete, Cem. Concr. Compos., vol. 34, no. 2, pp. 172–184, 2012.

[5] Funk J.E.; Dinger, D.R.: Predictive Process Control of Crowded Particulate Suspensions: Applied to Ceramic Manufacturing. Boston: Kluwer Academic Publishers, 1994.

Tensile behaviour of an Ultra-High Performance Fibre Reinforced Cementitious Composite incorporating spent equilibrium catalyst

Amin Abrishambaf[1], Mario Pimentel[2], Sandra Nunes[3]
1,2,3: CONSTRUCT-LABEST, Faculty of Engineering (FEUP), University of Porto, Portugal
1: aminab@fe.up.pt, 2: mjsp@fe.up.pt, 3: snunes@fe.up.pt

1 Introduction

Spent Equilibrium Catalyst (ECat) is a waste material generated by the oil refinery industry. ECat [1] was shown to act as an internal curing agent in UHPFRC, since the absorbed water in the porous ECat particles is released in matrix and provides a beneficial effect to reduce the autogenous shrinkage. This research focuses on the characterization of the tensile behaviour of the optimized UHPFRC_ECat mixture. The results are compared to a previously developed conventional UHPFRC, both exhibiting a close compressive strength.

2 Mixes, specimens and test setup

Mixes

The mix compositions with 3% fibre volume fraction are shown in *Table* in which U and U_ECat designate the conventional and new mixture with ECat [1], respectively. Smooth brass coated high-strength steel fibres with l_f =13 mm and d_f = 0.2 mm are used. U and U-ECat mixtures exhibited a slump flow diameter of 280 and 282 mm, respectively, without any compaction energy; and close 28-day compressive strength between 140-150 MPa, without heat/pressure treatment.

Table 1: Mix compositions (kg/m^3).

Mix	Cement	Silica fume	ECat	Filler	Water	SP	Sand	Fibres
U	794.90	39.74	---	311.43	185.20	30.03	940.96	235.50
U_ECat	690.19	33.56	155.45	250.58	207.50	19.48	775.01	235.50

Specimens and test setup

The interfacial bond properties were characterized through one-sided single fibre pullout tests performed in both the conventional and ECat plain UHPCs matrixes. An embedment length $l_f/2$ = 6.5mm was adopted and three fibre orientation angles 0°, 30° and 60°, were tested. For each mixture, two series of dog-bone specimens with different fibre orientation profiles were cast for testing under direct tension: one series of specimens with randomly oriented fibres and another with well-oriented fibres. In the latter, the matrix was subjected to an electromagnetic field during casting to align the fibres parallel to the loading direction [2]. The uniaxial tensile tests were performed on the dog-bone specimens with hinged-hinged boundary conditions.

3 Results and discussion

Interfacial bond properties

Figure 1 shows the interfacial bond properties between fibre and matrixes. The influence of fibre orientation is noticeable. Both mixtures show a similar fibre debonding load for the tested fibre orientation angles. However, when it comes to the maximum load and pullout work, higher values are observed for U_ECat. This confirms higher friction between the fibre and the U_ECat mixture during the pullout stage, which needs to be further studied by microscopic analysis of the surface of pulled out fibres. In the case of inclined fibres, two failure modes were observed during the tests: fibre pullout and fibre rupturing. A higher number of fibres ruptured in U than

U_ECat. This depends on the strength of the matrix at the fibre exit point, in which a matrix wedge is formed and detached during the fibre pullout. In the future works, SEM analysis and micro-hardness measurements will be used to examine the quality of interfacial transition zone between the fibres and each of the mixtures.

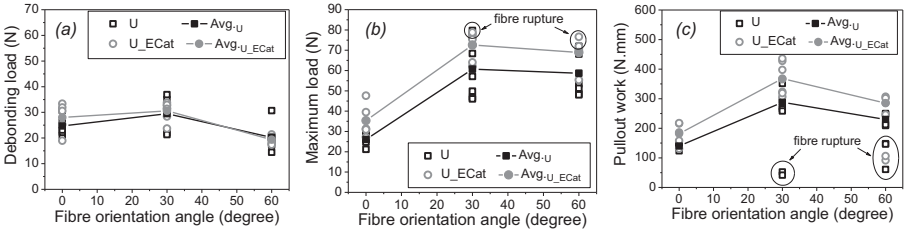

Figure 1: Interfacial bond properties: (a) debonding load, (b) maximum load and (c) pullout work.

Uniaxial tensile behaviour

Figure 2 shows the tensile behaviour of U and U_ECat. The tensile stress at crack initiation is nearly the same for both mixtures. The behaviour is significantly improved by orienting fibres parallel to the loading direction (well-oriented). Due to the variation in the fibre orientation profiles of the randomly oriented specimens, scattering is observed during the post cracking stage. This makes it difficult to compare the tensile fracture parameters without a detailed analysis of the fibre orientation profiles. However, similar fibre orientation profiles are expected within the well-oriented series. The analysis of the post cracking parameters of the well-oriented series reveals that post-cracking tensile strength, f_{Utu}, slightly increased from 14.9 MPa to 16.1 MPa, while strain at the onset of crack localization reduced from 0.0047 to 0.0043 for U to U_ECat mixtures, respectively. In the next stage, image analysis will be performed on each specimen to determine the fibre structure parameter and then correlate it to the tensile fracture parameters, as discussed in reference [2].

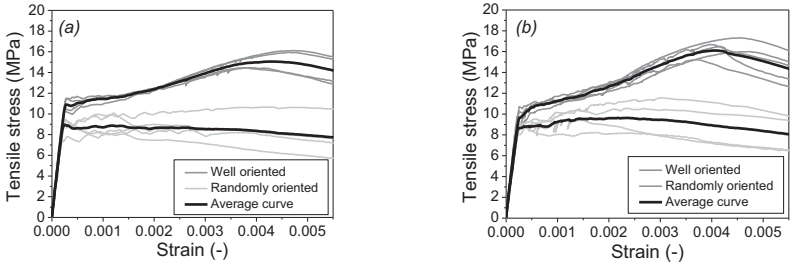

Figure 2: Uniaxial tensile behaviour: (a) U and (b) U_ECat.

4 Conclusions

Marginal differences between the tensile behaviour of UHPFRC and UHPFRC_ECat in meso- and macro-scale were observed. This seems to confirm the adequate performance of the new UHPFRC_ECat mixture for structural applications.

References

[1] Matos, A.M; Nunes, S.; Costa, C.; Barroso-Aguiar.: Spent equilibrium catalyst as internal curing agent in UHPFRC. *Cement and Concrete Composites* 104, 103362, 2019.

[2] Abrishambaf, A.; Pimentel, M.; Sunes, S.: A meso-mechanical model to simulate the tensile behaviour of ultra-high performance fibre-reinforced cementitious composites. *Composite Structures* 222, 110911, 2019.

About the biaxial flexural strength, the size effect and the correlation with uniaxial mechanical properties of UHPC

Milan Schultz-Cornelius, Matthias Pahn
Institute of Concrete Structures and Structural Engineering, Technische Universität Kaiserslautern, Germany

1 Introduction

The biaxial flexural strength of unreinforced concrete structures is hardly investigated because of a former lack of applications. Nowadays the applications, where a biaxial resistance is needed, increase. There are for example single unreinforced foundations, temporary shotcrete applications in tunnels and point supported slabs as facades. While the knowledge for normal strength concrete is already developed [1,2,3], nearly nothing is known for Ultra High Performance Concrete (UHPC). This applies especially to test methods as well as the scale effect. The uni- and biaxial flexural strength of concrete structures depends on the centric uni- and biaxial tensile strength and the height of the structure. An increasing height causes a decreasing of flexural tensile strength which reduces the tensile strength. The size effect on uniaxial tensile strength and uni- and biaxial flexural tensile strength of UHPC has been investigated at TU Kaiserslautern. The aim of the experimental series was to investigate and increase the knowledge on biaxial flexural strength, the size effect and to enable the calculation of the biaxial flexural tensile strength of any thin structural component on the basis of the test results of a standard prism-shaped specimen with a standardized height of 40 mm to be used it for structural design.

2 Experimental investigations

Geometry and production of the specimens

For the testing of the uniaxial bending tensile strength prisms and for the tensile strength, dog bone shaped tensile test samples were produced where the component height h varies. The dimensions of the specimens were based on [4,5]. Circular discs were used as supports for biaxial flexure tensile tests with a ratio of component thickness to diameter from approximately 1/10, which are also used for normal concrete [2] and natural stone [6]. After concreting, the specimens were wetted and covered with foil. After one day, the formwork was removed and the specimen were stored wet for 28 days, then stored dry for three days at 20°C until testing.

Results

With a decreasing depth from 50 mm to 15 mm an increase in mechanical tensile strength could be observed in all tests. In numbers an increase by 39 % for uniaxial tensile strength f_{ct} by 70 % for uniaxial flexural strength $f_{ct,fl,I}$ and by 40 % biaxial flexural strength $f_{ct,fl,II}$ could be determined.

3 Conclusions

In the Figure 1 (left) the calculations based on the existing approaches, which describe the ratio between flexural tensile strength and tensile strength for $h \geq 50$ mm, are mathematically extrapolated for $h < 50$ mm and graphically illustrated. The results of the experiments serve as a reference. The diagram shows an accordance of the experimental results with the calculation approach of DAfStb Heft 444 [7]. from depths between of 40 mm and up to the results. The high accuracy of the calculations with the help of this approach can be observed for $h \geq 40$ mm up to the tested depth range. According to [7] the ratio should grow non-linearly for depths of $h \leq 35$ mm, however the experimental results show an approximately linear relation. This linear correlation shows an increase similar to the approach of the Eurocode [8]. In order to enable

the conversion between flexural tensile strength and tensile strength for thin structural elements a theoretical formulation for depths h ≤ 35 mm is derived:

$$\frac{f_{ct}}{f_{ct,fl,I}} = \frac{1}{2{,}12 - \frac{h}{2100}} \qquad (1)$$

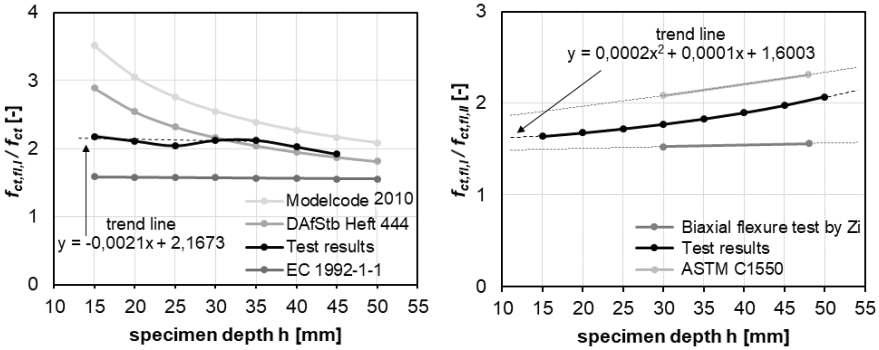

Figure 1: left – uniaxial bending vs tension: Comparison between MC 2010 [9], Heft 444 [7], EC2 [8] and exp. results; right – uniaxial vs biaxial bending: Comparison between Zi [2] and ASTM C1550 [3] and exp. results

In the Figure 1 (right), a good accordance of the test results with the results reported in [2,3] can be seen. The results from [3] show a similar slope as the own test results, while the results from [2] predicts an almost constant ratio between biaxial and uniaxial flexural tensile strength. An empirical calculation model is then derived from the polynomial regression curve shown in Figure 1. The function is converted for $h \leq 55\,mm$ to the following equation:

$$\frac{f_{ct,fl,II}}{f_{ct,fl,I}} = 2 \times 10^{-4}\left(h^2 + \frac{h}{2}\right) + 1{,}6 \qquad (2)$$

Furthermore, by inserting equation (1) into (2) the tensile strength or biaxial flexural strength can be calculated using the other mechanical property determined in a test. The proposed model is valid for UHPC with a largest grain diameter of 8mm.

References

[1] Kim, J.; Kim, D. J.; Zi, G.: Improvement of the biaxial flexure test method for concrete, in: Cement and Concrete Composites 37, 2013.

[2] Zi, G.; Kim, J.; Bažant, Z. P.: Size Effect on Biaxial Flexural Strength of Concrete, in: ACI Materials Journal 111, 2014.

[3] ASTM C1550 C09 Committee: Test Method for Flexural Toughness of Fiber Reinforced Concrete (Using Centrally Loaded Round Panel), West Conshohocken, PA, ASTM International, 2012.

[4] Fehling, E.: Entwicklung, Dauerhaftigkeit und Berechnung ultrahochfester Betone (UHPC), Kassel, Kassel Univ. Press, 2005.

[5] Mühlbauer, C.: Fügen von Bauteilen aus ultrahochfestem Beton (UHPC) durch Verkleben. PhD Thesis, 2012.

[6] Sattler, L.: Untersuchungen zur Wirkung und Dauerhaftigkeit von Sandsteinfestigungen mit Kieselsäureester. Unveröffentlichte DIssertation, Ludwig-Maximilians-Universität München, 1992.

[7] Deutscher Ausschuss für Stahlbeton: Zum Zug- und Schubtragverhalten von Bauteilen aus hochfestem Beton – Heft 444, Berlin, 1994.

[8] Deutsches Institut für Normung: Bemessung und Konstruktion von Stahlbeton- und Spannbetontragwerken – Teil 1-1: Allgemeine Bemessungsregeln und Regeln für den Hochbau – DIN EN 1992-1-1, 2011.

[9] CEB-FIP Model Code 2010: Design Code, 1993.

Ductility of GGBS-based UHPFRC incorporating amorphous metallic fibres: Applying an inverse analysis

Jean Bertrand[1], Anaclet Turatsinze[1], Ahmed Toumi[1], Thierry Vidal[1], Florian Bernard[2], Cédric Boher[3], Eric Buriot[4], Ludovic André[1,5]

1: LMDC, Université de Toulouse, INSA/UPS Génie Civil, Toulouse, France
2: Saint Gobain SEVA, Chalon-sur-Saône, France
3: Orano Temis - Activité Béton, Valognes, France
4: ERI-PBHP, Escassefort, France
5: Ecocem Materials Ltd, Paris, France

1 Research significance

The poor residual post-cracking strength of ordinary cement-based materials is substantially enhanced by a fibre-reinforcement [1]. At first glance, processing data collected from uniaxial direct tensile tests controlled by crack mouth opening displacement appears to be the most straightforward way to assess the tensile post-cracking behaviour of Fibre-Reinforced Concrete (FRC) and thus determine the ductility provided by fibre addition. However, carrying out uniaxial tensile tests (UTTs) on a concrete-based composite is a challenge for most laboratories, mainly due to the difficulty to attach properly the specimen to the platens of the testing machine [2].

Thus, and with the aim to facilitate the design of Ultra-High Performance Fibre-Reinforced Concrete (UHPFRC), the recent French standard NF P18-470 [3] allows the post-cracking behaviour of such materials to be assessed by applying an inverse analysis using data derived from three-point and four-point bending tests. More details on the implementation of this method are given in [4].

This study investigates the relevance of the NF P18-470 [3] inverse method applied to a UHPFRC incorporating Ground Granulated Blast-Furnace Slag (GGBS) as ultrafine and reinforced by Amorphous Metallic Fibres (AMFs).

2 Raw materials and methods

Raw materials

The granular spectrum of the mix is optimised by applying the Andreasen & Andersen packing method [5]. The GGBS-to-cement ratio is 1.50, the polycarboxylate-based superplasticizer-to-binder ratio is 1.6% and the efficient water-to-binder ratio is 0.19. AMFs are used at 1.5% by concrete volume.

Compared to conventional metallic fibres, due to their chromium content as well as to an isotropic atomic organisation, AMFs exhibit higher corrosion resistance and resistance to aggressive environments. They are consequently most suitable for sanitation networks, road buffers, sealing mortars, technical slabs, prefabricated products such as nuclear waste containers, etc.

Regarding UHPFRC binder design, the choice of GGBS as a total substitute for the most commonly used ultrafine, i.e. silica fume, is aimed to secure steady raw material supplies over time.

Methods

Uniaxial tensile tests are carried out on 70x70x140 mm^3 prisms notched at mid-height, while bending tests are conducted on 70x70x280 mm^3 prisms. All tests are carried out on specimens after 28 days of curing (20°C and 95% RH).

The ductility is assessed from tensile stress-Crack Mouth Opening Displacement (CMOD) curve, and the UHPFRCs covered by NF P18-470 [3] must satisfy the following inequality:

$$\frac{1}{w_{0.3}}\int_0^{w_{0.3}}\frac{\sigma_f(w)}{1.25}dw \quad \geq \quad \max\ (0.4\cdot f_{ctm,el}\ ;\ 3\ MPa) \qquad (1)$$

where w is the CMOD, $\sigma_f(w)$ the post-cracking stress in MPa, $w_{0.3}$ the upper limit of CMOD, i.e. 0.3 mm, and $f_{ctm,el}$ the mean value of the limit of elasticity under tension in MPa.

3 Results

For the record, the compressive strengths of the composite measured on 7x7x7 cm^3 cubes and on cylinders of 11 cm in diameter and of 22 cm in height are of 140 and 115 MPa respectively.

The experimental tensile stress vs. CMOD curve and the one derived from bending tests using inverse analysis are shown in Fig. 1. The values of the tensile limit of elasticity and of the ductility are given in Table 1.

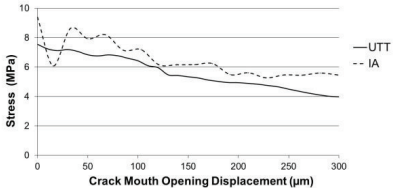

Figure 1: Tensile stress-CMOD curve from uniaxial tensile tests (UTT) and the one derived from bending tests using inverse analysis (IA).

Table 1: Mechanical properties of the UHPFRC.

		Tensile limit of elasticity	Ductility
Uniaxial tensile test	MPa	7.6	4.4
Bending test	MPa	9.4	5.4
Required value according to NF P18-470 [3]	**MPa**	**6**	**3.8**

4 Conclusions

This study compares two methods of post-cracking behaviour assessment of UHPFRCs: implementation of uniaxial tensile tests and an inverse analysis applied to the data from bending tests according to NF P18-470 [3].

The tensile stress-CMOD curves obtained from both methods are quite similar. However, it is found that the curve obtained by inverse analysis yields higher values both for the tensile limit of elasticity and for ductility. With regard to post-cracking, results also show that GGBS-based UHPFRC reinforced with 1.5 vol.% AMF complies with NF P18-470 [3].

References

[1] Brandt, A.: Fibre reinforced cement-based (FRC) composites after 40 years of development in building and civil engineering. Composite Structures 86, p. 3-9, 2008.

[2] Hordijk D.A., Reinhardt H.W.: Fracture of concrete in uniaxial tensile experiments as influenced by curing conditions. Engineering Fracture Mechanics 35, p. 819-826, 1990.

[3] AFNOR. NF P18-470 standard: Bétons – Bétons fibrés à Ultra Hautes Performances – Spécification, performance, production et conformité. Concrete - Ultra-high performance fibre-reinforced concrete - Specifications, performance, production and conformity, 2016.

[4] Bertrand J., Turatsinze A., Toumi A., Bernard F.: Design of a UHPFRC using amorphous metallic fibres. Proc. International Conference on UHPFRC, Montpellier 2017.

[5] Andreasen A.H.M., Andersen J.: Ueber die Beziehung zwischen Kornabstufung und Zwischenraum in Produkten aus losen Körnern (mit einigen Experimenten). Kolloid-Zeitschrift 50, p. 217–228, 1929.

Pedestrian bridge of UNAL in Manizales: A new UPHFRC application in the Colombian building market

Joaquín Abellán[1,2], Andrés Núñez[3], Samuel Arango[3]

1: Ph.D. Candidate, Department of Civil Engineering, Polytechnic University of Madrid (UPM), Madrid, Spain.
2: Department of Construction, Escuela Colombiana de Ingeniería Julio Garavito, Bogotá, Colombia.
3: Cementos Argos SA, Medellín, Colombia.

1 Introduction

To break into a new consolidated market with a new product is a challenge even for those products like ultra-high-performance concrete (UHPC) which has proven its worth outside the borders of Colombia. Even more so if this product does not have a local regulation that endorses it, as is the case of UHPC. That is why local developments, both dosages, and applications, are of vital importance. In this sense, it is important to highlight the execution of the pedestrian bridge in the National University of Colombia in Manizales (Colombia), connecting different educational areas within the institution, using Advanced Concrete ®, a UHPC proprietary formulation using local materials developed by the company Argos SA.

The pedestrian bridge is part of a new building at the Nacional University campus. The footbridge is composed of 14 UHPC premanufactured segments joined by non-adherent post-tensioning. Each keystone has a 3-ton weight. The total length of the structure is 26 m containing two 13 m spans.

Initially, the design involved a metallic structure, however, Argos proposed to the University to change the steel for Advanced Concrete ®. The decision to opt for this material represented a saving of 33% of the total cost of the work.

2 Pedestrian Bridge Architectural and Structural Design

The architectural design is inspired by a fish skeleton. The structural system of the footbridge is composed of the main girder with a plug-socket joint system. 3 post-tensioned cables were used to get the 14 segments together. The compressive strength of the segments exceeded the 150 MPa, while foundations were poured on-site using regular f'_c=50MPa concrete. Three columns were disposed to support the main structure. The cross-section and the structural conception of the UNAL pedestrian bridge are depicted in Fig.1.

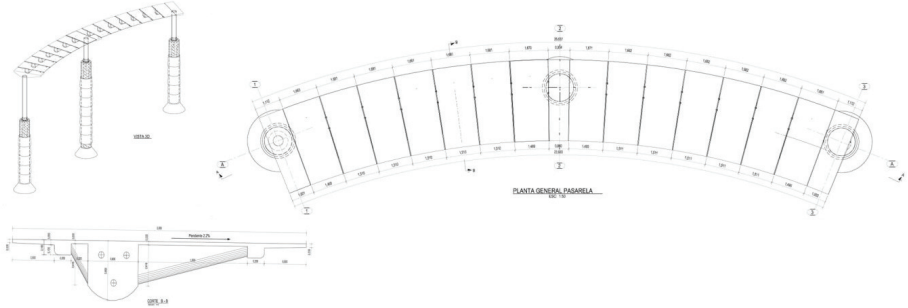

Figure 1: Cross-section and the structural conception of the UNAL pedestrian bridge.

3 Construction of the Keystones

Starting in July 2018, the construction of 14 keystones using Advanced Concrete ® was performed at Bieton field office in Medellín, Colombia. Pre-mixed UHPC was delivered through

the concrete batch plant. In order to improve the packing density of concrete, a slight vibration was applied to the mold during the pouring, prolonging it until one minute after completed. Several steps of the construction of the keystones are shown in Fig. 2.

Figure 2: Different stages of the keystone construction at Bieton field office in Medellín (Colombia).

4 Pedestrian Bridge Installation

On November 1, all 14 keystones were installed at the National University of Colombia in Manizales. At the Bieton field shop in Medellín, the 14 keystones were delivered using five semi-trucks (with a maximum load of three keystones each truck). At the pedestrian bridge site, the keystones were moved by crane. Once the keystones were in position, joints were realized with field-cast UHPC. After that, the post-tensioning process was performed, creating a continuous girder.

5 Conclusions

Material mechanical properties of UHPC makes possible the development of new infrastructure such as the UNAL pedestrian bridge in Manizales (Colombia) under four main objectives: fast construction, minimal affectation to concomitant uses, building long-lasting facilities with low maintenance cost (thanks to high durability) and building cost reduction compared to other alternatives of less efficient materials. Furthermore, this paper shows good practices, large applications of UHPC and attractive potential market in Colombia.

Acknowledgments

Authors want to acknowledge R&D division of Cementos ARGOS SA, BIETON Concrete + Design, Mario Barbosa engineers S.A.S, Escuela Colombiana de Ingeniería Julio Garavito, and UNAL Manizales University for bringing us the confidence, support, and opportunity to launch special concretes like UHPC in Colombia.

References

[1] Abellan, J.; Torres, N.; Núñez, A.; Fernández, J.: Ultra high preformance fiber reinforced concrete: state of the art, applications and possibilities into the latin american market. In XXXVIII Jornadas Sudamericanas de Ingeniería Estructural. Lima, Peru. 2018

[2] Blaise, P.Y.; Couture, M.: Precast, Prestressed Pedestrian Bridge—World's First Reactive Powder Concrete Structure, PCI Journal, Vol. 44, No. 5, September/ October 1999, pp. 60–71.

[3] Graybeal, B.; Stone, B.: Compression Response of a Rapid-Strengthening Ultra-High Performance Concrete Formulation, FHWA, U.S. Department of Transportation, Report No. FHWA-HRT-12-065, National Technical Information Service Accession No. PB2012-112545, 2012.

[4] Iowa Department of Transportation, "Special Provisions for Ultra High Performance Concrete," SP-090112a, Effective Date, February 15, 2011, Available at http://www.iowadot.gov/us6kegcreek/documents/SP-concrete.pdf [Cited May 29, 2012].

First UHPC pedestrian bridge in Belgium

Julie Piérard[1], Niki Cauberg[1], Pieter van der Zee[2]
1: Belgian Building Research Institute (BBRI), Limelette, Belgium.
2: Ergon / CRH Structural Concrete, Lier, Belgium.

1 Introduction

Ultra-high Performance Concrete (UHPC) is an advanced cementitious material that is attracting attention in the construction industry due to its exceptionally high strength and durability, leading to structures having low maintenance requirements. In the last few years, research works on the mix design of fibre reinforced UHPC using local materials have been conducted in Belgium. Consequently, reflections were held to promote the use of this concrete in specific applications. This led to the design and construction of the first Belgian precast bicycle/pedestrian bridge made of UHPC in cooperation with Infrabel, the Belgian railway infrastructure manager.

2 Previous research works

During previous research works, a UHPC mix has been optimized using local aggregates. The average mix proportions are given in Table 1. The 100 mm cube compressive strength at 28 days is about 160 MPa.

Table 1: UHPC mix

		UHPC mix
Quartz sand 0/0.5 mm	kg/m³	335
Quartz powder (d_{50} = 12 µm)	kg/m³	83
Porphyry 2/4 mm	kg/m³	723
CEM I 42.5 R HSR LA	kg/m³	830
Silica fume (slurry – 50% water)	kg/m³	332
Mixing water	kg/m³	12
Superplasticizer (polycarboxylate con. 30%)	kg/m³	up to 24
Steel fibres (6 and 30 mm length)	vol.%	up to 2
(water/cement)-ratio	-	0.23
(water/binder)-ratio	-	0.20

Up to 2 vol.% (i.e. 156 kg/m³) steel fibres of 6 mm and 30 mm length are added to the mix to enhance the load carrying capacity and ductility of the concrete. Silica fume slurry and quartz powder are used to densify the matrix. The addition of high dosages of polycarboxylate based superplasticizer ensures a suitable fluidity, close to that of a self-compacting concrete (slump-flow around 700-800 mm, as measured according to EN 12350-8).

Lab experiments at the BBRI showed among others that this UHPC mix has an excellent resistance to carbonation, to freezing and thawing, to alkali-silica reaction and against ingress of aggressive substances such as chloride ions and sulphates [1]. These results are in good agreement with other studies and existing recommendations [2].

In a second stage, the industrial feasibility of this type of concrete was evaluated by the production and experimental investigation of 7 m long prestressed I-girders [3][4]. Thanks to the sustained post-cracking tensile capacity of UHPC, the moment capacity of the tested girders was approximately 750 kNm.

3 Pedestrian bridge

Based on these previous results, a UHPC footbridge was designed to cross a 2-track railway line in Brussels. This new one was installed in December 2018 and replaces the first Belgian prestressed footbridge built in the 50's. It consists of a thin slab (10 cm thick) of 36 m long and 4 m wide, supported by two slender ribs (see Fig.1). The choice of the UHPC was made in regards of the lightness (weight reduced by half compared to C50/60 option), limited access for erection and extended lifespan.

In this mix, 1 vol.-% steel fibres were used. The concrete element was steam treated to accelerate the strength development, limit the residual shrinkage and reduce even more the porosity of the concrete.

The calculations were verified by full-scale loading tests (500 to 750 kg/m²) using water-filled containers.

Figure 1: UHPC pedestrian bridge in Brussels (left: production; right: final realisation)

4 Conclusion

In Belgium, UHPC so far has been used exclusively in applications such as street furniture or local repair works. This first experience of a civil engineering work in UHPC is a great success and should give rise in the future to other applications in the same vein.

5 Acknowledgements

The authors gratefully acknowledge the Flanders Agency for Innovation for the financial support during the research works, as well as Infrabel, the project owner of the UHPC footbridge.

References

[1] Piérard, J.; Dooms, B.; Cauberg N.; Durability Evaluation of Different Types of UHPC. Proceedings of the International RILEM-*fib*-AFGC Symposium on Ultra-High Performance Fibre-Reinforced Concrete (UHPFRC 2013), Marseille, France, 1-3 October 2013.

[2] Ultra-High Performance Fibre-Reinforced Concrete: Recommendations. AFGC, France, Revised edition, June 2013.

[3] Tronci, C.; Cauberg, N.; Piérard, J.; Van Der Zee, P.; Case Study Ultra-High Performance Concrete. Prestressed I-Girders: Part I – Material Characterization. CPI – Concrete Plant International, Issue 5, 2013.

[4] Tronci, C.; Cauberg, N.; Piérard, J.; Van Der Zee, P.; Case Study Ultra-High Performance Concrete. Prestressed I-Girders: Part II – Fabrication and testing. CPI – Concrete Plant International, Issue 6, 2015.

New UHPFRC footbridges in Czech Republic

David Citek[1], Jiri Kolisko[1], Petr Tej[1], Martin Kryštov[1], Adam Citek[1], Jan Marek[2]
1: Klokner Institute, Czech Technical University, Prague, Czech Republic
2: KS Prefa s.r.o., Prague, Czech Republic

1 Introduction

UHPC, Ultra High Performance Concrete, usually reinforced with steel (usually high strength) or polyolefin fibres (PP, PA or PVA), is therefore better named as UHPFRC, (Ultra High Performance Fibre Reinforced Concrete). It is a modern material based on principles similar to normal strength concrete (NSC), but applied in the smaller scale, characterized by its material optimization: fine-grained sand, silica fume, fibres, Portland cement with no large aggregates.

The used mixture was finally developed in 2017 after several years of research and applied tests in cooperation of KŠ PREFA company and Klokner institute of CTU. The exact design of the mixture cannot be published, but it is quite similar to standard UHPC mixtures as described above. There are no valid (or validated by legislative) normative standards in the Czech Republic concerning UHPC, except three methodical manuals published in 2015 by Klokner institute.

2 UHPFRC bridges

2.1 Footbridge over the Lubina river in city Příbor

The load bearing structure of the footbridge is a single span prismatic rectangular beam. A span of almost 36 meters and the height of cross section 800 mm declares boldness of structural engineer working with concrete and the ratio 1:45 fulfils the requirement of the architect. The structure itself is made of 5 elements connected by post tensioned monostrand cables, injected in three channels with parabolic shape. Connections of the elements were sealed by epoxy mortar, four channels were used special waterproof connectors. The casting of the elements was preceded by tests of testing elements. At first, elements with volume of 1.0 and 2.0 m^3 were tested for development of hydratation heat. After that, two elements, each in half volume of a typical element, were casted simultaneously as a test of batching, casting and test of the mould. In that moment it was the largest UHPFRC casting in CR of all the time. These elements were used for sealing, cable tensioning test and testing of the handrail anchoring.

2.2. Pedestrian and cycle bridge in the vicinity of Black Bridges in city Tábor

The presented footbridge creates an essential part of a complex of pavements and bike paths over the Budějovická street and its access roads in densely built-up part of the city Tábor. The footbridge is parallel to the steel railway bridge, in the vicinity ca 1.1 m. Load bearing structure is single span Pi - beam, with height of 0.94 m, width 3.0 m and length of 27.0 m; prefabricated as one prestressed element consisting of 12 m^3 UHPFRC. Bridge deck with thickness of 60 mm is reinforced only by ribs in the distance 1000 mm. Steel rebars are not used in the deck itself. Structure is designed according to EN 1991-2 and methodical manual for designing of UHPC structures by Klokner institute of CTU, 2015, uniform load caused by crowd of people of 5 kN/m^2, single load of service vehicle of total weight 3.5 t with dynamic coefficient $\delta = 1.10$ and special vehicle of 12 t. UHPFRC casting in one step for one element with volume of 12 m^3 is unique in Europe. After casting elements for the footbridge in Příbor, gained experience allowed to cast whole load bearing beam for the footbridge in Tábor in one 2-hour long work. Detailed preparation, comprehensive planning and on scale testing established the casting process without any pause, which was essential to avoid cold joints and to achieve optimal scatter of steel fibres, flawless surface and unexceptionable serviceability and durability of the finished UHPFRC element. One of the largest UHPFRC element poured in one take in Europe was successfully created, assembled and put in use by the public.

2.3 Footbridge over Dřetovice stream in Vrapice - city part of Kladno

Single span footbridge with unique U-shaped cross section leaps over the stream in two arches, vertically and horizontally. Beam with its length of 10.5 m, thickness of the walls 40 mm, thickness of the deck from 45 to 55 mm, without any steel rebars or prestressing cables, made of this experimental structure unique footbridge in the world. Volume of used UHPFRC ca 1.6 m^3 was casted in specially designed mould twice, first attempt was success in casting but unsuccessful in load testing of the whole bridge element. Second attempt was casted with thicker walls and modified geometry of wall-deck connection. The second bridge beam successfully accomplished load testing and was assembled in place over the stream.

2.4 Bridges over the railway tracks in city Přerov

Both bridges are over the railway track Přerov – Bohumín and Česká Třebová – Přerov. General constructor, Strabag, was recovering old steel loadbearing structures of both bridges with new one. Support structures were repaired. Bridge deck was casted over the steel crossbeams with NSC, but as the lost formwork were used thin UHPFRC slabs, both inside between the main steel girder and outside as sidewalk deck. Thickness of the NSC deck varied from 220 to 400 mm. UHPFRC slabs with a thickness of 60 mm covered the distance between steel crossbeams with a span of ca 1.7 m. For the sidewalk part the NSC deck was 190 mm thick and the UHPFRC slab was 50 mm thick. Lost formwork for bridge cornices were 1900x600 mm and 50 mm thick. Before casting the thin slabs, the initial testing of the early age elements had to be performed. The early loading of the slabs is the reason for a different control testing schedule, where had to be proved enough safety of 7-day old slabs.

Fig.1 – 3: Footbridges in Příbor, Tábor and Vrapice (left to right)

3 Conclusions

Four modern bridge constructions from UHPFRC were successfully designed and built in the Czech Republic in the last two years. More and more knowledge of this modern material is used in transport infrastructure same as in civil engineer structures nowadays. At this momet new projects using UHPFRC are under construction in the Czech Republic.

4 Acknowledgements

The support of the project GACR 17-22796S was gratefully acknowledged.

References

[1] Kalny, M., Komanec, J., Kvasnicka, V., Fiala, C., “Experience with UHPFRC applications in the Czech Republic”, UHPFRC 2017, Montpellier, France.
[2] Vítek, J. L., Coufal, R., Čítek, D.: UHPC - Development and Testing on Structural Elements. Concrete and Concrete Structures 2013, Žilina, 2013, University of Žilina, pp. 218-223.
[3] Abbas, S., Nehdi, M.L., Saleem, M.A.: Ultra – High Performance Concrete: Mechanical Performance, Durability, Sustainability and Implementation Challenges, International Journal of Concrete Structures and Materials, Vol.10, No.3, pp. 271-295, September 2016.
[4] Kolísko,J.- Čítek,D.- Tej,P.: Technologie výrobytenkostěnné obloukové dvojitězakřivené lávky z UHPFRC - 14. konference TECHNOLOGIE 2017, Jihlava, Sborník přednášek Česká betonářská společnost ČSSI, ISBN 978-80-906097-9-2.
[5] Kolísko, J.; Čítek, D.; Tej, P.; Rydval, M. Production of Footbridge with Double Curvature Made of UHPC In: Fibre Concrete 2017., Bristol: IOP Publishing Ltd, 2017. IOP Conference Series: Materials Science and Engineering. vol. 246. ISSN 1757-899X.

Analysis of the behaviour of bridge piers retrofitted with UHPFRC jackets

Renaud Franssen[1,2], Mathias Langer[2], Luc Courard[2], Boyan Mihaylov[2]
1: FRIA (F.R.S.-F.N.R.S), National Fund for Scientific Research, Brussels, Belgium
2: ArGEnCo Department, Research Unit in Urban and Environmental Engineering, University of Liège, Allée de la Découverte 9, Liège (4000), Belgium

1 Introduction

This project focuses on a durable rehabilitation and strengthening method of wall-type bridge piers. This method consists in the jacketing of the bottom part of the piers where deterioration typically occurs.

Bridge piers are exposed to de-icing salts, water projection, carbon dioxide, and other aggressive environment. Therefore, they can suffer high degradation involving concrete spalling and corrosion of the reinforcement. The corrosion of the transverse reinforcement can in turn lead to a lack of shear resistance and susceptibility to brittle failures. In order to solve both corrosion and shear resistance issues, a jacket of ultra-high performance fibre-reinforced concrete (UHPFRC) is applied on the bottom part of the pier.

2 Experimental campaign

In order to prove the effectiveness of this retrofitting method, an experimental campaign was carried out at the University of Liège. As shown in Fig. 1, four large-scale walls were built and tested to failure in the structural laboratory.

The variables of the tests are presented in Table 1. The reference specimen (M0) only consisted of reinforced concrete (RC) with a relatively low amount of stirrups, and therefore it was susceptible to brittle shear failure. The other specimens featured the same amount of stirrups, but they were retrofitted with an UHPFRC jacket of variable thickness.

Table 1: Variables

Wall name	Thickness of UHPFRC (mm)	Surface preparation	Vertical load, N (kN)	$N/(A_g f'_c)$ (%)
M0	0	/	1200	6.7
M30S	30	Smooth	1200	6.6
M30W	30	Water jetting	1200	7.5
M50W	50	Water jetting	2200	14.0

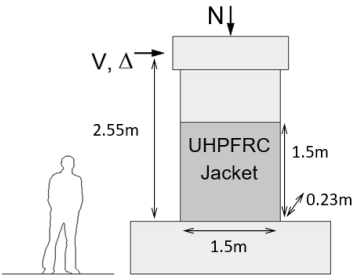

Fig. 1 Description of specimens

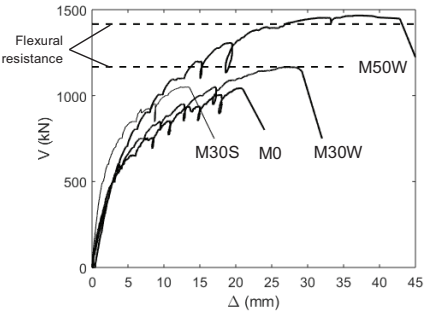

Fig. 2 Behaviour of walls

3 Behaviour of walls

The main results from the tests are presented in Fig. 2 in terms of shear force vs. top lateral displacement. As expected, the reference wall M0 failed in shear in a very brittle manner.

The behaviour of walls M30S and M30W demonstrated the effect of UHPFRC jacketing with 30mm thickness. These tests revealed that the effectiveness of the strengthening method depends very much on the surface preparation. When UHPFRC is applied on a smooth surface as in wall M30S, debonding develops and the two materials (RC and UHPFRC) stop working together. On the other hand, UHPFRC cast on a rough surface enhances significantly the performance as evident from wall M30W. The longitudinal reinforcement yielded before failure and thus wall M30W reached its flexural resistance. Curve M30W shows larger strength and displacement capacity as compared to curves M0 and M30S.

Because the UHPFRC jacket on wall M30W was sufficient to reach the flexural capacity, it was decided to increase the axial load on wall M50W, and in this way to tests whether the 50mm jacket will be sufficient to reach the flexural capacity again. Indeed, as evident from Fig. 2, wall M50W exhibited flexural yielding, large displacement capacity and enhanced ductility.

4 Digital Image Correlation (DIC) measurements

The DIC techniques was used to measure the complete displacement field of the walls. The DIC allowed to obtain the principal tensile strains in the wall, and in this way to trace the cracks as shown in Fig 3. Additionally, the kinematics of the main diagonal cracks was measured in terms of opening and slip displacements as illustrated in Fig 4. These results will be used to validate and extend a kinematics-based modelling approach for the behaviour of shear walls [1]. It is the final objective of this research to adapt this model to UHPFRC-jacketed piers.

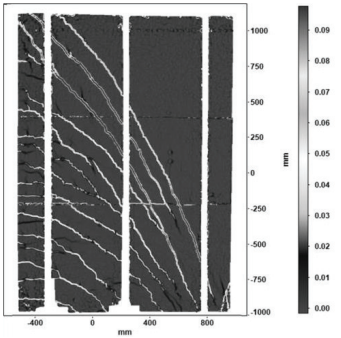

Fig. 3 Principal maximal strains at peak (Wall M0)

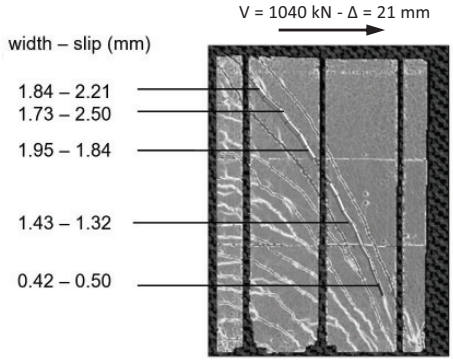

Fig. 4 Measurement of cracks at peak (Wall M0)

5 Conclusion

This paper presented results from an experimental study on the UHPFRC jacketing of RC wall-type bridge piers. The study demonstrated the effectiveness of the method when applied to a well-prepared concrete surface. Insight into the behaviour of the walls was provided by detailed DIC measurements which will be used to develop a kinematics-based modelling approach.

References

[1] Mihaylov, B. I.; Hannewald, P.; Beyer, K.: Three-parameter kinematic theory for shear-dominated reinforced concrete walls. *Journal of Structural Engineering*, *142*(7), 2016.

Composite UHPC facade elements with self-cleaning surface: Aspects of technological manufacturing

Julia von Werder[1], Serdar Bilgin[2], Johannes Hoppe[1], Patrick Fontana[3], Birgit Meng[1]
1: Bundesanstalt für Materialforschung und -prüfung, Fachbereich 7.1, Baustoffe, Berlin, Germany
2: Deutscher Beton- und Bautechnik-Verein E.V., Berlin, Germany
3: RISE Research Institutes of Sweden, Division Built Environment, Stockholm, Sweden

1 Materials and Methods

Introduction

In the framework of the European collaborative project H-House (grant agreement no. 608893) self-supporting façade panels were developed as composite elements made of ultra-high-performance concrete (UHPC) and autoclaved aerated concrete (AAC). On the elements the self-cleaning properties of the exposed concrete surfaces are achieved through imprinting a microstructure and adding chemical agents on the formwork directly in the casting process [1].

Test Series

Within series of tests, starting with small specimens of 10 x 10 cm² and ending with full-scale prototypes of 500 x 300 cm², the manufacturing technology was continuously refined. The mixture used was based on the Nanodur® fine mix. It was designed to reach a minimum compressive strength of 100 N/mm² [2] and allows to accurately shape very fine structured concrete surfaces.

In a first step, different textural moulds were manufactured and analyzed. To imprint the microstructure on the formwork, an acrylic glass sheet was covered with a textile sheet, and the freshly mixed melted polymer mass poured into a PVC frame (Figure 1a and b). After hardening, the polymer mat was reversed, cleaned and further used as a textural mould for the concreting of specimens (Figure 1c). In some tests a hydrophobic or releasing agent was applied to the microstructured substrate 20 minutes before concreting. The quality and durability of the microstructured concrete surface and the formwork substrate were assessed over the course of ten consecutive concrete casts into the same formwork by measurements of roughness, hydrophobicity, lightness and porosity. By concreting larger specimens of 160 x 60 cm² in size (Figure 1d), the impact of the amount and dilution with water of the hydrophobing agent as well as its flow behavior and the way of application (spray or brush) on the hydrophobicity of the concrete surface was assessed. For this purpose, 11 cores were drilled out at different positions of the element and the water contact angle and the roll-off angle, i.e. the minimum inclination angle necessary for the water droplet to roll off the surface, were measured.

2 Results

The best results in terms of hydrophobicity were achieved for a substrate of polyurethane rubber (PU), to which 80 g/m² of hydrophobing agent based on silane and siloxane were applied, before the concreting. The polymer mats showed an excellent stability over the course of ten concrete casts. The produced concrete specimens exhibited consistent superhydrophobic and self-cleaning properties, which are characterized by contact angles about 140° and roll-off angles around 10° respectively (Table 1). The lightness measured in % referring to a white surface as well as the root mean squared roughness of the surface did not show significant changes. The proportion of pores measured was always below 0,9 % of the surface area assessed, so that the requirements for architectural concrete class 3 [3] are fulfilled.

When concreting the larger specimens, the best results were achieved if the lowest amount of hydrophobing agent (80 g/m²) was applied undiluted with a roller-brush. When compared to the values measured at all the other positions along the specimen the contact angle measured below the position of the pouring funnel was slightly reduced, but it was still higher than 140°. Correspondingly, the roll-off angle measured below the position of the pouring funnel was slightly increased to 16 °. A high dosing of hydrophobing agent lead to bleeding of the material at the corners causing visual and mechanical defects. Based on the results of the preliminary studies the full-scale prototypes were successfully produced in a concrete pre-cast factory.

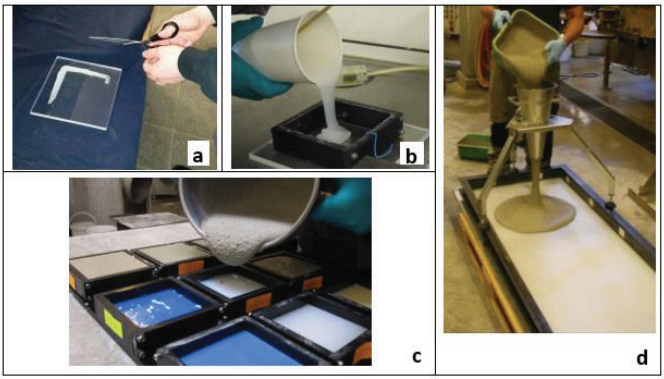

Figure 1: Sample preparation. a) microstructured textile sheet, b) pouring of polymer into the textile mould, c) pouring of concrete into the textural moulds, d) concreting of large specimen.

Table 1: Parameters evaluated for substrate (PU) and UHPC over 10 consecutive pours.

parameter	unit	Time step / Component							
		initial state		after 1st concreting		after 5th concreting		after 10th concreting	
		substrate	UHPC	substrate	UHPC	substrate	UHPC	substrate	UHPC
surface roughness	µm	19.4	n/a	17.6	25.0	19.4	25.3	20.7	21.5
contact angle	°	104.2	n/a	114.3	139.8	126.0	142.9	117.4	138.9
roll-off angle	°	n/a	n/a	n/a	8.0	n/a	10.8	n/a	9.2
lightness	%	n/a	n/a	n/a	64.5	n/a	62.9	n/a	64.8
porosity	%	n/a	n/a	n/a	0.76	n/a	0.01	n/a	0.02

3 Conclusions

The upscaling process for the manufacturing of microtextured self-cleaning UHPC using textural moulds showed that low dosages of the hydrophobing agent, applied on the surface of the formwork directly before concrete cast, lead to satisfying results in terms of hydrophobicity and homogeneity of the UHPC surface.

References

[1] Fontana, P.; Miccoli, L.; Kocadag, R.; Silva. N.; Qvaeschning, D.; Kreft, O.; Cederqvist, C.: Composite UHPC façade elements with functional surfaces, Proc. 4th International Symposium on UHPC and High Performance Materials – HiPerMat, Kassel, Germany, 2016

[2] Deuse, T.; Mutke, S.; Parker, F.; Qvaeschning, D.; Wulff, M.: Nanotechnically optimized binders for the production of user-friendly high-performance concrete, Part 1, Cement International, Vol. 16; 1/2018, Part 2, Cement International, Vol. 16; 5/2018

[3] Deutscher Beton- und Bautechnik-Verein E.V. (DBV); Verein Deutscher Zementwerke E.V. (VDZ), Merkblätter, Bauausführung, Sichtbeton Exposed Concrete, 2015.

Properties of electrically cured Ultra-High Performance Fibre Reinforced Concrete (UHPFRC) with carbon nanotubes (CNTs) and its self-sensing capability

Jung Myungjun, Hong Sung-Gul
Department of Architecture & Architectural Engineering, Seoul National University, South Korea

1 Introduction

Herein, electrically cured Ultra-High Performance Fibre Reinforced Concrete (UHPFRC) incorporated with Carbon Nanotubes (CNTs) (UHPFRC-CNT composite) was investigated to provide a compressive strength of ≥ 150 MPa on construction sites as an alternative to steam curing. In addition, the self-sensing capability of the composite was examined for applications in health monitoring.

2 Experimental program

The specimens were composed of a dispersed CNT suspension (50 g of CNTs dispersed in 1 L of water), Type I Portland cement, silica fume, silica powder, silica sand, and steel fibres. 0.24 wt% CNTs were incorporated with the base UHPFRC mixtures instead of water, and two curing methods were applied 24 h after specimen casting: steam curing (SC) at 90 °C for 2 d and electrical curing (EC) at low voltages of 20–23 V using a power supply for 2 d (Table 1). Cubic-shaped specimens with volumes of 50 × 50 × 50 mm^3 were fabricated for the compressive strength test, and two copper plates were embedded into the specimens as electrodes. During the curing and compressive strength tests, changes in the specimen resistance were measured using an LCR meter. The compressive strength was tested in accordance with ASTM C109.

Table 1: Mix proportion and curing conditions of the specimen (weight percent of cement).

Table	w/c	Water	CNT suspension	Cement	Silica fume	Silica powder	Silica sand	Super-plasticizer	Steel fibre	Curing condition
Ref._SC	0.24	0.24	-	1	0.25	0.35	1.1	0.05	0.17	SC
Ref._EC		0.24	-							EC
CNT_SC		-	0.24							SC
CNT_EC		-	0.24							EC

3 Results

Fig. 1 shows the change in temperature and resistance of the specimens during each curing method. For the reference specimen, the resistance was low at approximately 300–400 Ω before curing, but it sharply increased after curing to approximately 15,000 Ω using SC and 2,000 Ω under EC (Fig. 1a and 1b). In particular, the low voltages could not increase the temperature of the specimen to 90 °C because of the high resistance (Fig. 1b). In contrast, for the specimens containing CNTs, the resistance was not significantly changed and ranged from 20 to 40 Ω during curing regardless of the curing method (Fig. 1c and 1c). In addition, only low voltages of 20–23 V increased the temperature of the specimen to approximately 90 °C within 2 h and was maintained during curing.

Fig. 2 shows the compressive strength and fractional change in resistance (FCR) of the UHPFRC-CNT composites. For the specimens containing CNTs, the compressive strength was maintained or slightly improved compared to that of the reference specimen, while the FCR increased significantly at the time of yield.

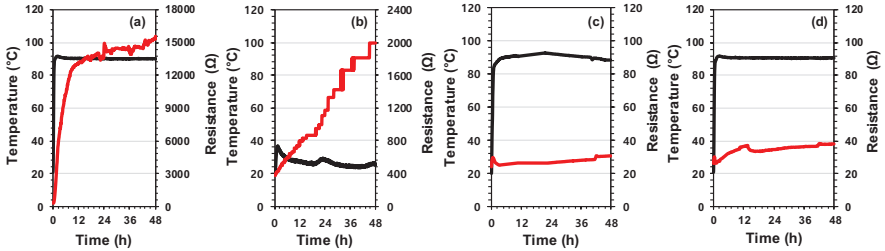

Figure 1: Change in temperature and resistance during curing: (a) Ref._SC, (b) Ref._EC, (c) CNT_SC, and (d) CNT_SC.

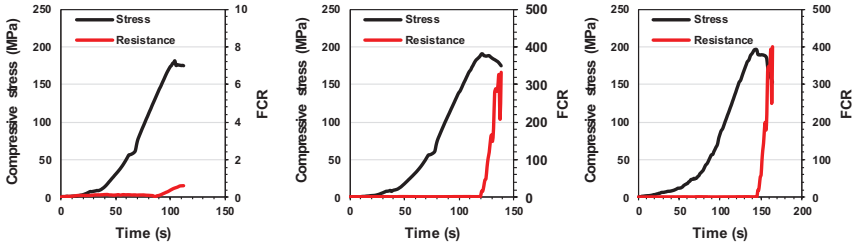

Figure 2 : Compressive strength and fractional change in resistance (FCR): (a) Ref._SC, (b) CNT_SC, (c) CNT_EC.

4 Discussion

For the reference specimen, since the ionic conduction by water was dominant in the resistance of the matrix, the resistance significantly increased due to decreasing water content in a given volume of matrix as hydration progressed. However, for the specimens containing CNTs, because the electronic conduction by CNTs was dominant and the conductive path in the matrix was completely constructed, the resistance remained largely unchanged regardless of curing method and low voltages were sufficient to increase the matrix temperature. In addition, the compressive strength slightly improved owing to the extraordinary mechanical properties of the CNTs and the FCR significantly increased at the time of yield. This was sufficient to identify the structural status as the constructed conductive path in the matrix by CNTs collapsed.

5 Conclusions

CNTs can improve the electrical conductivity of UHPFRC, enabling EC that can produce the same effect as SC at only low voltages of 20–23 V. Using this approach, UHPFRC can exhibit compressive strengths of ≥ 150 MPa on construction sites an alternative to steam curing which is difficult to apply on sites. In addition, UHPFRC-CNT composites can be used as a self-sensor for structural health monitoring.

References

[1] D.D.L. Chung: Carbon Composites (2nd Ed). Butterworth-Heinemann, pp.333-386, 2017.

[2] Jung, M.J.; Lee, Y.S.; Hong, S.G.: Study on Improvement in Electromagnetic Interference Shielding Effectiveness of Ultra-High Performance Concrete (UHPC) / Carbon Nanotube (CNT) Composites. Journal of the Korea Concrete Institute 31(1), pp. 69-77, 2019

Surface treatment of architectural High-Performance Concrete (HPC): Identifying the factors being crucial for successful implementation

Tobias Bader[1,2], Roman Lackner[1,2]

1: Unit of Material Technology, Department of Structural Engineering and Material Sciences, University of Innsbruck, Austria
2. Christian Doppler Laboratory for Performance-Based Optimization of Binder Composition and Concrete Manufacturing, University of Innsbruck, Austria

1 Motivation

The durability and aesthetic qualities of High-Performance Concrete (HPC) in combination with textile reinforcement make this type of concrete particularly suitable for architectural applications (e.g. cladding panels). The growing interest in the use of HPC for architectural purposes demands high-quality surfaces, as the front is essential for the perception of the entire building. However, facades are permanently exposed to weathering (e.g. rainwater runoff) with the impact of weathering (e.g. efflorescence, staining) over time becoming here visible. For the preservation of the aesthetic appearance of architectural HPC against weathering, surface treatment can be applied.

Currently, different types of treatments as well as chemical formulations are available on the market that differ among others with respect to their mode of action (penetrant – film former). However, the random selection and application of surface treatment due to initial cost or appearance considerations can result in early failure. Within this study, a combination of different test methods will be presented, which later allows to elaborate recommendations for the selection and the application of surface treatment in order to avoid misapplication requiring expensive and time consuming maintenance work.

2 Experimental setup

Materials

A high strength fine-grained concrete with textile reinforcement was produced using CEM I 42.5 R, admixtures (silica fume, metakaolin), calcareous aggregates (maximum size 0.8 mm) and a water-binder ratio of 0.33 as well as pigments to achieve a dark colouring (brightness L^* ~ 40). After 28 days of curing, the compressive strength was 110 MPa. The total porosity of the investigated HPC was determined using mercury intrusion porosimetry (MIP) showing an average pore size of 0.013 µm and a total porosity of about 9% [1]. Two supplied formulations were investigated: a water-borne acrylic dispersion with matt finish (film former) and a silane-based cream (penetrant).

Methods

Artificial weathering experiments (alternating cycles of UV light and moisture at elevated temperatures) on surface-treated HPC were conducted with the help of the accelerated weathering tester Q-Lab QUV spray and analysed by direct and indirect methods. The direct methods (scanning electron microscopy, Fourier-transform infrared spectroscopy, X-ray diffraction) give access to the formation of efflorescence and degradation of surface treatment, while the indirect methods (contact angle measurement, colourimetry) allowed the quantification of water-repellent modification and changes in colour of HPC surfaces. Detected changes in colour are expressed by the colour difference (ΔE^*) with changes that are visible with the naked eye amounting to ~ 3.

3 Results and discussion

Both, penetrant and film former led to water-repellent concrete surfaces as observed by contact angles for water > 90°. The application of the penetrant was not appreciable (ΔE^* ~ 0.5), while the application acrylic film was visible with the naked eye (ΔE^* ~ 2.7). The experiments revealed that HPC surface characteristics (low sorptivity) seem to have influenced the performance of the investigated two types of surface treatment. The acrylic film former successfully prevented efflorescence formation by acting as a physical barrier (Fig. 1a), while the penetrant was not able to prevent water from extracting the calcium-bearing constituents most likely due to the small penetration depth of < 0.5 mm (Fig. 1b). This resulted in discolouration of surface-treated HPC due to deposition of granular efflorescence crystals (calcium carbonate polymorph calcite).

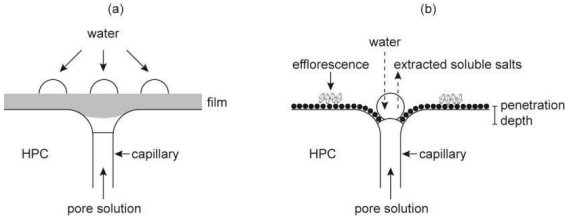

Figure 1: Schematic illustration (not to scale) of (a) efflorescence prevention due to application of film former and (b) efflorescence formation in case of HPC surface treated with penetrant [2].

The artificial weathering experiments revealed that the aesthetic deterioration of HPC surfaces treated with the acrylic film former is characterised by the proceeding opacity of the former transparent films (ΔE^* > 3) and the separation of small pieces of the films from the concrete surface (flaking). The time of occurrence as well as the degree of weathering-induced degradation of acrylic surface treatment was revealed to be influenced by substrate moisture content and application amount.

4 Conclusion and outlook

Acrylic surface treatment can be applied to architectural HPC in order to prevent efflorescence formation. The combination of the employed test methods can be useful for evaluating the performance of other types of surface treatment and formulations in terms of efflorescence prevention and weathering resistance.

Acknowledgements

The financial support by the Austrian Federal Ministry of Science, Research and Economy, the National Foundation for Research, Technology and Development as well as the associated industrial partner is gratefully acknowledged.

References

[1] Weisheit, S.; Unterberger, S. H.; Bader, T.; Lackner, R.: Assessment of test methods for characterizing the hydrophobic nature of surface-treated high performance concrete. *Construction and Building Materials* 110, pp. 145-153, 2016.

[2] Bader, T.; Waldner, B. J.; Unterberger, S. H.; Lackner, R.: On the performance of film formers versus penetrants as water-repellent treatment of High-Performance Concrete (HPC) surfaces. *Construction and Building Materials* 203, pp. 481-490, 2019.

Heat-resistant UHPC for use as baking plate - increased stability under thermal stress due to cellulose fibres

Niels Wiemer, Alexander Wetzel, Bernhard Middendorf
Department of Structural Materials and Construction Chemistry, Institute of Structural Engineering, University of Kassel, Germany

1 Introduction

The main properties of Ultra-high performance concrete (UHPC) are a high compressive strength and a good durability. These are due to the high packing density resulting from a very low water-binder ratio and the use of fine reactive components. With regard to thermal resistance these properties do not lead to good material performance. This is because of the water pressure which could not evaporate due to the dense microstructure. The UHPC fails even with steel fibre reinforcement brittle and abruptly [1]. Considering a standard concrete, there is no failure due to high temperature as long as its moisture content is less than approx. 2.5 wt % [2]. With a high ratio of capillary pores, the water vapour can evaporate directly out of the structure. In comparison to a standard concrete, the internal vapour pressure of UHPC rises faster.

In [3], a UHPC fine grain mixture M_3Q (SPP 1182; [4]) was subjected to thermal stress of up to 500°C. The compressive strength of the not adapted mix design of M_3Q increased by approx. 16% at a temperature up to 250°C (good post-treatment method). Above 250°C the UHPC is thermally instable.

Aim of the study

The aim of this research was to develop an UHPC for the use of backing plates with a thickness of 13 to 30 mm and optimized for cyclic, thermal loading. The plates are used in large bakeries and have a length/width of up to 2.85/1.25 m. In order to increase the thermal resistance, the UHPC was optimized with regenerated cellulose (CR) fibres. The CR-fibres shrink under thermal stress and leave thin, elongated cavities like capillary pores. The water vapour pressure created by thermal stress can dissipate and counteract the material failure (Fig. 1).

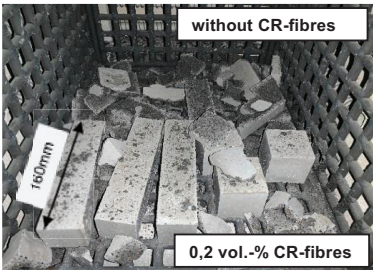

Figure 1: Picture of UHPC specimens after thermal treatment (500°C). Failure under thermal stress without CR-fibres (back row).

2 Material and methods

The raw materials used for the material development have been selected in cooperation with a manufacturer of baking plates. In the reference mix design of this plant a high w/b ratio ensures the thermal stability. This is associated with low mechanical properties. Therefore, the packing density was optimized and the w/b ratio was reduced. Furthermore, compared to the standard M_3Q formulation, quartz sand was replaced by limestone and basalt sand (Table 1). The low thermal expansion of the basalt sand is supposed to have a positive effect on the heat resistance. The risk of a sudden increase in volume due to the transition from alpha to beta quartz was noticed. For the investigation of the thermal resistance, the compressive strength according to German standard DIN EN 12390-3 on cubes with a length of 50 mm after a temperature load of 500°C as well as a heating and cooling rate of 10 K/min has been determined. Furthermore, the flexural strength of prisms (40 x 40 x 160 mm^3) and plates (30 x 30 mm^2) was tested.

Table 1: Compounds of the M2 mixture and their amounts in kg/m³ and wt %.

Compounds	kg/m³	wt %	
CEM III B	581.5	25.0	
Silica fume:	176.4	7.6	
Limestone sand 0_1 mm:	104.3	4.5	
Basalt sand 0_1 mm:	120.3	5.2	
Basalt sand 1_3 mm:	1,323.3	56.8	
Cellulose Fibres:	3.0		0.2 vol.-%
Superplasticizer: ViscoCrete2810	20.84		3.6 bwoc
w/b-ratio*	0.23/0.25		

*w/b: water / binder ratio.

3 Results

The results of the compressive strength after thermal stress on cubes showed that a fibre content of 0.2 vol.-% of the dry mix design is sufficient to ensure thermal resistance at 500°C. The samples were thermally stable up to a temperature of 300°C without CR fibres. Higher compressive strengths as the reference backing plate were determined by modifying the mixture by changing the fibre content (Fig. 2a). In contrast to the results of M_3Q, it is noticeable that higher compressive strengths are achieved after heating up to 500°C. A comparison between the mixtures M3 and M4 shows that an increase of the fibre content leads to a reduction of the compressive strength by approx. 18% after 500 °C. The flexural strength (Fig. 2b) also showed an increase after 500 °C for all mixtures. Only the flexural strength of the M4 mixture decreased, but a higher proportion of CR fibres leads to a approx. 22% higher flexural strength without thermal treatment. The grey area in Fig. 2b showed the flexural strength of the plates. The reference oven plate and the M5 mixture without basalt sand 1-3mm were compared. In comparison, the reference oven plate had a flexural strength that was approx. 50% lower. After the thermal loading the flexural strength of the M13-mixture decreases because of strong bending deformation.

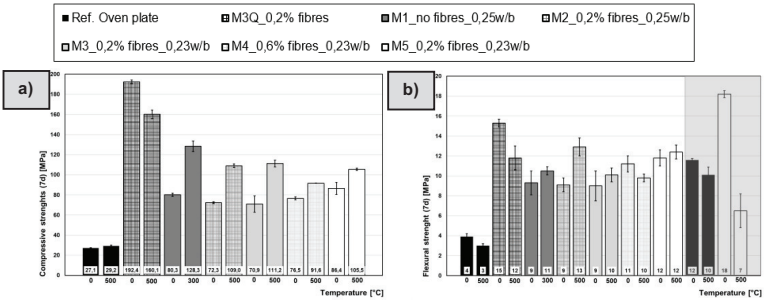

Figure 2: a) Results of the compressive strength (7d) compared to the reference mixture and M3Q with fibres (28d/90°C). b) Results of the flexural strength of prisms (7d) and plates in grey background (14d).

4 Conclusions and outlook

Based on a UHPC mixture, a baking plate was developed which can resist temperatures up to 500 °C. By adapting it to the factory conditions, an HPC results, which will be further developed in the next step by post-treatment and drying conditions.In addition, the durability of the surface will be tested for chemical resistance.

References

[1] Horvath, J.: Beiträge zum Brandverhalten von Hochleistungsbeton. Dissertation, Technische Universität Wien,2003.

[2] Meyer-Ottens, C.: Zur Frage der Abplatzungen an Betonbauteilen aus Normalbeton bei Brandbeanspruchungen. Schriftreihe des Instituts für Baustoffe, Massivbau und Brandschutz, Heft 23, Braunschweig, 1972.

[3] Scheffler, B.; Wetzel, A.; Sälzer, P.; Middendorf, B.: Thermische Stabilität von UHPC. Celluloseregeneratfasern zur Steigerung der Stabilität unter zyklischer thermischer Belastung, Beton- und Stalbetonbau Fachaufsatz/Bericht, 2019.

[4] Schmidt, M.; Fehling, E.; Fröhlich, S.; Thiemicke, J, Eds.: Sustainable Building with Ultra-High Performance Concrete, Kassel:University Press, 2014.

Experimental Investigations on glued composite beams of glass and UHPC

Hannes Eichler, Jenny Thiemicke, Roland Vollmar, Ekkehard Fehling
Institute of Structural Engineering, Department of Concrete Structures, University of Kassel, Germany

1 Introduction, motivation and objectives

The growing popularity of glass as an architectural element increases the request to use glass as a load-bearing structural component. While most common structures behave in a ductile manner, glass is charactarised by its very brittle failure mode without any plastic deformation (see Fig. 1). In order to design glass structures safer and more predictible, previous research projects have investigated on glass composite systems. [1], [2], [3]

2 Development and construction of glass-composite bending beams

Objective and constructional design

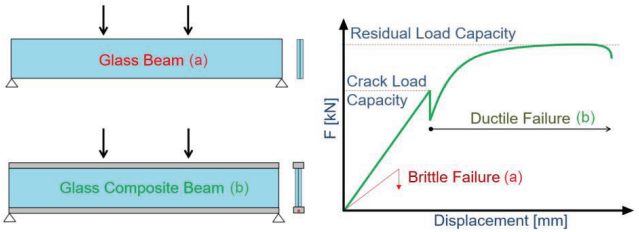

Figure 1: Glass concrete composite Beams, Objective

By designing hybrid glass - UHPC beams, the mechanical properties of glass and fibre-reinforced UHPC are combined in order to create an improved load-bearing behaviour.

As shown in Figure 2, the main objectives are to increase the beams' crack load capacity and to provide a residual load capacity after the glass has already cracked. In addition, it should be possible to further increase the load after the first crack event has occurred. In this way, the load-bearing capacity of the composite beams can be separated from the glass quality by offering a reliable capacity against bending tensile failure.

Test specimens

The composed beams had a length of 2000 mm and a height of 261 mm. The flanges of the beams (45 mm x 50 mm) were made of UHPC with a compression strength of 170 MPa. They were reinforced with 9 mm long steel fibres (2% by vol.) as well as a reinforcing bar with a diameter of 8 mm (f_y = 500 MPa). The web was formed by triple laminated glass (1950 mm x 190 mm). In each case, two beams were made of conventional float glass as well as of heat strengthened glass. To assemble all components, the glass was glued into a manufactured H-shaped metal profile which could be successfully anchored into the concrete by developing "concrete dowels".

3 Experimental investigations and modelling

Test setup and test results

The composite beams were tested in 4-point-bending tests at the University of Kassel. Besides the applied load, the vertical deformation in the load application centrelines as well as horizontal deformations in the area of the maximum bending moment on the flanges and on the glass web

were measured. The left side of figure 2 shows the load-deformation-curves of both kinds of beams, the rigth side shows the cracked beams after testing.

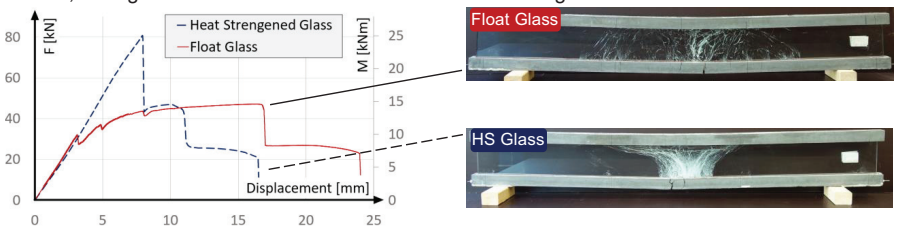

Figure 2: Test results of heat strenghened and float glass beams (left); cracked beams after testing (right)

Modeling with method of slices

As part of an Excel®-based calculation, the cross section of the composite beam is segmented into several lamellas. This model is updated with the material properties from preceding bonding and material tests. Using this iterative and simple model, the most important parameters (crack load, maximum load, residual load capacity) can be successfully verified without the need for complex FE-models. Figure 3 compares the test results of a float glass beam (left) with the subsequent calculation (right). The crack load is based on the bending stiffness of the composite beam, considering the non-linear failure of the concrete element. The residual load-bearing capacity can be completely attributed to the properties of the lower flange and the lever arm of inner forces-independent of the glass quality.

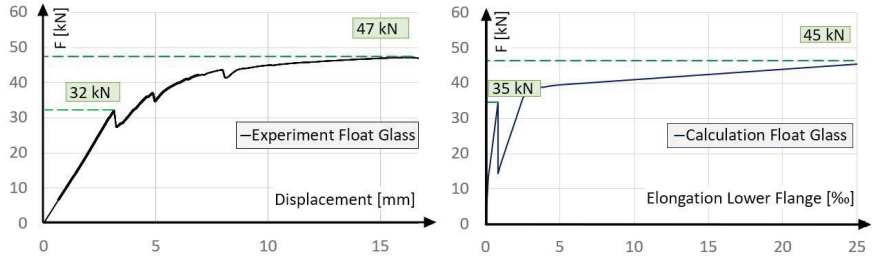

Figure 3: Float glass beams – comparison of test results (left) and modelling (right)

4 Conclusion and outlook

The results of the experimental investigations are:

- the developed bond construction enables the transfer of high bond forces,
- the composite beams of glass and UHPC possesed a high crack load capacity as well as increasing load bearing capacity after cracking of the glass web,
- the steel fibre reinforced UHPC-flanges allow a ductile behaviour of the composite beam and therefore,
- composite beams of glass and UHPC show a signalised failure.

References

[1] Freytag, B.: Die Glas-Beton-Verbundbauweise, Dissertation, Technische Universität Graz, 2002.

[2] Louter, C.: Fragile yet ductile. Structural aspects of reinforced glass beams, Dissertation, Technische Universität Delft, 2011.

[3] Härth-Großgebauer, K.: Beitrag zum Tragverhalten hybrider Träger aus Glas und Kunststoff, Dissertation, Technische Universität Dresden, p. 53 – 69, 2018.

Effect of thixotropy enhancing agents on extrudability of lightweight concrete

Carla Matthäus, Daniel Weger, Thomas Kränkel, Christoph Gehlen
Center for Building Materials, Chair for Materials Science and Testing, Technical University of Munich, Germany

1 Research Question and Methods

Motivation

Extrusion is an additive manufacturing technique in which a component is built up layer by layer from concrete strands. The extrusion of lightweight concrete poses material challenges due to the contradictory requirements of pumpability and buildability. Buildability is thereby defined as the ability of a deposited material strand to maintain its shape without deformation under increasing load [1]. This short paper aims to analyse the use of polymer based thixotropy enhancing agents (TEA) in lightweight concrete to improve pumpability and buildability.

Materials and Test Setup

The lightweight concrete consists of OPC, lightweight aggregate (0.1 mm to 2 mm expanded glass granulates), 10 V.-% limestone and a w/b-ratio of 0.56, including the water absorbed by the porous glass granulates. Two chemically distinct TEA on polymer basis are added at a dosage of 0.8 g/l water and compared to the reference without TEA. TEA 1 is a synthetic co-polymer and TEA 2 a sphingan. Furthermore, a PCE is used to achieve a comparable yield stress of all concretes. The investigations are based on a combination of pumpability and buildability tests. The pumpability is investigated in a progressive cavity pump at a hose length of 5 m and diameter of 25 mm. Simultaneously, dynamic rheological experiments are carried out with a six-bladed vane-in-cup rheometer and evaluated by Herschel-Bulkley. For buildability, static rheological experiments with vane-in-cup to determine the evolution of static yield stress over time of the concrete were carried out. Finally, the buildability was verified by 3D-printing of a cylindrical geometry in order to evaluate the maximum achievable vertical building rate, i.e. the maximum number of layers per time unit.

2 Effect of Thixotropy Enhancing Agents on Pumpability and Buildability

Pumpability

At constant pumping frequency of 7.2 Hz the addition of TEA to the lightweight concrete leads to an increased flow rate. Furthermore, TEA1 induces a lowered change of temperature and density during pumping, see table 1. Up to shear rates of 100 s^{-1} the apparent viscosity of the mixtures decreases with increasing shear rate. Above 100 s^{-1} the mixtures with TEA show a shear thickening behavior. It can be found in literature, that a material with a Herschel-Bulkley flow index above 1 might exhibit shear thinning behavior for low shear rates, followed by a shear thickening behaviour at higher shear rates [2]. Assuming that the shear rate for pumping with the progressive cavity pump lies in the range of 10-50 s^{-1}, the apparent viscosity of the mixtures correlates with their pumpability. The pumpability enhances with decreasing apparent viscosity (increasing thixotropic behaviour). This is in line with the findings in [3]. The pumpability of the three mixtures is comparable, with TEA1 being the easiest to pump.

Buildability

Based on the static rheological measurements, figure 1 shows the development of the static yield stress of the mixture without TEA and the mixtures with TEA as a function of time at rest. It can be seen that the increase in static yield stress is predominant within the first 5 minutes at rest. Afterwards there is just a further slight increase, whereby this can be approximated with a

smaller gradient using a separate linear equation. TEA1 shows the highest structural build-up rate followed by TEA2. The yield stress over time on the first (lowest) layer is calculated on basis of structural build-up and static yield stress. The comparison of this value with the stress applied by the subsequent layers over time, leads to the number of layers that can theoretically be printed before plastic failure occurs (see [4,5]).

Table 1: Pumping properties of selected mixtures.

Mixture	Change in temperature	Flow rate	Change in density	Mean Yield stress	Mean Apparent Viscosity at $\dot{\gamma}$ =25 s^{-1}	Mean Flow index
	[°C]	[kg/min]	[%]	[Pa]	[Pas]	[-]
without TEA	3.5	2.2	7	226	11.2	0.8
TEA 1	2.4	3.3	3	171	8.9	1.5
TEA 2	4.9	3.2	11	262	10.9	2.1

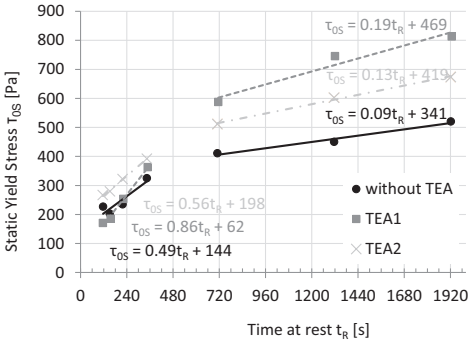

Figure 1: Increase in static yield stress at time at rest as a measure of structural build-up with and without TEA

Assuming a layer height of 15 mm and a vertical printing speed of one layer per minute, the failure is calculated to occur at 6 layers without TEA and 12 layers with TEA1. In verification tests an even more pronounced influence of the TEA was recognized: without TEA the structure failed as expected, while with TEA1 no collapse occurred even up to 40 layers. Therefore, due to addition of TEA the green strength development of the material seems to increase although the static yield stress development is only slightly different. This might be due to the water retention effect of the TEA.

3 Conclusions

The use of thixotropy enhancing agents allows the development of well pumpable mixtures with higher green strength than the reference material. However, the calculation of the number of printable layers directly on basis of the lightweight concrete properties leads to an underestimation of the mixtures with TEA. It is therefore necessary to investigate the effect of TEA on lightweight concrete under pressure more closely in further investigations and to develop a better estimate for the buildability of lightweight structures.

References

[1] Lim, S.; Buswell, R.; Le, T.; Austin, S.; Gibb, A.; Thorpe, T.: Developments in construction-scale additive manufacturing processes. Automation in Construction 21, p. 262-268, 2012.

[2] Roussel, N.; Lemaître, A.; Flatt, R.; Coussot, P.: Steady state flow of cement suspensions: A micromechanical state of the art. Cement and Concrete Research 40, p. 77-84, 2010.

[3] Matthäus, C.; Weger, D.; Kränkel, T.; Santos Carvalho, L.; Gehlen, C.: Extrusion of lightweight concrete: rheological investigations. In Rheology and Processing of Construction Materials, p. 409-416, 2019.

[4] Roussel, N.: Rheological requirements for printable concretes. Cement and Concrete Research 112, p. 76-85, 2018.

[5] Perrot, A.; Rangeard, D.; Pierre, A.: Structural build-up of cement-based materials used for 3D-printing extrusion techniques. Materials and Structures49, p 1213-1220, 2016.

The influence of simple polymers on the dispersion of colloidal nanosilica in Ultra-High Performance Concrete

Douglas Hendrix[1], Kay Wille[2]
1: Materials Science and Engineering, Institute of Materials Science, University of Connecticut, USA
2: Department of Civil and Environmental Engineering, University of Connecticut, USA

1 Introduction

In a concrete system, there can be several types of particles in an aqueous environment. The two most commonly researched particle systems are cement and silica. Without the addition of polymeric additives or superplasticizers, a significant amount of water is required to disperse cement and silica and therefore turn the mixture from solid particle agglomerations to a fluid state. Superplasticizers provide dispersion to cement through two primary mechanisms: electrostatic repulsion and steric hindrance. Cement particles possess a positive charge, causing the particles to be electrostatically repulsed and the long polymer chains provide a physical barrier to agglomeration. These two mechanisms in tandem provide a strong dispersion of cement particles, allowing for a maximum amount of surface area to be available for reaction.[1]

These same commercially available superplasticizers not only work inefficiently in the process of dispersing colloidal nanosilica (NS), they can also have an adverse effect on the dispersion of NS. There are two main reasons these superplasticizers do not work with NS. First, the superplasticizers are tailored to adsorb to positively charged cement particles. The anionic backbone, typically a modified polycarboxylate, adsorbs to the positive cement surface, with the cationic or nonionic side chains perpendicular to the surface. The NS has a negative surface charge which repulses the anionic backbone and can attract the side chains. Secondly, these long polymer chains can interact with multiple NS particles, causing permanent agglomeration. Therefore, the use of compatible polymers is essential for the dispersion of NS. It is hypothesized that the introduction of well-dispersed NS will further densify the microstructure of ultra-high performance concrete (UHPC) and thus further enhance the mechanical and durability properties.

2 Polymers & Nanosilica Investigated

The exact polymeric composition and structure of commercially available superplasticizers is not publicly available but the main polymer components are polyacrylic acid (PAA), polyethylene glycol (PEG), and PEG methyl ether (mPEG). In order to better understand the interaction of superplasticizers with NS, simple low molecular weight polymers were added to colloidal NS sols.

The polymers investigated in this study were PAA, PEG, mPEG, poly(acrylic acid-co-maleic acid) (PAACOM), poly(acrylic acid sodium salt) (PAANa), poly(vinylpyrrolidone) (PVP), and poly(N-isopropylacrylamide) (PNIPAM). The amount of polymer was varied from 10% to 200%. The percentage of polymer is proportional to the solid content of NS. For example, 100% polymer corresponds to a 1:1 ratio of the solid content of NS to the solid content of the polymer. In addition to these simple polymers, a commercially available superplasticizer, was used for comparison.

Six types of NS sols were investigated. These sols varied in size, solid content, pH, and stabilizing ion. The three NS sols referenced in this work are NS20Na, NS5Am, and NS20Al with an average particle size of 20 nm, 5 nm, and 20 nm, respectively, as supplied by the manufacturer. A Zetasizer Nano ZS was used to measure the particle size distribution and the

zeta potential (ZP) with the dip cell accessory. Dynamic light scattering (DLS) and ZP provide a quantitative analysis of the dispersion state of colloidal NS.

The dispersion of NS in concrete is difficult to measure and quantify. Therefore, these particles were added to a synthetic pore solution (PS) that represents the chemistry and ionic concentration of UHPC. This allowed for isolated quantitative measurements using DLS and ZP.[2]

3 Results

The addition of polymers to NS increased the apparent size due to adsorption. The apparent size was dependent on the type of polymer, the amount of polymer, the type of NS, and the pH. Increasing amounts of polymer or a higher molecular weight polymer increased the apparent size. The apparent size was often directly correlated to the zeta potential.

Two types of polymers (PAA, PEG) and three types of NS (NS20Na, NS5Am, NS20Al) will be discussed in more detail. The results from the other polymer and NS combinations will be provided outside the framework of this paper.

The addition of PAA resulted in the agglomeration of NS20Al but did not significantly affect the dispersion of NS20Na and NS5Am. The apparent size of these two was increased by about 15% and the magnitude of zeta potential was reduced by about 60%. While this may seem detrimental initially, upon the addition of PS, the average size remained consistent. At the full strength of PS, both NS20Na and NS5Am were dispersed, with an average size of 35.8 nm (SD = 0.2) and 16.9 nm (SD = 0.4), respectively. The zeta potential was -0.2 mV (SD = 3.1) and -4.5 mV (SD = 0.6), respectively. The PAA concentration for both of these samples was 100% and the pH was 4.0. In this high ionic concentration medium, the NS was only temporarily stabilized, as all samples sedimented within 12 hours. One reason the NS stays stabilized at low pH is because the polymer remains in a tightly coiled conformation, whereas at higher pH, the polymer chain unravels and stands perpendicular from the surface. When the polymer is standing out from the surface, this pushes the electrical double layer farther from the surface, reducing the zeta potential and increasing susceptibility to agglomeration by calcium ions.[3]

On the contrary to PAA, the addition of PEG was beneficial for NS20Al. The apparent size increased by about 10% and the zeta potential decreased by about 30%. Upon the addition of PS, the average size increased to 37.8 nm (SD = 0.6) and the zeta potential decreased to 27.7 mV (SD = 1.1). The difference between the polymer:NS combinations is due to the difference in surface charge and stabilizing ion. PAA is weakly anionic while PEG is nonionic.

4 Conclusion

Due to the high surface area to volume of NS, it is necessary to achieve a uniform dispersion of particles to enhance the particle packing of UHPC. This dispersion can be improved with the use of simple low molecular weight polymers. PAA seems to be a promising polymer for the use with NS in UHPC, however the surface characteristics of the NS and pH play an important role in determining the overall stability of particles in a high pH, high ionic concentration environment.

References

[1] Yoshioka, K.; Sakai, E.; Daimon, M.; Kitahara, A. Role of Steric Hindrance in the Performance of Superplasticizers for Concrete. *J. Am. Ceram. Soc. 80* (10), p. 2667–2671; 1997.

[2] Hendrix, D.; McKeon, J.; Wille, K. Behavior of Colloidal Nanosilica in an Ultrahigh Performance Concrete Environment Using Dynamic Light Scattering. *Materials (Basel).* 2019, *12* (12), 1976.

[3] Whitby, C. P.; Scales, P. J.; Grieser, F.; Healy, T. W.; Kirby, G.; Lewis, J. A.; Zukoski, C. F. PAA/PEO Comb Polymer Effects on Rheological Properties and Interparticle Forces in Aqueous Silica Suspensions. *J. Colloid Interface Sci.*, *262* (1), p. 274–281; 2003.

Flow-enhancing PCE-based superplasticizers for concretes of low W/C ratio such as UHPC

Manuel Ilg, Johann Plank
Chair for Construction Chemistry, Department of Chemistry, Technische Universität München, Germany

1 Introduction

Applicators often report about a sticky and cohesive consistency of concretes prepared at low water to cement ratios ≤ 0.30. Even though those concretes can be highly fluidized with polycarboxylate superplasticizers (PCEs), they often exhibit a creeping flow behavior which impedes a fast placement on the job site. Such a rheology is highly disadvantageous for the processing (pumping, placing etc.) as it often leads to an incomplete filling of the formwork and hence to defects of the hardened concrete structure. Mechanistic studies revealed that the low flow speed of those concretes particularly originates from a high plastic viscosity of the lime phase [1, 2]. Unfortunately, the plastic viscosity cannot be substantially reduced by conventional PCEs, which is why new approaches have to be found, how the rheological properties can be improved. This paper aims to present recent advances and strategies that are currently discussed for lowering the sticky consistency of concretes at low w/c ratios.

2 Phosphate-group modified superplasticizers

One promising concept to improve the flow speed of concrete is to introduce highly negative phosphate groups into the PCE polymers. The chemical structures of such novel superplasticizers are illustrated in *Figure 1*. Recently, phosphated phenolethoxlyates *(a)* were brought on the market, which are synthesized by polycondensation from phenolethoxylate, a phenol ethoxy phosphate ester, phenol and formaldehyde. Thus, a polymer is obtained with a polyaromatic backbone holding polyethylene glycol side chains and phosphate ester groups. An alternative product is a polymer prepared by aqueous free radical copolymerization of hydroxyethylmethacrylate phosphate ester (HEMAP), methacylic acid and a polyethylene glycol methacrylate ester *(b)* [3]. It was found that such phosphated polymers exhibit a high dispersing capability and an excellent robustness in the presence of sulfates and other chemical additives. However, the most striking feature is their ability to enhance the flow speed of concrete and to reduce the stickiness at low w/c ratios. This can be attributed to their high adsorption affinity and the high hydrophilic character of the trunk chain resulting from the phosphate groups which effectuate a low plastic viscosity. Contrary to common PCEs, the phosphated polymers affect the yield stress as well as the plastic viscosity of the lime phase.

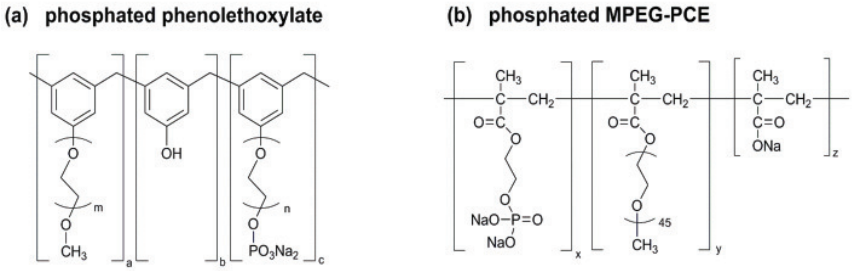

Figure 1: Chemical structures of phosphate-group bearing superplasticizers: (a) phosphated phenolethoxylate (polyarylether-based polymer) and (b) methacrylate-ester PCE exhibiting phosphate anchor groups.

3 Non-ionic small molecules as flow enhancers

Even simple blends of non-ionic small molecules like diethylene glycol with conventional PCEs can be used to improve the rheological properties. As can be seen from *Figure 2*, the effect of such auxiliary dispersants is particularly strong at very low w/c ratios (e.g. 0.22) where the cement particles are densely packed and the pore space becomes quite limited. However, the non-ionic co-dispersants not only increase the spread flow, but also enhance the flow speed as was confirmed by much faster V-funnel empty times of mortars exhibiting the same spread flow value [4]. Interestingly, the non-ionic molecules do not produce any fluidity when individually admixed to the cement and only work in combination with a PCE superplasticizer.

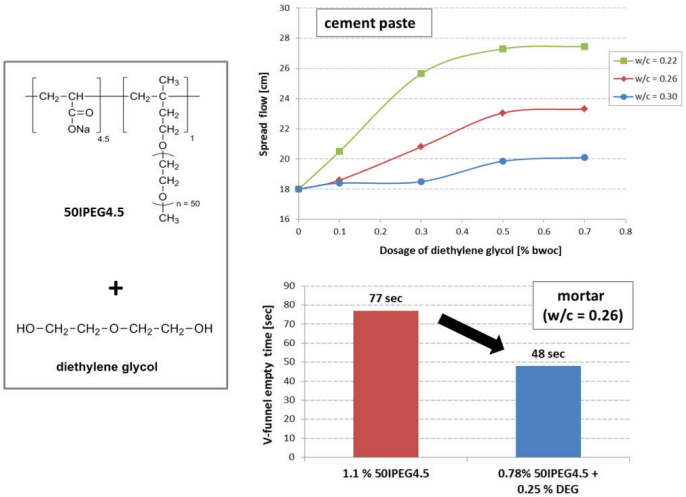

Figure 2: Effect of diethylene glycol as auxiliary dispersant on the spread flow of cement pastes and the V-funnel empty time of mortars at low w/c ratios.

The fluidizing effect of the co-dispersants can be explained by an osmotic spacer effect. Adsorption measurements have shown that the non-ionic molecules remain freely dissolved in the interstitial pore solution where they induce repulsive depletion forces, thus hindering the cement grains from flocculation. Otherwise, some parts of the pore solution would be depleted from the non-ionic molecules, which is energetically unfavourable and therefore avoided. Furthermore, it is assumed that such non-ionic co-dispersants create a lubricating layer around the particles and hence reduce the friction during flow.

References

[1] Banfill, P. F. G.: Additivity effects in the rheology of fresh concrete containing water-reducing admixtures. *Construction and Building Materials* 25, pp. 2955-2960, 2011.

[2] Liu, J.; Wang, K.; Zhang, Q.; Han, F.; Sha, J.; Liu, J.: Influence of superplasticizer dosage on the viscosity of cement paste with low water-binder ratio. *Construction and Building Materials* 149, pp. 359-366, 2017.

[3] Stecher, J.; Plank, J.: Novel concrete superplasticizers based on phosphate esters. *Cement and Concrete Research* 119, pp. 36-43, 2019.

[4] Ilg, M.; Plank, J.: Novel admixtures to reduce the stickiness of low w/c concretes. Proc. 12th International Conference on Superplasticizers and Other Chemical Admixtures in Concrete, Beijing 2018, pp. 77-88.

Bond behaviour of embedded FRP rebars in HPC and UHPC

Martin Empelmann, Vincent Oettel, Sara Javidmehr, Marcel Wichert
Institute of Building Materials, Concrete Construction and Fire Safety (iBMB), Division of Concrete Construction, TU Braunschweig, Germany

1 Introduction

Application of non-metallic rebars in HPC and UHPC is advantageous e.g. to achieve structural members with ultra-high durability in corrosive environment and maritime regions, as it combines the high performance of HPC and UHPC with the non-corrosive properties of non-metallic rebars. Using HPC and UHPC, it can be presumed that the interface bond strength between FRP rebar and concrete increases compared to normal strength concrete. Existing pullout tests on embedded FRP rebars in normal strength concrete show, however, that the bond failure mode can change from debonding in the concrete interface to delamination of rebar ribs or internal delamination depending on the concrete strength [1], [2].

To evaluate the above-mentioned effects on the bond behaviour of embedded FRP rebars such as basalt fibre and glass fibre reinforced polymers (BFRP, GFRP) is evaluated using pull-out tests. The influence of concrete strength (HPC and UHPC) and bond length (2ϕ and 3ϕ) of embedded FRP rebars are investigated in comparison to conventional reinforcement (B500).

2 Experimental Programme

Rebars with a diameter ϕ = 10 mm are used in the investigations (Table 1). The ribs of the FRP rebars were produced by winding of a tape, which was unwinded after the curing process of matrix. Two concrete mixtures HPC and UHPC are implemented with mean concrete compressive strength values of f_{cm} = 82.4 N/mm² and f_{cm} = 136.7 N/mm², respectively. 32 pull-out tests are performed in eight series on specimens with different rebar types (Figure 1, left) and two bond lengths 2ϕ = 20 mm (L1) and 3ϕ = 30 mm (L2). The test setup and the specimen designations are illustrated in Figure 1 (middle and right).

Table 1: Mechanical properties of evaluated rebars.

Rebar type		BFRP rebar (B)	GFRP Rebar (G)	B500 (S)
Young's modulus	N/mm²	53,190	50,687	208,900
Tensile strength f_u	N/mm²	1,313.25	1,311.30	625.17
Ultimate tensile strain ε_u	‰	33.84	34.44	30.68
Specific rib area f_R	-	0.074	0.080	0.071

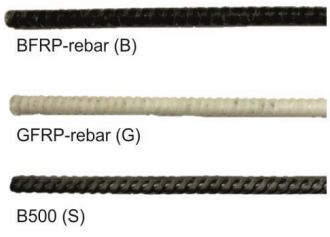

Specimen	No.	rebar type	bond length
HPC-L1-B	4	BFRP	2ϕ
HPC-L1-G	4	GFRP	2ϕ
HPC-L1-S	4	Steel	2ϕ
HPC-L2-B	4	BFRP	3ϕ
HPC-L2-G	4	GFRP	3ϕ
UHPC-L1-B	4	BFRP	2ϕ
UHPC-L1-G	4	GFRP	2ϕ
UHPC-L1-S	4	Steel	2ϕ

Figure 1: Evaluated rebars (left), experimental setup (middle) and overview of specimen designations (right)

3 Results and Discussion

The bond-slip behaviour for test specimens with embedded rebars in HPC and the bond length L1 is shown in Fig. 2.

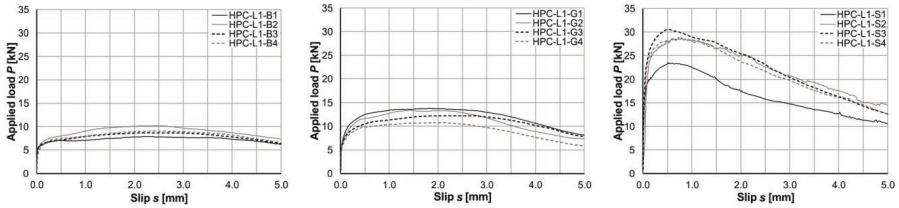

Figure 2: Bond-slip curve of embedded BFRP rebar (left), GFRP rebar (middle) and steel rebar (right)

For HPC-L1-B and HPC-L1-G, the failure happened as successive delamination of ribs, which occurred at the peak load levels with the corresponding mean bond strength values of τ_m = 14.3 N/mm² and τ_m = 19.9 N/mm², respectively. For steel rebars (HPC-L1-S), a higher mean bond strength of 44.3 N/mm² was reached, with the bond failure occurring in the concrete interface. During the tests, increasing the bond length of BFRP and GFRP rebars caused higher ultimate loads. This increase is, less than proportional to the increase of bond surface area for BFRP causing a lower bond strength τ_m = 11,1 N/mm² (Fig. 3, left) and proportional in case of GFRP rebars probably due to the slightly higher f_R (Fig. 3, middle). Fig. 3 also shows that the increased concrete strength of UHPC has no significant influence on the bond strength of BFRP and GFRP rebars. For steel reinforcement, the bond strength increases for UHPC specimens to τ_m = 66.3 N/mm² with the bond failure occurring at concrete interface (Fig. 3, right).

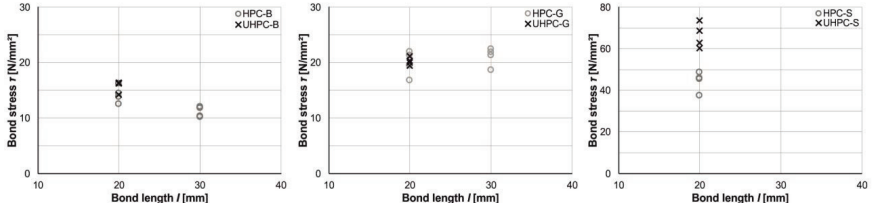

Figure 3: Correlation between bond length and bond strength for BFRP (left), GFRP (middle) and B500 (right)

4 Conclusion

The different bond behaviour of non-metallic rebars and steel rebars in HPC and UHPC was investigated. Based on the experiments, it was shown that for conventional steel rebars, the bond strength increases with increasing concrete strength. The bond strength of FRP rebars was almost not affected by an increase in the bond length or concrete compressive strength as delamination of ribs is the decisive bond failure mode for the investigated FRP rebars.

References

[1] Baena, M.; Torres, L.; Turon, A.; Barris, C.: Experimental study of bond behaviour between concrete and FRP bars using pull-out test. Composites: Part B 40, p. 784-797, 2009.

[2] Yang, Y.; Li.; Z.; Zhang, T.; Wie, J.; Yu, Q.: Bond-slip behaviour of basalt fiber reinfored polymer bar in concrete subjected to simulated marine environment: Effect of BFRP Size, Corrosion Age and Concrete Strength. International Journal of Polymer Science, Vol. 17, 2017.

[3] Moghaddam, O.; Wichert, M.; Empelmann, M.: Neuartige, mit nicht-metallischer Basaltbewehrung (BFRP) vorgespannte Rohrprofile aus Ultra-Hochleistungsbeton (UHPC) für außerordentlich dauerhafte, materialsparende Betontragkonstruktionen unter klimatisch und chemisch extremen Beanspruchungen. BBSR-Schlussbericht SWD-10.08.18.7-14.30, „Zukunft Bau“, 2018.

Shape memory alloy microfibres in UHPC – possibilities and challenges

Maximilian Schleiting, Alexander Wetzel, Niels Wiemer, Bernhard Middendorf
Department of Structural Materials and Construction Chemistry, Institute of Structural Engineering, University of Kassel, Germany

1 Introduction

Especially with Ultra-High Performance Concrete (UHPC), fibre reinforcement is a common method to enhance tensile and flexural strengths as well as to introduce a more pseudo ductile cracking behaviour of the material [1, 2]. The use of microfibres made of shape memory alloys (SMA) presents a new and innovative type of fibre reinforcement. Shape memory alloys have the ability to transform into an imprinted geometry due to a temperature and stress dependent phase transformation from martensite to austenite [3].

This “smart” material behaviour allows an advanced and functional type of fibre reinforcement that leads to more options and possibilities for construction. In contrast to these options and possibilities, there are also challenges to overcome, ensuring an effective usage of the material.

Aim of the study

This work will present two possible functionalities of shape memory alloy fibres in UHPC. These are on the one hand the enhancement of rheology of fibre reinforced fresh UHPC (Figure 1) and on the other hand the internal prestressing of UHPC by contraction of the fibres due to the shape memory effect of prestretched SMA fibres that transfers a compression stress by the bond between fibre and cementitious matrix onto the concrete.

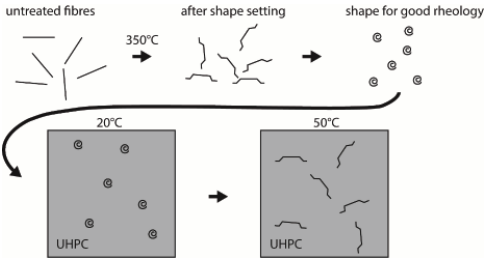

Figure 1: High-volume fibre-reinforced UHPC with low viscosity using SMA-microfibres.

Challenges

For both methods several challenges have been detected and have to be solved. In case of workability optimisation, an effective shape of the fibres has to be identified. This shape must fulfil several requirements. This study focuses on viscosity optimisation of fresh UHPC due to fibre shape modification. To get a better insight into the material behaviour, tests were done with fresh UHPC and additionally with a transparent silicon oil that has similar flow characteristics (plastic viscosity) compared to fresh UHPC [4].

In case of the prestressing method, the bonding and interfacial transition zone between fibre and cementitious matrix is an essential factor as the complete stress is transferred by bond.

2 Material and methods

A standard mixture based on the mixture M3Q known quite well from former investigations (SPP 1182; [5]) is used for all measurements. The used SMA fibres were made of nickel and titanium (NiTi).

For the rheology optimisation plastic viscosity was measured via rotation rheometer for UHPC mixtures and silicon oil with similar flow characteristics containing circular fibres. For the internal prestressing, fibre pullout tests with different SMA fibres were carried out and maximum

bond stress was compared to regularly used steel fibres. Therefore, these results do not show the prestress itself, but discuss the suitability of the SMA material for this method.

3 Results and discussion

The results regarding rheology show that a circular geometry of the fibres decrease the viscosity of fresh UHPC compared to straight fibres (Figure 2a and b). The viscosity of fresh UHPC containing circular fibres is about 33% lower than the mixture containing straight fibres. Therefore, the workability is improved. In silicon oil, the effect of the circular shape is less pronounced compared to UHPC (Figure 2c). Furthermore, the circular fibres sedimented much faster than the straight fibres.

The fibre pullout tests have shown that NiTi fibres have a much lower bonding stress than regular used coated and uncoated steel fibres (Figure 2c), indicating worse mechanical properties of fibre reinforced UHPC compared to steel fibres. Furthermore, the transfer of the compression stress that should induce the prestress, could be critical due to the low bonding strength.

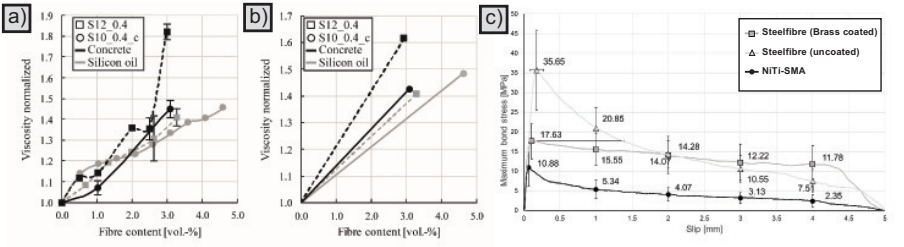

Figure 2: a) Normalised viscosity of fresh UHPC (black graphs) and silicon oil (grey graphs) containing 2 % by volume of straight (squares) and circular fibres (circles). b) Trend lines of the graphs in a). c) Results of the fibre pullout tests [4].

4 Outlook

To counteract the problems mentioned above, further research with regard to fibre sedimentation and distribution will be done using µ-CT measurements. In addition, fibre-shape transformation in UHPC will be investigated. Furthermore, surface treatment of the NiTi fibres as well as changes in matrix composition will be examined to enhance the bonding strength between fibre and UHPC.

References

[1] Bornemann, R.; Schmidt, M.; Fehling, E.; Middendorf, B.: Ultra-Hochleistungsbeton UHPC – Herstellung, Eigenschaften und Anwendungsmöglichkeiten. *Beton- und Stahlbetonbau* 96 (7), p. 458-467, 2001.

[2] Leutbecher, T.; Fehling, E.: Tensile Behavior of Ultra-High-Performance Concrete Reinforced with Reinforcing Bars and Fibers: Minimizing Fiber Content. *ACI Structural Journal* 109, p. 253-263, 2012.

[3] Otsuka, K.; Wayman, C.: Shape Memory Materials, Cambridge University Press, 1999.

[4] Schleiting, M.; Wetzel, A.; Gerland, F.; Niendorf, T.; Wünsch, O.; Middendorf, B.: Improvement of UHPFRC-Rheology by Using Circular Shape Memory Alloy Fibres. In: V. Mechtcherine, K. Khayat and E. Secrieru (eds.): Rheology and Processing of Construction Materials. RheoCon 2019, SCC 2019. RILEM Bookseries, vol. 23. Springer, Cham, 2020.

[5] Schmidt, M.; Fehling, E.; Fröhlich, S.; Thiemicke, J. (eds.): Sustainable Building with Ultra-High Performance Concrete. Kassel: Kassel University Press, 2014.

The effects of fiber surface treatment with abrasive paper on the pullout behavior of steel fiber in Ultra-High Performance Concrete

Booki Chun, Doo-Yeol Yoo, Hong-Joon Choi, Wonsik Shin, Yun-Sik Jang
Department of Architectural Engineering, Hanyang University, Republic of Korea

1 Introduction

In ultra-high-performance concrete (UHPC) using steel fibers, slip-hardening behavior is hard to be seen because the micro hardness of the steel fiber is too high to be damaged by the matrix. Therefore, we tried to change the factors that affect the interfacial properties between the fiber and the matrix, by treating the surface of steel fiber with abrasive paper.

In this study, abrasive papers with five different grits (120, 220, 320, 400, 800) were used to treat the fiber with two sanding direction i.e., parallel and perpendicular to the fiber axis. Treated fibers were embedded in the UHPC mixture with a compressive strength of 190.2 MPa. Quasi-static fiber pullout tests were conducted and surface roughness was evaluated using scanning electron microscope (SEM) and atomic force microscope (AFM) images.

2 Test results

Surface roughness analysis

After the sanding treatment, the surface roughness of the fiber was evaluated quantitively and qualitively using AFM and SEM, respectively. As a result, R_a, the arithmetical mean value of the height profiles within the measured area, was used to understand how roughness affects the bonding and bridging of the fibers. The increase of R_a varied from 1.5% to 157.9%, representing that the sanding treatment evidently has the effect of improving the surface roughness. In both fibers treated parallel and perpendicularly, the roughness increased when the smaller grit of the abrasive paper was used.

The average bond strength between the fiber and the matrix are calculated under the assumption that the bond stress is evenly distributed throughout the whole contact area, as follows.

$$\tau_{av} = P_{max} / \pi \cdot d_f \cdot L_e \quad (1)$$

Herein, τ_{av} is average bond strength, P_{max} is maximum pullout load, d_f is fiber diameter, and L_e is embedment length.

There was a clear correlation between the average bond strength and the surface roughness where the coefficient of determination was found to be 0.8319. The mechanism of the pullout behavior of steel fiber can be largely classified into two kinds: chemical adhesion and frictional shear resistance. Since the surface treatment increased the coefficient of friction as well as the surface roughness, it consequently inflates the frictional shear resistance. Unlike the pullout behavior of deformed fibers where the matrix breaks up due to the tremendous anchorage force, surface treatment on fibers are simply to improve the frictional shear resistance and therefore, it is expected that this improvement will be maintained in the composites behavior as well.

Fiber pullout test

From the pullout load versus slip curves, the slope of the curve after the debonding point eventually determines the slip behavior. In the case of plain fiber, the pullout load decreases linearly to the end of the embedment length due to the reduced bonding area. However, as shown in the Fig. 1, some sanded fibers exhibited distinctive slip hardening behavior which has

a clear ascending curve after the chemical debonding phase. It is very similar to the pullout behavior of PVA fiber within ECC, which is well-known for its outstanding strain hardening. The bridging of the fiber is not deteriorated despite of the reduced bonding area. The traces formed by the abrasive particles created uneven surface and it weaken the surface hardness. Thus, uneven exterior can be easily delaminated by the surrounding UHPC matrix and generate debris made of brass coating. These byproducts constrict the fiber and increase the frictional resistance. It is more remarkable from the perpendicularly sanded fibers compare to the parallel sanded fibers, where the traces act as canals allowing the byproducts to move relatively easily.

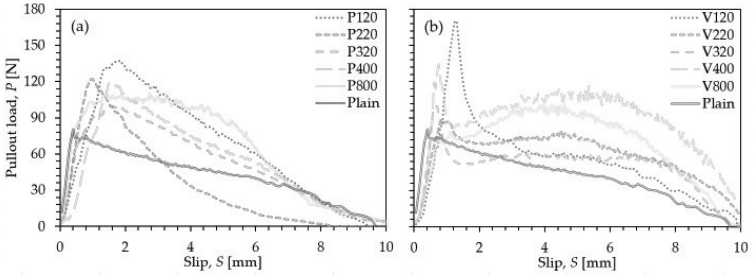

Figure 1: Pullout load versus Slip curves of (a) parallel treated and (b) perpendicularly treated fiber

The weakened surface and the delamination of brass coating can be explained with the difference of R_a after the pullout test. R_a of the plain fiber increased about 10% during the fiber pullout, whereas that of the V800, which exhibited the most distinct slip hardening behavior, decreased about 32%.

3 Conclusions

As an effort to make difference in interfacial properties between the fiber and the UHPC matrix, a surface treatment was applied to the conventional steel fibers. Based on the pullout test results and AFM analysis, following conclusions are drawn.

1. The sanding treatment was effective in increasing the surface roughness as well as enhancing the bond strength of the steel fibers. In general, larger grit of abrasive paper led to smaller improvement of average bond strength.
2. Because of the weakened surface hardness, byproducts were generated from the pullout process and they constricted the fiber to increase the shear resistance. As a result, surface treated fiber exhibited the slip hardening behavior and it was more pronounced when the sanding treatment was processed perpendicular to the fiber axis, and abrasive paper with higher grit was used.

Acknowledgements

This research was supported by a grant(20CTAP-C152069-02) from Technology Advancement Research Program funded by Ministry of Land, Infrastructure and Transport of Korean government.

References

[1] Redon, C.; Li, V.C.; Wu, C.; Hoshiro, H.; Saito, T.; Ogawa, A.: Measuring and modifying interface properties of PVA fibers in ECC matrix. *Journal of Materials in Civil Engineering* 13, p399-406, 2001.

[2] Stengel, T.: Effect of surface roughness on the steel fibre bonding in Ultra High Performance Concrete (UHPC). *Nanotechnology in Construction* 3, p371-376, 2009.

[3] Wille, K.; Naaman, A.E.: Pullout behavior of high-strength steel fibers embedded in ultra-high-performance concrete. *ACI Materials Journal* 109, p479-488, 2012.

Sustainable High and Ultra-High Performance Concrete – the next generation binders

Erik Pram Nielsen, Carmen Maria Quist Batista and Jesper Sand Damtoft
Cementir Holding SpA

1 Background

In the 1980's, the laboratories of Aalborg Portland A/S in Denmark, now the Research and Quality Centre for the Cementir Group, conducted pioneering research to develop very dense cement based binder-matrices. These efforts based on AALBORG WHITE® portland cement resulted in the first ever patented ultra-high performance steel fibre reinforced concrete – Compact Reinforced Composite, CRC® [1].

The technology and know-how from those findings, form still the basis for most modern HPC and UHPC mixtures. In spite of the mixture technology being almost 40 years old, it has changed little from the original recipes based on silica fume and quartz flours.

Unfortunately, it took decades before the construction market would begin realizing the advantages offered by fibre reinforced high and ultra high performance concrete, including its potential for highly efficient material optimization, provided excellent strength to mass ratios. Properly designed and installed UHPC building elements yield high energy efficiency, great resilience and durability, and are low maintenance. However, together with the growth in demand, some of the main challenges related to the technology and its complexity, become increasingly apparent, such as sourceability of the key ingredient, silica fume in terms of availability, price and quality, fresh concrete properties, such as fast loss of workability, and hardening properties, such as strong retardation and increased shrinkage.

2 Re-engineering HPC and UHPC binder technology

Sustainable HPC and UHPC binder technology

An Innovation Team in Cementir Group is further developing the very complex binder technology behind High and Ultra High Performance Concrete. The solution is based on a further refinement of Cementir Holdings recently patented sustainable binder technology, FUTURECEM™, which combines Portland cement clinker and supplementary cementitious materials derived from heat-treated aluminosilicate materials, and limestone[2]. The formulation does not include the use of scarce natural materials or waste materials from other industries which can be subject to volatile swings in quality, availability and cost. Furthermore, heat curing is not necessary for a succesful use of this technology.

Predictable and Reliable Performance

A successfull implementation of a technology assumes that what can be designed, mixed and manufactured in small specimens under laboratory conditions becomes transferrable to the conditions applicable to a full-scale production facility, where completely new requirements become decisive for the quality of the placed concrete in the final structure/element. A couple of examples of typical challenges are, ensuring a proper open time of the fluid UHPC mix to enable a controlled casting operation, and minimizing shrinkage potentially leading to cracks.

The challenges above require, among many others, an extensive investment and commitment to develop and document the properties of workable mixes, building up suitable quality control systems, knowhow, casting techniques, etc. Such challenges may seem a substantial mouthful to some manufacturers wanting to explore the possibilities of such a unique material. To support and sustain the increased demand for HPC/UHPC solutions,

Cementir Group has launched commercial UHPC ready to use, premixed products (see Table 1 for properties of AALBORG EXTREME™ Light120) based on this sustainable and reliable binder technology. These self-compacting products can be combined with fibres depending on the application served.

Table 1: Some key poroperties of AALBORG EXTREME™ Light 120

Table		**AALBORG EXTREME™ Light 120**
Aggreate size	mm	<3
Flow (EN-206)	mm	>900
Flow (ASTM C230/C1437-15)	cm	29±2 (initial and at 45´)
Hydraulic shrinkage	µm/m	<600
Compressive Strength (EN 12390-3)	MPa	1D: >75 / 28D: >120
E-modulus (EN 12390-13)	GPa	50
Flexural Strength (EN 12390-5)	MPa	>14
Splitting Tensile Strength (EN 12390-6)	MPa	12
Durability		
Chloride Migration Coefficient (NT Build 492)	$x10^{-12}$ m^2/s	28D: 0.35 / 56D: 0.27
Freeze/Thaw Resistance – Scaling (EN 12390-9)	kg/m^2	0.00
Water absorption, EN 1015-18	$kg/(m^2min^{0.5})$	<0.02
Oxygen Permeability (UNE 83981)	m^2	$<2x10^{-21}$
Carbonation Rate (UNE EN 13295)	$mm/day^{0.5}$	0 (at 1 and 3% CO_2)

An obvious advantage of the binder technology results from the high flexural and tensile strength obtained at any given compressive strength. This becomes even further improved upon combination with suitable selection of fibre types and dosages.

A binder technology linked to the framework of the EN standards

The composition of the binder used in AALBORG EXTREME™ Light 120 fulfills the chemical requirements of a CEM II/B-M (Q-LL) according to EN 197-1, including a total SO3 content lower than 3.5% suitable for all strength class nominations. The chloride content of the premixed concrete is less than 0.09 wt%, possing thereby no limit in respect to combination with standard reinforcement steel solutions.

3 Conclusions

Regardless of a HPC or UHPC mixture's makeup to be commercially viable, the technology must solve the persistent placement and workability issues these materials commonly experience today, such as flow retention and rheology. Following the binder technology principles in Cementir Goup´s patented FUTURECEM™, the Group has recently developed, tested and commercialized sustainable UHPC products which provide a safe and reliable solution to the issues mentioned above, which is based on AALBORG WHITE® cement, limestone and calcined clay.

References

[1] Bache, H.H., "Introduction to Compact Reinforced Composite," Nordic Concrete Research, No.6, 1987, pp. 19-33.

[2] Dai Z., Kunther W., Ferreiro S., Herfort D., Skibsted J. "Phase Assemblages in Hydrated Portland Cement, Calcined Clay and Limestone Blends From Solid-State 27Al and 29Si MAS NMR, XRD, and Thermodynamic Modeling". In: Scrivener K., Favier A. (eds) Calcined Clays for Sustainable Concrete. RILEM Bookseries, vol 10. Springer, Dordrecht, 2015.

Effect of Alccofine powder on the properties of Portland cement paste

Miliyon Yohans[1], N.B.Singh[2]
1: Department of Physics, Sharda University, Greater Noida, India
2: Department of Chemistry and Biochemistry, SBSR, Research and Technlogy Development Centre, Sharda University, Greater Noida, India

1 Introduction

Concrete is one of the most widely used construction material in spite of some inherent drawbacks such as brittleness, weak in tension, etc. and Portland land cement (OPC) is an important binding material in concrete. Portland cement manufacture emits huge amount of CO_2 gas. High rise buildings demand the use of high performance concrete (HPC) and ultra-high strength concrete(UHSC) in construction work as they lead to reduction in the size of structural elements and silica fume is the key ingredient of HPC and UHSC [1]. Recently it is found that Alccofine powder (AF) is a better substitute for silica fume but its action in cement is not understood well [2]. Alccofine powder (ultra fine slag) is a micro fine material obtained from low calcium silicate slag. When AF is mixed with OPC, properties are changed. Experiments were carried out with addition of 1, 3 and 5 mass % AF in OPC. Water consistency, setting time and compressive strengths were determined. Mechanism of action of AF during the hydration of OPC is discussed.

2 Materials and Experiments

The chemical compositions of Portland cement and Alccofine used in this paper are given in Table 1.

Table 1 Composition

Materials	SiO_2	Al_2O_3	Fe_2O_3	CaO	MgO	Na_2O	K_2O	SO_3	LOI
Portland cement	20.50	5.05	2.99	62.00	2.07	0.48	0.09	2.40	3.10
Alccofine	96.10	0.52	0.70	0.21	0.48	0.31	0.49	0.10	1.14

AF is a specially processed product based on slag of high glass content with high reactivity obtained through the process of controlled granulation [2]. It is amorphous in nature and X-ray diffraction pattern and SEM picture are shown in Fig. 1.

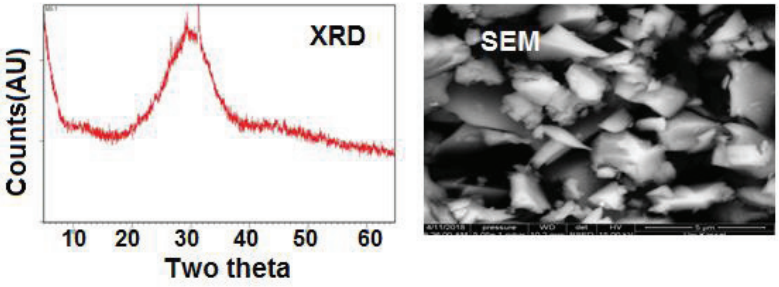

Figure 1: X-ray diffraction pattern and SEM picture of Alccofine

OPC was mixed with 0, 1, 3 and 5 wt% AF and pastes were prepared by adding water with W/S=0.33. Initial and final setting times were measured with Vicat apparatus. Hydrations were stopped at 3 and 7 days of hydration and non-evaporable water contents were determined by heating 1.0g hydrated samples at 1000 ^{o}C.

Rate of heat evolution (w/s=0.5) was determined at 27 ^{0}C with Calmetrix ICL 8000 isothermal calorimeter. After vibrating the samples for 30 s in order to have a homogeneous mixing, the samples were placed in the calorimeter chamber. In each case 2 g samples were taken.

OPC pastes containing 0, 1, 3 and 5% AF with a w/s=0.33 were made and kept in moulds of size 7.5 x 7.5 x 7.5 cm^3. The pastes in the moulds were vibrated with vibrating machine for 2 minutes with RPM 12000±400. The cubes were then demoulded after 12 hours and kept in water till measurements were made (1, 3 and 7 days). The compressive strengths were determined with a compressive strength testing machine. Each value was and average of three measurements.

3 Results and Discussion

Results showed that setting time decreased with addition of AF. Non-evaporable water contents which is related to degree of hydration also decreased with increase of AF both at 3 and 7 days of hydration.This indicated that there is a very little role of AF in the hydration process and the decrease may be due to dilution effect. Rate of heat evolution also decreased with increase of AF content (Fig.2). This supports the results of non-evaporable water contents.

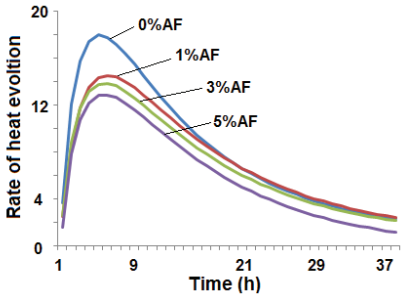

Figure 2 Rate of heat evolution

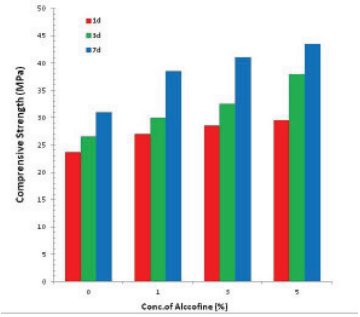

Figure 3 Compressive strength

However compressive strengths increased at all the days (Fig.3) and the values increased with concentration of AF. This indicates that AF being a fine powder fills the pores and makes the structure compact. Further there may be morphological changes also. Detailed investigations are needed.

4 Conclusions

Results showed that AF decreases the setting time. AF improved the pore structure and enhanced the compressive strength at all the concentrations and all the times. So AF may be an alternative material for enhancing the strength of cement and concrete.

References

[1] Madhurima, B.; Venkatanarayanan, H.K.: An integrated approach for studying the hydration of portland cement systems containing silica fume, Construction and Building Materials 188,1179–1192, 2018.

[2] Abhishek, S.; Rajesh, K.V.: Replacement of Portland cement with Alccofine: A Review, Int. J. Res. App. Sc. & Eng. Tech.,6(III)1285-1288,2018.

UHPFRC as maintenance and repair material for enhanced durability of transport infrastructure- mix optimizing with reduced clinker content

Louise Andersson[1], Nelson Silva[2], Andrzej Cwirzen[3], Ankit Kothari[3]
1: RISE Research Institute of Sweden, Built Environment, Stockholm, Sweden
2: SIKA, Stockholm, Sweden
3: Luleå Technical University, Luleå, Sweden

1 Background

In Sweden, there are approximately 16 000 road bridges with an average age of around 50 years old [1]; with a long coastal line and harsh winters, most of these structures often experience premature degradation due to combined effects of frost action and chloride induced corrosion.

State-of-the-art maintenance and repair solutions rely on the application of polymer-based cementitious materials, conventional reinforced concrete and hydrophobic surface treatments. These solutions bring a series of problems associated with durability of conventional reinforced concrete and its compatibility with polymer-based systems, and environmental aspects related to the impregnations.

The application of ultra-high performance fibre reinforced concrete (UHPFRC) for repair and strengthening of reinforced concrete structures has a number of advantages: it can be easily produced by any concrete plant and cast as self-compacting material in a regular manner known to contractors; the strength development is rapid enabling fast repairs; it does not require any additional steps such as vibration, heat treatment or surface finish. Such a solution is durable, cost effective and environmentally sustainable; it minimizes the frequency of maintenance interventions and traffic constrains thus minimizing associated costs and answers to future demands, e.g. increased traffic circulation.

The present study aims to investigate the possibility of using UHPFRC to cast “mantels” around damaged elements using regular formwork, without additional reinforcement. UHPFRC with reduced clinker content and optimal rheological properties will enable an efficient cast between tight reinforcement, the old concrete surface and the formwork without additional vibration. The compatibility as well as long-term durability pertaining to the UHPFRC will be investigated in detail using experimental methods. In the first part of the study, optimization of mix design with reduced clinker content have resulted in good properties in both fresh and hardened state.

2 Method

The aim of the optimizing of UHPC was to achieve a flow spread ≥ 270 mm (fresh state) and a compressive strength ≥ 100 MPa at 28 days, with a cement content in the range of 500-600 kg/m^3. The reason for the flow spread requirement of at least 270 mm was to have a good margin for the flowability when later adding steel fibres to create UHPFRC. The optimizing process of UHPC recipe consisted of examining the effect of different types of cements (CEM I & II) and their quantities, different supplementary products such as fly ash, limestone, quartz fillers and blast furnace slag. Also, silica fume, water content, superplasticizers and aggregate content were also varied but to a lesser degree. An underlaying aim is to create a recipe as user-friendly as possible by minimizing the number of products used and that can be mixed in

ordinary concrete mixers. Due to the requirement of fast demoulding the early compressive strength, preferably after 1 day, should not be too low.

3 Results

The first mixture was a “typical” UHPC with a cement content of 960 kg/m^3. The cement content was then reduced with most of the recipes after M3 using a cement content between 500 and 650 kg/m^3, still with various types of cement. It became clear that the use of a CEM I· (42.5 N-SR 3 MH/LA) with fly ash, was best when adding on flowability, compressive strength after the first 24 mixes. Mix 23 was then further developed using a cement content of 650 kg/m^3 before creating a final mix called FA1 with a cement content of 550 kg/m^3 with an acceptable flow spread and compressive strength. The flow spread and compressive strength of the mixtures can be seen in Figure 1 and the final recipe can be seen in Table 1.

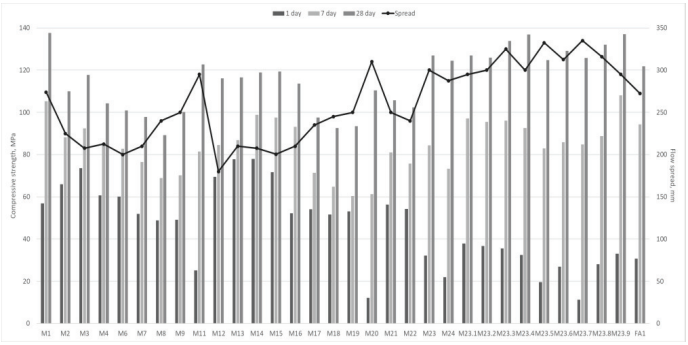

Figure 1: Flow spread and compressive strength of mixture during the initial optimization.

Table 1: Proportions of FA1 the final recipe.

Table		Density ρ	kg/m^3
CEM I 42.5 N - SR 3 MH/LA	kg/m³	3200	550
Fly Ash	kg/m³	2550	400
Silica Fume	kg/m³	2230	100
Quartz sand 0-0.2 mm	kg/m³	2650	575
Quartz sand 0-3 mm	kg/m³	2650	575
Water	kg/m³	1000	140
Superplasticizer	kg/m³	1090	25

4 Discussion

There are several ways to create an UHPC with reduced clinker content. The chosen final product met the expectations of flowability and compressive strength, both early and at 28 days. The recipe is relatively simple for an UHPC, with fewer components and even numbers which usually preferred on site. The next step is to optimize and evaluate with added fibres. There will also be durability test of chloride ingress, freeze-thaw and shrinkage. In the final stage, UHPFRC will be cast as an overlay on 4-meter high columns than have been water jetted.

References

[1] BaTMan, Swedish bridge and tunnel management system and database (2018).

Importance of secondary chemical reaction on mechanical evolution of UHPC

Prof. Juhyuk Moon, Dr. Sung-Hoon Kang
Department of Civil and Environmental Engineering, Seoul National University, Republic of Korea

1 Chemical reaction in Ultra-High Performance Concrete (UHPC)

Introduction

UHPC consists of various physical or chemical fillers to enhance materials properties including workability, strength, and durability. However, the role of each filler has not been clarified yet due to the material complexity of UHPC. Here, instead of silica fume which is the key ingredient for UHPC production, differently treated rice husk ask (RHA) fillers have been tested to compare its material performance and seek further potential to enhance material properties. RHA can be used as a supplementary cementitious materials (SCM) in cement based materials. Basically, it has been known that it has pozzolanic reactivity to consume portlandite (i.e., from hydration reaction of belite and alite) and water to produce more calcium-silicate-hydrates. However, the performance of the RHA is highly depending on the combustion conditions [1].

Materials and Methods

This study follows mix design proportion of our previous research on UHPC [2]. The UHPC samples were prepared using ordinary Portland cement (OPC), silica fume, quartz powder, silica sand, RHA, and water with polycarboxylate-ether based superplasticizer. For the chemical treatement of rice husk, firing temperature of 400 °C and 650°C was selected and each produces black color RHA and white color RHA, respectively (Figure 1). Based on different substitution ratio (50% or 100%), it has different trend of development of compressive strength which was obtained by 5 cm cubic samples from 7 to 71 days.

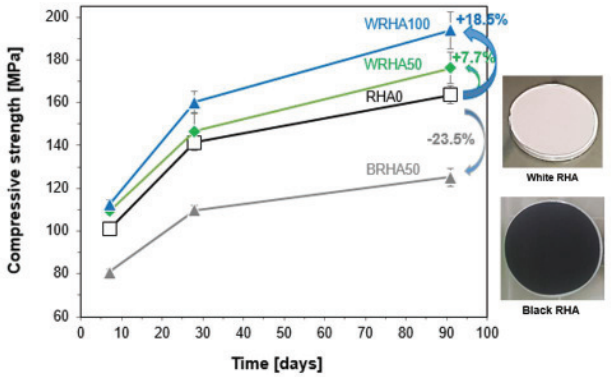

Figure 1: Strength evolution of UHPC with differently prepared rice husk ash instead of silica fume.

At each date for strength measurement, thermogravimetric experiment was conducted after hydration stoppage to accurately measure the amount of portlandite. The relationship between strength data at 28 days and the amount of portlandite content at 28 days was presented in Figure 2.

2 Pozzolanic reactivity in UHPC

As can be confirmed by the figure 2, there is a inverse relationship between the obtained strength and portlandite content. The portlandite was produced due to the cement hydration reaction from alite and belite. In UHPC formulation, the amount of those components is actually quite small due to the existence of large amount of different physical fillers such as quartz powder and sand. Nevertheless, we found out that approxiately 3~4 % of portladite was produced due to the hydration reaction. Furthermore, the amount is highly critical to control the secondary reaction of cement hydration in UHPC formulation, resulting the inverse relationship with compressive strength.

.

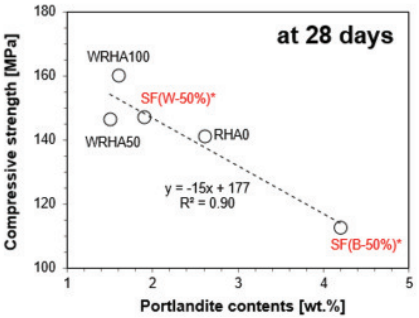

Figure 2: Inverse relationship between portlandite contents and compressive strength at 28 days. Data with red dots from [3]

3 Conclusions

Due to the complexity of UHPC at material scale, people may think high a degree of hydration of main clinker materials will increase the compressive strength of UHPC. However, this study clearly revealed that the strength evolution in UHPC does not depend on the degree of hydration (i.e., portlandite production reaction) but, is more importantly related to the portlandite consumption reaction. This is the pozzolanic reaction. Therefore, in terms of degree of secondary reaction, the degree of hydration of chemical filler of silica fume is much more dominant to determine the dense microstructure of UHPC although UHPC intrinsically has less amount of available water to facilitate pozzolanic reaction. This observation is used to understand how we can further improve the materials properties of UHPC because well-treated RHA can be a better pozzolanic material than silica fume.

References

[1] Zhang, M.; Lastra, R.; Malhorta, V.: Rice-husk ash paste and concrete: Some aspects of hydration and the microstructure of the interfacial zone between the aggregarte and paste. Cement and Concrete Research 26[6], pp.963-977, 1996.

[2] Kang, S.; Lee, J, Hong, S.; Moon, J.: Microstructural investigation of heat-treated ultra-high performance concrete for optimum production. Materials 10[9], pp.1106, 2017.

[3] Kang, S.; Hong, S.; Moon, J.: The use of rice husk ash as reactive filler in ultra-high performance concrete. *Cement and Concrete Research* 115, pp.389-400, 2019.

20-Years field durability experience of oldest UHPFRC structural elements

F. Toutlemonde[1], B. Terrade[1], T. Pons[1], F. Guirado[1], J. Billo[1], J.-C. Renaud[1], T. Vidal[2], P. Nicot[3], M. Fourré[3], A. Simon[4], J. Derimay[5], M. Lion[6], N. Schmitt[7]

1: Paris-Est University, IFSTTAR, Materials and Structures Department, France
2: Université de Toulouse; UPS, INSA; LMDC (Laboratoire Matériaux et Durabilité des Constructions), France
3: Toulouse Tech Transfer (TTT), France
4: Eiffage Génie Civil, France
5: LafargeHolcim Distribution, Ductal®, France
6: EDF Direction Industrielle, Département TEGG, France
7: EDF CNEPE, France

1 Context of investigation

UHPFRC are known for their exceptional structural and durability performance. Yet, durability assessment has been often based so far on samples cast in laboratory conditions, and feedback of UHFPRC ageing in existing structures is rather rare or recent. Conversely, the present study deals with the durability characterization of the oldest industrial application of UHPFRC in France and one of the oldest under such severe exposure conditions in the world [1]. Samples were drilled from two control girders made of UHPFRC of “Chinon” type (Tab. 1), cast in May 1996 [2], 23 years after their installation (August 1996) in the bottom part of one of the cooling towers of Cattenom nuclear power plant. Exposed to intense water dripping and forced wind circulation above a water basin containing salts, these pre-stressed I-shaped girders were maintained under permanent bending. They constitute durability warning samples with respect to the beams situated above. The program of investigations, following the one conducted after 10 year-exposure [3], was launched thanks to EDF support (owner and operator of the plant) and cooperation of Eiffage, LafargeHolcim, LMDC, TTT and IFSTTAR.

2 Specimens and results

On-site observations and coring

Access to the 6.50 m-long specimens was made possible during a maintenance operation (Fig. 1). Two to five mm-thick scale deposits are observed on the beams, their metallic supports and surrounding structures, identified as a porous layer of magnesian calcite with possible SiO_2 / SO_4 impurities. Namely, under operation, temperature of the water droplets varies from 35°C to 10°C, evaporation due to air flow concentrates the salt contents. Referring to the water of the basin, its pH ranges from 7.0 to 7.8; main ions contents are as follows: chlorides, 1 to 2 g/l; sulfates, 500 to 1000 mg/l. Periodic acid water treatments have used hydrochloric acid at 33% content, then sulfuric acid from 2017. 50 mm-diameter cores have been drilled transversally through the 50 mm-thick beams web (Fig. 2). Despite such aggressive conditions, no sign of fiber corrosion was visible on the core sides.

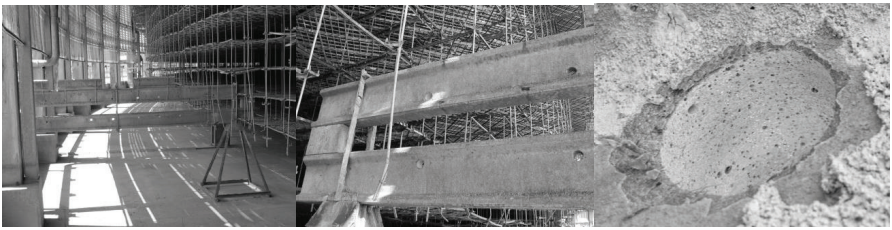

Figure 1: Situation of the beams in the cooling towers with location of the drilled specimens (no rust spots).

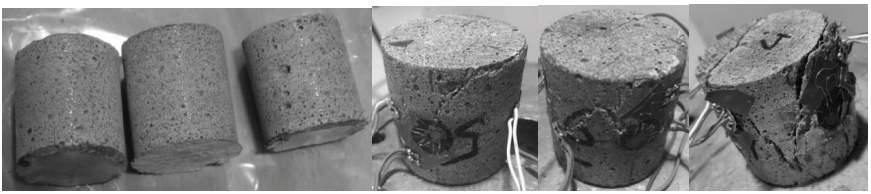

Figure 2: Cored specimens before and after compression testing.

Table 1: Nominal UHPFRC mix-proportions (kg/m³) [1].

Cem I	Zr Silica fume	Quartz flour (10µm)	Quartz sand (300 µm)	Steel fibers (Lf 13 mm)	Superplasticizer (dry extract)	Total water
714	232	214	1021	160	12.1	139

Measurements

Possible chlorides ingress or any alteration were investigated by chemical analysis of layers sawn from cores, resulting in absence of pH nor chloride content variation over time and along the cores depth (Tab. 2). Results of compressive tests carried out on 3 of the cores, 45.6 mm-diameter and 47.2 mm-high after surface preparation, are displayed in Table 2 with initial and 10 years determination [3], and can be related to the nominal mix used for casting these control girders (Tab. 1). The initial strength was measured on moulded 70 mm-diameter, 140 mm-high cylinders at 7 days of age, the day after the 48 hour-long thermal treatment. Slump measured during the fabrication was 16 cm (final selection of the admixture and associated placement protocol may not have been fully optimized when casting these prototype “Chinon” beams).

Table 2: Mechanical properties and durability indicators at the different ages.

Age	Mechanical properties			Durability indicators			
	Compressive strength	Young’s modulus	Poisson’s ratio	pH		Chlorides	
				near surface	core	near surface	core
7 days	207.8 MPa	56.0 GPa	0.21	-	-	-	-
10 years	240.4 MPa	54.4 GPa	0.19	12.4	12.4	< 0.1% of cem. mass	< 0.1% of cem. mass
20 years	237.7 MPa	53.6 GPa	0.18	12.7	12.7	< 0.1% of cem. mass	< 0.1% of cem. mass

3 Conclusions

Some scatter in interpretation comes from the significant air bubble content and differences in the specimens size and aspect ratio. Moreover, observations of tendons and additional tests have been planned to confirm the durability of the beams (first implementation of prestressed concrete – namely, UHPFRC – in a cooling tower). Whatsoever, it can be concluded at this stage that UHPFRC constitutive characteristics in compression are unaltered and that no fiber corrosion nor chemical degradation has occurred after 23 years under such exposure.

References

[1] Birelli, G.; Chauvel, D.; Dugat, J.; Adeline, R.; Bekaert, A.: RPC Industrialization. Using in cross flow air cooling towers and first design rules. The French Technology of Concrete, 13th FIP congress, 1998.

[2] Birelli, G.: UHPFRC development: Review of a determining application, in Designing and Building with UHPFRC, Toutlemonde & Resplendino eds, ISTE-Wiley, 2011, pp. 21-41.

[3] Toutlemonde, F.; Bouteiller, V.; Platret, G.; Carcasses, M.; Lion, M.: Field demonstration of UHPFRC durability. Girders shown to perform well in a cooling tower. Concrete International, Nov., pp. 39-45, 2010.

Adhesive bond strength of grouted joints between UHPC segments under static and cyclic loads

Marcel Wichert, Martin Empelmann
Institute of Building Materials, Concrete Construction and Fire Safety, Division of Concrete Constructions, Technische Universität Braunschweig, Germany

1 Introduction

Ultra-high performance concrete (UHPC) offers new opportunities for innovative and highly durable constructions. The application of UHPC can be advantageous in prestressed segmental structures like segmental bridges and precast towers. A further, pioneering approach is the application in framework structures (jackets) for foundations of offshore wind energy plants. For the structural design and the deformation behaviour of such foundations the joints between the UHPC segments are crucial. The implementation of grouted joints is a persistent solution to compensate manufacturing tolerances as well as to obtain force-locked connections.

The joints of such jackets are designed in such a way that they remain under compression during loading. The respective load-bearing capacity of the grouted joint under shear and compressive forces is investigated in [1] and [2]. However, unplanned tensile stresses may occur e.g. due to unexpected occurrences. Then, the adhesive bond strength of the grouted joint as a residual resistance will get relevant.

In order to investigate the adhesive bond strength of grouted joints between UHPC segments under static and cyclic tensile loads, uniaxial tensile tests are carried out at iBMB, Division of Concrete Construction of TU Braunschweig, which are introduced and analysed in the following.

2 Experimental Program

The test specimens consist of two UHPC segments with different surface characteristics of the interfaces, which are grouted with a high-performance mortar (HPM). The tests include series on smooth (S) or sandblasted (B) interfaces as well as nubbed (N) and trapezoidal (T) joint profiles. For series N, the influence of a pre-wetting (w) during the production is investigated in comparison to dry (d) joint surface production. The specimen and the surface characteristics are illustrated in Fig. 1. The mean compressive strengths of the UHPC and the HPM were $f_{cm,c} \approx 150$ and $f_{cm,m} \approx 120$ N/mm². First uniaxial tensile tests under static loads were carried out to determine the adhesive bond strength σ_u of grouted segment joints and to define the upper load levels σ_{sup} for cyclic loads. Afterwards, the specimens were tested under cyclic loads with a frequency $f = 2$ Hz until failure occurred or one or two million load cycles were reached (run-out). For the run-out specimens, the residual adhesive bond strength after preloading was determined. The lower load levels were $\sigma_{inf} \approx 0.1\sigma_u$.

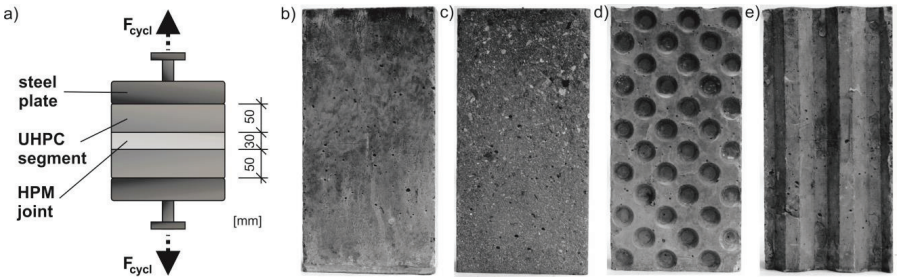

Figure 1: Specimen (a) as well as surface characteristics of series S (b), B (c), N (d) and T (e).

3 Results and Discussion

All specimens showed failure in one of the surfaces between UHPC segments and HPM joint. Fig. 2 presents the results of the static (left) und cyclic loaded (right) specimens. As expected, the specimens with the smooth surface (S-w) showed the lowest ultimate tensile stresses with a mean value σ_u = 0.33 N/mm². The results for series T-w (trapezes) were nearly the same but with less scattering. For series B-w (sandblasted) and N-w (nubbed) more than two times higher tensile stresses (σ_u = 0.72 and 0.75 N/mm²) were determined, which is due to the larger specific surface area. Series N-d showed that a dry concrete surface before grouting leads to an adhesive bond strength, which is 44 % higher (σ_u = 1.1 N/mm²) than pre-wetted joints.

All the cyclically loaded series (after preloading) exhibited an increase of residual adhesive bond strength: Series B-w (+28 %), N-w (+20 %) and N-d (+36 %). This effect can be explained with an ongoing hardening of UHPC and HPM during testing and a reduction of internal stresses due to cyclic loads.

For tensile stress levels $\sigma_{sup} < 0.8\sigma_u$ no failure under cyclic loading occurred. Furthermore, no influence of stress level or number of load cycles (one or two million) on the residual adhesive bond strength could be observed.

However, the adhesive bond strength was always considerably below the tensile strength of plain UHPC ($f_{ct,c}$ = 5,5 N/mm²) or HPM ($f_{ct,m}$ = 6,0 N/mm²), respectively.

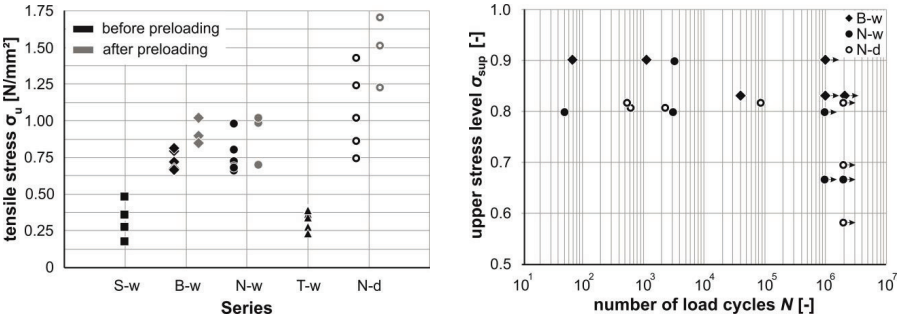

Figure 2: Test results of specimens under static (left) and cyclic (right) loads.

4 Conclusions

The adhesive bond strength between UHPC segments under static loads highly depends on the surface characteristics of the interfaces. With higher specific surface area, the tensile load capacity increased. Under cyclic loads with tensile stress levels $\sigma_{sup} < 0.8\sigma_u$ no failure could be observed for the investigated number of load cycles. All series exhibited an increase in residual bond strength after cyclic loading. However, the investigated grouted joints showed adhesive bond strengths considerably below the tensile strength of plain UHPC or HPM, respectively. Grouted joints of UHPC-jackets for foundations of offshore wind energy plants must be designed so that they remain under compressive stresses in any case during loading.

References

[1] Wichert, M.; Matz, H.; Empelmann, M.: Grouted segment joints for structures made of ultra-high performance concrete. In: Derkowski, W. et al. (Ed.): Proceedings of the fib Symposium 2019, 27.-29.05.2019 in Krakau (Polen), S. 2231-2238 (full paper digital).

[2] Matz, H.; Wichert, M.; Empelmann, M.: Numerical Investigations on Grouted Segment Joints for UHPC-Strucutres. In: Proceedings of the 7th International Conference on Structural Engineering, Mechanics and Computation (SEMC 2019) in Kapstadt, Südafrika, 02.-04.09.2019, S. 1421-1426.

UHPC overlay projects in the United States

Peter J. Seibert[1], Gilbert S. Brindley[1], Jerry W. Reece[2]
1: UHPC Solutions, New York, USA
2: WALO US Holdings Inc., New York, USA

1 Introduction

In North America, Ultra High Performance Concrete (UHPC) has been typically used in accelerated bridge construction as field cast connections for precast elements for either new or rehabilitation/replacement for over a decade [1]. Only recently, UHPC has been placed as a thin bonded overlay for bridges in the United States of America. UHPC overlays are an excellent rehabilitation method for existing bridge decks to extend their service life time and to enhance their long-term durability performance in a cost effective way.

2 Successfully Completed UHPC Overlay Projects in the US

US 18 over Floyd River Bridge, Sheldon, IA

This 2018 project was the first machine placed UHPC overlay in the United States which utilized a two-layer approach with different fiber contents per layer and multiple passes to achieve a 45 mm (1 ¾") depth overlay. This thin UHPC layer on the bridge deck acts as a protective waterproofing layer and helps the owner to save on any future costs by eliminating any additional deck repairs or even a full deck replacement. The goal of the bridge rehabilitation was to repair the existing concrete deck and extend the service life at a minimal traffic interruption.

Prior to installation, the deck surface was roughened using hydrodemolition and was pre-wetted for few hours before placement of the overlay. The UHPC for the 838 m^2 (9,020 ft^2) overlay was mixed onsite and was placed with a fully mechanized paving machine (Fig. 1). A two layered overlay was requested to minimize any steel fibers extrusions on the UHPC surface. Installation occurred in four stages where one lane of each direction remained open for the public at all times during the 10 days of construction. Diamond grooving was applied to achieve the final surface finish of the overlay (Fig. 2).

Figure 1: Fully mechanized paving machine


Figure 2: Diamond grooved UHPC overlay surface

SR1 Bridge, Little Heaven, DE

Two new 36.5m (120ft) long and 12.8m (42ft) wide bridges (Fig. 3) were constructed with a cast-in-place concrete deck on steel girders. Uneven chambers and grades resulted in having the top rebar mat in the center of the bridge deck with insufficient concrete cover and protection. The bridge owner searched for a solution that would provide enough protection of the top rebar mat, while keeping the designed cross slopes and horizontal curve of the bridges.

An UHPC overlay was the preferred repair method due to its great durability resistance and minimum required overlay thickness for grade repair. The UHPC overlay thickness varied between 45mm (1¾") to up to 127mm (5") in local areas with an overall average thickness of approximately 76mm (3"). The surface of the existing concrete deck was prepared using hydrodemolition at a depth of 6mm (¼") and prior installation the existing concrete surface was saturated with water. FHWA has demonstrated and validated that this is the best performing surface preparation to ensure sufficient bond of the UHPC overlay to the concrete substrate [2]. The low temperatures in February 2019 required winter heating installation procedures to ensure proper strength gain. Staging of the overlay construction included three paving lanes (Fig. 4) and construction joints were installed between the paved lanes. The entire UHPC placement was completed within a two week time period. Diamond grinding of the UHPC surface was applied to meet the road surface requirements for smoothness and microtexture.

Figure 3: SR1 Bridges during Construction

Figure 4: UHPC Overlay after Stage #1

Thin Lift UHPC Paving Machine Advancements

Manny lessons were learned on proper mix preparation, feeding of the paving machine, finishing the overlay surface and curing the overlay from all previous projects. This prompted the development of a new thin lift UHPC overlay paver (Fig. 5) capable of paving lanes in widths from 2.4m (8') to 9.1m (30') for the U.S. market in 2019. This thin lift UHPC paver can be utilized for smaller single-span to larger multi-span bridge rehabilitation projects. Bond tests validated strong performance.

Figure 5: Highly Specialized Thin Lift UHPC Paver

3 Conclusions

Even though overlays are still in the infancy for UHPC applications in the US, these projects illustrate successful and high quality installations with minimized traffic interruption. The most important success factors of an UHPC overlay are proper surface preparation, compaction and curing. Utilizing specifically developed paving machines for UHPC and an experienced workforce are essential to achieve these success factors in a fast and cost-effective way. Specialized UHPC paving machines help bridge owners to minimize traffic interruptions and to shorten the total construction time of the bridge rehabilitation project.

References

[1] Haber Z.B.; Graybeal B.A.: Performance of Grouted Connections for Prefabricated Bridge Deck Elements. *Report No. FHWA-HIF-19*-003, Federal Highway Administration, Washington, DC, 2018.

[2] Graybeal B.A; Haber Z.B.: Ultra-High Performance Concrete for Bridge Deck Overlays. *FHWA-HRT-17-07*, Federal Highway Administration, Washington, VA, 2018.

Composition and microstructure stability of cement compound under cyclic hydrothermal condition

Hongwei Tian[1], Marieke Voigt[2], Christian Lehmann[1], Birgit Meng[2], Dietmar Stephan[1]
1: Institute of Civil Engineering, Technische Universität Berlin, 13355, Berlin, Germany
2: Division 7.1 Building Materials, Bundesanstalt für Materialforschung und -prüfung (BAM), 12205 Berlin, Germany

1 Discussion

Thermal storage has been considered as a promising approach to realize energy recirculation, real-time supplement, and efficient utilization. This research aims to find an appropriate mixture composition for the construction of accumulator with the purpose of thermal storage where hot water is used as storage medium and the highest operating temperature can reach 200 °C. The cement compound used in this study is Nanodur® Compound 5941 by Dyckerhoff GmbH, produced for simple production of UHPC which contains 59 wt. % CEM II/B-S 52.5 R and 41 wt. % fine quartz powder. There are three series of samples tested in this research, NC, FNC20, and FNC40 referring to pure Nanodur® Compound 5941, the compound with 20 wt. % and 40 wt. % fly ash respectively.

Mineralogical analysis

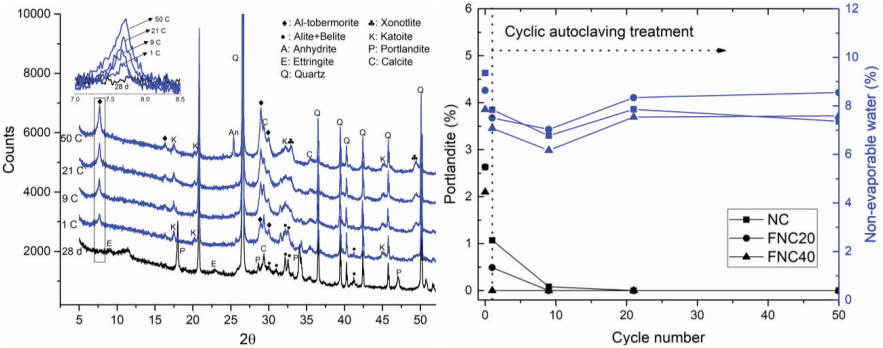

(a) (b)

Fig. 1 Influence of cyclic autoclaving treatment on composition stability (a. XRD results of FNC20 and b. TGA analysis)

Once autoclaved by cyclic hydrothermal treatment (200 °C, 15.5 bar and 6 h for one cycle), the phases formed show a great difference compared with the samples cured at standard condition. As for NC samples, the peak of portlandite disappears after 9 cycles while it is only 1 cycle for F20 indicating the strong pozzolanic reaction between portlandite and silica and the addition of fly ash accelerates the consumption of portlandite. Conversely, there are also some new phases formed. Xonotlite gradually grows and dominates in NC samples after 50 cycles while Al stabilized tobermorite (Al-tobermorite) governs in FNC20. Furthermore, Al-tobermorite grows faster and keeps stable after 21 cycles in FNC40 compared with that in FNC20 implying that sufficient Al supplied by fly ash favours the Al-tobermorite formation. Besides, katoite [$Ca_3Al_2(OH)_{12}$] also forms and is more evident in the samples with fly ash probably because the incorporation of fly ash supplies excess Al. It is reported that ettringite will decompose into monosulfate phase and then into hydrogarnet and insoluble anhydrite β-$CaSO_4$ [1] which are both detected in our study and keep stable within the tested cycles.

The results shown in Fig. 1(b) are extracted from the thermogravimetry (TG) curves which are not present here. As for the samples subjected to autoclaving treatment, the content of

portlandite in NC samples decreases and then disappears completely after 21 cycles while it depletes after 9 cycles for FNC20 and only 1 cycle for FNC40 indicating the accelerating effect introduced by fly ash. The content of non-evaporable water (NEW) which is generally used to evaluate hydration degree also decreases in the first 9 cycles probably because on one hand the amorphous C-S-H bound with a large number of water converts into crystalline phases losing the redundant water; on the other hand, the pozzolanic reaction accelerated by high temperature and/or fly ash releases some bound water from portlandite. In the subsequent autoclaving, the content of NEW starts to increase indicating that the hydration continues and more hydrates form which can be also verified by XRD results. We can see that the NEW content of pure samples is slightly lower than that of FNC20, but larger than that of FNC40 which is believed to originate from that the NEW content of xonotlite dominated in NC series is much lower than that of tobermorite and the large replacement by fly ash reduces clinkers content. It should be noted that the NEW content barely changes after 21 cycles for FNC20 and FNC40 indicating a relatively stable composition.

2 Final comments

Although xonotlite has better thermal stability, its strength and impermeability are generally weaker than that of tobermorite [2]. Incorporation of aluminous components such as fly ash should be a complementary method for cement paste served in such severe condition as Al-tobermorite has not only decent thermal stability but also high strength and low permeability. It seems that FNC40 has the better composition in this study concerning that the Al-tobermorite in this sample grows faster and stronger, and keeps stable after reaching the maximum value. Besides, in order to confirm the best composition, the samples with larger dosage of fly ash and other kinds of supplementary cementitious materials also need to be tested. It should be mentioned that the existence of excess Al or fly ash will lead to considerable formation of hydrogarnet which is unfavorable for strength and anti-permeability.

3 Conclusions

In the presence of sufficient fly ash, Al-tobermorite dominates in the sample subjected to cyclic hydrothermal condition rather than xonotlite. The hydration of cement compound proceeds further in hydrothermal environment as the content of chemically bound water increases after an initial decrease. However, the phases in the sample incorporated with 40 wt. % fly ash barely changes after 21 cycles indicating a relatively stable composition.

References

[1] V. SATAVA, O. VEPREK, Thermal Decomposition of Ettringite Under Hydrothermal Conditions, Journal of the American Ceramic Society 58 (1975) 357–359.

[2] P.C. Hewlett (Ed.), Lea's Chemistry of Cement and Concrete (Fourth Edition), Butterworth-Heinemann, Oxford, 1998.

Experimental resistance of composite UHPFRC-RC beams under impact

Carlos Zanuy, Gonzalo S.D. Ulzurrun
Dept. Continuum Mechanics and Structures, Universidad Politécnica de Madrid, Spain

1 Introduction

Strengthening of reinforced concrete (RC) with a thin tensile layer of ultra-high performance fiber-reinforced concrete (UHPFRC) is an efficient structural concept under quasi-static loading scenarios. Because of its excellent tensile properties, UHPFRC has an interesting potential for high-energy solicitations like impacts. So far, research on UHPFRC-RC beams under impact has focused on the application of the UHPFRC as a thin overlay, whereby the UHPFRC mainly works as a protective layer in charge of receiving the impact [1]. In the present contribution, it is analyzed how the UHPFRC tensile layer can improve the impact performance of RC.

2 Experimental research and results

Impact tests have been carried out on 6 configurations of UHPFRC-RC beams (Figure 1a). Two series were tested, without and with stirrups (Φ8 @ 150 mm), named RC- and RCS- samples respectively. The former are shear-critical and the latter are flexure-critical under quasi-static loading. Each series included unstrengthened (h_U = 0 mm) and UHPFRC-strengthened (h_U = 35 and 55 mm) beams, with 2 specimens of each type. The UHPFRC consisted of CRC (portland cement- and microsilica-based dry mortar premix including dry superplasticizer and fines of 4 mm maximum size) supplied by Hi-Con A/S, with 2% by volume of 12.5 mm straight steel fibers.

Previous research on RC structures [2] has shown that impact loading leads to two types of diagonal cracks, even for flexure-critical members: a shear plug at the midspan (type I cracks) and flexure-shear cracks between the midspan and the supports (type II). Type I cracks are due to the local effect produced by the projectile upon impacting, while type II cracks are a result of the global beam behavior once the impact and inertia forces have propagated to the supports.

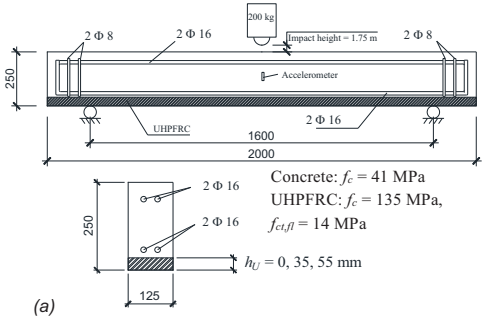

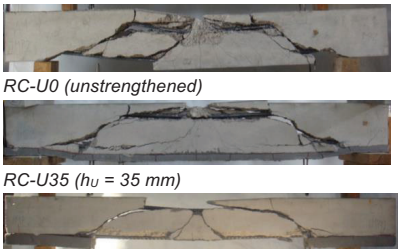

Figure 1: (a) Test configuration and geometry (in mm); (b) Crack pattern of shear-critical beams after impact.

The crack pattern at failure of RC-series (Figure 1b) demonstrates that both types of shear cracks formed in the present tests. For RC-U0, multiple type I and II cracks, spalling and fragmentation produced the collapse. Large concrete cover pieces were split out, leading to debris, which is an undesirable hazard for structures protecting humans or goods. The addition of a 35 mm UHPFRC was very positive: even though both type I and II cracks were visible, the UHPFRC layer kept the integrity and reduced debris. According to video records, the UHPFRC provided a resisting mechanism by working as a kind of stress ribbon able to withstand the

damaged RC above it. In contrast, specimens with a 55 mm UHPFRC layer behaved worse, as the UHPFRC between the type II cracks was spalled. It has to be noted that the UHPFRC-RC interface of RC-U55 beams was at the level of the longitudinal reinforcement, which might have decreased the interfacial strength with respect to that of RC-U35 beams. The smaller concrete-to-concrete area of RC-U55 beams was not enough to resist the bottom-up reflected tensile wave induced by the impact. The debris can be evaluated by means of the mass loss produced by the impact, which was on average: -16% (RC-U0), -9% (RC-U35), -20% (RC-U55).

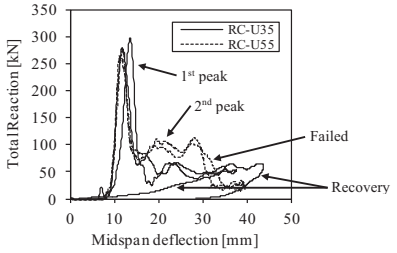

(a)

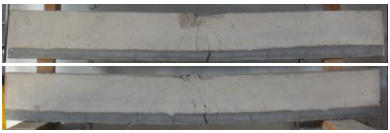

RCS-U55 (h_U = 55 mm)

(b)

Figure 2: (a) Total reaction-midspan deflection curve of shear-critical beams; (b) Crack pattern of RCS-U55.

The global behavior can be also studied from the load-deflection diagrams derived from dynamic measurements (Figure 2a). The 1st peak, which corresponds to the initial local effect and type I cracks, was similar for both series because it is governed by the contact condition between the projectile and the specimens. The 2nd peak is related with the global response and type II cracks. Thus, it can explain the different behavior of RC-U35 and RC-U55 beams: on the one hand, the 2nd peak load of RC-U35 was almost 2 times that of RC-U55; on the other hand, the 2nd peak ends with different slopes for RC-U35 and RC-U55: positive stiffness and negative stiffness, respectively. The former has been associated to residual strength in previous tests [3], which agrees with the integrity shown by the UHPFRC layer in RC-U35 beams.

The stirrups of RCS-series have improved the impact strength in two ways: 1) controlling the full propagation of type I and II cracks, 2) avoiding the debonding at the UHPFRC-RC interface of beams with 55 mm UHPFRC layer (Figure 2b).

3 Conclusions

Strengthening of RC beams with a thin UHPFRC tensile layer can improve the impact strength. An additional contribution was provided by the UHPFRC by working as a stress ribbon which reduces debris generation. The UHPFRC-RC interface should not be placed at the level of the reinforcement in order to avoid interfacial debonding. Otherwise, it is recommended to use shear reinforcement to avoid debonding.

Acknowledgements

Following supports are appreciated: Spanish ministry for science (Project ID BIA2016-74960-R AEI/FEDER, UE); Hi-Con A/S (Denmark); “Fundación José Entrecanales Ibarra”.

References

[1] Habel, K.; Gauvreau, P.: Behavior of reinforced and posttensioned concrete members with a UHPFRC overlay under impact loading. *Journal of Structural Engineering* 135, p. 292-300, 2009.

[2] Yi, W.J.; Zhao, D.B.; Kunnath, S.K.: Simplified approach for assessing shear resistance of reinforced concrete beams under impact loads. *ACI Structural Journal* 113, p. 747-756, 2016.

[3] Zanuy, C.; Ulzurrun, G.: Residual behavior of reinforced SFRC beams damaged by impact. *Structural Concrete* 20, p. 597-613, 2019.

Thermoplastic reinforcement for Ultra-High Performance Concrete panels

Reagan M. Smith Gillis[1], Todd S. Rushing[2], Roberto Lopez Anido[1], Eric N. Landis[1]
1: Advanced Structures & Composites Center, University of Maine, USA
2: Geotechnical and Structures Laboratory, U.S. Army Engineer Research and Development Center, USA

1 Introduction

Recent studies investigating the impact performance of ultra-high performance concrete (UHPC) report a quasi-brittle flexural failure that transitions to a brittle punching-shear failure as the size of the impact head is reduced [1]. In the study presented here, E-glass fiber reinforced thermoplastics were investigated as a potential reinforcing material to shift the failure mechanism and improve toughness. The advantages of the thermoplastic composites include rapid fabrication, automated manufacturing and weldability with other thermoplastics.

2 Materials and Methods

Sixteen 305 x 305 x 12 mm UHPC panels were fabricated using the mix shown in Table 1. This mix produced a concrete with a compressive strength of 200 MPa. The UHPC was reinforced by 12 mm by 0.2 mm-diameter brass-coated steel fibers at a volume fraction of 1.5%. Half of the panels included a small addition of cellulose nanofibrils (CNFs), which were added as a way to potentially improve toughness of the UHPC matrix.

Table 1: UHPC Constituents and proportions.

Table	Proportion by weight
Type I/II Portland Cement	0.384
Silica fume	0.067
Silica sand (max. size 0.6 mm)	0.475
Water	0.068
Water reducing admixture	0.006

Two systems of thermoplastic reinforcement were investigated: thermoforming and vacuum infusion. For thermoforming, the UHPC panels, a collection of fiber reinforced pre-impregnated tapes, and a layer of thermoplastic resin were heated and pressed (consolidated) with a hydraulic actuator. Upon cooling the multiple layers of thermoplastic tapes formed into a complete laminate that was fully bonded to the UHPC core. The second system to reinforce the UHPC was vacuum infusion using a two-part liquid thermoplastic resin-system and a woven roving fabric. Details are presented in [2].

For mechanical testing, the panels were quartered into nominal 150 x 150-mm specimens, which were subjected to both quasi-static and low-velocity impact testing. In both tests, panels were simply supported on all four sides, and loaded at the panel center with a 16-mm diameter hemi-spherical load head. For brevity, only the impact tests are presented here. Force was measured during the test using a dynamic load cell in the impact head, and midspan deflection was measured using an in-line position sensor. Specimens were subjected to impact energies of either 16, 24, 32, or 40J.

Panel damage from the impact tests was quantified by loading the specimen in a load frame before and after impact test. This was done so that both the change in specimen compliance and the residual deformation after impact could be measured. An example illustrating this procedure is shown in Fig. 1.

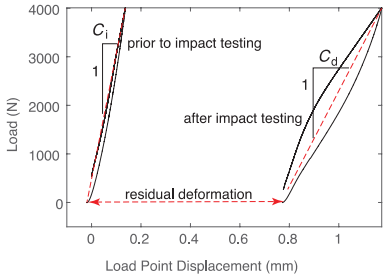

Figure 1: Illustration of terms used in damage assessment. C_i is initial compliance; C_d is damaged compliance.

3 Results and Conclusions

Fig. 2 illustrates the results of impact tests for panels subjected to an energy of 16 J. The plots illustrate damage observations made for all impact energies. In general, the addition of the thermoplastic reinforcement not only significantly reduces residual deflection and change in compliance (between 80 and 95%), but also significantly reduces the variability of damage. The addition of CNF to the UHPC mix had little to no effect on performance. Perhaps most significantly, there is little to no performance difference between the thermoformed reinforcement and the vacuum-infused reinforcement. The significance is that the thermoformed approach is far simpler to implement, and is more easily scaled up to larger panel sizes and to a more rapid fabrication process.

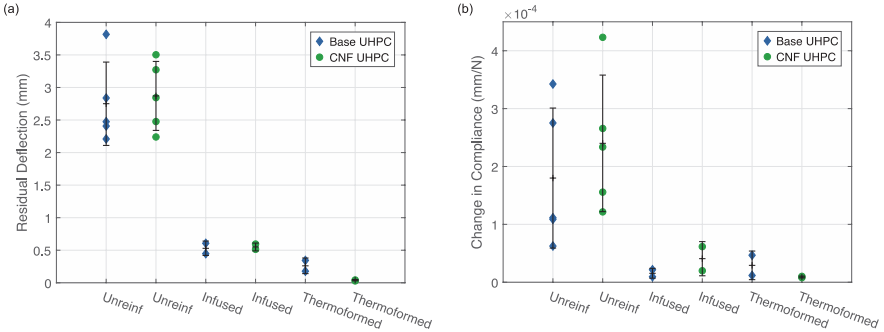

Figure 2: Results of impact tests at 16 J: (a) residual deformation; (b) change in specimen compliance.

The research results suggest that performance gains from the thermoplastic reinforcement warrant additional development steps, including optimizing the concrete/FRP bond, and developing an appropriate material model that will allow refinement of both FRP fiber layups and processing parameters for additional performance improvements.

References

[1] Ranade, R.; Li, V.C.; Heard, W.F.; Williams, B.A.: Impact resistance of high strength-high ductility concrete, Cement and Concrete Research 98 (Supplement C) (2017) 24 – 35. doi:10.1016/j.cemconres.2017.03. 013.

[2] Smith Gillis, R.: Development of thermoplastic composite reinforced ultra-high performance concete panels for impact resistance, MS Thesis, Civil Engineering, University of Maine, 2017.

Innovative UHPC-NSC composite members as substitution for structural steel

Goran Vojvodic, Duc Tung Nguyen, Viet Tue Nguyen
Institute of Structural Concrete, Graz University of Technology, Austria

1 Introduction

Considering that the compressive strength of UHPC nearly reaches the strength of conventional construction steel, a substitution of steel by UHPC in specific structural elements such as NSC composite members, could be possible. In this context, this contribution presents an experimental investigation on UHPC-NSC composite members, in which UHPC was used instead of conventional construction steel. As first composite member a UHPC hollow box girders were considered as a substitution for steel girders in composite superstructure of single span bridges with a span up to 30 m. Prefabricated, slender, thin-walled UHPC box girders beams are prestressed by pre-tensioning and supplemented by NSC slab as deck layer cast in place. The second member, a UHPC-NSC composite column, consisted of a precast spun NSC shell and a UHPC filled core. The spun NSC shell served both as the fire protection layer and a load-bearing element.

2 UHPC-NSC hollow box girder

The developed precast UHPC hollow box girder for composite bridge superstructures consist of thin deck slab, thin webs and thicker bottom slab. Pretension strands are mostly arranged in the bottom slab, a small number are also arranged in the deck plate, in order to prevent cracking of the deck plate during the prestressing. For simple construction and to keep the thickness of all sectional elements thin, the girders were designed without conventional reinforcement. Due to this a high amount of micro steel fibre is required in order to avoid the formation of splitting cracks due to the transfer of prestressing forces.

Fig. 1 shows as an example of construction with UHPC box girders.

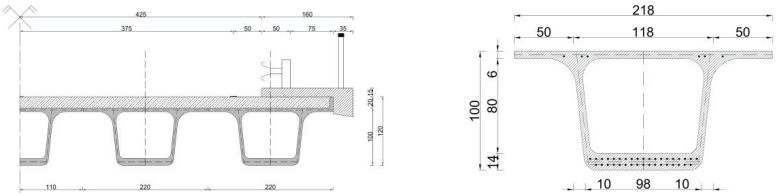

Figure 1: Possible bridge construction made of several UHPC box girder (left) and corresponding girder cross section for a bridge span of 30 m (right)

In order to investigate the load bearing behavior of hollow box girder and to valid prestressing test results, a 1:2 scaled UHPC hollow box girder was cast in a precast plant and tested. A self-developed fine grain UHPC mixture with the compressive strength higher than 180 N/mm^2 after 28 days without heat treatment, self-compacting properties and the Young's modulus of approx. 54000 N/mm^2 was used. The UHPC matrix tensile strength was approx. 8.5 N/mm^2 and the post-cracking tensile strength was amount to 9.0 N/mm^2. The steel fibers had a tensile strength of approx. 3800 N/mm^2 and are structured and brass-plated to improve the bond behavior, with a maximum fibre amount of 2% by volume. The prestressing strands were 0.62", 7-wire strands with a cross-section area of 150 mm^2, steel grade 1660/1860 N/mm^2 and the nominal diameter d_n of 15.7 mm.

Fig. 2 shows the tested 7 m long UHPC box girder at bearing load with corresponding cracks.

Figure 2: Specimen at bearing load (left) and corresponding bending cracks (left) from measurement with the digital image correlation system

The UHPC hollow box girder reached the bearing capacity at 950 kN when a ductile bending behaviour occurred. Clearly visible was the specimen stiffness declination at approximately 550 kN with increasing number of bending cracks. Besides the opening of bending cracks at mid span of bottom slab and webs, the shear cracks in girder webs were observed. The first shear cracks were observed at about 650 kN. No slip between strand and concrete as well at the joint between NSC and UHPC was detected, also no torsion effect through possible stiffness decline on one girder side.

3 UHPC-NSC composite column

At this innovative composite column, UHPC core is cast in a spun NSC shell and serves as the single load-bearing element in the fire design situation. The NSC shell serves primarily as fire protection layer and secondly as load bearing element in normal design situation. Besides, it is used as formwork for the UHPC core. In contrary to conventional steel-NSC composite columns, where the profiled steel core can reach its compressive strength at the maximum loading by crushing of the NSC, attentions should be paid to considerable difference in the axial strain by reaching the compressive strength between UHPC and NSC in UHPC-NSC composite columns.

Fig. 3 shows cross section of UHPC-NSC composite column and typical failures occurred.

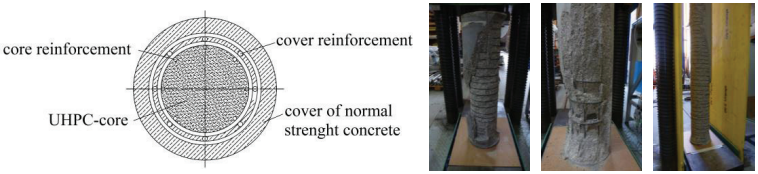

Figure 3: Schematic cross section of UHPC-NSC composite column (left) and typical failures (right)

The experimental program had three parts. In first part, 13 UHPC columns were tested in order to investigate the effectiveness of the fibre and transversal reinforcement regarding load bearing capacity and confinement action. At the second part, 18 short UHPC-NSC composite columns were tested. The distribution of longitudinal and transversal reinforcement was varied in order to identify the appropriate reinforcement arrangement regarding confinement and ductility. At third part, 3 UHPC-NSC composite columns with larger column length were tested in order to verify applicability for building construction columns.

For a core self-developed coarse grain UHPC mixture with the compressive strength higher than 180 N/mm^2 after 28 days without heat treatment and without self-compacting properties and for a shell a C 50 / 60 was used. The failure of UHPC-NSC composite columns occurred very ductile with the spalling of NSC cover.

4 Conclusions

An experimental investigation on presented innovative UHPC-NSC composite structures pointed out that both structural composite members showed excellent composite action.

Resistance to high velocity projectile impact: A comparative investigation of UHPFRC, FRHSC, and SHCC

Rui Zhong, Fengling Zhang, Leong-Hien Poh, Shasha Wang, Hoang Thanh Nam Le, Min-Hong Zhang

Department of Civil and Environmental Engineering, National University of Singapore, Singapore

1 Introduction

Previous studies have indicated that several parameters affect the concrete resistance to high velocity projectile impact (HVPI) including compressive strength and coarse aggregate among others. On the one hand, the significantly higher compressive strength of ultra-high performance fiber reinforced concrete (UHPFRC) under quasi-static state suggests its enhanced effectiveness against HVPI over fiber reinforced high strength concrete (FRHSC) and strain hardening cement-based composites (SHCC). On the other hand, elimination of coarse aggregates from UHPFRC and SHCC may undermine their ability to resist HVPI. The intrinsic advantages and drawbacks of individual advanced cement composites raise a question: which of these advanced cement composites is the most effective one when penetration resistance against HVPI is of concern. This study provides preliminary experimental data and insights into this question.

2 Experimental Program

Two proprietary UHPFRCs, three FRHSCs, and two SHCCs were examined in this study. The mixture proportions of these materials are provided in Table 1.

Table 1: Mix proportions of different advanced cement composites

Mix	*w/cm*	*C*[1]	*SF*[2] *or FA*[3]	*W*[4]	*CA*[5]	*S*[6]	*SPL*[7]	*f*[8]	*PE*[***]	*PVA*[****]
UHPFRC-S	Proprietary							3.0% (SS1-3)[*]	-	-
UHPFRC-A								3.0% (HS)[**]	-	-
FRHSC-60	0.50	410	-	205	946	760	3[b]	0.5% (SS4)[*]	-	-
FRHSC-85	0.35	480	-	168	946	776	10[b]	0.5% (SS4)[*]	-	-
FRHSC-110	0.28	450	45[2]	139	946	772	10[c]	0.5% (SS4)[*]	-	-
SHCC-ST+PE	0.25	1478	148[2]	414	-	-	17[b]	0.5% (SS4)[*]	1.5%	-
SHCC-PVA	0.25	587	704[3]	323	-	469[a]	10[c]	-	-	2%

[1]Cement; [2]Silica fume; [3]Fly ash; [4]Water; [5]Coarse aggregate; [6]Sand; [7]Superplasticizer; [8]Steel fiber; [a]Maximum size 0.25 mm; [b]Naphthalene based; [c]Polycarboxylate based; *Straight; **Hook-end; ***Polyethylene fiber; **** Polyvinyl alcohol fiber

The dimensions of the HVPI test specimens were 600×600×400 mm. A large gas gun facility (Figure 1) and non-deformable ogive-nosed projectiles (Figure 2) weighing about 250 g were utilized for the HVPI tests with impact velocity of approximately 400 m/s. The detailed experiment method can be found in Wang et al. [1]. In this preliminary study, emphasis is placed on the depth of penetration (DOP) which is defined as the distance from the impact surface to the deepest point in the crater.

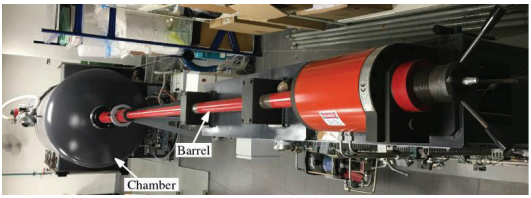

Figure 1: Large gas gun facility

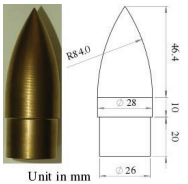

Figure 2: Details of the projectile

3 Results and Discussion

The dependency of the DOP on the compressive strength f_c for these advanced cement composites is illustrated in Figure. 3a. In contrast to previous results for normal concrete (NC) which typically show a monotonic decrease in the DOP with increasing f_c, a turning point is observed at approximately 90 MPa after which no appreciable decrease in DOP is observed as f_c increases. This suggests mechanisms other than f_c that determine the DOP of concrete subjected to HVPI. It is generally accepted that f_c alone cannot adequately describe the DOP. The compositions of concrete, such as coarse aggregate, also play an important role. It is also observed that commonly used empirical equations [1] for the prediction of DOP may not be applicable to these advanced cement composites as indicated by the generally large deviations from experimental results. This may be explained by the fact that these equations are calibrated using test data on NC which typically has lower f_c and includes coarse aggregate.

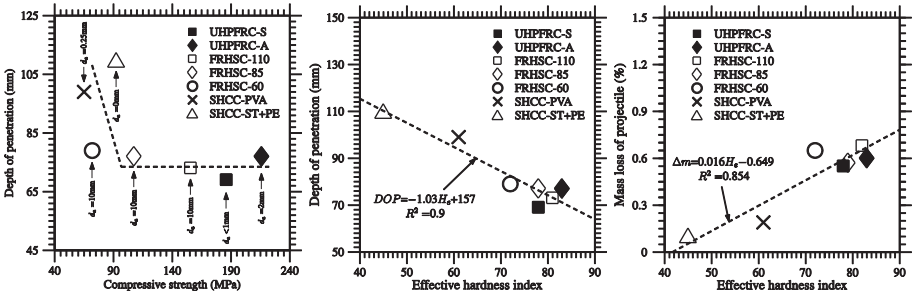

(a) DOP vs f_c (b) DOP and Δm vs H_e (c) DOP vs Δm

Figure 3: The relationship between f_c, H_e and DOP or projectile mass loss Δm.

Figure 3b illustrates the dependency of the DOP on the effective hardness H_e, calculated by the weighted Rockwell hardnesses of matrix and coarse aggregate in concrete according to their idealized relative fractions along the projectile trajectory. Detailed derivation can be found in Wang et al. [1]. A good linear relationship between the DOP and H_e is observed. This is ascribed to the fact that H_e accounts for the influence of both mortar and coarse aggregate. Higher H_e due to the incorporation of coarse aggregate led to improved resistance against HVPI. The improved resistance may also be ascribed to more severe abrasion between the coarse aggregate and projectile as indicated by the increase in projectile mass loss with H_e (Figure 3c).

4 Conclusions

Preliminary experimental results for a comparative study on the resistance of UHPFRC, FRHSC, and SHCC to HVPI indicate that the decrease in DOP with the increase in f_c is not monotonic. There is a turning point after which no further reduction is observed. In contrast, there exists a close correlation between effective hardness and DOP. The improved resistance to HVPI with increased H_e may be ascribed to the incorporation of coarse aggregate and more severe abrasion between the coarse aggregate and projectile.

References

[1] Wang, S.; Le, H.T.N.; Poh, L.H.; Feng, H.; Zhang, M.H.: Resistance of high-performance fiber-reinforced cement composites against high-velocity projectile impact. Int. J. Impact Eng. 2016, 95: 89-104.

Development of cost-efficient UHPC with local materials in Colombia

Joaquín Abellán[1,3], Andrés Núñez[2], Nancy Torres[3], Jaime Fernández[4]

1: PhD Candidate, Department of Civil Engineering, Polytechnic University of Madrid (UPM), Madrid, Spain.
2: Cementos Argos SA, Medellín, Colombia.
3: Department of Materials and Structures, Escuela Colombiana de Ingeniería Julio Garavito, Bogotá, Colombia.
4: Department of Civil Engineering, Polytechnic University of Madrid (UPM), Madrid, Spain.

1 Introduction

Compared with normal strength concrete, ultra-high-performance concrete (UHPC) is characterized by high particle packing density, combined with the use of superplasticizer to reduce the water-to-cementitious materials ratio. These extremely low porosity and low permeability characteristics of UHPC give it improved durability and mechanical properties over other types of concrete [1] [2].

However, in terms of sustainability and cost, this class of material must still be evaluated regarding its value of the higher average dosage of binder compared to regular concrete.

The research program reported on herein was aimed at determining eco-friendly UHPC dosages in which the cement content was kept as low as possible while reaching compressive strength al 28 days (R28) over 150 MPa using local available components in the Colombian market and without using any heat treatment.

2 Materials

The materials used to manufacture the concrete were local available in Colombia. In all dosages, ASM Type HE cement (C), 100 kg/m^3 of silica fume (SF), silica sand (SS) with maximum particle size of 600 μm, tape water and polycarboxylate-ether-superplasticizer (HRWR), were used. As suppelementary cementitious materials (SCM) several options were tested: Electric Arc Slag Furnace (EASF), Ground Granulated Blast Slag Furnace (GGBSF), Limestone Powder (LP), Micro-Limestone Powder (MLP), Recycled Glass Powder (RGP), Recycled Glass Flour (RGF), local high unburned carbon fly ash (FA), and fluid catalytic cracking catalyst residue (FC3R), as partial substitution of cement and silica fume. A reference dosage without restrictions in the amount of silica fume which doesn't use any of the SCM aforementioned, was used as reference.

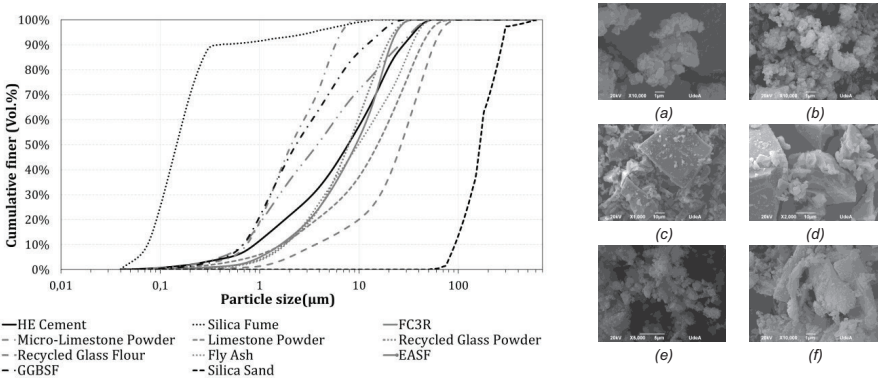

Figure 1: On the left: Particle size distribution of the components used in this research. On the right FSEM of several supplementary cementitious materials used: a)FC3R, b)MLP, c)RGP, d)RGF, e)EASF, and d)FA.

3 Mixture design and results

Statistical tools such as Design of Experiments (DoE) and multiobjective optimization were used to better adjust the goal of compressive strength while using the less amount of cement and maintaining the mixture in a reasonable cost. The factors analysed in each combination of components were cement content in kg/m^3 (Factor A), water to binder ratio (Factor B) and percentage of superplasticizer in volume used (Factor C). The rest of components were adjusted to the A&Amod curve using q=0.264 [3]. The optimization was based on the desirability approach developed by Derringer and Suich [4]. In every combination an 18-run DoE was used. The combinations analysed are depicted in Table 1 as well as their mathematical optimization and the respective experimental verification.

Table 1: Combinations analysed in the research. COP = Colombian Pesos. R28 in MPa. Cement in kg/m^3

DoE	SCM	Cement	w/b	HRWR	Model R28	Experimental R28	Cost/m^3 *(x1000COP)*
REF	-	870	0.191	3.05%	174	170	1350
DoE01	LP+MLP+EASF	651	0.161	2.62%	155	152	900
DoE02	RGF+MLP+EASF	621	0.164	2.55%	158	156	848
DoE03	RGP+MLP+FC3R	654	0.172	2.83%	153	150	900
DoE04	RGF+RGP+MLP	603	0.165	2.05%	155	152	809
DoE05	MLP+RGF	590	0.163	2.11%	157	155	806
DoE06	MLP+FA	711	0.168	2.86%	151	148	890
DoE07	GGBFF+RGF	674	0.164	2.57%	153	157	841
DoE08	GGBSF+RGP+RGF	681	0.166	2.28%	152	151	876

4 Conclusions

Based on the obtained results from this analysis, the following conclusions can be drawn: (i) Partial substitution of cement and silica fume is possible with different options, however there is a drop in the resistance in all cases;(ii) limestone powder and especially recycled glass allow to reduce the superplasticizer content which has a notable impact on the final cost;(iii) local fly ash dosage presents the greater need for cement due to the high unburned carbon obver 12%;(iv) lower final cost an cement content is achieved when blending micro-limestone powder and recycled glass flour as partial substitution of cement and silica fume.

References

[1] Soliman, N. A. and Tagnit-Hamou, A., “Using particle packing and statistical approach to optimize eco-efficient ultra-high-performance concrete”, ACI Mater. J., vol. 114, no. 6, pp. 847–858, 2017. doi: 10.14359/51701001.

[2] Abellán, J., Fernández, J., Torres, N., and Núñez, A.“Statistical Optimization of Ultra-High-Performance Glass Concrete,” ACI Mater. J., vol. 117, no. M, pp. 1–12, 2020. doi: 10.14359/51720292

[3] Abellan, J., Torres, N., Núñez, A. and Fernández, J. ,“Influencia del exponente de Fuller, la relación agua conglomerante y el contenido en policarboxilato en concretos de muy altas prestaciones”, in IV Congreso Internacional de Ingenieria Civil, La Havana, Cuba, 2018.

[4] Derringer, G., & Suich, R. “Simultaneous Optimization of Several Response Variables.” Journal of Quality Technology, 21(4), 214–219, 1980.

High Performance (HPC) Concrete with construction and demolition wastes (CDW) implemented in prefabricated sandwich panel

Miguel Prieto[1], Linus Brander[1], Mathias Flansbjer[2], Urs Mueller[1]
1: RISE Research Institutes of Sweden, CBI Swedish Cement and Concrete Research Institute, Borås, Sweden
2: RISE Research Institutes of Sweden, Mechanics Research, Borås, Sweden

1 Introduction

Within the scope of EU funded RE4 project [1] a high-performance concrete (HPC) together with a self-compacting concrete (SCC) based on ordinary Portland cement and mineral construction & demolition waste (CDW) aggregates were developed to be used in a concrete sandwich panel. The sandwich panel had an inner layer of 120 mm of SCC CDW concrete with reinforcing steel, combined with a layer of PE-PIR insulation of 60 mm and an external layer of 40 mm thickness of HPC CDW concrete reinforced with 1 layer of carbon textile reinforcement.

2 HPC CDW concrete development

The HPC requirements were C60/75 strength class, SF1 slump flow class and 15 MPa of cubic concrete compressive strength at 16 hours in order to be demoulded from the tilting table. For the SCC concrete all requirements were identical except for the concrete strength class that was C40/50. Due to the production site of the concrete elements (Creagh Facilities in Northern Ireland), CDW aggregates used came from 2 different sources. The CDW fractions consisted of concrete, stone, bricks, glass, ceramics, etc. The initial development of the HPC mix was performed with CDW coming from Southern Europe (SE) with 0/2 and 2/8 fractions. The HPC CDW SE was casted with 655 kg/m^3 of CEM I 52 R, fly ash and silica fume. The aggregate replacement level of CDW was 90% and the flow was 600 mm with a mean compressive strength of around 80 MPa. For the upscaling of the elements, the CDW aggregate came from United Kingdom (UK) with 0/4 and 4/10 fractions. The HPC CDW UK was casted with 725 kg/m^3 of CEM I 42.5 R, fly ash and silica fume. The replacement level achieved was 50% due to poorer quality of the CDW and also the compressive strength at 28 days was around 70 MPa. In addition, the flow obtained was 800 mm. Both concretes achieved the 15 MPa requirement at 16 hours, but the compressive strength of HPC SE CDW was around 45 MPa compared to HPC UK CDW that was 21 MPa.

3 Mechanical performance of HPC layer and sandwich panel

For the investigation of flexural properties of the HPC layer using carbon textile reinforcement, 4-point bending tests were performed. Three specimens for each type of panel were tested, which consisted of a reinforced panel shape in the size of 700 mm x 100 mm with 2 different thicknesses (30 and 40 mm) and 1 or 2 layers of carbon textile reinforcement.
It can be observed that that with one layer carbon textile reinforcement (30 and 40 mm thickness) following the initial cracking, multiple crackings are formed and stabilized and afterwards the mechanical properties are mainly governed by the textile reinforcement. In the case of the two-layer carbon textile reinforcement (30 and 40 mm thickness) there is no multiple crack formation but only a discrete crack with a higher load compared to the test results of one-layer reinforcement followed by a huge drop in the load afterwards. This is a more brittle behaviour than the observed in the one layer specimens.

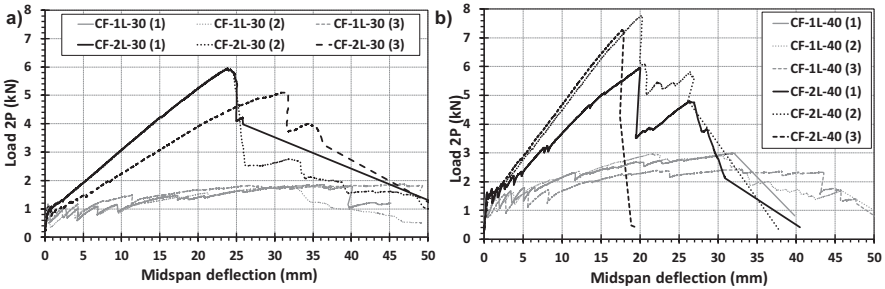

Figure 1: Load vs displacement of 1 and 2 layer carbon textile with: a) 30 mm thickness; b) 40 mm thickness.

The mechanical overall performance of the sandwich panels was analized with 4-point bending tests. The panel dimensions were 2.5 m. long, 1.0 m. width and 0.22 m thick. The connection between layers was achieved by MC/MS series pin connectors from Thermomass every 350 mm. Two Sandwich panels were casted with one-layer textile reinforcement and the other with 2 layers of carbon textile reinforcement and all 3 specimens were casted with a HPC layer of 40 mm thickness.

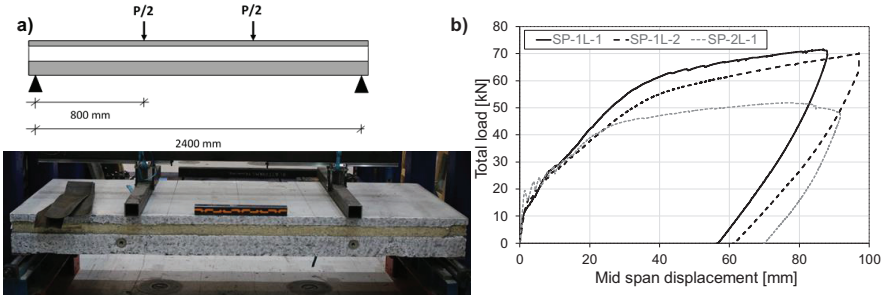

Figure 2: a) Schematic of 4-point bending test and photograph; b) Load vs displacement of tested specimens

The results of these tests were also useful to determine the bending stiffness, cracking moment and bending moment resistance of the developed elements. After the initial cracking was reached in all specimens, the ones with one-layer textile (SP-1L) had a strain hardening behaviour with an increase in the load, reaching a 20 % higher load than if the specimens worked with only the inner layer (non-composite behaviour). On the other hand, sandwich panel with 2 layers of textile reinforcement (SP-2L) worked like a non-composite panel probably caused by the behaviour of the 2 layers of textile reinforcement not letting work properly the pin connectors.

4 Concluding remarks

The use of HPC concrete with a high replacement level of CDW aggregates was achieved obtaining adequate compressive strength and good workability. Moreover, the implementation of the HPC in the external layer of sandwich panel combined with one layer carbon textile reinforcement showed a good performance according to the mechanical tests performed. This sandwich panel is already placed at the mock-up building of RE4 project in Madrid (Spain).

References

[1] RE4 project, www.re4.eu.

Use of resource-saving, finely grained recycling calcium silicate units filler in UHPC

Tim Schade[1], Wolfgang Eden[2], Bernhard Middendorf[1]
1: Institute of Structural Engineering, Department of Building Materials, University of Kassel, Germany
2: Forschungsvereinigung Kalk-Sand e.V., Hannover, Germany

1 Theoretical basics and target idea

The global construction boom is associated with a large amount of resource consumption. Due to the economically significant production and processing of the raw materials, the construction industry is more resource-intensive than any other sector. Moreover, in the construction industry an upcoming shortage of sand is expected. As a result, a very large market results for demolished building materials and thus also for recycled aggregates [1]. Consequently, the recycling of concrete in pure form has been regulated in a normative manner in recent years. Nevertheless, there are still problems with the reuse of masonry building materials from building construction. Recycled calcium silicate units (CS-units) belong to the masonry building materials and consist of a compound of CS-units and adhering plaster and mortar. This plaster and/or mortar almost always consists of cement and/or lime cement.

While coarse recycling aggregates are generally accepted by the market in their pure form, the use of finer recycled aggregates < 4 mm is not yet widespread; for example, these finer aggregates are only used in mixed material quality for backfilling earthworks (downcycling) or are sent to landfill in large quantities. In general, fine-grained fillers are added to concrete to achieve special requirements. Quartz powders are used especially in packing density-optimized systems. As an inert additive, they ensure a high packing density and are a component in the formulation of Ultra High Performance Concretes, UHPC.

In the context of this work, the acceleration effect of recycled fine grained CS-units is analysed. Thus, the resource intensive quartz powder was replaced by recycling material of fine grained CS-units. In addition, a positive effect of the fine Calcium-Silicate-Hydrate phases (CSH) on the reaction behavior was analysed. In further AiF projects [2] it was shown that fine CSH-phases in fillers will act as crystal seeds.

2 Methodological approach

Two different recycled CS-units as fillers were investigated to check the reactivity. Besides a pure CS-units recycling filler (A2), a building material with adhering plaster (A4) was grained and used as a filler in a well-known M3Q mixture (reference) developed at the University of Kassel [3]. The following investigations were carried out:

chemical mineralogical investigations
- X-ray powder diffraction (XRD)
- environmental scanning electron microscopy (ESEM)

physical investigations
- grain size distribution
- measurement of the released heat quantity using an isothermal calorimeter

mechanical investigations
- compressive strength.

3 Results

First, the particle size distribution of the used fillers was checked by means of laser granulometry. With the aid of precise grinding technology and the corresponding grinding time, a comparable particle size with regard to the quartz flour and the recycling filler was achieved. The grain size distribution of all samples was within d_{50}=15±1 µm.

The hydration tendency was checked by means of isothermal calorimetry. As suspected in advance, the use of recycling fillers as CSH seeds increased the hydration heat quantity after 24 hours from 53.3 J/g to 55-56 J/g, see crosses in figure 1. This property is also reflected in the compressive strength development. The compressive strength of the samples A2 and A4 increased about 3 MPa by the use of recycled CS-unit fillers compared to the reference mixture. However, after 28 days these differences in strength do not exist and the strength of the reference mixture is even higher (161.9 MPa compared to 151.3 and 154.1 MPa).

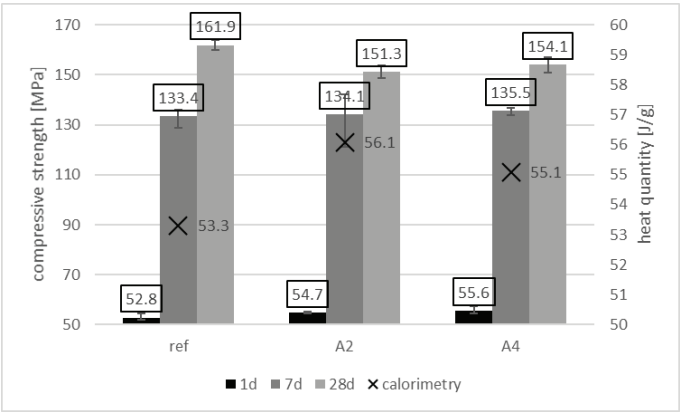

Figure 1: Compressive strength (related to the left axis) as well as the hydration tendency (right axis)

In addition, the samples were examined by XRD after 28 days. No foreign phases could be detected by the analytics.

4 Summary and outlook

The use of recycled and finely grained CS-units represent a promising method for the use in UHPC. Thereby, natural resources can be reduced. In addition, the use of CS-units recycling material leads to a CSH-seeds effect in the early hydration process. This effect is responsible for an improvement in the early strength.

References

[1] Deilmann, C.; Materialströme für den Hochbau, Forschung für die Praxis, Band 6, Zukunft Bauen, Bundesministerium für Bau-, Stadt, und Raumforschung, Berlin 2017

[2] Eden, W.; Middendorf, B.; Otten, S.; Einsatz von CSH-Phasen als Reaktionsbeschleunigern bei der Herstellung von Kalksandsteinen zur Reduzierung des Energieverbrauchs und der klimaschädlichen Emissionen - Teil 2, Forschungsbericht Nr. 125 der Forschungsvereinigung Kalk-Sand eV, Hannover, 2017.

[3] Schmidt, M.; Fehling, E.; Ultra high performance concrete (UHPC): 10 years of research and development at the University of Kassel - 10 Jahre Forschung und Entwicklung an der Universität Kassel, Kassel: Kassel Univ. Press, 2007.

Recycling of concrete fine from demolition

Simone Stürwald, Ronny Meglin, Susanne Kytzia
University of applied sciences Rapperswil, Institute for Civil and Environmental Engineering, Rapperswil, Switzerland

1 Introduction

In Switzerland, around 15 million tons of construction & demolition waste (C&DW) were produced in 2014 [1], of which approximately 7 million tons are concrete and mixed demolition waste (e.g. masonry). According recent studies [2], [3] the amount of construction waste from building construction will increase significantly due to a higher demolition and renovation ratio.

As result of the increasing amount of waste, the Federal Office for the Environment of Switzerland (FOEN) declared in 2016, that all waste such as municipal waste or construction and demolition waste "must be recycled or recovered for energy" [4]. Around 70-80 % of the overall C&DW, as of today, is recycled for building materials, while the rest is deposited or burned in waste incineration plants [1], [5]. However, most of the processed C&DW is "down-cycled" into materials with subordinate technical requirements such as lean concrete or as road subbase material [6]. One reason for the Downcycling is the crushed concrete sand with grain sizes smaller than 4 mm, the quality of the crushed sand has a significant influence on the possibilities of returning the crushed sand to cement and concrete production. It depends on the methods of concrete demolition treatment [7], [8]. Furthermore, the European Cement Research Academy [9] states, that the re-use of crushed concrete is a challenge due to the less favourable properties of the crushed concrete fines.

In this study, three technically viable applications of this crushed concrete sand are evaluated according to sustainability criteria with a focus on climate protection, resource conservation and waste avoidance. Possible applications of crushed concrete fine are: (i) as a raw meal substitute, (ii) as additives in cement mills or concrete production or (iii) as aggregates in concrete production.

Based on these interrelationships, an evaluation of the possible application of crushed sand represents an essential prerequisite for the development of suitable processing methods in order to obtain a high performance.

2 Methodology

To estimate the potential for the use of the crushed concrete fine, several testing methods and calculations will be used to determine the properties of real and laboratory samples.

Based on chemical analyses of the samples, simulations will evaluate the use of ground crushed sand in clinker production. The result of this step are statements as to whether the raw material can be used in clinker production. Mortar samples produced with the ground crushed sand as an additive will be subjected to tests in accordance with the SN EN 196 series of standards. The results are then compared with the current standards and allow statements about the possible use of the crushed concrete fine as additive and the possible amount to be added. In a further step, crushed sand samples are used as a substitute for primary sand in the production of concrete. The concretes produced will then be subjected to comprehensive testing. On the basis of these results and a comparison with the standards, the maximum substitution rate of the primary sand is determined. Finally, the results are evaluated and the reduction potential of CO_2, the effects on the consumption of natural raw materials and the effect on costs are estimated

3 Discussion and conclusions

Efforts to optimise the recycling of mineral construction waste today focus on mixed demolition, as there are currently too few recycling possibilities for this secondary building material. The demolition of concrete is not yet considered as a problem and the potential of its recycling is not yet sufficiently recognised. This will change in the coming years or decades, because:

(i) The amount of concrete demolition will increase once the concrete structures from the second half of the last century have reached the end of their useful life. Therefore, the proportion of mixed demolition in mineral construction waste will decrease in the future and the proportion of concrete demolition will increase accordingly.
(ii) The possible uses of RC concretes in structural engineering will increase and with it the demands on the building material. Today, qualitative deficiencies in the concrete granulate are compensated by adjustments in the concrete mix design (more cement, more admixtures). This leads to higher costs and environmental pollution. In the future, attempts will be made to improve the quality of concrete demolition.
(iii) The pressure on the cement industry to make its contribution to climate protection is increasing (e.g. through higher CO_2 fees and measures taken by public clients). Many representatives of this industry see a promising approach to solving this problem by rebinding CO_2 in concrete. For this, the greatest potential lies in the rebinding capacity in the crushed sand of the concrete demolition.

For these reasons, efforts to develop new processes for the separation and processing of C&DW will increase significantly in the coming years and further investigations for the usage of C&DW will be necessary. The here described research project improves the decision-making basis for the development of new technologies to close the material cycles and obtain high-quality results.

Acknowledgment
Supported by the Federal Office for the Environment FOEN (UTF 591.03.19) and the Gebert Rüf Foundation (GRS-049/18).

References

[1] Hiltbrunner, D.: Das Bauwerk als Rohstofflager, vol. 22, pp. 65–69, 2017.
[2] Guerra, F.; Kast, B.: Bauabfälle in der Schweiz - Hochbau Studie 2015 [Construction waste in Switzerland - Building Construction Study 2015], Bern, 2015.
[3] Schubert, S.; Hoffmann, C.: Grundlagen für die Verwendung von Recyclingbeton mit Mischgranulat, EMPA, Abteilung Ingenieur-Strukturen, 2011.
[4] Swiss Waste Ordinance, *Ordinance on the Avoidance and the Disposal of Waste*. 2015, pp. 1–46.
[5] Almeida, J.; Wälti, C.: Ent-Sorgen? Abfall in der Schweiz illustriert, Bern, Nr. 1615, 2016.
[6] Galbenis, C.T.; Tsimas, S.: Use of construction and demolition wastes as raw materials in cement clinker production, *China Particuology*, vol. 4, no. 2, pp. 83–85, 2007.
[7] Müller, A.: *Baustoffrecycling*, vol. 63, no. 11–12. Wiesbaden: Springer Fachmedien Wiesbaden, 2011.
[8] Hoffmann, C.; Jacobs, F.: Recyclingbeton aus Beton- und Mischabbruchgranulat, 2007.
[9] Müller, C.; Reiners, J.; Palm, S.: Closing the loop: What type of concrete re-use is the most sustainable option?, 2015.

Mechanical properties and bond behaviour of fibre-reinforced UHPC based on alkali activated slag

Daniela Göbel, Alexander Wetzel, Bernhard Middendorf
Institute of Structural Engineering, University of Kassel, Germany

1 Introduction

Alkali activated materials (AAM) are considered as promising alternative to cementitious systems due to the excellent mechanical properties and their environmentally friendly raw materials. The production of traditional Portland cement is energy intensive and contributes significantly to CO_2 emissions, on this account climate-friendly binder systems are of great interest for the development of building materials. The aim is to avoid the use of Portland cement clinker as binder. Through the appropriate use of secondary raw materials a comparable sustainable binder systems can be produced and the CO_2 emissions could be reduced up to 75 % [1].

Based on the principles of ultra-high performance concrete (UHPC) a Portland cement free, alkali-activated material base on blast furnace slag was developed and the effects of different fibres on the fresh and hardened concrete properties were investigated.

2 Material and Methods

AAMs consist of a reactive solid component, which must contain SiO_2 and Al_2O_3 in sufficient quantity and form, and an alkaline solution [2]. The hydration and/or polymerization reactions with the release of water result in strength-forming reaction products which remain solid under water and are stable in atmosphere [3]. The durability of the material is positively influenced by the small amount of capillary pores as well as by the addition of silica fume [2]. The formulation used and developed in this research is based on ground granulated blast furnace slag with a potassium water-glass solution as an activator. The basic mixture is a self-compacting material with a w/b ratio of 0.23 and compressive strength of 160 MPa after 7 days. As another advantage compared to other high alkaline AAM, the initial setting of this mixture is more than 60 minutes.

The influence of different fibres on the fresh and hardened concrete properties are compared to the formulation without fibres. Different straight fibre types (basalt, polyvinylalcohol and steel) in different volume proportions (0.25 vol% and 0.5 vol%) were compared in this study. In addition to these investigations some fibre pullout tests with steel fibres were done and compared to the results of fibre pullout tests on OPC based UHPC. The nominal embedded length of the steel fibres was 5 mm.

3 Results

All used fibre types have an effect on the workability. This is noticeable at the slump flow, which carried out with the mini slump according to German standard DIN EN 1015-3 [4]. If the results exceed a value of 250 mm, the material is refered to as self-compacting concrete (SCC) [5].
With an increasing fibre volume, the slump is getting smaller (Figure 1a, dots) and thus the workability decreases. The use of fibres in the AAM mortar has no significant influence on the compressive strength (Figure 1a, bars). With a w/b ratio of 0.23 the steel fibres are sedimented. The subsequent reduction of the w/b ratio to a value of 0.18 resulted in an increase in compressive strength to over 200 MPa after 7 days.

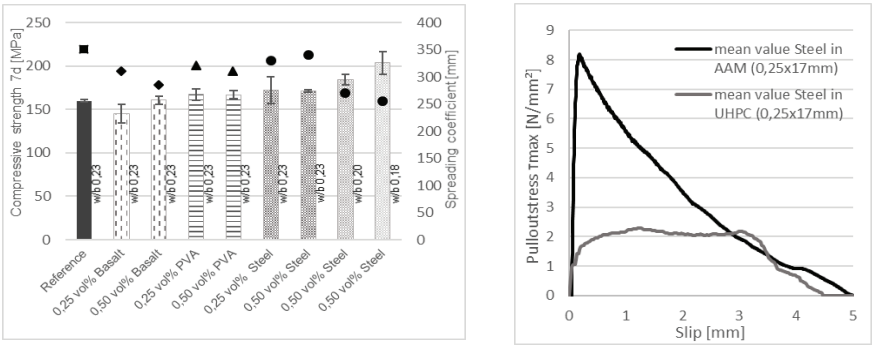

Figure 1: a) Compressive strength and slump flow results of UHP-AAM formulations with different fibre contents and types. b) Results of the fibre pullout tests in AAM compared to UHPC [6].

In addition to these investigations, fibre pullout tests with 5 brass coated steel fibres (Figure 1b) have been carried out with the reference mixture in order to demonstrate the bond between fibres and UHP-AAM matrix. The pullout stress-slip relationship represents the forces applied in relation to the contact surface of the fibres with the binder matrix. To compare them with those in UHPC, where single fibre pullout was performed [6], the test results in AAM were calculated for one fibre. The single pullout stress in the AAM is higher with 8 MPa, compared to UHPC with 2 MPa.

4 Discussion and conclusion

This study showed that adding fibres to the AAM leads to a higher viscosity of the fresh mortar, however, SCC behaviour still exists for all observed mortars. With the use of steel fibres and a reduced w/b ratio a counteraction of sedimentation tendency and an increasing compressive strength is observed. The addition of different fibre types (with an equal w/b ratio) only slightly affects the compressive strength.

The fibre pullout tests have shown that the steel fibres in UHPC have much lower bonding strength compared to these in AAM. Whether the different and higher pullout stresses in AAM result from a chemical reaction with the surface of the materials or has other causes must be further investigated.

In this research a UHP-AAM material with very high compressive strength and properties of an SCC could be produced. But the material showed the same brittle post cracking behaviour, similar to the UHPC. Further tests on the variation of fibre contents and shapes can counteract the brittle failure of the material.

References

[1] Awoyera, P, et al.: A critical review on application of alkali activated slag as a sustainable composite binder, Case Studies in Construction Materials 11 (2019), e00268

[2] Wetzel, A. et al.: Influence of silica fume on properties of fresh and hardened ultra-high performance concrete based on alkali-activated slag, Cement and Concrete Composites 100 (2019) 53-59

[3] Provis, J.L. et al.: Geopolymers and related alkali-activated materials, Annu. Rev. Mater. Res. 44 (2014) 299–327

[4] EN 1015-3:1999+A1:2004+A2:2006 Methods of test for mortr for masonry – Part 3: Determination of consistence of fresh mortar (by flow table); German version

[5] Bergmeister, K. et al.: Beton Kalender 2016 – Konstruktiver Hochbau, Aktuelle Massivbaunormen Ernst und Sohn, (2016) 86-89

[6] Schleiting, M. et al.: Functional Microfibre reinforced Ultra-High Performance Concrete (FMF-UHPC), Cement and Concrete Research, Volume 130, April 2020

Damage behaviour of high-strength grouts under fatigue loading

Corinne Otto, Ludger Lohaus
Institute of Building Materials Science, Leibniz University of Hannover, Germany

1 Introduction

High-strength grouts are commonly used in the wind industry, where they are exposed to high cyclic loading. In fatigue tests with a load frequency f_p = 10 Hz and maximum stress levels $S_{max} \leq 0.75$, fine-grained high strength grouts reach lower numbers of cycles to failure than coarse-grained high-strength grout or high-strength concrete. These results indicate that the fatigue behaviour of fine-grained grouts might be different from the fatigue behaviour of coarse-grained grouts. At the same time, the fine-grained grout show a stronger increase in temperature and deviating characteristic of the temperature development. From this, it can be assumed that these differences are not only due to test-related influences such as the load frequency f_P, but also to material - or structure - related effects.

2 Experimental Investigations

The experimental investigations of the fatigue behaviour were conducted on three high-strength grouts of varying fineness, which are often used and were supplied by the wind energy industry. Hence, the exact compostions of those grouts are unknown. The blaine value of the materials was determined as the fineness parameter. The blaine value of VM3 is 2,417 cm²/g; the blaine value of VM1 is 2,696 cm²/g and the blaine value of VM0 is 4,391 cm²/g. The fatigue tests were conducted on cylindrical specimens with H/D = 180/60 mm. The PVC-framework was removed after two days and the specimens were stored under water until testing. Immediately before testing, the exterier surfaces of the specimens were sealed with butyl tape to avoid drying out during the fatigue test. The minimum stress level was kept constant at S_{min} = 0.05 for all tests, while the maximum stress level was either S_{max} = 0.75 or S_{max} = 0.65.

During the tests, the axial deformation and the surface temperature were measured continuously in order to calculate the damage indicators, e.g. strain, stiffness, dissipated energy and temperature development.The axial deformation is temperature-compensated for the evaluation of the deformation. As parameters of the damage indicators, the gradient of strain at the minimum stress level grad ε^{II}_{min} and the gradient of stiffness grad E_s^{II} and the heating rate $v_{T;II}$ in phase II of the strain development were analysed. The averaged gradient of strain and the averaged gradient of stiffness as function of the averaged heating rate are shown in Figure 1 and Figure 2 for both stress levels.

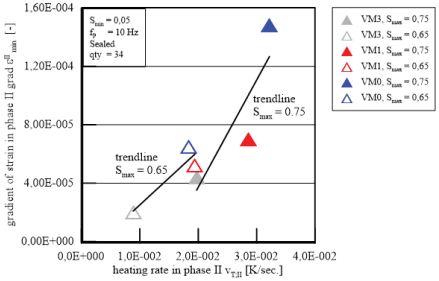

Figure 1: Gradient of strain as a function of the heating rate (averaged values)

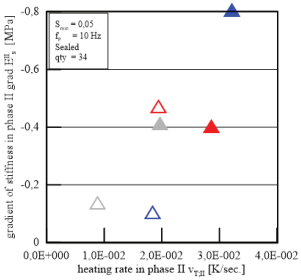

Figure 2: Gradient of stiffness as a function of the heating rate (averaged values)

3 Results

The expected drastic differences in logarithmised numbers of cycles to failure of several orders of magnitude based on the test results of e. g. [1] could not be determined for these materials and test boundary conditions examined here. The tested numbers of cycles to failure are in similar range. For S_{max} = 0.65, the grout VM1 has on average almost identical numbers of cycles to failure as for S_{max} = 0.75. Reducing the stress level by 10 % does not lead to an increase in the numbers of cycles to failure for VM1. This is a completely atypical behaviour, that has not been observed in the literature so far.

For all grouts, the gradient of strain and the heating rate in phase II are higher for S_{max} = 0.75 than for S_{max} = 0.65 (cf. Figure 1). The higher the gradient of strain in phase II and higher heating rate, meaning that the strain increase per load cycle and the increase in temperature is higher. With a higher stress level, the absolute applied force is higher and the increase in strain is higher and more energy is introduced in the specimen, which can be converted into heat. For both stress levels, a correlation between a higher heating rate and higher gradient of strain can be identified. Furthermore, it can be observed for both stress levels that the gradient of strain and the heating rate are higher for fine-grained grouts VM1 and VMO than for the coarse-grained grout VM3. Obviously, with increasing fineness of composition, the increase in strain per load cycle is higher.

For the respective grout, it can be seen that higher gradient of stiffness, except for VM1, correlates with higher heating rate (cf. Figure 2). VM1 shows an atypical behaviour for S_{max} = 0.65, which can explain the higher gradient of stiffness for S_{max} = 0.65. As expected, a higher gradient of stiffness for S_{max} = 0.75 could be determined for the other grouts. The comparison of the gradient of stiffness shows that the values of gradient of stiffness are in similar range depending on the stress level. A correlation between the fineness of the composition and the gradient of stiffness, as it could be oberserved for the gradient of strain, is not be seen. This means that a higher heating rate and increase in strain does not correlate with higher stiffness degradation in phase II. Similar results regarding the strain and stiffness development were observed for normal-strength concrete, mortar and hardened cement paste [2].

4 Conclusions

In summary, no drastic difference in the logarithmised numbers of cycles to failure could be determined, as was excepted. It can be said that fine-grained grouts have higher heating rates and higher increases in strain than the coarse-grained grout. Comparing all grouts, a higher heating rate and higher increase of strain correlate, but higher heating rate does not correlate with a higher gradient of stiffness. With a similar gradient of stiffness in phase II, a fine-grained grout can endure larger deformations. With a lower proportion of fines and a higher proportion of aggregates, the possible deformations could be limited [2]. Regarding the fatigue behaviour, the higher heating rate and higher increase in strain does not directly indicate lower numbers of cycles to failure, which means lower fatigue resistance, since the gradient of stiffness in phase II and the numbers of cycles to failure are in a similar range.

References

[1] Elsmeier, K. ; Hümme, J. ; Oneschkow, N. ; Lohaus, L.: Prüftechnische Einflüsse auf das Ermüdungsverhalten hochfester feinkörniger Vergussbetone, Beton- und Stahlbetonbau, Jahrgang 111, Heft 4, Ernst & Sohn, 2016, pp. 233-240

[2] Martin, J. L.; Darwin, D.; Terry, R. E.: Cement paste, mortar and concrete under monotonic, sustained and cyclic loading, Research Report University of Kansas, Kansas, 1991

Equi-biaxial flexural fatigue behavior of thin circular UHPFRC slab-like specimens

Xiujiang Shen, Eugen Brühwiler
Laboratory of Maintenance and Safety of Structures (MCS-ENAC), EPFL – Swiss Federal Institute of Technology Lausanne, Station 18, CH-1015 Lausanne, Switzerland

1 Experimental Campaign

The ring-on-ring test method is applied for equi-biaxial flexural fatigue testing, using circular slab-like UHPFRC specimens with a diameter R_0=600mm and a thickness h=50mm. The Digital Image Correlation (DIC) technique is used to observe the full-field fatigue damage propagation during the whole fatigue testing process.

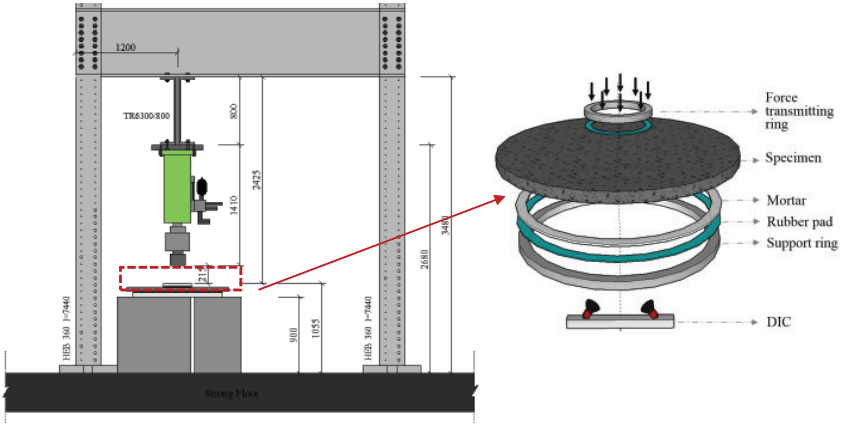

Figure 1. Schematic description of test setup

The chosen UHPFRC is an industrial premix containing 3.8% by volume of straight steel fibers with length of 13mm and diameter of 0.175mm, and its water/cement ratio is 0.15. After casting, the slab-like specimens were kept under moist curing conditions (20°C, 100% humility) for seven days, and stored inside the laboratory until testing. The test age was more than 60 days.

A total of sixteen slab-like specimens are prepared for the experimental campaign: four quasi-static tests are carried out first, and twelve fatigue tests with S (the ratio between the maximum applied fatigue force and the quasi-static ultimate resistance) ranging of 0.47~0.76 are performed with the aim to explore the fatigue endurance limit. The minimum fatigue force is always set to be 10% of the maximum fatigue force. And the sinusoidal cyclic loading with frequencey of 5Hz was imposed for the constant period of fatigue testing.

2 Quasi-static flexural behavior of UHPFRC slab

Based on F-δ curves, the equi-biaxial response of UHPFRC slabs is characterized by four phases: elastic phase (O-A), quasi-elastic phase (A-B), hardening phase (B-C) and softening phase (C-D) according to Figure 2:

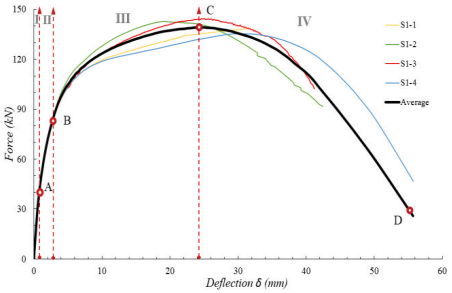

Figure 2. Force-deflection response

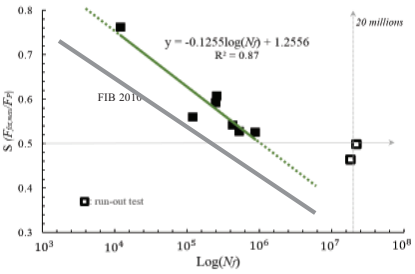

Figure 3. S-N diagrams

3 Flexural fatigue behavior of UHPFRC slab

The fatigue test results suggest a constant amplitude fatigue endurance limit at S=0.50 considering run-out results after 20 million fatigue cycles, as illustrated in Fig.3. Compared with the testing results in Fig.3, the S-N curve for concrete as taken from the fib Model Code 2010 obviously is conservative and does not apply to UHPFRC which is different to concrete.

Based on the fatigue damage evlotion, four stages of fatigue damage evolution are characterized for UHPFRC slab-like specimens showing fatigue failure, while run-out specimens show three stages. Figure 4 shows the increase of specimen deflection as a function of fatigue cycles represented in a normalized scale from two representative specimens. This deflection evolution can be considered as an indicator of fatigue damage. The specimen for S=0.53 (Fig.4-a) shows a fatigue fracture after 0.88 million cycles (LogNf=5.94)), although the applied stress level is slightly above the fatigue endurance limit. The run-out specimen for S=0.50 (Fig. 4-b) also shows some damage evolution but the damage propagation rate is much smaller than in the case of specimen with S=0.53, and no further deflection propagation was observed after 15 milliion cycles.

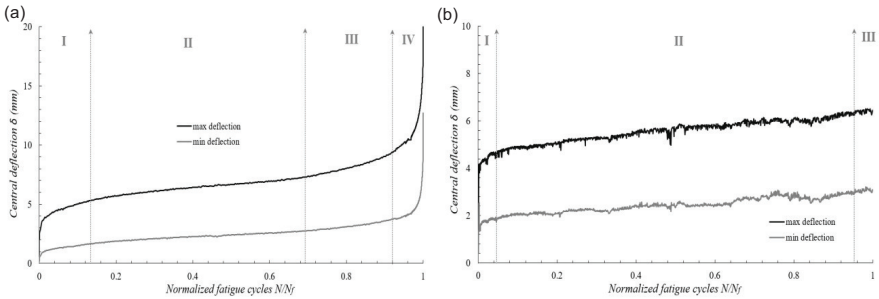

Figure 4. Evolution curve of central deflection under flexural fatigue loading
(a) S=0.53, Nf=0.88million, (b) S=0.50, run-out

Water-induced damage mechanisms in fatigue loaded high-performance concrete

Christoph Tomann, Ludger Lohaus
Institute of Building Materials Science, Leibniz University of Hannover, Germany

1 Introduction

The expansion of offshore wind energy systems increases the number of fatigue-loaded concrete structures that are permanent submerged in water. Comparatively few investigations of fatigue-tested concrete specimens immersed in water are documented in the literature (see e.g. Huemme [1], Nygard et al. [2] and Sørensen et al. [3]). Despite the fact that considerable scatterings occur in these results, a clear tendency can be observed. Concrete specimens, which are stored and tested submerged in water, show a significantly lower fatigue resistance compared to specimens which are stored and tested in air. This phenomenon was recognized in the past, but it is still unknown how the water influences the fatigue resistance of concrete and which water-induced damage mechanisms are involved in the degradation process.

2 Experimental Investigations

Cylindrical test specimens of a high-strength concrete with the dimensions of h/d = 300/100 mm were used to investigate how water influences the fatigue resistance of concrete. The test specimens prepared were divided directly after the manufacturing process into five series to adjust to different moisture contents. The influence of the moisture content in the microstructure and the influence of external surrounding water were investigated in tests with sealed and unseald specimens in dry conditions and fully submergend in water (cf. Tab. 1).

Tab. 1: Definition of the storage and test conditions investigated

acronym	*storage condition*	*sealing*	*test condition*
D	*dried (105 ± 5 °C)*	*(Al)-butyl tape*	*dry*
C	*climate chamber (20 °C, 65 % RH)*	*(Al)-butyl tape*	*dry*
M	*intrinsic moisture (sealed until testing)*	*(Al)-butyl tape*	*dry*
WS	*water storage (stored underwater)*	*(Al)-butyl tape*	*dry*
WST	*underwater (stored and tested underwater)*	*unsealed*	*under water*

The entire experimental investigation was performed in a servo-hydraulic testing machine, with a specially developed test set-up, which allows fatigue tests in air and submerged in water. The related minimum and maximum stress levels (S_{min} = 0.05, S_{max} = 0.65) were kept constant throughout the whole experimental investigation. A constant load frequency of f_P = 1.0 Hz (exept for the dried test specimen) was applied in the fatigue tests.

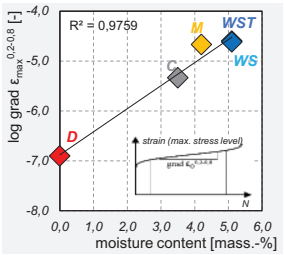

Fig. 1: Logarithmic gradient of strain at the maximum stress level

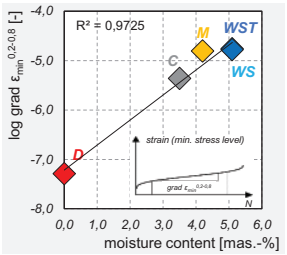

Fig. 2: Logarithmic gradient of strain at the minimum stress level

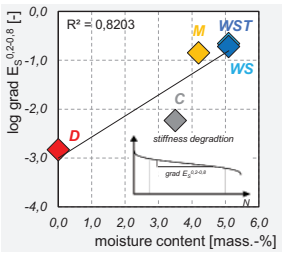

Fig. 3: Logarithmic gradient of the development of stiffness

During the tests, the axial deformations were measured continuously in order to calculate the damage indicators gradient of strain at the minimum and maximum stress level grad $\varepsilon_{min}^{0.2\text{-}0.8}$ and grad $\varepsilon_{max}^{0.2\text{-}0.8}$ and the gradient of stiffness grad $E_S^{0.2\text{-}0.8}$. The damage indicators were analysed between 20 % and 80 % of the numbers of load cycles to failure. In order to classify water-induced damages the acoustic emission activity was analysed additionally. The gradient of strain at maximum and minimum stress level and the gradient of stiffness as a function of moisture content are shown as average logarithmic values in Figures 1, 2 and 3.

3 Results and conclusions

For a better classification, the results of the numbers of cycles to failiure are presented first. The results show a decreasing fatigue resistance with an increasing moisture content in the microstructure of the concrete. The biggest deviation can be found with a value of 2.5 orders of magnitude between the storage conditions WST and D (note: the specimen of storage condition D refers to one fatigue-test without failure). Furthermore, the results show that external surrounding water reduces the fatigue resistance further, but only by a small amount (see [4]).

It is obvious from Figures 1, 2 und 3 that the analysed fatigue damage indicators gradient of strain at the minimum and maximum stress level and gradient of stiffness generally increase with an increasing amount of water in the microstructure of the concrete. The water-saturated test specimens of storage condition WS and WST show a higher increace in strain at minimum and maximum stress level and a higher stiffness reduction per load cycle compared to specimens of the storage condition C and D. Therefore, the results indicate a faster damage development with increasing moisture content, which correlates with the results of the number of cycles to failure.

In order to obtain more information about the damage mechanisms involved in the degradation process the acoustic emission activity was analysed. The results show an increasing trend of acoustic emission signals with an increasing amount of water in the microstructure of the concrete. Further, the results show acoustic emission signals of water-saturated test specimens (WS and WST) occurring over the entire fatigue process with signals located mainly near the minimum stress level (see [4]).

Consequently, the results of the damage indicators anaysed show that different damage mechanisms are acting depending on the moisture content in the micro-structure of the concrete. In addition to the mechanical damage mechanisms, these water-induced damage mechanisms act obviously substantially damaging.

References

[1] Huemme, J. (2018), Ermuedungsverhalten von hochfestem Beton unter Wasser, Berichte aus dem Institut fuer Baustoffe, Heft 18, Institut für Baustoffe, Hannover.

[2] Nygard, K., Petković, G., Rosseland, S., Stemland, H. (1992), The Influence of Moisture Conditions on the Fatigue Strength of Concrete. Cement and Concrete Research Institute, SINTEF report Nr. 70.

[3] Sørensen, E. V., Westhof, L., Yde, E., Serednicki, A (2011), Fatigue Life of High Performance Grout for Wind Turbine Grouted Connection in Wet or Dry Environment. Poster session presented at EWEA OFFSHORE, Amsterdam, Netherlands.

[4] Tomann, C., Oneschkow, N. (2019), Influence of moisture content in the microstructure on the fatigue deterioration of high-strength concrete. Structural Concrete. 2019; 1–8. https://doi.org/10.1002/suco.201900023

Low cycle fatigue of Ultra-High Performance Steel Fibre Reinforced concrete

Jens Peder Ulfkjaer
Department of Enngineering, University of Aarhus, Denmark

1 Introduction

The development of concretes with higher compressive strengths and high ductility provides the ability to construct slender and lightweight concrete structures. These differ from the more traditional concrete structures in the way that a reduced dead weight makes the structures more susceptible to dynamic loads. The development of Ultra High Performance Fiber Reinforced Concrete (UHPFRC) with high tensile and compressive strength combined with an extreme high fracture energy makes it possible to make e.g. Wind Turbine Towers of heights over 200 m. An example of such a tower is the Conelto tower [1] constructed of circular elements. In the concrete elements about 520 canals are embedded, which will be used to post-tensioning the rings together. When subjecting the rings to compressive stresses, tensile stresses will occur in certain zones around the vertical canals. FE calculations of the cross-section has shown the tensile stresses are up to 20% of the applied compression stress. It needs to be proven that there will not be a problem with fatigue in compression and in tension. Very few data exists and there is limited knowledge about fatigue for UHPFRC in tension. Due to the high fatigue, resistance of the material focus in this work has been on low cycle fatigue.

2 Experimets

Test of beams in three point bending has been performed on beams with depth 100 mm, height 100 mm and with a span of 400 mm. In order to relate the physical damage to the stiffness changes, a new test set-up for three point bending of notched beams was designed where the optical measuring systems ARAMIS was used. From the ARAMIS pictures, the crack growth can be observed. The pictures were taking without interrupting the loading cycles in order to avoid creep. Additionally displacement were measured at the two supports (to correct for rigid body motions), the stroke, an LVDT close to the notch at the midsection and a laser measured the crack mouth opening displacement over the notch (CMOD). Both static and fatigue loading have been performed.

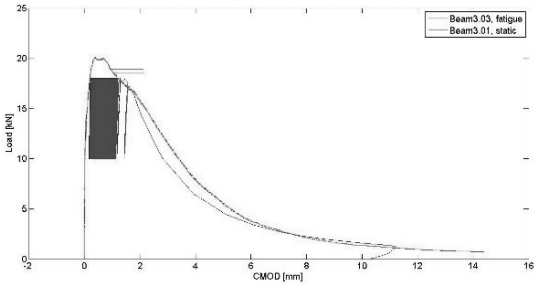

Figure 1: Load - CMOD curve for both static and fatiques test

In the fatigue test a stress ratio, ($R=F_{max}/F_{min}$) of 0.55 was used, and the stress level, $S_L=F_{max,fatigue}/F_{max,static}$ was varied between 0.9 to 0.8. In total 11 tests were performed and of these 5 failed prematurely. This was due to a bad distribution of the fibers in the failure surface, and initial rapid crack growth could be seen in the ARAMIS measurements.

The phenomenon of crack growth in three phases could be observed. The crack initiates during the first few cycles and then crack growth slows down during the next several cycles. Finally a phase with rapid crack growth that leads to failure.

In the tests, it is seen that the descending branch of the static experiments can be correlated to the fatigue life as can be seen in figure 1.

3 Modelling

A previous developed analytical model for predicting the complete load deflection curves of plan reinforced beams, [2], has been extended to cyclic loading, [3]. In the model, cyclic loading follows the model suggested by Yankelevsky, [4]. The calculations are then divided into three phases: I: An elastic state described by linear theory of elasticity. II: Development of a fictitious crack, and strain softening in the concrete. III: Development of a real crack in the concrete.

This makes it possible to have a stress-strain formulation for the crack band, and thus implement known un- and reloading models to model the fatigue behaviour.

This is done by implementing a cyclic loop on the constitutive relation and thereby calculating a new stress distribution per cycle including crack growth. By adapting the failure criterion seen in the experiments, an estimated relation between the inclinations of the cyclic loop and the stress level, it is possible to estimate the fatigue life of the beams and calculate an S-N curve with a good correlation to the experimental results

4 Conclusions

The purpose of this investigation was the understanding of the effects of low cycle flexural fatigue on UHPFRC. The understanding was obtained with experimental investigations together with the development of an analytical model based on a previous developed static model. From the experimental testing a fracture criterion for the models was found. It was shown that the Load-CMOD curve from fatigue loading could be compared to the static one and that fracture occurred when the deflection on the fatigue curve reached the static curve.

By implementing the analytical fatigue model it can be concluded that the Ulfkjær et al. model [2] can be further developed to estimate fatigue life. This is done by implementing a cyclic loop on the constitutive relation and that way calculating new stress distributions per cycle. Using the fracture criterion found from the experimental tests and an estimated relation between the inclinations of the cyclic loop and the stress level, it was possible to estimate the fatigue life of the beams, and calculate an S-N curve with a good correlation to the experimental results.

References

[1] "Conelto - concrete element towers" available at http://www.conelto.dk/.

[2] Ulfkjær, Jens Peder; Krenk, Steen and Brinker, Rune 1992, "*Analytical Model for Fictitious Crack Propagation in Concrete Beams*", Journal of Engineering Mechanics, No 34, vol R9206.

[3] Rikke Elbæk Sørensen and Morten Gabrielsen "*Experimental and Numerical Investigation of UHPFRC in Low Cycle Flexural Fatigue",* Aarhus University, Master Thesis, pp.1-67, 2016.

[4] Yankelevsky, David Z; Reinhardt, Hans W. 1987, "*Response of Plain Concrete to Cyclic Tension*", ACI Materials Journal, September-October 1987, No. 84-M37.

Performance evaluation of North American bridges with field cast UHPC connections

Peter J. Seibert[1], Vic H. Perry[2]
1: UHPC Solutions, New York, USA
2: ceEntek North America, Calgary, Canada

1 Introduction

Ultra-High Performance Concrete (UHPC) has been utilized in bridge construction across North America in various applications such as precast bridge elements, field cast connections, overlays, repairs and seismic retrofit for the past 20 years. The most popular and widely used North American UHPC application is to connect precast bridge elements with field cast UHPC due to its ultra-high strength, bond development, and durability. This solution speeds up construction, facilitates Accelerated Bridge Construction (ABC), allows for simpler connections with reduced reinforcing bar congestion and provides a longer lasting more robust connection than other conventional methods. Since 2006, over 250 bridges with UHPC field connections have been constructed in Canada and the USA [1].

2 Bridge Inspections

In 2012, more than 40 bridge structures with UHPC connections were visited and visually inspected [2]. Since November 2018, the authors visited and visually inspected 22 bridges with varying types of typical field cast UHPC connections for precast bridge elements in New York State and Ontario that have been constructed and in service for the past decade [3, 4]. Two of the inspected bridges are presented and concluding remarks for all 22 inspected bridges are included.

Whiteman Creek Bridge, City of Brantford, Ontario
In 2011, an existing three span concrete bridge was replaced with a 40m single span steel plate girder structure made composite with a 225mm thick concrete deck and asphalt waterproofing topping during a seven week full highway closure [5]. To reduce construction time, this ABC utilized precast concrete elements for all structurally reinforced concrete sections (except cast-in-place barrier walls). Field cast UHPC was utilized to develop: a) integral steel H-pile to precast abutment connections; b) composite shear connections between precast deck panels and supporting steel girders; c) deck-level connections between precast concrete panels; and d) connections between adjacent approach slabs.

Figure 1: Bridge Underside

Figure 2: Cracks in Vertical Connection (non-UHPC)

Figure 3: Longitudinal Cold Joint in Asphalt

A visual inspection of the bridge did not reveal any leakage through the transverse UHPC deck-level connections or the composite shear connections (Fig. 1). No rust stains or effloresce were evident. Even a UHPC repair patch along a precast deck panel has remained intact. No precast deck panels showed any signs of cracking. Even though this bridge has only been in service for 8 years, other deteriorations were noticed: a) ASR cracking in the cast-in-place barrier walls and precast deck panels; b) cracks in vertical foundation connections made of high performance concrete (Fig. 2); and c) longitudinal crack in asphalt along the centerline and along the width of a paver from the centerline (Fig. 3).

Canandaigua Outlet Bridge, Village of Lyons, New York

In 2009, this project was the first use of Side-by-Side Deck Bulb-Tees with longitudinal field cast UHPC connections topped with a waterproofing membrane and an asphalt wearing surface. A visual inspection of the deck surface (Fig. 4) showed no evidence of any reflective cracking in the asphalt surface on top of the longitudinal field cast UHPC connections due to a potential differential movement of the girders; except the longitudinal centerline joint appeared to have a cold joint along the length of the bridge. This may be a result of having a crown along the centerline. Other deteriorations such as ASR cracking in the barrier walls, excess scaling of the conventional concrete sidewalk (Fig. 5), rutting of the asphalt surface in the westbound lane, and failing of the eastside expansion joint were noticed (Fig. 5). A crack from the failed expansion joint has also formed in the sidewalk. None of this deterioration was a result of using field cast UHPC connections.

Figure 4: Top Surface

Figure 5: Expansion Joint & Normal Concrete Sidewalk Scaling

3 Conclusions

The 22 projects visited in 2018 and in previous years are a representative sample size of inspections that provide a level of comfort and added assurance to keep constructing bridges with field cast UHPC in the future. The absence of cracking, scaling, reflective cracking or other deterioration of UHPC supports that the material is performing as expected by the designers. In contrast, other deterioration mechanisms were observed on several bridges such as: pavement scaling, ASR, cracks in non-UHPC connections, asphalt rutting, longitudinal asphalt cracking, overlay groove wearing, panel cracking, and expansion joint failing.

References

[1] FHWA: Interactive Map – North American Developments of UHPC in Highway Bridge Construction. https://highways.dot.gov/bridges-and-structure/ultra-high-performance-concrete/deployments, 2019.

[2] Perry V.H.: An Eight Year Review of Field-Cast UHPC Connections for Precast Concrete Bridge Elements & ABC. 9th *Internat. Conf. on Short & Medium Span Bridges.* Calgary, AB, Canada, 2014.

[3] Seibert P.J.; Perry V.H.; Corvez D.: Performance Evaluation of Field Cast UHPC Connections for Precast Bridge Elements. *2nd International Interactive Symp. on UHPC.* Albany, NY, USA, 2019.

[4] Seibert P.J.; Perry V.H.; Doiron G.: Perfromance Evaluation of UHPC Field Connections for Hooper Road Bridge Project. *International Accelerated Bridge Construction Conf.* Miami, FL, USA, 2019.

[5] Young W.F.; Boparai J.; Perry V.H.; Archibald B.I.; Salib S.: Whiteman Creek Bridge – A Synthesis of Ultra-High Performance Concrete and Fibre Reinforced Polymers for Accelerated Bridge Construction. *Proceedings of HiPerMat – 3rd International Symposium on UHPC.* Kassel, 2012.

UHPFRC for jointless transition structures of integral bridges

Michael Mayer, Michael Huß, Hoang Huy Kim, Viet Tue Nguyen
Institute of Structural Concrete, Graz University of Technology, Austria

1 Introduction

Integral bridges are becoming increasingly popular. One of the main advantages are the low maintenance costs due to the missing expansion joints. However, the occuring deformations in horizontal direction, which are not absorbed by expansion joints anymore, must be transferred sufficiently to the ground without harming the surface of the pavement in this region. Therefore the development of special transition structures is required, especially for long integral bridges.

In [1] the basic operating modes of transition structures are shown. Recently, a number of different new concepts have been developed to satisfy the requirements on operational reliability. Some of these approaches are shown in [2] and [3].

This contribution presents a new approach using UHPFRC, which has already been realized at an integral bridge with a length of about 90 m in Fehring (Austria). For monitoring the behavior of this structure in service, measuring systems have been installed. Following, the functionality of the new system with UHPFRC will be exemplified with the before mentioned bridge in Fehring.

2 Approach with UHPFRC

The transition structure must be able to transfer the extension of the bridge in summer as well as the contraction in winter. Overall, the contraction is expected to be higher than the extension because of additional shortening of the concrete bridge due to shrinkage. For further explanations, however, the extension and the contraction are assumed to be the same.

In a simplified manner, the horizontal deformations of the bridge in Fehring can be assumed with about +/- 15 mm, which correspond to a difference in temperature of +/- 30 °C. Figure 1 shows an intersection and a bisected ground view of the new developed system with UHPFRC, in order to distribute these deformations uniformly in the transition zone without causing damages of the road surface (cf. [4]).

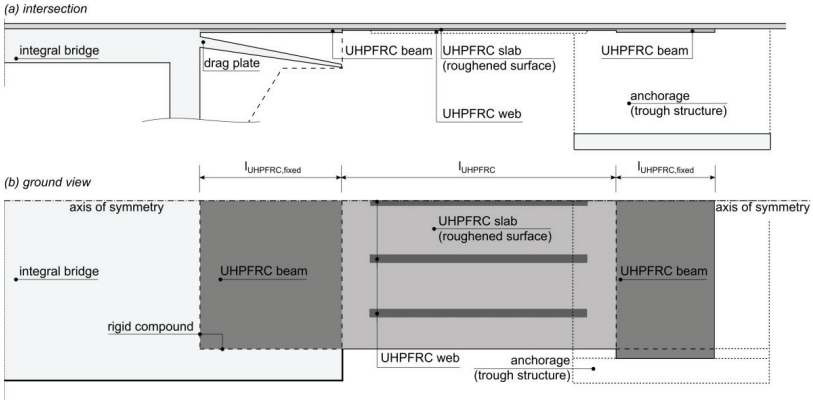

Figure 1: Principle of a transition structure made of UHPFRC (a) intersection, (b) ground view.

The functional principle of this new structure is that there is an UHPFRC slab, which can be extended without significant resistance. It is fixed at the beginning and at the end. In the free length of the UHPFRC slab, the horizontal deformations of the bridge should be distributed

uniformly. In winter, this distribution is done by fine cracks and in summer, the compression occurs by a uniform strain.

In case of the bridge in Fehring, the free length (l_{UHPFRC}) is 7.00 m. The UHPFRC slab with a thickness of 0.04 m is near to the surface and bonded with the asphalt. Hereby the fine cracks are directly transferred to the surface of the roadway. These fine cracks do not influence the driving safety.

On one extremity, the UHPFRC slab is fixed by an UHPFRC beam which is connected with the bridge, on the other extremity it is attached to an undisplaceable trough structure. Addtionally to the UHPFRC construction a standard drag plate is situated at the end of the bridge to cover possible settlement depressions in this zone.

In winter, the tensile force in the UHPFRC slab has to be anchored. This anchoring is achieved by additional reinforcement in the slab as well as in the beams. The UHPFRC beams have a thickness of 0.07 m. In the area of the slab, the reinforcement has a concrete cover of 0.01 m. Therefore, GFRP (glass-fibre reinforced plastic) bars are used in longitudinal direction to ensure durability despite a very small cover. The longitudinal tensile force, which occurs due to the contraction of the bridge, is transferred to the UHPFRC beams. In the beams, the load is distributed by compression arcs which causes transversal tensile forces. These transversal tensile forces are transferred and anchored to the bridge and the trough structure via transversal reinforcement bars made of steel.

A homogenous UHPFRC mixture was needed in order to guarantee fine cracks with an uniform distribution. For this construction, it is also necessary to reduce the tensile strength of the UHPFRC-matrix in order to minimize the forces to be anchored in the trough structure. The main reason is the exclusion of displacements of the trough structure, to provide the best possible serviceability.

The second load case for the transition structure is the extension of the bridge in summer. Because of the position of the UHPFRC structure near to the surface it is possible that the slab buckles. To avoid this, additional UHPFRC webs are included. This must be seen as a security measure to heighten the reliability of the structure. As mentioned before, the overall contraction of the bridge will be greater than the extension. As a result, the tensile strains exceed the compressive strains in the slab and the risk of buckling is significantly reduced.

3 Conclusions

The approach of using UHPFRC for the construction of jointless transition structures is novel. Therefore, long term experiences are not available at the moment. In order to gain such experiences the structure in Fehring is monitored. The first results confirm the planned functionality of the system. It is also intended to use this concept for another integral bridge (about 101 m), which will be built in 2020. Finally it should be mentioned, that the manageable costs of this UHPFRC transition system make it a promising solution for jointless transition structures.

References

[1] Österreichische Forschungsgesellschaft Straße-Schiene-Verkehr: RVS 15.02.12 – Bemessung und Ausführung von integralen Brücken, Wien, 2017-08-21.

[2] Eichwalder, B.: Fugenlose Fahrbahnübergangskonstruktionen für lange integrale Brücken, Technische Universität Wien, Dissertation, 2017.

[3] Brunner, A.T.: Untersuchung der schadhaften Belagsdehnfuge der semi-integralen Seitenhafenbrücke in Wien, Technische Universität Graz, Master's thesis, 2019.

[4] Mayer, M.; Nguyen, V.T.: Übergangskonstruktionen "Lückenschluss Fehring-Brunn, König und Heunisch Planungsgesellschaft mbH Leipzig – NL Graz, unpublished, Graz, 2017.

Pilot application of UHPFRC in railway bridge construction - Part 1: Background, conception, planning and scientific support

Oliver Fischer[1], Nicholas Schramm[1], Thomas Lechner[2]

1: Chair of Concrete and Masonry Structures, Technical University of Munich, Germany
2: SSF Ingenieure AG, Munich, Germany

1 Introduction

Ultra-high performance fibre-reinforced concrete (UHPFRC) is characterized by an extremely dense microstructure and thus very high strengths as well as excellent durability properties. This enables a material-saving and weight-reduced, slim construction method that opens up completely new possibilities and areas of application in precast bridge construction. In the course of the superstructure renewal of an existing old railway bridge over the creek Dürnbach, on the railway network of the Tegernseebahn close to the lake Tegernsee in Bavaria, the material could now be used for the first time in Germany for a railway bridge in a particularly practical and advantageous way. This part 1 of the contribution deals with the background, the conception as well as the planning and scientific supervision of the bridge.

2 Pilot application of UHPFRC in railway bridge construction

Background

With a view to the simplest possible construction process and a larger flow cross-section for the transferred stream, the aim was to achieve the most slender structure possible with a significantly lower construction height compared to a conventional solution. The use of UHPFRC made it possible to design a new bridge superstructure that could be lifted onto the existing abutments as a comparatively light prefabricated element during a short track closure break. For further information see also [1], [2], [3].

Conceptual design

The standard cross-section of the bridge can be seen in Figure 1.

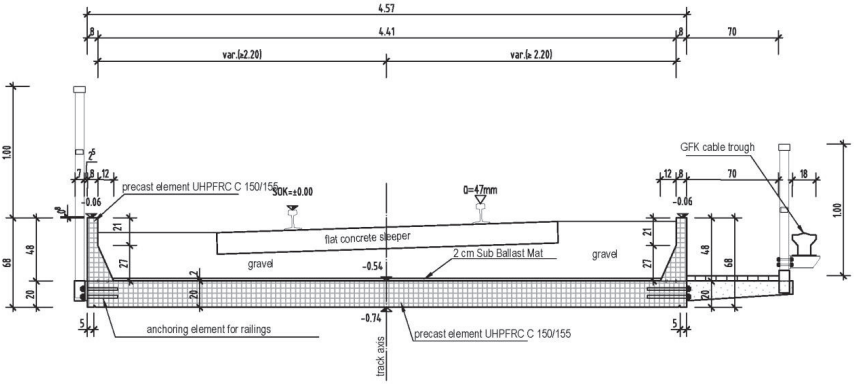

Figure 1: Standard cross section of the EÜ Dürnbach

The superstructure of the bridge was realised as a prestressed trough-shaped slab. Thanks to the use of the high-performance material, the slab thickness of the bridge under the rails was extremely low at only 20 cm. The overall height is only 74 cm and it was possible to integrate the ballast holders (with a minimum thickness of only 8 cm) into the component in a load-bearing manner. Due to the excellent durability properties as well as the high degree of density and resistance to mechanical stress, a separate waterproofing and the otherwise required protective concrete was not necessary. Together with a new type of flat concrete sleepers, the required clearance measured from the upper edge of the rail to the lower edge of the construction could be reduced by a total of about 25 cm compared to a conventional concrete solution and thus also the required increase in the flow cross-section during floods could be achieved. The precast element has a longitudinal prestressing and a transverse post-tensioning in the support areas. For the superstructure, a UHPFRC C 150/155 with 2.5 % by volume micro steel fibres was used. Conventional bar steel reinforcement was only installed locally and for the connection of the ballast holders, which were subsequently concreted in a second work step, and - to increase robustness and as minimum reinforcement to avoid failure without prior notice - in the central slab area as lower transverse reinforcement.

3 Scientific investigations and measurement supervision

In order to be able to determine in particular the losses of the prestressing due to creep and shrinkage as well as the development of the hydration heat in the real component, appropriate measurement equipment was integrated in the slab and the production was accompanied with measurement technology. In addition, a measurement supervision and scientific support in railway operation was carried out. Besides that, a test concreting in the mixing plant was carried out in advance. In this context extensive accompanying tests to determine the material properties and assumed values for the strengths were carried out. Furthermore, a mock-up slab element with a full-scale cross-section height of 20 cm was produced and then subjected to a 3-point bending test until failure, in order to determine the maximum bending moment that could be achieved for a fibre orientation similar to that in the later component, as well as the linear elastic tensile stress at the edge of the slab when cracking occurred and completed.

4 Conclusion

Within the framework of the pilot application of UHPFRC for the railway bridge "EÜ Dürnbach", important practical findings and experiences could be gained. The project shows the advantages of the construction method, such as the low superstructure height, the possible avoidance of coatings and a simple and fast lifting as well as the preservation of the old abutments due to the low dead weight. In addition to the laboratory experience, the measurement supervision could provide further insights in real operation.

References

[1] Schramm, N.; Fischer, O., (2019): “Precast bridge construction with UHPFRC—Shear tests and railway bridge pilot application.” Civil Engineering Design. 2019; p. 1–13.

[2] Fischer, O.; Schramm, N.; Lechner, T., (2019): „Deutschlandweit erstmalige Anwendung von UHPFRC im Eisenbahnbrückenbau, Teil 1: Konzeption, Realisierung und bauprаktische Erfahrungen mit einem vielversprechenden Werkstoff.“ Beton- und Stahlbetonbau 114, issue 2, p. 74-84.

[3] Schramm, N.; Fischer, O., (2019): „Deutschlandweit erstmalige Anwendung von UHPFRC im Eisenbahnbrückenbau, Teil 2: Flankierende wissenschaftliche Untersuchungen sowie messtechnische Begleitung der Herstellung und des Betriebs.“ Beton- und Stahlbetonbau 114, issue 5, p. 1-8.

Pilot application of UHPFRC in railway bridge construction - Part 2: Structural engineering

Thomas Lechner[1], Oliver Fischer[2], Nicholas Schramm[2]
1: SSF Ingenieure AG, Munich, Germany
2: Chair of Concrete and Masonry Structures, Technical University of Munich, Germany

1 Introduction

The bridge “EU Dürnbach” which is located close to the lake Tegernsee in Bavaria is the first railway bridge in Germany realized with ultra-high performance fibre-reinforced concrete (UHPFRC). The conception and the planning of this extraordinary bridge is described in part 1 of the contribution. This part 2 deals with the detailed design and the structural engineering.

2 Project overview

As reported in part 1 of this contribution the most important task for the renewal was to achieve a larger flow cross section for the stream Dürnbach. In addition, a fast construction process was necessary due to the short track closure break. For this reason, a modular building method with the superstructure as a prestressed trough-shaped UHPFRC-slab (see Fig. 1, part 1), was developed. The whole project consisted of five prefabricated concrete elements (see. Fig. 1). Due to the lightweight superstructure the lower part of the existing abutments could be preserved. On top of the old abutments new substructure precast elements made of normal strength concrete (NSC) were placed and connected to the abutments with grout and rebar elements. The elastomeric bearings were already fixed to the UHPFRC-superstructure when in the following step the precast element was lifted on top of the substructures. After positioning the superstructure in vertical direction, the bearing pedestals were grouted. The retaining wall precast elements, which are needed to keep the gravel in place, were then positioned next to the substructure elements. Due to the excellent durability of the UHPFRC no additional waterproofing was necessary so that immediately afterwards the gravel, the concrete sleepers and the railway track could be installed. For further information see also [1], [2] and [3] (part 1).

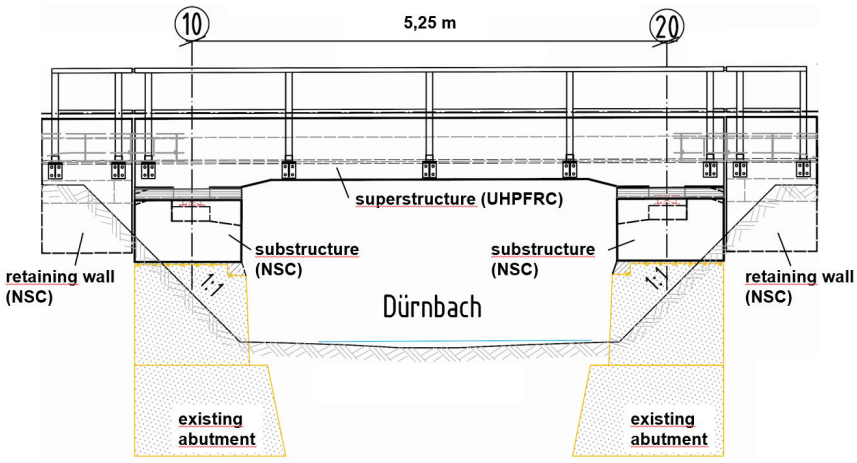

Figure 1: Longitudinal section of the EÜ Dürnbach

3 Design phases

The conception of the solution as well as the conceptional design were carried out by the Chair of Concrete and Masonry Structures of TUM in cooperation with the engineering office Büchting+Streit AG. Since until today no design rules for UHPFRC exist in German codes, the design rules for this project were defined in an expert´s report that was prepared by the Chair of Concrete and Masonry Structures of TUM. This report (carried out on the basis of the current draft of the DAfStb Code of Practice and international standards) was also needed to obtain an individual approval for this bridge, which was issued by the district government of upper Bavaria. Based on the expert´s report the structural engineering and the detailed design were carried out by the engineering office SSF Ingenieure AG. Max Bögl was commissioned with the production of the precast elements, using UHPC Compound of HeidelbergCement AG.

4 Structural Engineering

Bearing system

The bearing system of the superstructure is a single-span slab (see Fig. 1). There are four elastomeric bearings on each side of the bridge. One of the bearings is fixed in all directions and one is fixed in transverse direction. All other bearings are free to move in every direction.

Superstructure

The 52 strands for the longitudinal prestressing were arranged with a minimum distance of 4 cm in such a manner that the resulting tensile stresses on the bottom side of the plate in longitudinal as well as in transverse directions were reduced to a minimum. In addition, in transverse direction six post-tensioning tendons have been used in the support areas to minimize the tensile stresses in this direction even more. With a view to achieve the highest efficiency of the pre- and posttensioning a construction sequence was developed that guaranteed a minimum loss of initial tension due to creep and shrinkage. Because the tension stresses on top of the ballast holders (see Fig. 1, part 1) had to be limited, these elements had to be concreted in a second step after prestressing the slab. Conventional bar reinforcement was used to connect both elements and to transfer the shear forces resulting from shrinkage and additional loads. Apart from that, conventional reinforcement was only used in regions of splitting tensile forces and as lower transverse reinforcement in the central part of the slab. The posttensioning was carried out immediately before the transport to the construction site.

Detailed design

Since no design rules exist for UHPFRC in Germany, a couple of additional detailed designs had to be made for which typically guideline drawings and construction rules exist. This includes for example the definition of type and maximum number of spacers that should be used, when the tensile strength of the fibre reinforced concrete is considered, as well as all other built-in parts like the anchoring elements for the handrail and the walkway.

5 Summary

The structural calculations showed that (due to the minimal cross-sectional dimensions) the arrangement of the prestressing and the construction sequence have a big influence on the residual stresses in the plate and ballast holders. Therefore, it was not only necessary to know the mechanical parameters as tensile and compression strength, but also the creep and shrinkage parameters of the UHPFRC used for this project. After all, the detailed design for the railway bridge "EÜ Dürnbach" proved that a prestressed trough-shaped superstructure made of UHPFRC can be used as an interesting alternative to other typical construction methods for small railway bridges.

Pilot application of UHPFRC in railway bridge construction – Part 3: Concrete technology

Jennifer C. Scheydt, Lisa Wachter, Stefan Schöne
HeidelbergCement AG, Department Engineering & Innovation, Leimen, Germany

1 Introduction

For the first time in Germany, UHPC was applied for the renewal of an existing railway bridge over the Dürnbach creek within the railway network of the Tegernseebahn (Bavaria). Initiated by the Technical University of Munich (see part 1 of the contribution), the renewal was carried out in steel fiber reinforced UHPC.

For this, the new UHPC-Compound Effix® Plus by HeidelbergCement AG was chosen. In close cooperation with the planning and executive units, the resulting UHPC was adjusted to the requirements coming from the dimensioning and furthermore from the manufacturing process applied in the precast factory. The following part 2 of the contribution deals with the performance of the applied UHPC in fresh and hardened state.

2 Fresh concrete properties

Requirements resulting from planning

Resulting from the dimensioning of the pre-stressed and steel-fiber-reinforced precast bridge (2.5% by volume steel fibers, L / D = 12.7 mm / 0.175 mm), a strength class of C150/155 and a Young´s modulus of approx. 48,000 N / mm² were required.

In addition, the demanding requirements for the fresh concrete properties resulted from the manufacturing process and previous experience of the manufacturer Max Bögl. Accordingly, the mixing time of the UHPC should be less than 5 minutes in the conventional twin-shaft forced mixer at the precast factory. A self-compacting consistency with a slump flow of at least 700 mm and a working time of at least 90 minutes should be guaranteed.

Mix design and performance

In order to save on silo capacities and due to its performance, the compound EFFIX® PLUS from HeidelbergCement AG was used as the mortar matrix of the UHPC. The concrete recipe was adapted to the requirements resulting from the project. After adaption, an UHPC with 10% by volume basalt (maximum grain size 8 mm) and an w/c ratio of 0.27 was gained.

During production, the total mixing time of the UHPC in the twin-shaft forced mixer, including the introduction of the steel fibers of the precast plant, was less than 5 minutes. This is very short for an UHPC.

The resulting fresh concrete properties are shown in table 1. The self-compacting properties were maintained for the entire duration of concreting. No additional compacting was needed.

Table 1: Fresh concrete properties of the UHPC used for the Dürnbach bridge

Fresh concrete property (concrete age: 15 minutes)	**Unit**	**Value**
Slump flow	mm	700
Flow time t_{500}	sec	7
Temperature	°C	25
Air content	% by volume	2.4

In total, 8.8 m³ of UHPC were required for concreting the precast element. These were combined in four batches of 1.1 m³ in a truck mixer. In order to avoid interruptions during installation, two truck mixers were used. The self-compacting UHPC was inserted into the bridge formwork with a concrete bucket. Immediately after installation, an curing agent was sprayed on the surface and the finished part was covered with foil.

3 Mechanical properties

The properties of the hardened concrete were tested at several concrete ages as well in the laboratories at the Technical University of Munich as also in Leimen at the HeidelbergCement laboratory. A summary of the test results of the concrete used for the bridge production is shown in table 2.

Table 2: Hardened concrete properties of the UHPC used for the Dürnbach bridge after water curing at 20 °C

Hardened concrete property (concrete age: 28 days)	**Unit**	**Value**
Compressive strength	MPa	165 [1)]
Flexural tensile strength	MPa	26 [2)]
Young´s modulus	MPa	47.500 [3)]
Axial tensile strength	MPa	9 [4)]

[1)] Mean value of 12 individual values; tested on cubes with 150/150/150 mm³
[2)] Mean value of 3 individual values; tested on unnotched beams with 500/100/100 mm³
[3)] Mean value of 3 individual values; tested on cylinders with d/h = 150/300 mm³
[4)] Mean value of 3 individual values; tested on bones with l = 400 mm, cross section 50 mm/50 mm

In order to gain practical knowledge apart from the laboratory, a separate testing of the precast element under defined hubloads and crossing speeds took place by the Technical University of Munich after installation. The results of the monitoring showed a very good agreement with the assumed and calculated values. Thus, the load-bearing behaviour of the bridge was considered very positive.

4 Conclusion

The successful pilot application of UHPC for the Dürnbach railway bridge illustrates the efficiency and possibilities of this construction method. The new bridge superstructure, designed as a comparatively light prefabricated part, could be lifted onto the existing abutments of the old bridge due to its lower weight compared to a conventional prefabricated part. In addition, it was possible to dispense with a separate seal and the otherwise required cap concrete due to the good durability properties, the high density and the resistance to mechanical stress. Overall, the design with UHPC allowed a reduction of the required total height of about 25 cm and thus also the desired enlargement of the flow cross section at high water without any adaptation of the existing track position.

The pilot project has shown that the slender UHPC design, despite the comparatively high material costs of UHPC, represents an economically interesting alternative to the conventional construction method, especially when weighing up the technical advantages mentioned above. Anyhow, a very close cooperation and coordination of all project participants is essential for such a successful implementation.

Manufacturing and construction of 300-meter long Manong Bridge using standard 70-meter long UHPC precast post-tensioned U-girder

Yen Lei Voo[1,2,3], Jhen Shen Tan[1], Milad Hafezolghorani[1]

1: DURA Technology Sdn Bhd, Malaysia
2: School of Civil and Environmental Engineering, University of New South Wales, Australia
3: School of Civil and Environmental Engineering, Swinburne University, Australia

1 Introduction

This paper presents the design example of a 70m long UHPC composite bridge. In SLS condition, the calculation sample illustrated the stresses of the precast/prestressed girder at transfer stage, at different construction load history and at service stage. In ULS condition, the design moment and shear resistances are presented. The example used is an UHPC composite bridge (known as the Manong bridge) which has been constructed recently near Kuala Kangsar, Malaysia. Figure 1a shows the general arrangement of Manong Bridge which consists of five continuous spans with the total length of 308m and total width of 11.5m. Figure 1b shows the typical cross-section of the 70m span and it shows each span consists of three UHPC U-girders and topped with a 11.5m wide and 200mm thick cast in-situ RC deck. The RC deck will later be covered with 50mm thick asphalt wearing surface. The first and fifth spans are 45m long whereas the second to fourth spans are of 70m length. The UHPC used for the U-girder has characteristic compressive strength of f_{ck} = $f_{ck,cyl.}$ = 140MPa and characteristic post-cracking tensile strength of f_{ctfk} = 8 MPa. The composite bridge was designed as simply supported span and seated on elastomeric rubber bearings.

2 Description of UHPFRC U-Girder

Figure 1c shows that each 70m precast UHPC post-tensioned U-girder consists of twelve segments: two anchorage end segments (i.e. 5m long and weight 15.7 tonnes each); two anchorage end-internal segments (i.e. 6m long and weight 18.2 tonnes each) and eight internal segments (i.e. 6m long and weight 15 tonnes each). The U-girder consists of two 125mm thin webs, a 100mm thick bottom flange and they are post-tensioned with six external tendons of 27K15 strands and two internal tendons of 7K15 strands at the top flanges to ensure the joints are always in compression during prestressed transfer and service stages, no tensile stress is permitted in all the joints. The strands used are a seven-wire, low-relaxation type with diameter of 15.24mm with minimum breaking load of 260kN per strands. All the tendons to be stressed up to 75% of the breaking load and the 5% of immediate losses during stressing is taken into design. Unlike conventional concrete beams, this UHPC U-girder does not have any shear reinforcement at any part of its thin webs. There are only busting links at the anchorage zones and horizontal shear studs at the top flanges which acts as a shear connection to the cast in-situ deck and U girders.

3 Design Method

The applied design loads in this work example according to BS:EN 1991-2-2003 [2] are presented in Table 1 and the design bending moments and shear forces are presented in Table 2. The partial factor for the load cases is taken according BS:EN 1990:2002 [1]. The load cases were analyzed by using the MIDAS civil software to get the bending moment and shear forces.

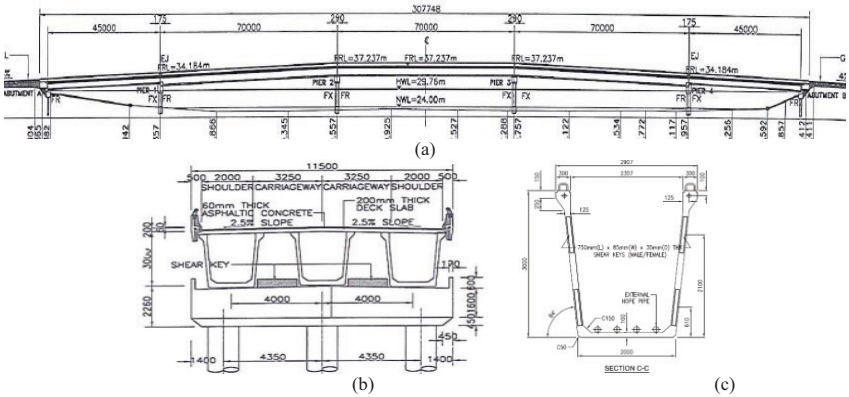

Figure 1. (a) Elevation view, (b) cross-section of Manong Bridge and (c) typical cross section of U-girder.

Table 1. Applied design load on bridge girder

	Load History	Load (kN/m)	SLS Factor [1]	ULS Factor [1]
G1	Self-weight of U-girder	27.0	1	1.35
G2a	Self-weight of internal slab (B=4m)	19.60	1	1.35
G2b	Self-weight of external slab (B=3.6m)	17.64	1	1.35
G3	Parapet load	10.0	1	1.35
G4a	Internal deck surfacing (premix)	5.52	1	2.0925
G4b	External deck surfacing (premix)	4.485	1	2.0925
Q	LM1+LM3 SV80	Refer to [2]	1	1.35

Table 2. Design bending moments and shear forces

	Load History	Edge Beam (Governing Values)			
		SLS		ULS	
		Moment (kNm)	Shear (kN)	Moment (kNm)	Shear (kN)
G1	SW of U-girder	16538	945	22326	1276
G2a	SW of slab	10805	631	14586	834
G3	Parapet load	4196	363	5665	490
G4a	SIDL (premix)	2950	164	6174	344
Q	LM1+LM3 SV80	19884	1414	26844	1909
	Total SLS	MSLS+ = 54372	VSLS = 3518	-	-
	Total ULS	-	-	MEd = 75593	VEd = 4852

4 Conclusion

In the SLS check, the UHPC composite bridge has satisfied all the stress limit criteria. The instantaneous deflection due to live load is less than the allowance deflection limit. The design cracking moment capacity is M_{cr} = 66615 kNm which is larger than the SLS maximum moment M_{SLS} = 54372 kNm. The design moment resistance is M_{Rd} = 104,792 kNm which is greater than the design moment effect M_{Ed} = 75593 kNm. The design shear resistance is V_{Rd} = 7923 kN which is greater than the design shear force effect V_{Ed} = 4852 kN. The use of UHPC girder in the bridge construction have enhanced the construction technology in the aspect of time and cost efficiency. The UHPC girder can achieve a long span with the shallower girder depth and reduce the number of piers which can significantly reduce the construction cost. UHPC is resistance to chemical attack, in result it can maximize the service life of the bridge.

References

[1] BS EN 1990:2002: Eurocode-Basic of structural design, 2002

[2] BS EN 1991-2:2003: Eurocode 1– Action on structure - part 2: traffic loads on bridges, 2003

Shear strengthening of prestressed concrete beams with UHPFRC – a numerical study

Mladena Luković[1], Nikhil Jayananda[1], Marco Roosen[1,2], Steffen Grünewald[1,3], Dick Hordijk[4]

1: Department of Engineering Structures, Delft University of Technology, The Netherlands
2: Rijkswaterstaat, Utrecht, The Netherlands
3: Magnel Laboratory for Concrete Research, Ghent University, Belgium
4: Adviesbureau Hageman, Rijswijk, The Netherlands

1 Research description

Research relevance

The growing need for strengthening of concrete structures to improve their structural performance challenges engineers to come up with a strengthening technique that is most effective, economical and such that out-of-use periods of these structures are minimized. The use of novel cement-based materials such as Ultra High Performance Fibre Reinforced Concrete (UHPFRC) might be promising in this respect due to its exceptional material properties, in particular, strain-hardening behaviour in tension, high compressive strength, excellent durability and compatibility with existing concrete. UHPFRC, which can be applied either as cast-in situ overlay or as prefabricated laminate, might lead to an effective and easily applicable strengthening solution.

Research approach

In order to investigate the effectiveness of using UHPFRC in shear strengthening of prestressed concrete elements, a numerical study was performed with ATENA FEM-software [1]. The post-tensioned T-girders of the Helperzoom bridge, Groningen, the Netherlands were chosen as reference case for this study. First, the reference beam (T-R0), without strengthening, was modelled. The beam was subjected to 3-point flexural testing such to determine its shear capacity. Simulated results of the reference beam were verified with experimentally obtained results from the literature in which similar girders were tested. Second, a detailed numerical study was performed to understand the shear behaviour of the reference beam. The contributions of shear reinforcement and prestressing strands, active in the critical shear region, to the shear capacity and the final failure mode were investigated through performing a number of simulations on imaginary beams in which the amount of shear reinforcement and prestressing strands was reduced compared to the reference beam (samples labelled as T-R1, T-R2 and TR-3). Shear capacities for these beams were also verified by Huber's analytical model [2]. Finally, the effect of strengthening by applying perfectly bonded layers of UHPFRC at both sides of the web was investigated for the reference and imaginary beams (Fig. 1).

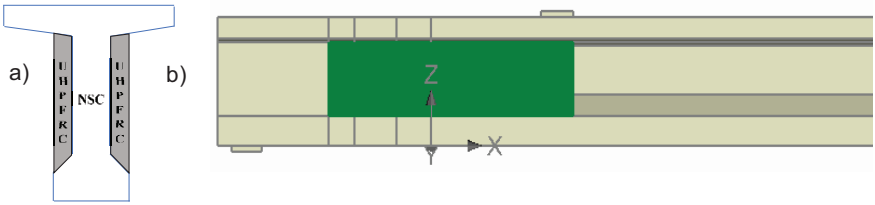

Figure 1: Configuration for strengthening a T-beam (a) cross-section & (b) part of the span (NSC=Normal Strength Concrete).

2 Numerical results obtained with ATENA

In the following, the outcomes of numerical simulations are compared for reference beams (R-series) with strengthed versions of the reference beams (U-series). The T-beams were strengthened with the UHPFRC composite on both sides of the web in the U-series. Perfect bond is assumed between the beam and the UHPFRC composite. The composite is added in the shear span of the beam, i.e., from 0.96 m from the left-hand support till the loading point. The direct tensile behavior of UHPFRC was assumed with a tensile strength f_t of 7.0 MPa, an ultimate tensile capacity f_{ut} of 8.0 MPa (at a strain of 2.5 promille) and a maximum strain of 3 promille.

The numerically predicted shear capacity of the reference beams (without strengthening) was found to be close to that calculated with the Flexural Shear Crack Model [2]. Figure 2 compares the load-deflection curves for reference and strengthened beams T-R0 (Fig. 2a) and T-R3 (Fig. 2b). TR-0 beams comprise of original reinforcement configuration, whereas in T-R3 beams, shear reinforcement and inclined prestressing cables crossing the shear span are removed. In T-R0 beam, although a critical shear crack opens at a load of around 1300 kN, this crack does not develop into failure mechanics, but the beam ultimately fails in shear compression failure at the load of around 1900 kN. On the other hand, the failure mode of the reference beam T-R3 is shear tension failure. It is found that the strengthening enabled a flexural failure for all simulated cases. However, the effectiveness of the strengthening varies, being the largest for the beams with the lowest initial shear capacity. The change in configuration of adding the UHPFRC - bonding UHPFRC to only the web region of the T-beam - showed the same effect as bonding UHPFRC to both the flange and web regions of the T-beam. The study also showed that the strain-hardening property of the UHPFRC material can be effective to prevent brittle shear failure and to increase the ultimate load-bearing capacity.

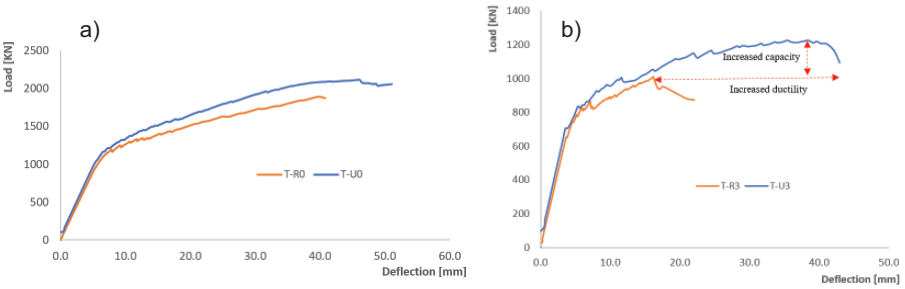

Figure 2: Comparison of load-deflection curves for reference beams and for the same beams, which were strengthened with UHPFRC (a) T-R0 vs T-U0, (b) T-R3 vs T-U3.

3 Conclusions

Although these results still need to be further verified by experimental testing, they confirm the potential of UHPFRC strengthening, but also highlight the need for thorough and accurate assessment of the structural behaviour and capacity of the existing structure prior to considering any strengthening method.

References

[1] Jayananda, N.: Shear Strengthening of Prestressed Concrete Beams with Ultra High-Performance Fiber Reinforced Composite – Numerical analysis by ATENA model, MSc-thesis, TU Delft, 2018.

[2] Huber, P. et al.: Approach for the determination of the shear strength of existing post-tensioned bridge girders with a minimum amount of transverse reinforcement, Bauingenieur, 2016. (in German)

Energy-based determination of maximum force to be transferred by bond

Ekkehard Fehling, Paul Lorenz
Institute of Structural Engineering, Department of Concrete Structures, University of Kassel, Germany

1 Differential Equation of Bond

A mechanical model introduced in [1] describes the bond behaviour between steel and concrete under cyclic loading, taking into account energy dissipation. An analytical model introduced in [2] leads to the well known differential equation of bond:

$$s''(x) = \frac{U}{E_s \cdot A_s}\left(1 + \alpha_E \rho_{s,eff}\right) \cdot \tau(x) = C \cdot \tau(x) \tag{1}$$

The relationship between the second derivative of the slip s and the bond stress $\tau(x)$ is based on a constant C which implies the contact area U between the two materials, the elastic moduli ratio (α_E) and the cross sections ratio (ρ_{eff}) of both.

2 Energy-Based Description of Bond Behaviour

Following an idea of the first author it is possible to formulate the equation in terms of the first derivative of the slip s and moving all parts of the equation tho the left side. Partial integration and separation of variables leads to the following expression.

$$W_\varepsilon = \frac{1}{2C}\left[s'(x_2)^2 - s'(x_1)^2\right] = \int_{s(x_1)}^{s(x_2)} \tau(s)ds = G_b \tag{2}$$

The right side of this expression represents the area under the bond stress-slip law between two values x_2 and x_1 of slip at the sections x_2 and x_1. This side can be seen as a length specific bond energy G_b or work done when increasing the slip from $s_2=s(x_2)$ to $s_1=s(x_1)$. The left side of equation (2) represents the energy or work of strains W_ε. The first derivative of s (along the x-axis) is the strain difference between the two materials. The difference between the squares of the strains at the positions x_2 and x_1 corresponds to the energy due to the stresses and strains for both materials at the mentioned positions. Figure 1 shows the mentioned relationships which, like equ. (2), imply linear elasticity for the two materials, and the same bond stress-slip law for each section along the reinforcement.

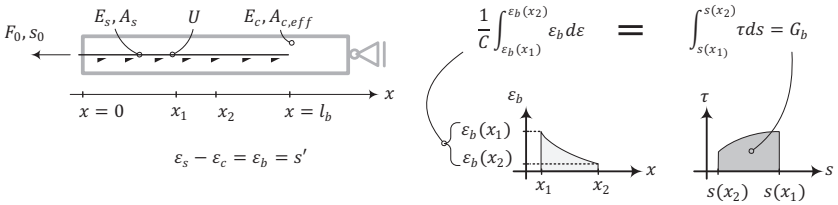

Figure 1: Strain and bond energy relationship between the concrete and the reinforcement for any given load

3 Energy-Based Determination of Maximum Force to be transferred by Bond

The proposed energy-based approach enables to compute the maximum possible force to be transferred by bond without solving the differential equation explicitly. Besides the elastic and geometric properties expressed by the coefficient C, it is sufficient to know the ultimate bond energy G_b while the shape of the bond stress-slip law plays no role in this regard.

At the loaded section of the reinforcement the strain difference has a maximum value and at the unloaded end section it is equal to zero, because here the strains of both materials are equal. Using the left side of equation (2) it is possible to calculate the strain energy which must be smaller than - or equal to - the ultimate bond energy.

If, however, the required transmission length or the distribution of the strains (or that of the slip) is the objective of the calculations, further considerations become necessary. This is also the case when the required bond length exceeds the possible length available in a structure. In this regard, it should be noted that the bond stress-slip law influences how “fast” the strain difference is reduced along the reinforcement position and how “fast” the slip is reduced from s_0 (at the loaded section) to zero (at the unloaded section). Figure 2 shows the development of the bond length for three different bond stress-slip laws (decreasing, constant, increasing with the slip) for the same value of the bond energy G_b. The relationships presented here can also be applied to treat bond of reinforcement in UHPC, reinforcement glued to concrete or masonry, long fillet welds, and long connections in steel structures with many bolts in one line after each other.

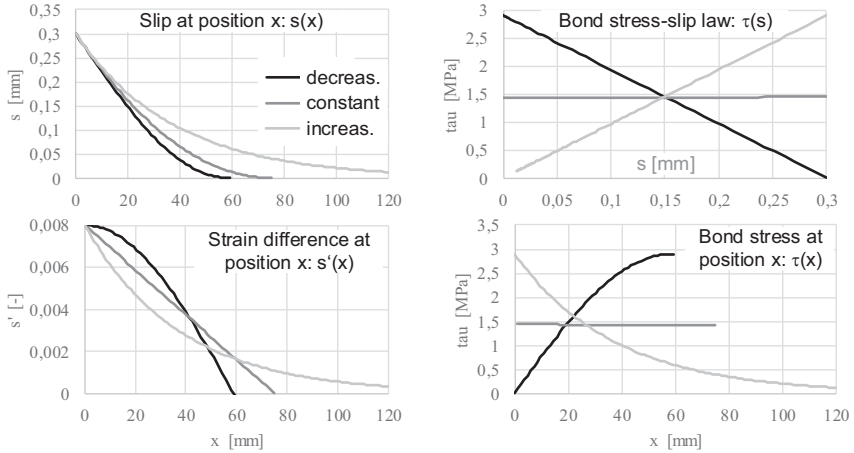

Figure 2: Bond length, slip, strains and bond stresses for same bond energy but different bond stress-slip laws

4 Conclusions

In this paper, it has been concluded that the specific bond energy G_b is the only parameter – and not the shape of the bond stress-slip law – which is decisive for the quantification of the maximum force to be transferred by bond. The proposed energy-based approach can help to find the slip, strain and stress development along the bonded length and the required (activated) bonded length by solving the differential equation of bond. In the case of short existing bonded length, where the slip at the unloaded end is not equal to zero, further considerations are needed. The proposed approach can be extended to any long connection, whatever the bonding materials are.

5 References

[1] Fehling, E.: Zur Energiedissipation und Steifigkeit von Stahlbetonbauteilen unter besonderer Berücksichtigung von Rißbildung und verschieblichem Verbund. Darmstadt, 1990.

[2] Rehm, G.: Über die Grundlagen des Verbundes zwischen Stahl und Beton. Deutscher Ausschuss für Stahlbeton, Heft 138, Verlag Wilhelm Ernst & Sohn, Berlin, 1961.

Experimental research on grouted connections for offshore wind turbine structures using UHPC

Attitou Aboubakr, Ekkehard Fehling, Jenny Thiemicke , Yuliarti Kusumawardaningsih
Institute of Structural Engineering, Department of Concrete Structures, University of Kassel, Germany

1 Introduction and objectives

The effect of using different fibre ratio as well as the effect of increasing the thickness of the grout on the behaviour of the connection are analysed and discussed in this paper. Five specimens (SHC-20N-Q0, SHC-20N-Q1, SHC-20-N-Q2, SHC-30-N-Q1, and SHC-30-N-Q2) were tested for this purpose. UHPC M3Q mixture (appr. f_c = 180 MPa) with a fibre ratio of 0, 1 and 2% by vol. for specimens SHC-20N-Q0, SHC-20N-Q1 and SHC-20-N-Q2 was used as a grout for these tests. To study the effect of increasing the thickness of the grout, specimens SHC-30-N-Q1 and SHC-30-N-Q2 were tested. The tests were performed at the Institute of Structural Engineering Laboratory at the University of Kassel.

2 Fabrication of test specimens

The trapezoidal shaped shear with a height of 3 mm and a width of 10 mm were created by drilling on the pile and sleeve. Figure 1 shows the shear keys shape, specimen with 20 and specimen with 30 mm.

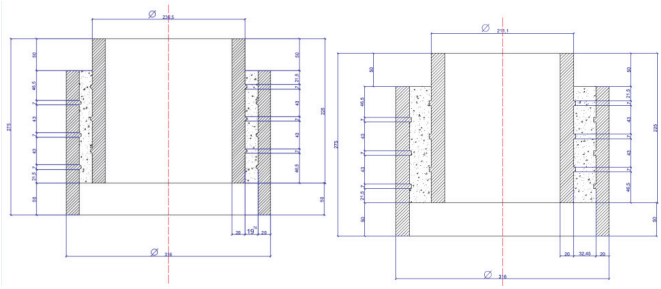

Figure 1: The dimension of specimens with grout thickness of 20 and 30 mm.

UHPC M3Q mixture was elaborated at Kassel University during the work on the priority programme (SPP1182) of the German Research Foundation. The M3Q mix provided an average compressive strength of concrete cylinders at about 180 MPa . Only one type of steel fibres with a length of 13 mm and a diameter of 0.175 mm was used for all tests with equal tensile strength of 2500 MPa.To assure that the steel tubes remained concentric during the process of concrete pouring a wooden template was manufactured on an European pallet. Figure 2 shows the specimens during the fabrication and after pouring the concrete.

Figure 2: The specimens during the fabrication and after pouring the concrete.

Reference tests have been done to control the quality of the mix and to make a comparison with other previous studies. Reference tests referred to testing of fresh grout by slump cone test and testing of hardened grout by compressive strength test, direct tensile test, splitting tensile test and flexural strength test.

3 Loading and experimental test procedures

Thirty-six strain gauges were installed in both the axial and hoop direction and placed at 120° spacing around the sleeve and pile perimeter. The relative axial displacement of the connection was recorded by using four Linear Variable Differential Transducers (LVDTs) which were located at 90° apart from each other. The specimens were tested in a universal hydraulic testing machine with a capacity of 6.3 MN. The specimens were loaded till the connection failed. The load was applied with a constant displacement rate of 0.002 mm/s. Mostly, it was observed that the performance of the specimens, after the peak at a displacement of 5 mm, had no significant change with time, therefore, the displacement rate then was increased up to 0.02 mm/s.

4 Test results and discussions

The results of the tests show that the stiffness of the grouted connection was somehow affected by the fibre ratio for specimens with grout thickness of 20 mm while there is not a significant increase in ultimate load or in ductility for connections with 20 mm grout thickness. However, for specimens with grout thickness of 30 mm, there was a significant increase in ultimate load and ductility while the stiffness of the grouted connection was not affected by the fibre ratio for these specimens. Furthermore, the specimens with grout thickness of 30 mm have the same general shape of axial load-displacement curves.

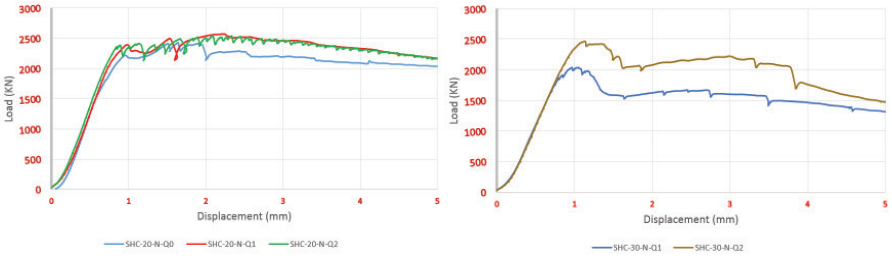

Figure 3: Load-displacement curve for the specimens.

5 Conclusions

Five specimens were tested to study the effect of using different fibre ratio and the effect of increasing the thickness of the grout on the behaviour of the connection The test result indicates that there is a fibre ratio effect for the grouted connection with 30 mm and 20 mm grout thickness, which enhances the behaviour of the grouted connection.

References

[1] Dallyn, P.; El-Hamalawi, A.; Palmeri, A.; Knight, R.: Experimental testing of grouted connections for offshore substructures: A critical review, 2352-0124/© 2015, The Institution of Structural Engineers. Published by Elsevier Ltd

[2] Lamport, W.B.: Ultimate Strength of Grouted Pile-to-Sleeve Connections, PhD-Thesis, University of Texas at Houston, 1988.

[3] Aboubakr, A.: Behaviour Study of Grouted Connection for Offshore Wind Turbine Structures with Brittle Cement Based Grouts, PhD thesis, University Kassel (publication in preparation, 2020).

Use of UHPFRC as waterproofing & bridge reinforcement

Laurent Boiron[1], Marco Maurer[2]

1: Walo Bertschinger AG, Giessenstrasse 5, CH-8953 Schlieren, laurent.boiron@walo.com
2: Walo Bertschinger AG Bern, Feldstrasse 42, CH-3073 Gümligen, marco.maurer@walo.ch

1 Waterproofing of a railway bridge

Choose of UHPFRC as waterproofing

The Kanderviadukt is a railway bridge built in 1911 on the North-South axis from Lötschberg in Switzerland. It is a single-lane natural stone viaduct with 11 arches and a length of 280 m. In 2017, the bridge sealing was renewed with a 3cm layer of UHPFRC.

The engineer office (B+S AG Bern) suggested to the project owners to use a UHPFRC layer instead of a standard sealing due to the multiple advantages of this solution: independent of weather conditions, no protection needed between the sealing & the ballast, and insurance of successful project completion during the allotted time. In addition, the UHPFRC offers a significantly longer protection (reduction of the Life-cycle cost).

Realization

The entire rehabilitation of the bridge was carried out by Walo Bertschinger AG in a two-month intensive construction phase with a complete closure. The important elements of the project were the renovation of the concrete gravel trough, the local repair of joints in the natural stone masonry, the adaptation of the trough drainage, and a complete sealing.

The complexity of the project was to install different types of UHPFRCs with different flow characteristics. A fluid self-consolidating mix was poured in the formwork and a thixotropic formulation was placed on the top of the edges to hold the bridge slope (Fig. 1). This surface has been inlayed with gravel as it will be used for structural maintenance and as escape route. After the protection of the edges, the full length of the bridge was paved in one day (Fig. 2).

More than 120 m^3 of UHPFRC were produced and transported in a very limited construction area. Thanks to a great organization, cooperation between all parties and the use of UHPFRC, the project deadline was met and the traffic was able to resume on schedule.

Figure 1: Preparation work for UHPFRC

Figure 2: UHPFRC paving

2 Bridge reinforcement

Thanks to the high mechanical characteristics of the UHPFRC, the reinforcement of existing structures can be thought off in a new way. Thin bonded overlay layers can be placed on the deck to reinforce and to seal the structure. It is also possible to use the material in highly stressed areas to simplify the working steps or to limit the space required for reinforcements.

During the renovation of the Aufgeständerte Schwarzwaldalle bridge in Basel (CH), it was necessary to reinforce the upper layer of the deck due to tension. As the room to work was really restricted (rehabilitation under traffic), a UHPFRC Category UB (4% fibers) was chosen to reduce the length of rebar anchorage to 15 time the diameter of the rebars (according to Swiss standard [1]).

Since the Swiss standard indicates that reinforcing bars with a diameter of 8 mm to 20 mm are generally used, additional tests needed to be carried out to understand the rebar development of larger diameter. The samples cast on site during the renovation and under the same conditions, showed that the failure systematically and repeatingly took place in the reinforcing bar (Fig. 3). Those tests allowed the engineer Aegerter & Bossardt AG Basel to validate the development length of the rebars and to control the quality of the product poured on site.

Figure 3: Failure in reinforcing bar

Figure 4: UHPFRC overlay paving

An UHPFRC overlay layer with a thickness of 4 cm was installed on the entire bridge deck in order to increase the load carrying capacity of the bridge (Fig. 4).

3 Conclusions

UHPFRC allows a new way of thinking for the rehabilitation or the construction of bridge structures. The durability and the independence of weather conditions ensure a reduction of the construction duration. The structural performance of the material reduces the impact of the reinforcement and allows the project owners to extend the service life of existing structures. The watertightness efficiency of the UHPFRC has been proved on many projects since 2004 in Switzerland.

Reference

[1] SIA 2052:2016 – Ultra-Hochleistungs-Faserbeton (UHFB) – Baustoffe, Bemessung und Ausführung

Floating UHPFRC rafts for shellfish farming

Esteban Camacho, Juan Ángel López, Hugo Coll, Fernando Galán
Co-founders of Research and Development Concretes SL and Prefabricados Formex SL, Spain

1 Introduction

Nearly 45% of the EU mussel is produced in Spanish estuaries using a floating raft system made with eucalyptus wood. This 540 m^2 structure has a reduced lifetime and a high carbon footprint associated to the protection coatings. In 2015 the company RDC developed a raft (Utility Model nºES1147609U) made with Ultra-High-Performance Fiber-Reinforced-Concrete (UHPFRC) precast prestressed beams. The peculiarity of this application, under continuous movement in Aggressive Exposure Environment (EAE), made very convenient the installation of continuous site monitoring to control the evolution of its durability. In 2019, there are already more than 5.000 m^2 under operation and proving high resiliency and very low maintenance costs.

2 UHPFRC floating rafts

Design

Wooden rafts are used in Spain since 1900 due to their reduced purchase cost, lightness and flexibility. The structure produces up to 100 tons/year. However, its use has three main disadvantages: (i) Economic: it has an average durability of 12 years and needs periodic investment in maintenance. (ii) Industrial: each raft is built manually through a high-risk job in the inter-tidal zone using hammers. (iii) Environmental: it implies intense deforestation and the degradation of the wood and the products used to protect it cause water pollution.

A UHPFRC structure was designed with the same geometry as the wooden raft (20x27 m, Fig. 1), with 6 primary beams and 10 secondary beams (slenderness of 89 and 120 respectively) and with comparable weight (56 t), mechanical capacity and flexibility, but with the required resistance to the Aggressive Exposure Environment of the sea (XS2, XS3). The connection between the beams is bolted through a polyethylene prism that provides certain degree of flexibility, necessary to reduce the stresses produced by the continuous stochastic actions. Besides of the capacity under service, the design of the beam geometry and prestressing is constrained by several factors: (i) The release of the strands in production 18 h after casting, (ii) The handling of the beams during the assembling, (iii) The need of a minimum width to have a safe corridor for the farmers, (iv) The potential impact of a boat with the surface.

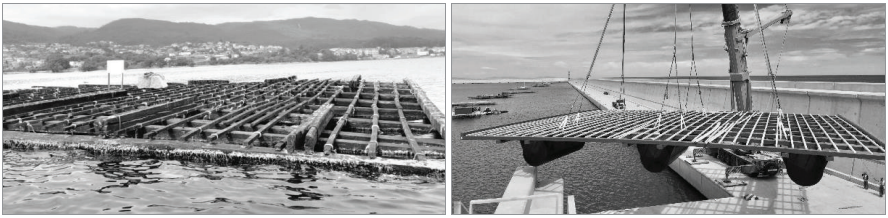

Figure 1: Traditional wooden raft (left) and UHPFRC raft floated in Valencia port (right)

The elements are produced at the precast company PREFFOR. The top face of the beams is textured to avoid slipping and the beam edges are rounded to reduce the friction with the ropes (Fig.2, left). The self-compacting UHPFRC fulfils the mechanical and durability requirements defined at the French Norm NF P18-470.

Figure 2: Detail of a connection (left) and placing of a beam (right)

UHPFRC rafts under service

The first raft was floated in October 2016. The sensors are proving no risk of corrosion in the beams, providing a resistivity more than 100 times higher than the value of the reference (a 25 MPa concrete beam on the raft). Periodic inspections to the farms have proven that the beams remain uncracked, as defined in the design, and only small rust spots are appreciated due to the corrosion of the fibers in contact with the surface. The UHPFRC connections have proven that they do not need retightening of the bolts as required for the wooden structures.

Future

In 2019, the European Commission launched the Blue Economy Report to support the sustainable development of the Blue Growth economy. The development of resilient and affordable infrastructures for the sectors of energy and aquaculture in open waters is crucial. Considering this, RDC is adapting now the design of the UHPFRC floating structure in the project OpenMode-863562 (co-funded by the European Maritime & Fisheries Fund (EMFF)). The new floating module has 140 m^2 and is adapted for open waters, connectable and sensor-equipped. The modules will measure remotely up to 14 parameters, correlating durability, mechanical, weather and water quality data. The project will test the capacity with eight pilots floated in five countries across three EU sea basins.

3 Conclusions

UHPFRC is an optimum material for a raft, a structure that needs to be light, slender and durable. The Integrated Sensor Network and cameras are proving their resiliency, so they are demanded by the Galician farmers because they are proving to minimize the operating expenses, being the most economical solution from the mid-term. The progress of the production experience curve for the aquaculture sector has led to a further development of the structure for multi-marine uses in open waters, which is now being tested under different marine, water and climate conditions.

Acknowledgements

The work presented has received funding from the European Union's Horizon 2020 research and innovation programme under GA Nº 738777 and with the contribution of the EMFF of the European Union under GA Nº 863562.

4 References

[1] AFNOR, NF P18-470, 'Complément national à l'Eurocode 2 – Calcul des structures en béton: règles spécifiques pour les bétons fibrés à ultra-hautes performances (BFUP), 2016.

Austrian UHPFRC – from mix design to applications

Michael Huß, Hoang Huy Kim, Viet Tue Nguyen
Institute of Structural Concrete, Graz University of Technology, Austria

1 Introduction

The great potential of Ultra High Performance Fibre Reinforced Concrete (UHPFRC) is widely known. A large number of research activities and application have confirmed that UHPFRC can be used, on the one hand, to build lightweight and sustainable structures and, on the other hand, to strengthen existing structures durably with low material input ([1], [2]). However, the realisation of structures made of UHPFRC is still challenging for the construction industry nowadays, as there is still a lack of guidelines and experience with this material. In recent years several applications have been realised under various conditions where experiences could be gained. Some selected projects as well as reference values for a robust mix design considering the special properties of UHPFRC are described below.

2 Mix design

Mix design of UHPFRC mainly depends on the required tensile properties. Therefore, the steel fibre content and the fibre geometry have to be selected in order to ensure the required post-cracking tensile strength. Depending on the fibre reinforcement, a certain amount of paste (particle size smaller 125µm + liquid) is necessary for a stable mixture with homogeneous fiber distribution, especially if self-compacting properties are desired. The higher the fibre factor (aspect ratio l_f/d_f x fibre content ρ_f), the better is the post-cracking tensile strength and the higher is the required paste volume. It should be noted, that an optimized paste composition regarding packing density and material compatibility is necessary for an efficient mix design.

Table 1 presents some reference values for the fibre factor and the paste volume depending on the required post-cracking tensile strength. Furthermore, a minimum cement content (CEM I) is shown to obtain a compressive strength f_{ck} of 150 MPa. The listed values are differentiated with regard to the use of fine or coarse grain UHPFRC. In the case of high requirements for post-cracking tensile strength, such as strain-hardening, usually fine grain UHPFRC will be preferred. Using coarse grain UHPFRC makes it possible to reduce the required amount of paste, which has a positive effect on material costs, hydration heat and shrinkage. In general, it is also possible to achieve a high post-cracking tensile strength with coarse grain UHPFRC. However, a higher paste content is needed and, as a result, the quoted advantages of coarse grain UHPFRC could not be taken into account. Consequently, no coarse grain UHPFRC with high post-cracking tensile strength is stated in the following table. The presented values are consistent with the recipes of the projects described below as well as many other applications that have already been realised. The post-cracking tensile strength refers to fiber orientation conditions which are usually obtained with micro steel fibers in bending tensile tests on thin plates.

Table 1: Reference values for UHPFRC mix design

	Fine grain UHPFRC (max. grain size <1 mm)			**Coarse grain UHPFRC** (max. grain size >1 mm)	
Required mean post-cracking tensile strength [MPa]	**4**	**7**	**10**	**-**	**4**
fibre factor [l_f/d_f . ρ_f]	> 0.4	> 1.0	> 1.8	-	> 0.4
paste volume [litre/m³]	> 520	> 570	> 650	> 450	> 500
cement content [kg/m³]	> 600	> 700	> 800	> 480	> 550

3 Recent applications

The following projects present some applications of UHPFRC which have been realised in the past years. The mix design was developed by the Institute of Structural Concrete, Graz University of Technology. It is based on the approach described in [3], whereby the material composition was modified to the framework conditions of the project.

UHPFRC-steel composite bridge

An existing single-track railway bridge, more than 100 years old, was replaced by a more modern structure. The new bridge was designed as a trough bridge with steel-UHPFRC composite slab to ensure that the bottom edge of the structure does not fall below the predefined limit. The span width is 8.46 m and the construction height is 0.82 m (0.17 m slab thickness). Puzzle shaped composite dowels are used for a sufficient shear resistance of the slab. The UHPFRC was produced in a stand-alone mixer next to the structure.

Reinforcing and waterproofing UHPFRC-layer for an overpass bridge

UHPFRC was used as a waterproofing and reinforcing layer for a two-span road bridge with a total length of 37.5 m in Germany. In order to guarantee the impermeability of the 7 cm thick UHPFRC layer, the requirements for the properties of the hardened concrete were high. Therefore, an UHPFRC with 3 vol.-% of fibres and a compressive strength $f_{cm,cube}$ of 168 MPa was applied. The slab has a slope of 3.5%, which requires thixotropic fresh concrete properties. The UHPFRC was produced in a concrete plant and cast on site.

Prefabricated edge beams

Edge beams of bridges are exposed to very strong environmental influences, which means that they frequently have to be rehabilitated or renewed. In order to prevent this problem, an edge beam made of prefabricated UHPFRC elements was used in the course of a bridge rehabilitation. An innovative dovetail connection enabled an easy mounting of the elements. Grit was sprinkled on the surface of the edge beam to ensure the necessary grip.

Transition structure of an integral bridge

UHPFRC was used for the transition structure of a 90 m integral bridge in Austria. The longitudinal deformation of the bridge can be dissipated by the UHPFRC construction via finely distributed cracks. The thickness of the slab is 0.04 – 0.07 m. The UHPFRC was mixed in a conventional concrete plant, transported with a truck mixer and finished with a vibrating beam at a slope of 2.5%.

4 Conclusion

This contribution presents some successfully realised projects which make use of the outstanding properties of UHPFRC, such as high compressive strength, durability, ductility and impermeability. It could be shown that the field of application of this material can be very diverse. In addition, reference values are presented for a robust mix design depending on the required tensile properties.

References

[1] Schmidt, M., et al.: Sachstandsbericht Ultrahochfester Beton. Deutscher Ausschuss für Stahlbeton Heft 436, 2008

[2] Brühwiler, E.; Denarié, E.: Stahl-UHFB – Stahlbeton Verbundbauweise zur Verstärkung von bestehenden Stahlbetonbauteilen mit Ultra-Hochleistungs-Faserbeton (UHFB). *Beton- und Stahlbetonbau* 108, Heft 4, 2013.

[3] Hoang, K., H.: A Systematic Mix Design Approach for UHPFRC, Dissertation, Graz University of Technology, 2017.

Strength and deformation behaviour of fibre reinforced UHPC; an experimental investigation using Digital Image Correlation (DIC)

Ingrid Lande Larsen, Rein Terje Thorstensen, Katalin Vertes, Anette Heimdal
Department of Engineering Sciences, University of Agder, Norway

1 Introduction

A wide range of studies is available, focusing on how the inclusion of fibres influences the strength properties of UHPC. A review article covering 26 such papers were presented at the fib congress 2018 [1]. It is concluded that the results span widely between the investigations. Hybrid configurations of different fibre types are frequently claimed to cause positive synergetic effects [2], where microfibres are expected to reduce the propagation of initial cracks in the weaker interfacial transition zones of the UHPC matrix. Macrofibres are explained to span larger cracks and thus maintain the material continuity during deformation of the structural members.

This paper presents an investigation on how compressive strength and flexural tensile strength is impacted by the inclusion of three alternative configurations of differently shaped steel fibres while keeping the fibre content constant at 2 vol.-%. The crack propagations were documented by the use of a Digital Image Correlation camera system (DIC) during the whole loading process where the beams were loaded in a three-point bending test until failure.

2 Experimental program

The fibre configurations were denoted SS (straight micro fibres only, l/d=13mm/0.2mm), HE (hooked-end only, l/d=50mm/1mm) and HY (a hybrid combination of 50% SS and 50% HE). 24 cubes (100 mm) were cured in water at 90 °C for 72 hours (including gradual increase and decrease of temperature) and then tested for compressive strength according to NS-EN 12390-3:2009 after a total of 28 days curing. 24 beams (500 mm x 100 mm x 100 mm) were cured in water at 20 °C for 7 days and then exposed to a three-point bending load until failure.

3 Experimental results and discussion

All results are average values from 6 to 9 cubes or 5 to 8 beams. Prior to this, outlying results deviating more than 10% from the average were excluded. The variations in compressive strength were found to be <3.5% between the varying fibre configurations (Figure 1). Also, results from other published studies have found a relatively low level of influence <10% on compressive strength (e.g. [3, 4]), for the same type of investigations.

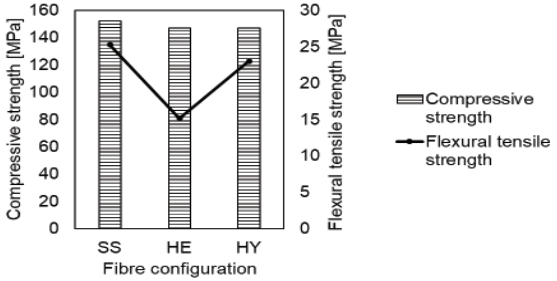

Figure 1: The effect of fibre configuration on compressive strength and flexural tensile strength.

The variations in flexural tensile strength due to fibre configuration was considerably larger; around 60% higher with SS than with HE. This difference seems not easily explained by straight shape being better than hooked-end. However, the differences in the volume of each fibre cause the number of SS fibres to be approximately 100 times that of HE fibres. The probability of any initiated crack to be spanned by fibres is thus much higher with SS, compared to the situation with the low number of fibres present with HE. The reduced number of cracks being able to propagate unhindered from initiation might explain the higher capacity for tensile strength with SS. Additionally, a high amount of fibres reduces the sensibility towards unfavourable fibre orientation. HY was found to perform correspondingly to SS, indicating a potential for an optimum hybrid configuration.

Some typical crack patterns recorded by the DIC are shown in Figure 2. At the load level immediately before the failure of the HE beams, the SS and HY beams showed only minor tendencies of cracking, while HE had typically a few severe cracks (Figure 2 a). Thus, the DIC recordings documented the increased capacity of SS and HY, compared to HE.

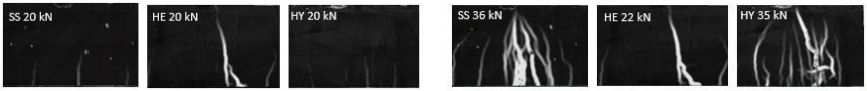

a) *Constant load level for all beams.* b) *Immediately before failure for each beam.*

Figure 2: Typical crack patterns derived from measurements of major principal strain registered by the DIC.

Immediately before the failure of each beam (Figure 2 b), the beams with SS and HY typically developed a high number of distributed cracks with a smaller width than the fewer cracks before failure with HE.

4 Conclusions

Based on this study, the following conclusions can be drawn:

1. The impact on compressive strength from variations in the fibre configurations was found to be <3.5%.
2. The inclusion of 2 vol.-% straight steel microfibres (SS) improved the flexural tensile strength by 60%, compared to the inclusion of 2 vol.-% hooked-end (HE) macro fibres.
3. Immediately before failure in bending, the beams with SS configuration exhibited multiple cracks of small width, compared to the few and larger cracks with HE configuration.
4. The benefits of SS to HE is believed to be caused by the superior number of fibres.
5. Hybrid fibre configuration (HY) were found to perform correspondingly to SS configuration, neither improving strength nor reducing crack width further.

References

[1] Larsen, I.L.; Thorstensen, R.T.; Vertes, K.: "Efficient use of fibres in UHPC - a structured scoping review," in *The 5th International fib Congress, Better - Smarter - Stronger, 7 – 11 October 2018*, Melbourne, Australia, 2018, pp. 458-469.

[2] Yu, R.; Spiesz, P.; Brouwers, H.J.H.: "Development of Ultra-High Performance Fibre Reinforced Concrete (UHPFRC): Towards an efficient utilization of binders and fibres," *Construction and Building Materials,* vol. 79, pp. 273-282, 2015/03/15/ 2015.

[3] Meng, W.; Khayat, K.H.: "Effect of hybrid fibers on fresh properties, mechanical properties, and autogenous shrinkage of cost-effective UHPC," *Journal of Materials in Civil Engineering,* Article vol. 30, no. 4, 2018, Art. no. 04018030.

[4] Wu, Z.; Shi, C.; He, W.; Wang, D.: "Static and dynamic compressive properties of ultra-high performance concrete (UHPC) with hybrid steel fiber reinforcements," *Cement and Concrete Composites,* Article vol. 79, pp. 148-157, 2017.

Cyclic deterioration of bond zone between fibres and UHPC

Martin Empelmann[1], Vincent Oettel[1], Jan-Paul Lanwer[1], Dieter Dinkler[2], Ursula Kowalsky[2], Svenja Höper[2]

1: Institute of Building Materials, Concrete Construction and Fire Safety, Division of Concrete Construction, Technische Universität Braunschweig, Germany
2: Institute of Structural Analysis, Technische Universität Braunschweig, Germany

1 Introduction

UHPFRC can preferably been used for lean and thin-walled structures due to its very high compressive strength. The combination of weight reduction and high slenderness make UHPFRC-structures susceptible to cyclic loading. Although the post-cracking tensile strength of UHPFRC under static loading is examined quite well, fundamental research on the damage propagation during fatigue loading is missing. Within the DFG-founded priority programme 2020 the degradation behaviour of UHPFRC under cyclic tensile loading is studied both experimentally and numerically. In order to achieve the objective of understanding the microphysical fatigue behaviour, methodical graduated experimental investigations of raw fibre material, plain UHPC, single and multiple pull-out tests as well as UHPFRC tensile tests have been conducted. Certainly, this paper focuses on the degradation processes that can be detected by multiple pull-out tests (groups of fibres). Simultaneously to the experimental programme, 3D finite element analyses are conducted to examine the damage mechanisms and processes regarding the deterioration of the bond behaviour on the mesoscale.

2 Experimental Investigations

The test programme contains multipe pull-out tests (groups of fibres) of straight, smooth micro steel fibres $(l_f/\emptyset_f = 13.0/0.19\,[\mathrm{mm}], f_{st}^f = 3.578.8^{80.2}\,\mathrm{N/mm^2})$ out of UHPC $(f_{cm} = 157.1^{2.3}\,\mathrm{N/mm^2})$ under monotonic (VMS) and cyclic (VMZ) loading (single amplitude, sinusoidal, $\Delta\sigma_{st}^f = 0.6,\ f = 0{,}25\,\mathrm{Hz}$). The desired embedded length is l_e = 6.50 mm (= l_f/2) and the angle of fibre alignment (α = 30°, 60° and 90°) is varied. Figure 1 shows the test specimen (left) and the σ-δ-curves (right).

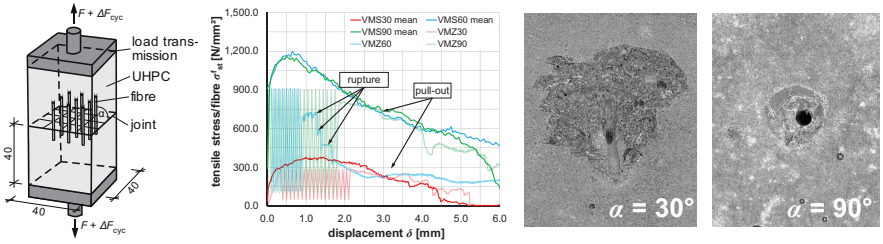

Figure 1: Test specimen (left), pull-out curves with schematic load changes (centre), concrete canals (right)

In both monotonic and cyclic pull-out tests, a gradual fiber pull-out always occurred. Exceptions were pull-out tests with a fiber alignment of 60°, in which fiber rupture occurred occasionally. Afterwards the surfaces with the cones of breakout (concrete canals) have been examined by digital microscopy. With regard to the angle of alignment, a pronounced cone of breakout could be observed at 30°, a very small cone of breakout at 60° and no cone of breakout at 90° in all monotonic as well as in all cyclic pull-out tests (figure 1, right). The cone of breakout is the reason why the pull-out resistance in pull-out tests with 30° aligned fibres is lower compared to the pull-out tests with 60° and 90° aligned fibres.

3 Numerical Simulations

Numerical analyses concerning the stress distribution around the embedded fibre rotated by different angles as well as the bond behaviour are conducted. Therefore, a new bond model is developed operating geometrically and physically non-linear on the mesoscale. This bond model is discretised with two-dimensional zero-thickness interface elements in the bond zone, which act in three-dimensional space and store the deformation and stress history of the bond layer on the surface of the surrounding concrete matrix [2]. Being in contact with the fibre surface, the bond response is calculated in dependency on the relative displacements of these surfaces. Simulating the full pull-out of a fibre from a concrete matrix within the theory of small strains, the mesh has to be flexible with respect to moving surfaces. Therefore, a repetitive mapping of the interacting fibre and matrix surface nodes is incorporated in the iterative calculation of every time step. The creation of bond forces due to the progressive fibre pull-out is modelled according to the theories of elasto-plasticity and continuum damage mechanics and separated by the relevant bond phases rigid and sliding bond [3]. The accumulated bond zone damage representing inelastic relative displacements in the bond layer displays the degradation of the capable bond stresses and can be evaluated in terms of cyclic tensile loading (figure 2).

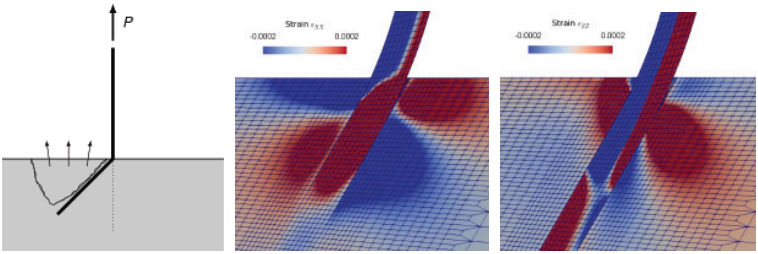

Figure 2: Numerical Simulation of oblique single-fibre pull-out tests (following [4])

4 Conclusions and Outlook

The pull-out tests subjected to both monotonic and cyclic loading show fibre pull-out as well as fibre rupture. For the future, the capacity of oblique-angled fibres bridging widening cracks will be investigated in comparison to orthogonally bridging fibres and according to the interaction of neighbouring fibres with different embedded lengths and orientation.

References

[1] Lanwer, J.-P.; Oettel, V.; Empelmann, M.; Dinkler, D.; Kowalsky, U.; Höper, S. (2019): Degradation Processes of UHPFRC under Cyclic Tensile Loading. In: Derkowski, W. et al. (Ed.): Proceedings of the fib Symposium 2019, Krakau (Polen), pp. 1912-1919.

[2] Höper, S.; Kowalsky, U.; Dinkler, D. (2018): Micro-structure related modelling of ultra-high-performance fibre reinforced concrete (UHPFRC) subjected to cyclic tensile loading. In: PAMM 18 (1), pp. 1–4.

[3] Lanwer, J.-P.; Oettel, V.; Empelmann, M.; Höper, S.; Kowalsky, U.; Dinkler, D. (2019): Bond behavior of micro steel fibers embedded in ultra-high performance concrete subjected to monotonic and cyclic loading. In: Struct. Concr. 20 (4), pp. 1243–1253.

[4] Makita, T.; Brühwiler, E. (2014): Tensile fatigue behaviour of ultra-high performance fibre reinforced concrete (UHPFRC). In: Mater. Struct. 47 (3), pp. 475–491.

Non-destructive evaluation of the fibre content and anisometry in thin UHPFRC elements

Aurélio Sine[1], Mário Pimentel[2], Sandra Nunes[3], Paria Mokhberdoran[4]
1,2,3,4: CONSTRUCT-LABEST, Faculty of Engineering (FEUP), University of Porto, Portugal
1: aurelio.sine@fe.up.pt, 2: mjsp@fe.up.pt, 3: snunes@fe.up.pt, 4: pmokhber@fe.up.pt

1 Introduction

It is well known that the tensile response of UHPFRC is governed by the fibre content and orientation [1], [2]. This leads to an anisotropic tensile behaviour that needs to be characterized, especially in the case of thin elements or thin layers without conventional steel reinforcement. Here we present further developments on a non-destructive test (NDT) method [3] that allows determining suitable fibre content and anisometry indicators.

2 Non-destructive method

Fundamentals

The NDT method consists on measuring the inductance of the magnetic circuit generated by placing a U-shaped inductor (or probe) over a UHPFRC layer (see Figure 1). In reference [3] is shown how to obtain the relative magnetic permeability of the composite, $\mu_{r,i}$, from the inductance measurements. It is also shown that $\mu_{r,i}$ is solely governed by the fibre fraction.

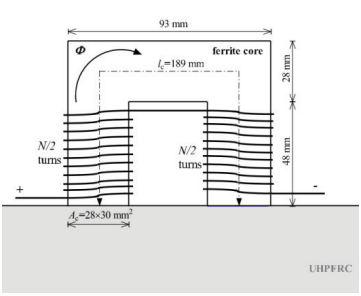

(a)

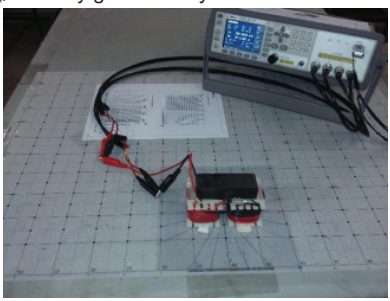

(b)

Figure 1: NDT method (a) magnetic circuit constituted by probe and UHPFRC layer; and (b) measurements on a 30mm thick UHPFRC plate.

Determination of the fibre volumetric fraction and fibre orientation factor

The mean of the relative magnetic permeability, $\mu_{r,mean}$, along any two orthogonal directions, *i* and *j*, was proposed [3] as an indicator of fibre content in UHPFRC element. For a given fibre type, element thickness and finishing of the measuring surface, $\mu_{r,mean}$ is shown to increase linearly with the fibre volumetric fraction, V_f.

The fibre orientation factor, $\alpha_{0,i}$, is selected as the scalar measure of the fibre anisometry, governing the tensile behavior of a crack normal to the i^{th} direction. The normalized difference of the relative magnetic permeability along two orthogonal directions, ρ_{ij}, is shown to be nearly linearly related to $\alpha_{0,i}$.

Approximation by a 2nd order tensor

The relative magnetic permeability of a thin UHPFRC layer is well approximated by a 2nd order tensor, as shown in Figure 2(a). Therefore, the relative magnetic permeability along a generic facet with orientation β, $\mu_{r,\beta}$, can be estimated from any three non-collinear measurements of μ_r. This allows determining the fibre orientation factor along any in-plane direction of a thin

UHPFRC element, as exemplified in Figure 2(b) for the case of a 0.03x0.85x1.10m^3 panel cast vertically with a flowable UHPFRC containing 9mm and 12mm long fibres (50% of each).

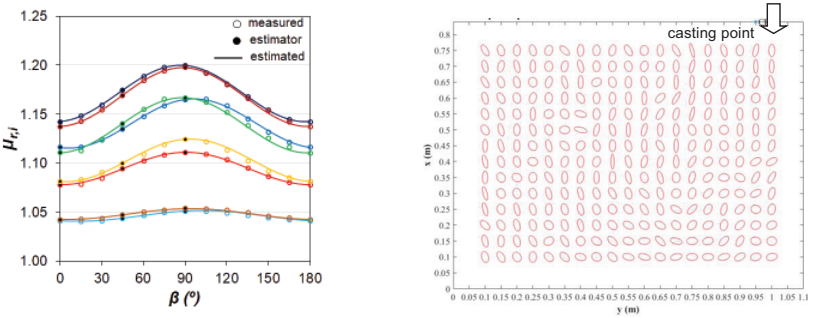

(a) (b)

Figure 2: (a) Relation between fibre orientation factor and fiber orientation indicator; and (b) ellipse representation showing the maximum and minimum fibre orientation factors in a vertically cast panel.

Estimation of tensile strength

The tensile strength of UHPFRC on a given *i*-direction, $f_{Utu,i}$, can be estimated using Eq. 1 [1,2]:

$$f_{Utu,i} = \tau_f \alpha_{0,i} \alpha_{1,i} V_f \frac{l_f}{d_f} = \tau_f.\lambda \qquad \text{Eq. 1}$$

where l_f and d_f are the length and diameter of the fibres and τ_f the effective bond strength. The parameter $\alpha_{1,i}$ is the fibre efficiency factor which can be determined from $\alpha_{0,i}$, as shown in references [1,2]. The fibre structure parameter, λ, can then be obtained knowing the fibre shape (l_f and d_f) and estimating V_f and $\alpha_{0,i}$ using the magnetic probe. This is shown in Figure 3, where the f_{Utu} values were obtained from DEWS tests with varying fibre contents and orientation profiles.

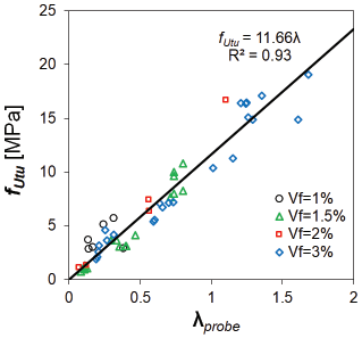

Figure 3: Tensile strength estimation.

3 Conclusions

The NDT method is shown to be an effective in the evaluation of both the fibre content and anisometry of the fibre distribution in thin UHPFRC elements. The approximation through the 2nd order tensor improves the efficiency of the method allowing the determination of the tensile strength of the material along any in-plane direction based on a minimum of three non-collinear measurements of the magnetic permeability.

References

[1] Bastien-Masse, M.; Denarié, E.; Brühwiler, E.: "Effect of fiber orientation on the in-plane tensile response of UHPFRC reinforcement layers," *Cem. Concr. Compos.*, pp. 111–125, 2016.

[2] Abrishambaf, A.; Pimentel, M.; Nunes, S.: "Influence of fibre orientation on the tensile behaviour of ultra-high performance fibre reinforced cementitious composites," *Cem. Concr. Res.*, pp. 28–40, 2017.

[3] Nunes, S.; Pimentel, M.; Carvalho, A.: "Non-destructive assessment of fibre content and orientation in UHPFRC layers based on a magnetic method," *Cem. Concr. Compos.*, vol. 72, pp. 66–79, 2016.

Pullout behavior of steel fibers under influence of impact loading rate and cryogenic conditions

Min-Jae Kim, Soonho Kim, Min-Chang Kang, Doo-Yeol Yoo
Department of Architectural engineering, Hanyang University, Korea

1 Introduction

This study aimed to investigate steel fibre pull-out behaviour from UHPC matrix, under impact loading rates and cryogenic temperatures (below –162°C) and the influence of the UHPC matrix-steel fibre interaction on the fibre pull-out behaviour. This was not only to verify the capability of the UHPC for building inner and outer walls of liquefied natural gas tanks which are frequently exposed to cryogenic temperatures but also to further investigate pullout behaviors of steel fibers under unusual conditions. The test results were analysed based on microscopic images of fibres and matrix including their interfaces, taken during and after the pull-out tests.

1 Experiment

The UHPC matrix was in accordance with the mix proportions applied in a previous study [1], which have been commercially used in North America. Silica fume replaced 25% weight ratio of Portland cement, and silica flour and silica sand were incorporated into the mix, along with polycarboxylate superplasticizer. Three types of steel (i.e. straight, half-hooked, and twisted, thus called S, H, and T, respectively) fibres were pulled out from the UHPC matrix. The S, H, and T fibers had a 30 mm length and 0.3, 0.375, and 0.5 mm diameters, respectively. Test conditions included aligned and 45° inclined conditions, static and impact loading conditions, and ambient and cryogenic temperature conditions. The specimen-naming process was based on temperature conditions (“” or “C” for ambient or cryogenic temperatures, respectively), fibre types (S, H, and T), and fibre inclination (“” or “-I” for aligned or inclined states, respectively).

2 Test result and analysis

Figure 1 shows that fibre pull-out properties were enormously influenced by cryogenic temperature, fibre inclination angle, and impact loading rate. Under cryogenic temperatures, bond strength of the S, H, and T fibres were considerably increased. For the inclined fibres, however, the increases in bond strength derived from the cryogenic condition were significantly smaller as compared to those of the aligned fibres. Although a slip capacity of the aligned S fibre was observed to be clearly higher under the cryogenic condition, that of the deformed H and T fibres remained the same or even decreased. In accordance with previous research [2], the inclined fibres showed increases in slip capacities, but no cryogenic effect was observed with respect to the slip capacity of the inclined fibres. The impact loading rate, in the meantime, also resulted in higher bond strengths of the aligned fibres under the ambient temperature. However, the increasing rates became lower or even negative, when the fibres were geometrically deformed, inclined, and pulled out under the cryogenic condition. Moreover, slip capacities were mostly reduced under the impact loading condition.

Figure 2 illustrates representative microscopic images on fibre pull-out ends after pull-out tests. It was noted that even the S fibre, without geometrical deformation and tilted angle, caused the matrix to be cracked and crushed. Furthermore, the matrix damage became much more severe under the cryogenic and inclined conditions. The impact loading rate, on the other hand, had less influence on the matrix damage as compared to the previous two experimental conditions.

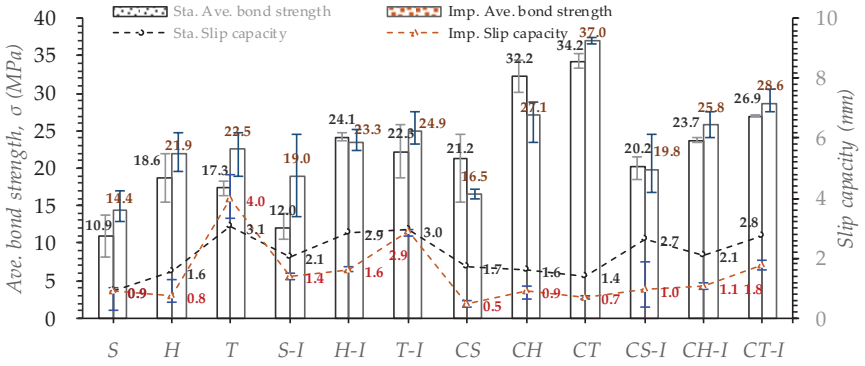

Figure 1: Average bond strength and slip capacities

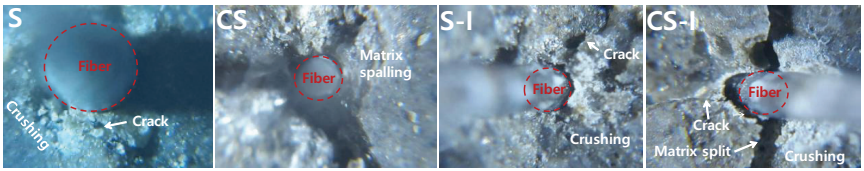

Figure 2: Micrograph on fibre pull-out ends

3 Conclusion

Steel fibre pull-out behaviours under the impact loading and cryogenic conditions were analysed with fibre-matrix damaging mechanism. Based on the analysis on test results and micrograph, the following conclusions were derived:

1. Average bond strengths of steel fibers considerably increased under the cryogenic temperature, and the increases were higher under the static loading rate. At the ambient temperature, the average bond strengths highly increased under the impact loading rate. At the cryogenic temperature, however, the increasing rates were considerably decreased.
2. The slip capacities generally increased under the static loading and cryogenic condition but decreased under the impact loading condition. The values were further deteriorated by the cryogenic temperature.
3. Stress concentration due to enhanced pull-out resistance at the cryogenic temperature or deformation and inclination of steel fibers caused premature fracture of fibers and larger matrix damage.

Acknowledgement

This work is supported by the Korea Agency for Infrastructure Technology Advancement(KAIA) grant funded by the Ministry of Land, Infrastructure and Transport (Grant 20SCIP-B146646-03).

References

[1] Kim MJ, Yoo DY, Kim S, Shin M, Banthia N. Effects of fiber geometry and cryogenic condition on mechanical properties of ultra-high-performance fiber-reinforced concrete. Cem Concr Res 2018;107:30–40.

[2] Cunha VMCF, Barros JAO, Sena-Cruz JM. Pullout Behavior of Steel Fibers in Self-Compacting Concrete. J Mater Civ Eng 2009;22:1–9.

Residual strength of UHPC exposed do sulfate and chloride attack

Aline Bensi Domingues[1], Pablo Augusto Krahl[2], Mounir Khalil El Debs[1]
1: São Carlos School of Engineering, Department of Structural Engineering, University of São Paulo, Brazil
2: State University of Campinas, São Paulo, Brazil

1 Introduction

Concrete structures built in aggressive environments like sea water, sewage or industrial effluents are typically susceptible to attack by inorganic acids. In this context, the use of ultra high performance concrete (UHPC) can increase the structure's lifetime due to lower porosity compared to conventional concretes due to particle packing. Silica fume and nano silica also influence on performance of cementitious materials under acid action [1-2]. So, due to the lower susceptibility of UHPC, new investigations are required regarding aggressive classes and ambients [3]. Therefore, this paper presents experimental finds on degradation processes of UHPC subjected to acid attack.

2 Experimental program

The UHPC utilized in the present research was developed in Krahl [4]. For characterization, cylindrical specimens (50x100 mm) were molded. After 28 days under moist chamber, six specimens were tested, which resulted in compression strength of 110 MPa. Other six speciments were immersed in hydrochloric acid solution (concentration 3%) and six in sulfuric acid solution (3% concentration) for 90 days. Figure 1 shows the specimens after removal from acid solutions. After drying, the speciments were tested under quasi-static strain rate and analyzed by scanning electron microscopy image (SEM image).

(a) *(b)*

Figure 1: Laboratory-accelerated degradation tests after 90 days (a) in hydrochloride acid solution (b) in sulfuric acid solution

3 Test results and discussions

The results of the compressive behavior are shown in Fig. 2. The specimens exposed to hydrochloric acid (HCl) presented a small reduction in modulus of elasticity of 6.4% compared to the reference samples. Also, the preapeak nonlinear behavior of the attacked samples was more pronouciated, which resulted in a greates peak strain, as shown in Figure 2(a). The color change in the external layer of the specimens indicates that chemical compounds were precipitated. The attack by chloride ions (Cl-) on harneded cement past results in formation of calcium chloride, which can be easily leached by water. However, analysis of pH variation and microscopy showed that chloride ions attacked only the outer layer. The peak strenght had insignificant variation.

In contrast, the samples subjected to sulfuric acid (H_2SO_4) had the strength reduced by 38.6% relative to the referece samples, and a more ductile behavior. This occurs due to reaction between ions sulfate (SO_4^{-2}) and the resistant compounds of concrete, such as calcium hydroxide (portlandite), hydrated calcium silicate (C-S-H) and monosulfate hydrate (AF_m) [5]. Figure 2(b) shows that specimens after sulfuric acid exposure had hard degradation with formation of expansive compounds and decrease in cross section.

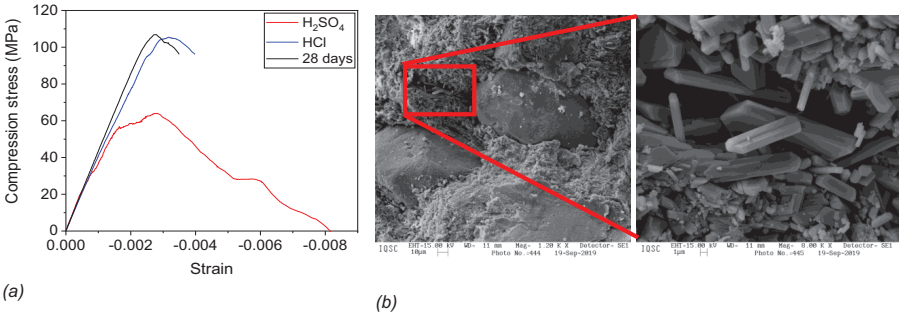

Figure 2: (a) Stress-strain curves (b) SEM image of gypsum crystals deposited in the corroded layer somewhere close to the unaffected section of the paste specimen after 90 days of exposure to sulfuric acid.

4 Conclusions

From the current research, it was found that the specimens immersed in aqueous solution with 3 % H_2SO_4 concentration had a reduction of 38.6 % in compressive strength. Such effect can be explained by the reduction in silica content of the cement paste in the outer layer of the specimens.

The samples immersed in water with 3 % of HCl had an insignificant reduction in strength. The major effect was the decrease in calcium content in a very small outer layer of the specimen with the effect of a slightly more nonlinear prepeak behavior.

References

[1] Poon, C. S.; Kou, S. C.; Lam, L.: Compressive strength, chloride diffusivity and pore structure of high performance metakaolin and silica fume concrete. Construction and Building Materials. 20.p 858-865. 2006.

[2] Mahdikhani, M.; Bamshad, O.; Shirvani, M. F.: Mechanical properties and durability of concrete specimens containing nano silica in sulfuric acid rain condition, Construction and Building Materials.167. p 929-935. 2018.

[3] An, M. Z.; Wang, Y., Yu, Z. R.; Ji, W. Y.; Han, S.: Durability of uhpc under complex environments. RILEM Proceedings. 1st International conference on uhpc materials and structures. V 105. P 380-394. Changsha. 2016.

[4] Krahl, P. A.: Lateral stability of ultra-high performance fiber-reinforced concrete beams with emphasis in transitory phases. Tesis (Doutorado em Estruturas) - São Carlos School of Engineering, University of São Paulo. São Carlos. 2018.

[5] Mehta, P.K.; Monteiro, P. J. M.: Concrete: Microstructure, Properties and Materials. 4. Ed. McGraw Hill Professional, 2013.

Investigation on the resistance of UHPFRC-RC composite beams to chloride ingress under mechanical loading

Toni Pollner, Christoph Dauberschmidt, Andrea Kustermann
Institute for Material and Building Research, Munich University of Applied Science (MUAS), Germany

1 Introduction

Ultra-High Performance Fibre-Reinforced Concrete (UHPFRC) has exceptional mechanical properties and a binder matrix that is virtually capillary pore-free. It is therefore particularly suitable for the repair and strengthening of reinforced and pre-stressed concrete structures that are exposed to both chlorides and high mechanical loads. Due to the high strength, RC-structures can be strengthened with very thin layers of UHPFRC in regard to their load-bearing capacity and serviceability. In combination with additional reinforcement, this effect is further enhanced. Furthermore, UHPFRC can serve as a protective layer against aggressive media such as chloride ions.

As in reinforced concrete, the question of the durability in the areas of cracks (or stress induced micro-cracks) in the UHPFRC layer also arises. Aggressive media can penetrate into the cracked concrete (or UHPFRC) much faster than into the non-cracked concrete. Many investigations show that the penetration resistance to aggressive media decreases with increasing crack width, for example [1]. Even in the non-cracked state, however, there is a possibility that high mechanical stresses may have a negative effect on the penetration resistance [2]. This circumstance has not yet been taken into account in durability design.

Therefore, investigations have been carried out at the Institute for Material and Building Research at the Munich University of Applied Science (MUAS), to determine the material properties of the UHPFRC used and the durability of UHPFRC-RC composite beams with simultaneous flexural tension and chloride exposure. The presentation focuses on the combined loading tests.

2 Materials and methods

A UHPFRC ready-mix was used as repair and strengthening material. The mixture consists of a premix with a maximum grain size of 0.6 mm, a superplasticizer and 2.11 Vol.-% steel wire fibres with a length of 14 mm and a diameter of 0.2 mm. The material has a compressive strength of 187 MPa after 28 days of water storage. The tensile strength has been determined with bending tests according to SIA 2052 and amounts to 13.1 MPa. There was no strain hardening effect assessed under axial tensile stress.

For the experimental investigations on combined loading, roughened and notched reinforced concrete RC-beams were produced in advance, loaded to initiate a crack width of 0.2 mm in four-point flexural tensile tests and then strengthened with a 30 mm thick UHPFRC layer. The substrate concrete was prepared by exposing the coarse aggregate with a high-pressure cleaner shortly before the concrete solidified. After sufficient hardening of the UHPFRC, the composite beams were subjected to a combined load of simultaneous bending tensile stress and chloride exposure with a 10 % NaCl solution. During the test procedure, the electrolyte resistance Z of the composite beam was recorded using Electrochemical Impedance Spectroscopy (EIS) between a titanium strip anode in the chloride container and the electric conductively connected reinforcement. The electrolyte resistance provides information on the charge transport in the pore solution of the concrete and can be used to estimate the chloride penetration resistance. The test setup is shown in Figure 1.

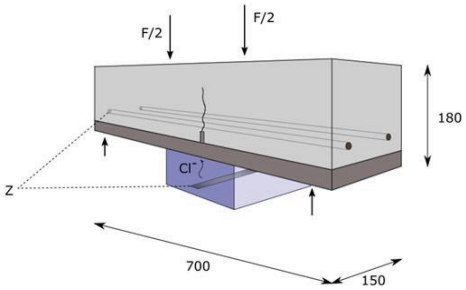

Figure 1: Experimental set-up for combined loading (dimensions in millimetres)

Subsequently, two samples were taken from the crack area of each composite beam and prepared for the following investigations. Half of the samples were examined at HafenCity University Hamburg (HCU) for their chloride distribution using Laser Induced Breakdown Spectroscopy (LIBS). The procedure is described in [1]. The other half of the samples was prepared according to [3] and examined under a digital reflected light microscope for crack formation.

3 Results and Discussion

The results show a decrease of the electrolytic resistance both under continuous static and cyclic mechanical stress. Depending on the type, level and duration of the load, the electrolyte resistance dropped by up to 73 % of the initial value. It is assumed that the loss of resistance is caused by microcracks in the UHPFRC layer, through which chloride ions dissolved in water can penetrate into the concrete. As a result, the conductivity of the electrolyte increased and the electrolytic resistance decreased accordingly.

The investigations on chloride distribution in the crack area revealed a high chloride content of up to 2 wt.% by cement directly in the crack area of the UHPFRC as well as in the substrate concrete and thus confirms the results of the electrolytic resistance measurements.

With the help of digital reflected light microscopy, it could also be shown that several micro cracks with remaining crack widths of about 30 µm were formed in the UHPFRC by applying increasing load and that the wide crack in the reinforced concrete was thus divided into several small cracks within the UHPFRC.

4 Conclusions and Outlook

As the investigation results show, the penetration of chloride ions under simultaneous mechanical stress and the resulting crack formation could not be prevented by the thin protective layer of UHPFRC. It can be stated, however, that the large crack widths or the crack width changes in the RC-beams are divided up into several small, presumably less harmful cracks in UHPFRC, even if the material is not strain-hardening.

The future investigation in the framework of a new research project on retrofitting with sprayed UHPFRC (i-SCUP) at MUAS will focus on the question: which modification of material, load and specimen layout can reduce the chloride ingress to a harmless value? The aim is to determine critical crack width, below which a chloride ingress can be significantly reduced. Furthermore, the investigations will be carried out with UHPFRC with strain hardening effect.

References

[1] Šavija, B., Schlangen, E., Pacheco, et al.: Chloride ingress in cracked concrete: a laser induced breakdown spectroscopy (LIBS) study. Journal of Advanced Concrete Technology 12 (2014), S. 425–442.

[2] Yao, Y., Wang, L., Wittmann, F. H., et al.: Test methods to determine durability of concrete under combined environmental actions and mechanical load: final report of RILEM TC 246-TDC. Materials and Structures 50 (2017), S. 105.

[3] Kustermann, A.: Einflüsse auf die Bildung von Mikrorissen im Betongefüge. Dissertation. München 2005.

Microstructure analysis of thermally treated ultra high performance concrete in the context of the durability performance

Marieke Voigt, Julia von Werder, Birgit Meng
Bundesanstalt für Materialforschung und-prüfung, Berlin, Germany

1 Thermal treatment of ultra high performance concrete (UHPC)

Thermal treatment is a common application in the production of precast UHPC elements to reach the characteristic compressive strength of over 150 MPa immediately after the heat treatment and to reduce the effect of autogenous shrinkage. Previous studies [1] tested and analysed different protection styles against desiccation during thermal treatment focusing on the performance in compressive strength. During these studies an inhomogeneity in form of a zonation over the cross section of selected samples was observed after the thermal treatment as can be seen in figure 1A. A correlation between the thickness of the outer zone and the degree of desiccation during thermal treatment was found by measuring the average width of the visible zonation. This study is focusing on the effect of the zonation and the detected change in porosity [2] on the durability performance.

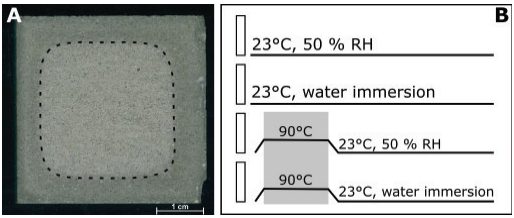

Figure 1: A. Cross section of a 4x4x16 cm specimen after 90°C thermal treatment for 6 days without protection against desiccation. B. Sample treatment incl. thermal treatment (grey) and storage conditions before testing.

2 Materials & Methodology

For the durability study a SiO_2-based UHPC mixture design after [1, 3] without the addition of fibres was chosen. For more detailed information on the mixture design and sample preparation see [2]. Four different treatment methods of the samples (Fig. 1B) were investigated to link the microstructure studied in [2] to different treatment effects and finally to the durability performance. A prolonged thermal treatment of 6 days at 90 °C without protection against desiccation was performed to produce a distinctive zonation. Afterwards, the UHPC samples were either stored in a controlled climate at 23 °C and 50 % RH exposed to air or immersed in water (Fig. 1B). The reference samples were stored at 23°C either at the air or submerged in water over the time of 28 days.

For testing of the durability performance three testing procedures were carefully chosen of the variety of tests available. In this study the acid resistance, the air permeability, and the capillary water absorption were investigated. For testing the sulphuric acid resistance, the German regulation NA 119-05-37-01 AKN 61 was adapted. As the concrete mixture analysed is not declared acid resistant the strength performance after immersion in sulphuric acid (pH 1) was neglected and merely the reduction in sample size was measured. To track possible shifts in chemical composition µXRF mappings of the cross sections of the specimen were taken after 28-days of acid immersion. The air permeability testing was conducted on cylindrical specimens with a diameter and height of 5 cm in a pressure range up to 4,5 bar after the RILEM TC 116-PCD. The capillary suction was conducted after DIN EN 13057 on cylindrical specimen

(diameter of 4 cm/ height of 5 cm) for a time period of 45 days. ^{1}H-NMR relaxometry of the cores visualises the water uptake additionally to the gravitational measurements.

3 Results

The thermally treated specimens show a higher resistance against sulphuric acid compared to the reference samples cured under ambient conditions (Fig. 2). Hence, the thermally treated samples exhibit 22 % less abrasion compared to the reference samples. The spatial distribution of major chemical elements was not altered during the test. Merely the homogeneous size reduction and the sulphur permeation on all sides of the samples could be confirmed via µXRF. The sulphur intrusion correlates with the values from the air permeability tests. The air permeability is 2.5 to 3 times higher in the reference samples cured at ambient conditions compared to the thermally treated samples. The sorption coefficient of the reference sample

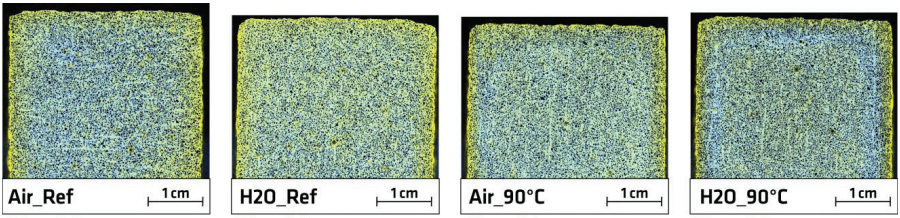

Figure 2: µXRF mappings of the samples after 28d acid immersion, blue = sulphur, yellow = potassium. AR_{70} = Acid resistance after 70d, K = permeability, WA = water absorption

stored in the water bath is the lowest whereas the sample cured at 90 °C and exposed to air exhibits the highest sorption coefficient (Fig. 2) and the deepest water intrusion (Fig. 3). For the latter it could be seen that the water absorption was influenced through inhomogeneities in the texture such as microcracks and lead to an inhomogeneous water distribution within the specimen.

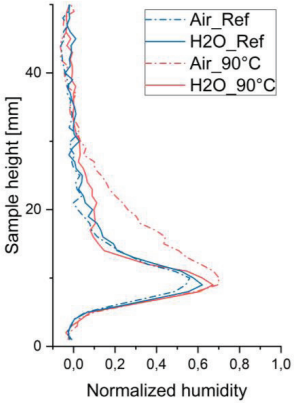

Figure 3: H1-NMR relaxomtery data of the humidity distribution through out the samples after 28d.

4 Conclusion

The durability tests illustrate that thermal treatment of UHPC even under severe conditions without protection against desiccation is improving the durability of UHPC compared to a UHPC cured under ambient conditions. Even though the mean porosity of thermally treated UHPC compared to UHPC cured under ambient conditions is larger [2] and suggested otherwise. The indication of microcracks after thermal treatment did not have a severe effect on the durability.

References

[1] Selleng, C., et al., Influencing factors for the effectivity of heat treatment of ultra-high performance concrete (UHPC). Beton- und Stahlbetonbau, 2017. **112**(1): p. 12-21.

[2] Voigt, M., J. von Werder, and B. Meng, Investigagtion of the zonation of thermally treated ultra high performance concrete. Construction and building Materials, 2020: (in review)

[3] Bornemann, R., et al., Ultra High Performance Concrete UHPC - Composition, Properties and Applications. Beton- und Stahlbetonbau, 2001. **96**(7): p. 458-467.

Effect of the liquid phase on the rheological properties of UHPC

H. Vacca[1], Y. Alvarado[1], J. Hurtado[1], D. Ruiz[1], M. Ocampo[1], A. Nuñez[2]
1: Pontificia Universidad Javeriana, Civil Engineering Department
2: Argos S.A., & + D. Colombia

1 Abstract

Rheology is a fundamental property to characterize the workability, consistency, and fluidity of a concrete. This study investigates the rheological behaviour of UHPC concrete for four (4) percentages of variation of superplasticizer, with respect to the reference dosage. A coaxial rheometer was used for determination of flow curves of tested samples. These flow curves and the relationship between the yield stress and mini-slump flow test [1] were measured from a time of 36 minutes and up to two (2) hours after having come into contact with the liquid phase and solid phase in the mixing process of the UHPC. The variation of the compressive strength for the different percentages of SP used in this study was determined.

2 Experimental program

Materials used in this study were of local origin (Colombia, Southamerica). The basic mixture of UHPC was prepared whit Portland cement, silica fume, sand, superplasticizer, water, and steel fiber. A polycarboxylate-based superplasticizer (SP) used in this study was formulated to meet ASTM C-494 [2]. Four (4) different mixes of UHPC was prepared. A reference mixture of UHPC was determined, which includes the use of superplasticizer (SP) to obtain a value of 220±10 mm of mini-slump and 150±10 MPa compressive strength at 28 days. The name of this mix is 100%-SP. The next mixture was made with 5% less of SP than a reference value, and was called is 95%- SP. In the same way, two additional mixtures were designated with the name of 90% -SP and 85% -SP.

3 Experimental results and conclusions

For the 100%-SP mixture, no measurement value was obtained in the standard slump, even after two hours (120 min). In contrast, the mini-slump test indicated that for the 100% SP reference mixture, the fluidity value was reduced to 34% after two hours, affecting the workability of the UHPC. If the mixtures are compared within 36 minutes, a decrease in workability of 38%, 48%, and 52% is observed for the 95%-SP, 90%-SP and 85%-SP mixtures respectively, (see figure 1.a). Moreover, for the yield stress parameter (τ_o), the situation is similar. Where when decreasing the percentage of additive and / or increasing the time, the value of τ_o increases, as shown in figure 1.b.

Figure 2.a, shows the dependency of τy on the diameter of the flowability Df. It is evident that the trend can be fitted by an exponential function in the form of $\tau_o = e^{A \cdot Df + B}$ and its linearization form $\ln \tau_o = A \cdot Df + B$. In comparison with results of other research, [3] the behavior of the workability is the same. However, in this case, the range of fluency is lower than in other studies, demonstrating that this exponential relationship can be acceptable in this range. However, the relationship of the yield stress with the slump test (Figure 2.b.) does not show a good correlation. Thus, it can be attributed to the fact that the slump test does not cover an appropriate range of flowability of UHPC concrete.

Finally, the behavior of the compressive strength is shown in Figure 3. It was observed that when the percentage of SP decreased, the compressive strength decreases, until finding that for the 85% -Sp mixture, the resistances would be out of range of a UHPC.

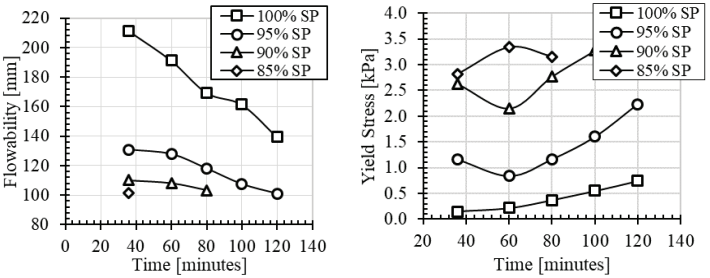

Figure 1: a) Flowability with different percentage of SP at time, and b) Yield stress with different percentage of SP at time.

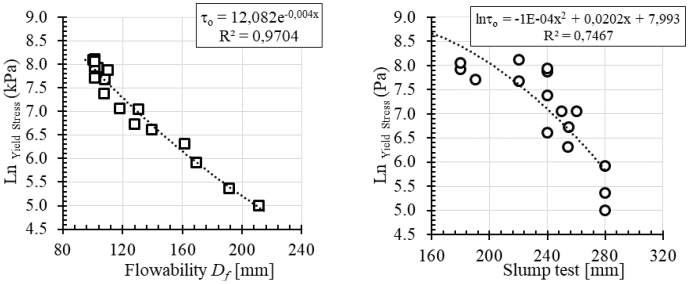

Figure 2: a) Relationship between yield stress and Flowability, and b) Relationship between yield stress and slump test.

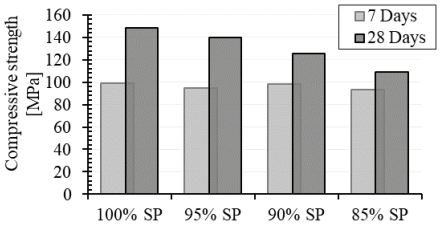

Figure 3: a) Compressive strength at 7 and 28 days, for each of the mixtures.

4 Acknowledgements

The authors of this work acknowledge and thank the support given by Cementos ARGOS S.A, COLCIENCIAS (Project No. 63881), and the Civil Engineering Department of the Pontificia Universidad Javeriana.

References

[1] European Standard, «EN 12350-8: testing fresh concrete – Part 8: self-compacting concrete – Slump-flow test». 2008.

[2] I. ASTM, «Standard Specification for Chemical Admixtures for Concrete. C494/C494 M-17». 13-feb-2019.

[3] O. Koutný, D. Snoeck, F. Van Der Vurst, y N. De Belie, «Rheological behaviour of ultra-high performance cementitious composites containing high amounts of silica fume», Cement and Concrete Composites, vol. 88, pp. 29-40, abr. 2018.

Behaviour of fasteners in steel fibre reinforced concrete under tension loads

Norbert Vita, Akanshu Sharma, Jan Hofmann
Institute of Construction Materials, Department of Fastening and Strengthening Methods, University of Stuttgart, Germany

1 Introduction

In the present work, tension tests on single bonded anchors in two different types of normal concrete (low- and high strength) as well as in corresponding steel fibre reinforced concrete (SFRC) are presented. The main objective of the work was to investigate the influence of SFRC on the performance of anchors including its resistance, displacement behaviour and ductility. In order to reach that aim, a number of test parameters had to be adapted to the properties of the basematerial (SFRC).

State of the art and Motivation

In the past, the positive influence of the SFRC on the load bearing behaviour of anchors (cast-in or post-installed), due to crack bridging mechanism and higher fracture energy, was reported in a few tests. The recent investigations by Tóth et al. [1] have shown that a positive influence on the load-bearing behaviour of anchorages in SFRC can only be observed if the type of failure in plain concrete (PC) as well as in corresponding SFRC is concrete breakout (concrete cone or concrete edge), and the test parameters, such as fiber length, effective depth of the anchor, edge distance of the anchor, aggregate size etc. lie in a certain range. The paper by Tóth et al. [1] summarizes and evaluates the most relevant articles on this topic in the recent years.

2 Experimental investigations

Test program, setup and procedure

The experimental program focussed on investigating the influence of steel fibres on concrete cone resistance of the anchors with regard to the following parameters: concrete grade, fiber content, anchor size, effective depth, edge influence and concrete condition (uncracked or cracked concrete). Therefore, tension tests (on surface, on the edge, in crack) were carried out on single bonded anchors, in two concrete grades (C25/30 and C50/60) and in corresponding SFRC with different amount (20, 40 and 80 kg/m^3) of steel fibres. Hooked-end steel fibre with a length/thickness ratio of 35/0.55 [mm] and tensile strength of app. 1200 N/mm^2 were used. The standard tension test setup acc. to ETAG 001, Annex A was used for all test series.

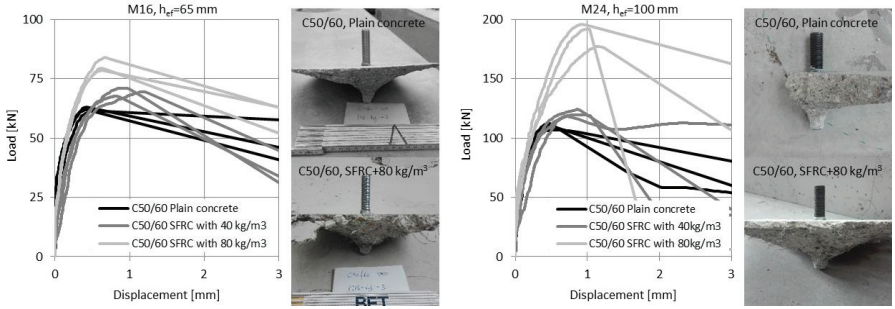

Figure 1: Load-Displacement curves from tension tests with bonded anchor on surface in different concrete types (Plain, SFRC with 40 and 80 kg/m^3) and the corresponding failure mode, concrete cone breakout.

Tests Results and Discussion

Due to space limitation, Figure 1 shows the typical load displacement curves from the tension tests with bonded anchor (left M16, right M24) in SFRC with low and high (40/80 kg/m^3) steel fiber content, as well as the corresponding reference curves in PC. The diagrams clearly show a beneficial influence of the presence of steel fibers on the concrete cone resistance of the anchors. As expected, a higher tension resistance was obtained in case of tests with high fiber content and with larger effective embedment depth due to the activation of more fibers.

Figure 2 (left side) summarizes the results of all tension tests in terms of the ratio of failure load in SFRC to corresponding load in PC as a function of fiber content. As the steel fiber content increases, the beneficial influence of the fibers on concrete cone resistance of the anchor also increases both for the anchors away from the edge as well as those close to an edge. The comparison of the test results with the recommendation from [1] shows a very good correspondence.

Additionally, load-displacement curves from tension tests on M16 bonded anchors in cracked and uncracked SFRC are shown in Figure 2 on the right. The results indicate that the factor 0.7 for the ratio of concrete cone resistance in cracked to that in uncracked concrete is valid also for anchorages in SFRC.

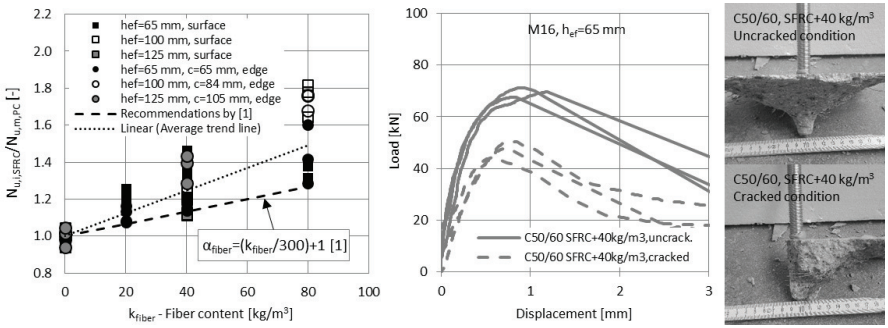

Figure 2: Left: Increasing factor ($N_{u,l,SFRC}/N_{u,m,PC}$) as a function of steel fibre content for 46 tests in SFRC and 28 reference tests in PC, Right: Load-Displacement curves on bonded anchors M16, in uncracked (solid) and cracked SFRC (dashed), high comp.strength and 40 kg/m^3 amount of fiber and pictures of failed anchors

3 Conclusions

Anchorages can achieve a better performance in SFRC (failure load, displacement) in comparison to PC, provided the anchor geometry and base material properties are favourable and concrete breakout is the dominant failure mode. If the design parameters (anchor/fiber geometry and concrete mix design) are optimized to activate a large amount of fibers, it can result in a significant increase in the concrete cone resistance of the anchors. For all other types of failure (pullout, splitting or combined concrete cone and pullout), further tests need to be carried out to verify the load-bearing behaviour. Although the tests were performed in SFRC, it is presumed that the load-bearing behaviour of the anchors in UHPC should be similar due to better properties of UHPC such as increased tensile strength, better post-crack behaviour compared to PC. The behaviour of anchorages in UHPC will be investigated in future research.

References

[1] Tóth, M., Bokor, B., Sharma, A.: Anchorage in steel fiber reinforced concrete concept, experimental evidence and design recommendations for concrete cone and concrete edge breakout failure modes - Engineering Structures , Vol. 181, pp.60 75, 2019

Validation and adaptation of Dewar's packing model for mix design of UHP(FR)C

Elke Gruyaert, Pieter Caerels, Iben Delameilleure, Peter Minne
KU Leuven, Department of Civil Engineering, Gebroeders De Smetstraat 1, B-9000 Ghent, Belgium

1 Introduction

Conventional concrete is a versatile material, abundantly available and simple to manufacture, has preferable characteristics and the cost of the raw materials is low [1]. However, it has some shortcomings as a low tensile strength, brittle behaviour and relatively low compressive strength.

The aim of this study is to develop a method to design ultra-high performance (fibre reinforced) concrete (UHP(FR)C). This UHP(FR)C is characterized by a very high compressive strength (≥ 150MPa), a low W/B-ratio, an improved flexural tensile strength, sufficient fluidity, a low porosity and an excellent durability [2]. The current study focuses on two methods to optimize the packing density: (i) the method developed by the research group of Brouwers [3], based on the modified model of Andreasen & Andersen and (ii) the particle theory of Dewar [4], based on the interaction diagrams of Powers. The effect of the chemical and mineralogical properties of the cement and the silica fume (SF) in combination with the chemical structure of the superplasticizers (SP) on the flowability of the fresh mix was studied and the compatibility of the binder with the SP was evaluated.

2 Materials and methods

Materials

The materials applied in the current research were: (i) Ordinary Portland Cement (OPC) CEM I 52.5R, provided by two suppliers, (ii) polycarboxylate-based SP, to optimize the water reduction and flowability of the concrete, (iii) quartz powder Silverbond M800 and Micosil M4, to optimize the cement content, (iv) SF and nanosilica in slurry, (v) different fractions of quartz sand and (vi) basalt and porphyry, as the coarse aggregate fraction in some mixtures.

Mix design methodology

The size distribution of the modified Andreasen & Anderson model is given by Eq. (1) [3]:

$$P(D) = \frac{D^q - D_{min}^q}{D_{max}^q - D_{min}^q} \quad (1)$$

Where D is the particle size $[\mu m]$, D_{min} and D_{max} represent the minimum and maximum particle size $[\mu m]$ resp.; $P(D)$ is the cumulative fraction of the total solids being smaller than size D and q is the distribution modulus, which can be related to the fineness of the mix.

The model acts as a target function for the optimisation of the composition of the mixture. The least squares method is used to determine the proportions of each material in the mix.

According to the particle packing theory of Dewar, the proportions of each individual material in the mix can be calculated. When two groups of particles (e.g. fine and coarse particles) are mixed together, the small particles will fill the voids between the larger particles. However, this effect is disturbed by particle interference (wall effects and loosening effects) [4]. The advantage of a packing model is that in addition to the particle size distribution, the voids, which are related to the particle shape, particle texture, particle distribution, packing energy, etc. are taken into account. In Dewar's packing model, the fineness of the mix can be controlled by the cohesion factor (CJ).

A new mixing procedure was developed in the current study based on the mixing procedures for UHP(FR)C of De Larrard & Sedran and Tafraoui [1].

Testing

A total of 32 UHP(FR)C mixtures were manufactured and tested.

The reference target compressive strength on cubes 70x70x70 mm³ was 150 MPa and reference the mini slump flow value was 200 – 250 mm. Flowability was evaluated by the mini slump flow test (EN 1015-3 (1999)). Compressive and flexural strength of the specimens were determined according to NBN EN 12390-3 (2009) resp. NBN EN 196-1 (2016).

3 Results and discussion

An evaluation of Dewar's packing model to design UHPC was established and a comparison was made with the design method of Brouwers. It was found that in the modified model of Andreasen & Anderson the proposed q-value of 0.23 is too high to achieve the proposed requirements, as indicated also by [5]. Better results were obtained with a q-value between 0.12-0.18. With the model of Dewar, good results were obtained for a CJ between 9-15 (Table 1). In addition, the water demand and the flowability of the mixture could be predicted accurately.

Based on a more extended analysis of the results, it is shown that the chemical and mineralogical properties of the cement and the SF have an influence on the flowability of the fresh concrete. On the one hand, the carbon content of the SF must be limited. On the other hand, we believe that mainly the C_3A-content of the cement should be kept to a minimum. Also, Plank et al. [6] discovered that PCE-intercalation cannot occur when the SO_3/C_3A ratio is higher than 1. It also seems that the alkali sulphates show a good correlation with the flowability, in case of delayed addition of SP. Apparently, alkali sulphates dissolve faster than the calcium sulphates. Therefore, the alkali sulphates determine whether the SP can intercalate or not. Further, it is observed that nanosilica strongly raises the water demand and the concentration of the slurry limits the maximum dosage.

Table 1: Influence of the cohesion factor on the mixture composition and compressive strength.

	CJ 15	CJ 11	CJ 9
Aggregates D_{max} = 2 mm (kg/m³)	1149.5	1293.1	1360.8
Cement CEM I 52.5R (kg/m³)	737.7	664.3	623.1
Silica fume (kg/m³)	105.4	94.9	89.0
Quartz flour (kg/m³)	210.8	189.8	178.0
Water (kg/m³)	182.1	165.4	159.9
Superplasticizer: dry matter (kg/m³)	13.1	9.5	8.9
W/(C+SF)	0.216	0.218	0.225
Voids ratio (-)	0.21	0.20	0.19
Mini slump flow (mm)	225	235	223
7 days compressive strength (MPa)	135	133	134
28 days compressive strength (MPa)	166	157	150

4 Conclusions

In comparison to the method of Brouwers, which is easy to apply, the Dewar's model is more fundamental and can be used to design UHP(FR)C, predict the water demand and flowabillity.

References

[1] Sohail, M.G., et al.: Advancements in Concrete Mix Designs: High Performace and Ultrahigh-Performance Concretes from 1970 to 2016. *J. Mater. Civ. Eng.* 30(3), 2018

[2] Cauberg, N.; Piérard, J.; Parmentier, B.; Wastiels, J.: Ultrahogesterktebeton, een nieuwe stap in de betontechnologie. *WTCB-Dossiers,* NR4/2008, Katern nr.11, 2008

[3] Yu, R., Spiesz, P., Brouwers, H.J.H.: Mix desigofsn and properties assesment of Ultra-High Performance Fibre Reinforced Concrete. *Cem. Concr. Res.* 56, pp. 29-39, 2014

[4] Dewar, J.D.: Computer Modelling of Concrete Mixtures. Int E&FN Spon, London, 1999

[5] Li, P.P., et al.: Effect of coarse basalt aggregates on the properties of ultra-high performance concrete (UHPC), Constr. Build. Mater. 170, 2018

[6] Plank, J., et al.: Fundamental mechanisms for polycarboxylate intercalation int C_3A hydrate phases and the role of sulfate present in cement, *Cem. Concr. Res.* 40(1), pp 45-57, 2010

Effect of wet curing time on the pull-out behavior of steel fibers in UHPFRC

Pablo Augusto Krahl[1], Gustavo de Miranda Saleme Gidrão[2], Gustavo Henrique Siqueira[1], Ricardo Carrazedo[2]

1: University of Campinas, São Paulo, Brazil
2: São Carlos School of Engineering, Department of Structural Engineering, University of São Paulo

1 Introduction

Very high strength in compression, strain-hardening behavior in tension, and the possibility of developing lighter components make Ultra-High-Performance Fiber-Reinforced Concrete (UHPFRC) a promising material for application in the precast industry. As is known, UHPFRC has typically high volumes of binders that require appropriate curing for adequate hydration. However, fast construction can restrict the curing time, for example, for elements that are shipped to construction sites in one day after casting without any curing. Therefore, the characterization of UHPFRC subjected to different curing periods is essential for its application in precast construction. In this context, it should be emphasized that many research has been developed to understand fiber interaction with the Ultra-High-Performance Concrete (UHPC) matrix. However, the topic concerning the influence of early age exposure of UHPFRC to ambient curing on the pull-out behavior was not significantly explored.

2 Experimental program

The UHPFRC utilized in the present research was developed in Krahl [1]. Fibers for pullout tests were fixed vertically in an acrylic plate of 150 x 500 x 6 mm dimensions. Pouring of UHPFRC in the mould covered the fibers, which had a diameter of 0.2 mm a length of 12 mm. Also, a test apparatus was developed for the pullout, as shown in Figure 1 (a) and (b).

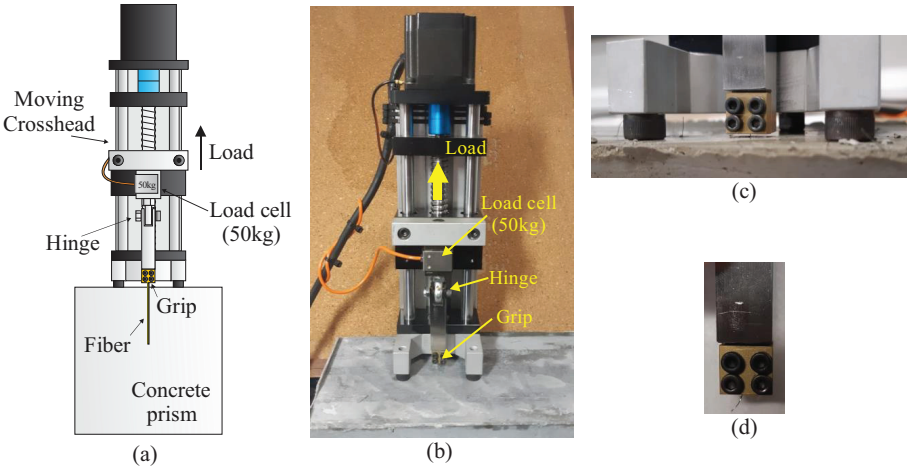

Figure 1 – (a),(b) Portable test apparatus for single fiber pull-out (c) detail of the grip and the supports, and (d) pulled fiber cramped at the grip

The portable machine rests on three points of the concrete surface for testing, Figure 1 (c), which gives the stability for applying the pullout load. Figure 1 (c) shows a fiber clamped at the grip after pull-out. In the current research, the fibers were pulled at a speed of 0.005 mm/s. One concrete prism was taken from the moist chamber after 1, 3, 7 and 28 days to be subjected to

ambient curing. All tests were performed at 28 days. The average compressive strength, tensile strength, and modulus of elasticity at 28 days were 129.6 MPa, 11.11 MPa, and 44 GPa, respectively.

3 Results

The pull-out performance is represented in the current paper by average bond strength τ_{av}, calculated with equation (1), as in Yoo and Kim [2], versus dimensionless slip S/L_E, obtained from the force-slip curve, where S is the current slip and L_E is the initial fiber embedded length.

$$\tau_{av} = \frac{P_{\max}}{\pi d_f L_E} \qquad (1)$$

Where P_{max} is the maximum load of the pull-out test, df is the fiber diameter. Figure 2 presents average curves for the pullout behavior of UHPFRC subjected to different curing periods.

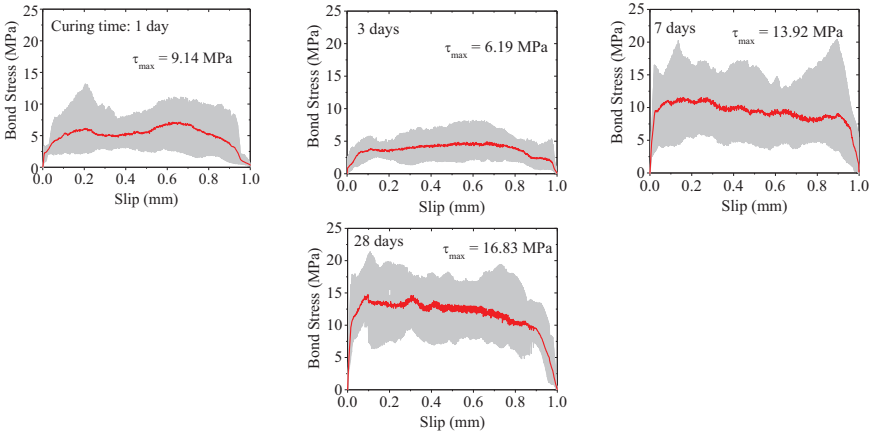

Figure 2 – Pull-out curves for UHPFRC subject to different curing times. All tested at 28 days

The developed UHPFRC did not develop significant bond strength when it was left under ambient curing from 1d and 3d until the date of the test (28d) when compared to the samples left 28d in wet curing (reference case). However, the samples left 7d in the moist chamber reached average bond strength which was 83 % of the maximum bond reached by the reference samples.

4 Conclusions

Based on the experimental results of pullout tests in UHPFRC left different times in the moist chamber, it can be concluded that the time of wet curing had a significant effect in the bond strength of the fibers, which is attributed to the loss of hydration water necessary for developing stronger interfacial properties. However, the samples left 7d in wet curing presented 83% of bond strength reached by the samples left 28d in the chamber.

References

[1] Krahl, P.A.: Lateral stability of ultra-high performance fiber-reinforced concrete beams with emphasis in transitory phases, University of São Paulo, 2018.

[2] Yoo, D.; Kim, S.: Comparative pullout behavior of half-hooked and commercial steel fibers embedded in UHPC under static and impact loads, Cem. Concr. Compos. 97 (2019) 89–106.

Strengthening and/or retrofitting of reinforced concrete elements with thin UHPFRC layers

Andre Strotmann[1], Andrea Kustermann[2], Christoph Dauberschmidt[2], Jörg Jungwirth[1]
1: Structural Engineering, University of Applied Sciences Munich (MUAS), Germany
2: Institute for Material and Building Research, Munich University of Applied Science (MUAS), Germany

1 Research project i-SCUP "Instandsetzung (Retrofitting) – Shotcrete Ultrahigh Performance"

In the sector of infrastructure and building construction, the structures are typically up to 80 years old. Many of the structures are in damaged condition due to chloride attack and loading [1]. The established retrofitting methods are usually associated with major intervention in the structure, therefore they are expensive and time-consuming.

In the research project "Retrofitting and strengthening of reinforced concrete structures by using thin UHPFRC shotcrete layers: application areas, design, durability, processing technology", a holistic investigation of the strengthening system is carried out.

This paper provides research results of cast UHPFRC concrete elements as a pre-study for UHPFRC shotcrete project. Out of this an optimized retrofitting and strengthening systems is developed by using the innovative material ultra-high performance fibre reinforced concrete (UHPFRC) as shotcrete in thin layers.

2 Investigations

General

When retrofitting/strengthening concrete elements by using UHPFRC shotcrete one obtains composite elements of UHPFRC and concrete, which are characterized by two cementitious materials featuring different material properties and ages. As a basis for the research, a detailed investigation of the composite action is carried out. This investigation with main focus on cracking and load bearing properties is based on already existing design approaches for cast UHPFRC-concrete composite elements. To consider specific aspects of spayed UHPFRC, a test series with varying parameters off spayed UHPFRC-concrete composite elements is conducted. To calculate the stresses in the cross-section, restrained stress during the curing process are determined as well as stresses caused by external load. The stresses have been derived from the material-specific stress-strain curves, for which accompanying material tests have been carried out. The results are compared with the existing design approaches of UHPFRC concrete composite elements. In addition, the degree of restrain μ of the UHPFRC layer due to the thickness ratio of new and old concrete can be determined in the future. The results and knowledge are used as a basis for the investigation of the UHPFRC shotcrete. The main factor for the durability of the UHPCFRC layer is the cracking characteristics.

Analytical Investigation

First, an analytical investigation of the specimens was carried out. The calculation is based on SIA 2052 [2]. The calculation focussed under special consideration of the strains and stresses in serviceability limit state and ultimate limit state. For this an Excel sheet has been developed, which allows an efficient calculation of the composite elements with different material properties. Material models for the UHPFRC and interaction approaches of the different materials have been defined for the design of the UHPFRC concrete composite elements.

Experimental Investigation

There have been four point bending tests on beams with a length of 1.15m, width of 15cm and height of 12cm plus 5 different UHPFRC layer thicknesses à 3 samples. The specimens were tested under positive or negative bending.

	Specimen 1	Specimen 2	Specimen 3	Specimen 4	Specimen 5
reinforment	rebars	unreinforced	unreinforced	unreinforced	unreinforced
concrete	rebars	rebars	rebars	rebars	rebars
length	1050 mm	1050 mm	1050 mm	1050 mm	1050 mm
width	150 mm	150 mm	150 mm	150 mm	150 mm
heigth	120 mm	120 mm	120 mm	120 mm	120 mm
UHPFRC	40 mm	40 mm	20 mm	15 mm	8 mm

Strain gauges were placed on the rebars in order to determined the induced stresses from shrinkage and creep during the curing process of the concrete. These measurements provid information on the restrain stresses and the degree of restrain μ of the thin UHPFRC layers.

The strain gauges on the rebars were able to provide strain data during the four-point bending test. The specimens were also equipped with optical and inductive measuring technology. Figure 1 shows the position of the strain gauges in different heights over the UHPFRC-concrete composite element. On the specimen surface, the deformation of the composite element is shown.

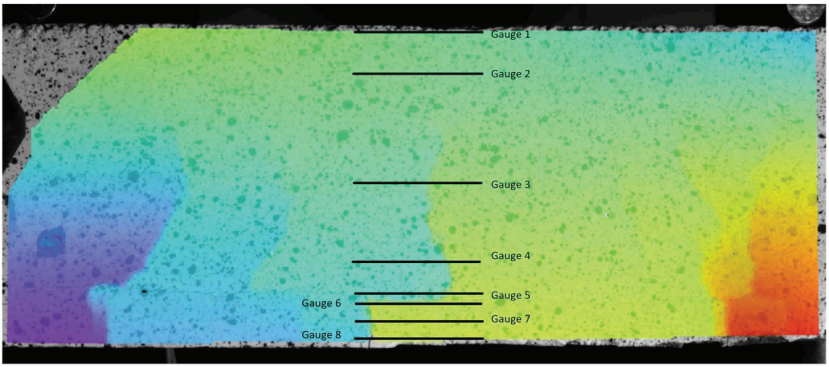

Figure 1: Deformation X-direction and arrangement of digital strain gauges

Comparison

The comparison of the analytical and the experimental investigations enable conclusions on the applicability of the simplified design approach for practical application. The design approach serves as a simple tool to design appropriate retrofitting and strengthening of reinforced concrete components with thin UHPFRC layers as well as shotcreted UHPFRC. These investigations will verify the accuracy of the simplified design approach.

3 Conclusions

First recalculations have confirmed the optimized design approach of UHPFRC concrete composite elements. Further investigations are required for a final confirmation of the approach.

During the test, problems occurred with the joint load-bearing behaviour. Further investigations are necessary. The complete bending load bearing capacity can only be activated if the strength of the joint is sufficient.

References

[1] Bundesanstalt für Straßenwesen (BASt), „Verstärkungen älterer Beton- und Spannbetonbrücken," 2016.

[2] Schweizerischer Ingenieur und Architektenverein: Ultra-Hochleistungs-Faserbeton (UHFB) – Baustoffe, Bemessung und Ausführung. SIA 2052, Zürich, 206.

Bond strength of steel bars in basalt fibre reinforced High Performance Concrete

Piotr Smarzewski
Faculty of Civil Engineering and Architecture, Department of Structural Engineering, Lublin University of Technology, Poland

1 Introduction

Basalt fibres produced from molten basalt rock have very good strength properties as well as high resistance to fire and an alkaline environment, and are relatively cheap at the same time. These features determine their use in concrete [1]. However, the cost in addition to the chemical and mechanical properties of basalt fibres vary depending of the type and quality of the raw material and the production process of the fibres [2]. Basalt fibre reinforced high performance concrete (BFRHPC) is widely regarded as an excellent composite for use in sustainable construction [3]. Nevertheless, concrete structures reinforced with basalt fibres generally include steel bars to obtain an efficient and reliable structural member. A good interfacial bond of BFRHPC to steel bars is an important factor conditioning the interaction of these two materials in the structure. Therefore, this study investigates the pull-out resistance of steel bar embedded with short length in BFRHPC. The specimens were designed to examine the influence of concrete cover to bar diameter ratio (c/ϕ_b) and of the fibre content on the local bond strength between BFRHPC and the reinforcing bar.

2 Materials and Methods

Deformed bars with nominal diameters of 12 mm and 16 mm were used in pull-out test specimens. Specimens were made for each bar using basalt fibre contents of 0, 1, 1.25, 1.5, 1.75, and 2%. All the specimens were cast parallel to the bar. The details of the test specimens are shown in Table 1 and Fig. 1.

Table 1: Details of test specimens.

Bar diameter, ϕ_b (mm)	Bottom concrete cover, c_y (mm)	Side concrete cover, c_x (mm)	Embedded length, l_e (mm)	c_y/ϕ_b	Number of specimens
12	94	94	60	7.83	18
12	44	94	60	3.67	18
16	92	92	80	5.75	18
16	42	92	80	2.63	18

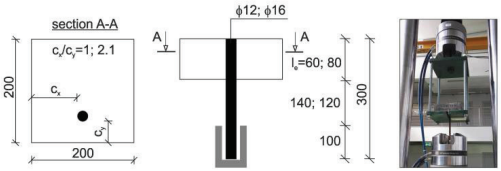

Figure 1: Test specimen details (dimensions in mm) and test set-up.

The quantities used in the reference mixture were as follows: cement CEM I 52.5R – 670.5 kg/m^3, tap water – 210 kg/m^3, basalt coarse aggregate ranging in size from 2 to 5 mm fractions – 990 kg/m^3, fine quartz sand with a maximum particle size of 2 mm – 500 kg/m^3, and superplasticizer based on polycarboxylate ethers – 20 kg/m^3. The control mixture did not contain any fibres. The following five contained basalt fibres (l/d = 12/0.013 mm) with a

percentage ranging from 1% to 2% and with a reduced quartz sand amount equal to the weight of the added fibres.

3 Results and Discussion

The bond strength was calculated by means of the relation $\tau_b = F/\pi\phi_b l_e$ where F is the measured load. Fig. 2 compares the bond strength versus the fibre content relationships using two different c_y/ϕ_b relations for two bar diameters ϕ_b. The error indicator denotes the standard deviation.

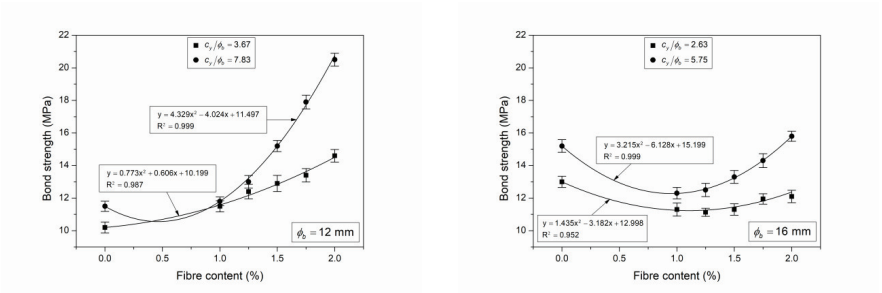

Figure 2: Variation in bond strength with fibre content for different bar diameters ϕ_b and relations c_y/ϕ_b.

Comparison of the results in Fig. 2 shows that for different values of c_y/ϕ_b, the bond strengths of the 12 mm bar increase with a growing basalt fibre content and with an increasing concrete cover. In contrast, the bond strength of the 16 mm bar falls when the fibre content is 1-1.25%. In the case of concrete without fibres, the bond strength was greater for the 16 mm bar. This can be explained by the larger rib face angle between 44 to 73° of the 16 mm bar than in the 12 mm bar with a rib face angle from 37 to 73°. The lower values of bond strengths of BFRHPC for the 16 mm bar can be clarified by the larger distances between the ribs from 6 to 12 mm compared to the 12 mm bar in which these distances are between 3 to 6 mm. At larger distances between the lugs on the bar, the basalt fibres could be oriented parallel to the rod between the ribs causing faster bond failure occurring as a result of shearing off and crushing the concrete. This effect was observed for the smallest concrete cover. This indicates that the bond strength of the steel bar depends on the concrete strength. The BFRHPC compressive strength used in this study was 17-22% lower compared to the concrete without fibres, and the splitting tensile strength was 20-22% higher [3].

4 Conclusions

1. The bond strength rises with increasing the concrete cover.
2. The bond strength of HPC without fibres is greater for the bar with the larger rib face angle.
3. The bond strength of BFRHPC is lower for the bar with the larger distances between the lugs on the bar.

References

[1] Jiang, C.; Fan, K.; Wu, F.; Chen, D.: Experimental study on the mechanical properties and microstructure of chopped basalt fibre reinforced concrete. *Materials & Design* 58, pp. 187-193, 2014.

[2] Fiore, V.; Scalici, T.; Di Bella, G.; Valenza, A.: A review on basalt fibre and its composites. *Composites Part B* 74, pp. 74-94, 2015.

[3] Smarzewski, P.: Flexural toughness evaluation of basalt fibre reinforced HPC beams with and without initial notch. *Composite Structures* 235, 111769, pp. 1–12, 2020.

Variability of tensile properties of UHPC within the continuous production quality programme of two factories

Juan Ángel López, Esteban Camacho, Fernando Galán, Hugo Coll
Co-founders of Research and Development Concretes SL and Prefabricados Formex SL, Spain

1 Introduction

Despite fibre-reinforced concrete technologies have been understood for many years and advantages of their use clearly proved, their extensive use in construction and industry has been delayed over the years until the present. The reason for this delay may be found in the lack of reliability in conventional fibre-reinforced concrete tensile response and difficulties found by companies when trying to ensure specific characteristic values within strict quality control programmes due to its high variability.

Traditionally, tensile behaviour of UHPC has been described using a stress-strain relationship up to maximum load and a stress-crack opening relationship after it. A simplified UHPC behaviour often used is shown in Fig. 1.

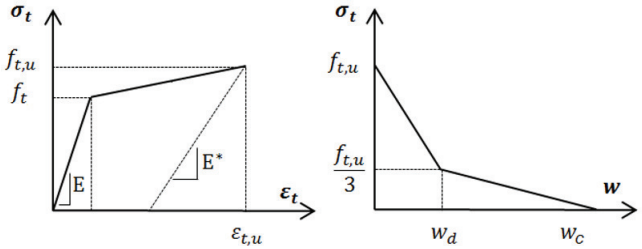

Figure 1: Simplified constitutive behaviour in tension of UHPC

Characterisation of this behaviour is completely necessary for design; ensuring it in production is mandatory a suitable quality control programme. However, large variability is often obtained in a continuous production in factory which greatly decreases characteristic properties. It may lead to a misperception of the produced UHPC in such a way that reliable production of it may seem difficult if additional notions are not considered.

Table 1 shows coefficient of variation results of tensile behaviour properties of three different mixes made in two different factories obtained from inverse analysis methodology applied on four-point bending tests [1]. Sample size for the determination of coefficient of variation is 34, 32 and 25 three different mixtures, respectively.

Table 1: Coefficient of variation of different tensile parameters obtained

CoV (%)		MIX 1	MIX 2	MIX3
f_t	MPa	14%	15%	10%
$f_{t,u}$	***MPa***	***22%***	***15%***	***25%***
E	MPa	6%	11%	6%
$\varepsilon_{t,u}$	**-**	***39%***	***44%***	***54%***
w_{dT}	Mm	18%	18%	21%

2 Analysis of the results

According to data in Table 1 one could think that (i) parameters $f_{t,u}$ *and* $\varepsilon_{t,u}$ are not suitable to define UHPC design properties; or (ii) UHPC production is unreliable; or (iii) inverse analysis procedure and four-point bending tests are not adequate for this purpose.

In an attempt to prove (i) and prove wrong (ii) and (iii), number of fibres in a cross-section next to the failure one were counted through image analysis. Moreover, crack spacing in the constant moment area of the bending test was also determined. The aim of that was substituting design parameters $f_{t,u}$ *and* $\varepsilon_{t,u}$ by a parameter describing average bond between matrix and fibres (τ_{av}) and average crack opening at debonding (w_{deb}) according to Equation 1.

$$w_{deb} = \varepsilon_{t,u} \cdot s_{av} \qquad f_{t,u} = \kappa \cdot \tau_{av} \qquad (1)$$

being, s_{av} the average crack spacing and κ a global fibre efficiency parameter [2] that takes into account the ratio between number of fibres counted and theoretical maximum number of fibres in a cross-section assuming them perfectly aligned, percentage of fibres in volume, fibre slenderness ratio, and fibre efficiency coefficient. Coefficient of variation of parameters w_{deb} and τ_{av} derived from the previously obtained $\varepsilon_{t,u}$ *and* $f_{t,u}$ are shown in Table 2.

Table 2: Coefficient of variation of different tensile parameters obtained

CoV (%)		MIX 1	MIX 2	MIX3
w_{deb}	MPa	-	21%	18%
τ_{av}	Mm	13%	14%	9%

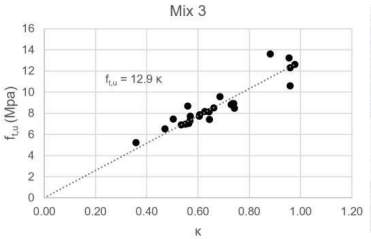

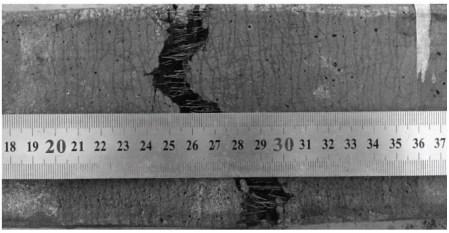

Figure 2: Relation between tensile strength and global fibre efficiency parameter (τ_{av}) (left); crack spacing measurement (right)

3 Conclusions

Reliable UHPC tensile parameters needs to be defined in order to guarantee suitable designs and ensure quality of concrete during production. As fibre orientation and the discontinuous nature of fibre reinforced concrete are the highest source of variability $f_{t,u}$ *and* $\varepsilon_{t,u}$ should be reconsidered as either design or constitutive parameters. A proposal of substituting them by w_{deb} and τ_{av} is proposed and justified in this paper. These parameters can be deduced from easy to perform four-point bending test and simplify inverse analysis methodologies.

Acknowledgements

The presented results were obtained in the context of the “Reshealience” project with reference 760824 funded by the H2020 European Union funding for Research & Innovation.

References

[1] López, J.A.; Serna, P.; Navarro-Gregori, J; Coll, H.: A simplified five-point inverse analysis method to deterine the tensile properties of UHPFRC from unnotched four-point bending tests. *Composites Part B 91 189-204.* 2016

[2] Abrishambaf, A.; Pimentel, M.; Nunes, S.: A meso-mechanical model to simulate the tensile behavoiur of Ultra-High Performance Fibre-Reinforced Cementitious Composites. *Composites Structures 222:110911*, 2019

The effects of resonant acoustic mixing on the microstructure of UHPC

Aileen Vandenberg, Kay Wille
Advanced Cementitous Material Composites Laboratory, Department Civil Engineering, University of Connecticut, USA

1 Introduction

Current mixing technologies for the concrete industry have not changed much in the last century relying heavily on planetary type mixers with shearing tools that provide low mixing energies to the system [1]. High-intensive mixers that provide high energy input to the system and have power consumption instrumental capabilities have advanced the field of high performance concretes and concretes with supplementary cementitious materials [2]. However, these improvements still rely on tool agitation as a means for mixing which provides non-uniform energy profiles during the mixing. Exploring mixing technologies used in other fields that provide more uniform energy mixing profiles in combination with improved built-in mixing monitoring techniques [3] is one possible avenue to take.

This research study presents a novel type of UHPC mixing technology called Resonant Acoustic® Mixing (RAM) Technology [4]. The effects of RAM on the microstructure of a designated UHPC mix are studied and compared to UHPC samples mixed with a conventional table top paddle mixer. Conclusions are drawn based on the results of back-scattering electron scanning microscopy (BSE-SEM), mercury intrusion porosimetry (MIP), and mechanical strength.

2 Experimental Program

Materials

Type I white cement conforming to ASTM C150 was used in all the mixtures due to its high amount of $C_3S + C_2S$ content (18.4%), low amount of C_3A content (less than 5%), and moderate fineness [5]. A commercially available high-range water reducer conforming to ASTM C494 Type A & F polycarboxylate superplasticizer (HRWR), with specific gravity 1.060 and solid content of 29%, was used at 1% by weight of cement. White silica fume (SF) and quartz powder (QP) were used as secondary cementitious and filler materials, respectively. Aggregates consisted of extra fine (QS1, d_{50} ~0.10 mm, d_{max} ~0.21 mm) and coarse quartz sand (QS2, d_{50} ~0.42 mm, d_{max} ~0.60 mm). Table 1 gives the composition of the mix used with respect to weight of cement.

Table 1: UHPC mix composition

C	SF	QP	QS1	QS2	HRWR	W
1	0.25	0.25	0.304	0.709	0.01[a]	0.21

Experimental Methods

UHPC specimens were prepared using a four-step mixing protocol. First the dry materials were mixed together from lowest to highest bulk volume density. Then the liquid materials were added to complete the mixing. The time of wet mixing for the RAM specimens was 5 minutes and for the table top paddle mixer it was around 20 minutes.

Back-scattering scanning electron microscopy, mercury intrusion porosity, and mechanical strength experiments were performed on small specimens. Results for one specimen are presented in Figure 1, Figure 2, and Figure 3, respectively.

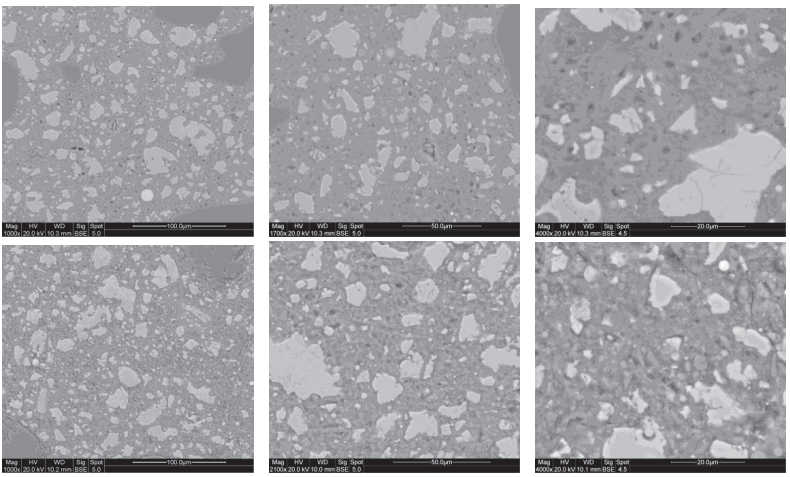

Figure 1: BS-SEM images for a Hobart (top) and a RAM (bottom) specimen.

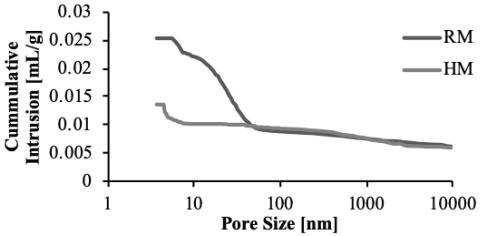

Figure 2: MIP results for UHPC mixed with a paddle mixer (HM) and with RAM at room temperature (RM)

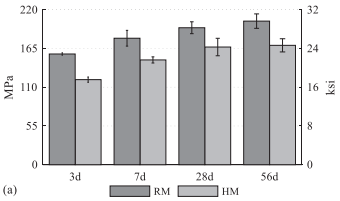

Figure 3: Mechanical Strength results for UHPC specimens.

3 Conclusions

In this research, the effects of RAM on the microstructure of a designated UHPC mix through back-scattering electron scanning microscopy, mercury intrusion porosimetry, and mechanical strength were presented. A table top paddle mixer was used as a comparison tool. The results show that RAM mixing produces a dense UHPC matrix with low porosity and suggest that RAM mixing has the potential to enhance the physical and chemical microstructure.

References

[1] Dils, J.; De Schutter, G.; Boel, V.: Influence of Mixing Procedure and Mixer Type on Fresh and Hardened Properties of Concrete: A Review. *Materials and Structures* 45 (11), p.1673 –1683, 2012.

[2] Chopin, D.; Cazacliu, B.; de Larrard, F.; Schell, R.: Monitoring of concrete homogenisation with the power consumption curve. *Materials and Structures* 40 (9), p. 897 – 907, 2007.

[3] Danilevskii, L. N.; Korobko, E. V.; Terekhov, S. V.: Vibroacoustic Monitoring of the Homogeneity and Workability of Concrete Mixes by their Hydromechanical State in the Process of Mixing. *Journal of Engineering Physics and Thermophysics* 82 (2), p.338 – 345, 2009.

[4] Wille, K., Boisvert-Cotulio, C.: Material Efficiency in the Design of Ultra-High Performance Concrete, *Construction and Building Materials (86)*, p. 33 – 43, 2015.

[5] Vandenberg, A., Wille, K.: Evaluation of Resonance Acoustic Mixing technology Using Ultra High Performance Concrete. *Construction and Building Materials* (164), p. 716-730, 2018.

Finite element investigation of the influence of fiber orientation on the pullout behavior of rebar embedded in Ultra-High Performance Concrete

Manish Roy, Kay Wille
Department of Civil and Environmental Engineering, University of Connecticut, USA

1 Introduction

Background

When a rebar is pulled out of conventional concrete (CC), the bearing of the ribs on the concrete plays the most important role in transferring tensile stresses across cracks. The perpendicular component of the bearing force causes a tensile ring of radial stresses to develop along the perimeter of the bar leading to radial cracks as soon as the matrix tensile strength is exceeded [1-4]. Fibers in Fiber Reinforced Concrete (FRC) are able to transfer tensile forces across those cracks, resulting in a re-distribution of the tensile ring after the initial cracking [5]. If the longitudinal cracks are bridged by the fibers without being opened excessively, a relatively ductile pullout failure will occur. Otherwise, a sudden splitting failure will happen with further opening of the longitudinal cracks [5]. Since Ultra-High Performance Concrete (UHPC) has much higher bond stress than CC [6-7], fibers in UHPC prove to be effective when covers are small enough to induce a splitting failure before the rebar can develop the full bond strength.

Goal

Since fiber orientation influences the crack bridging effect in UHPC, it is expected that it would also have an impact on the bond behavior between rebar and UHPC, especially at a low concrete cover. Hence, the present study investigates the effect of fiber orientation on the pullout behavior of rebar embedded in UHPC with a low cover (effective cover = 25 mm) using finite element simulation.

2 FE modelling of pullout tests

The geometry of the pullout test, investigated in the present study, is based on the specimen used in the laboratory experiment by Roy et al. [6]. A small elastic volume is added around the end of both the pullout and the support bar in order to avoid the application of the load or constraints directly to a reinforcement point outside the concrete. Symmetry boundary conditions are applied to the surfaces at the plane of symmetry of the specimen (Figure 1). To prevent any unrealistic response, the lateral movements of the elastic volumes are restrained perpendicular to the pullout bar as well as the support bar. The end of the elastic volume around the support bar is constrained in all the three directions to simulate the laboratory testing condition. The load is applied as a prescribed displacement to the end of the elastic cube around the pullout bar. The displacement on the pullout bar is measured at the bar end inside the elastic cube and at the junction of the bar in air and the concrete and thus similar to the experimental setup in the lab. Then the displacement at the pullout screw position is interpolated from these two values. The displacement on the side bar is measured at the bar end. The slip is calculated by subtracting the displacement of the side bar from that of the pullout bar. The load is calculated by adding the nodal reactions on the loading surface.

'Reinforced Concrete Model' in ATENA (v. 5.6.1) [8] is used as the material model for UHPC. In order to capture the anisotropic behavior of UHPC, the fibers are modeled as smeared reinforcement with 1D elements and the concrete matrix is modeled with volume elements (8-node linear hexahedra elements). An idealized sketch is shown in Figure 2. The spacing 'S' of

the smeared reinforcement is assumed to be infinitely small. The directional vector of the smeared reinforcement represents the orientation of the fibers inside the matrix. The fiber properties are calibrated using the stress-stain data obtained from uniaxial direct tensile tests of UHPC (14-day compressive strength = 162 MPa, 14-day tensile strength = 13.43 MPa, fiber volume fraction = 2%). 1D Reinforcement material model is used for the pullout bar (diameter = 9.375 mm, yield strength = 700 MPa, ultimate strength = 1102 MPa, and elastic modulus = 222 GPa), the side bar, and the support bar.

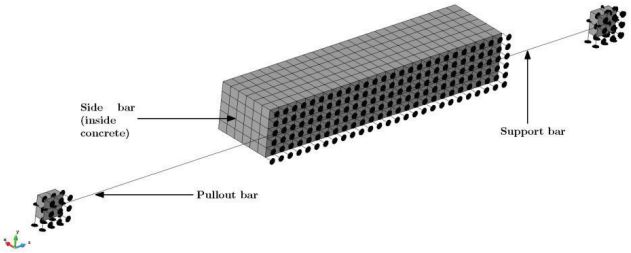

Figure 1: Boundary conditions.

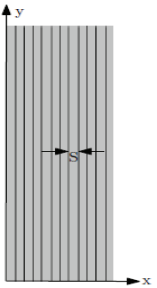

Figure 2: Smeared fibers.

3 Conclusions

The pullout test results show that the pullout force for the random orientation and the perpendicular orientation is 16% and 23% higher than that for the parallel orientation, respectively. Also, the slip at the peak load is maximum for the perpendicular orientation of fibers and minimum for the parallel orientation of fibers. The value for the random fiber orientation lies in between. Due to the low concrete cover, the specimens fail due to radial splitting cracks. Hence, perpendicularly oriented fibers bridge the cracks more effectively as compared to the other two types of fiber orientation.

Acknowledgements

The authors acknowledge the support from Cervenka Consulting for providing the free upgrade to ATENA v.5.6.1.

References

[1] Joint ACI-ASCE Committe 408, Report on Bond of Steel Reinforcing Bars Under Cyclic Loads, in: American Concrete Institute, ACI 408.2R-12, 2012.

[2] Tepfers, R.: A theory of bond applied to overlapped tensile reinforcement splices for deformed bars, Doctoral thesis, Chalmers University of Technology, 1973.

[3] Uijl, J.A.; Bigaj, A.J.: A bond model for ribbed bars based on concrete confinement, Heron 41 (1996) 201–226.

[4] Azizinamini, A.; Chisala, M.; Ghosh, S.K.: Tension development length of reinforcing bars embedded in high-strength concrete, Eng. Struct. 17 (1995) 512–522.

[5] Chao, S.H.; Naaman, A.E.; Parra-Montesinos, G.J.: Bond behavior of reinforcing bars in tensile strain-hardening fiber-reinforced cement composites, ACI Struct. J. 106 (2009) 897–906.

[6] Roy, M.; Hollmann, C.; Wille, K.: Influence of volume fraction and orientation of fibers on the pullout behavior of reinforcement bar embedded in ultra high performance concrete. Constr Build Mater 146 (2017) 582-93.

[7] Roy, M.; Ray, I.; Davalos, J.F.: High-performance fiber-reinforced concrete: development and evaluation as a repairing material. J Mater Civ Eng 26 (2014) 04014074.

[8] Červenka Consulting s.r.o., ATENA Program Documentation - Part 1: Theory, 2018; 5.6.1.

Experimental Investigations on bond between glass and UHPC

Hannes Eichler, Jenny Thiemicke, Roland Vollmar, Ekkehard Fehling
Institute of Structural Engineering, Department of Concrete Structures, University of Kassel, Germany

1 Introduction, motivation and objectives

Glass composite systems combined with steel, timber or concrete are a practical way to realise glass structures as architectural elements with a ductile load-bearing behaviour. The key factor for such a construction is a suitable bond between the glass element and the composite partner [1]. Since UHPC has a strong adhesive effect on rough surfaces, the bond between glass and UHPC can be achieved by mechanically roughening the glass surface. In preceding studies, such methods have often led to damages on the surface, which reduced the tensile strength of the glass [2]. In order to create a strong, smooth and controllable bond without damaging the glass surface, different joining technologies were tested in this study.

2 Development of alternative joining technologies

General options

Glass components can be most effectively integrated within a composite system by creating a shear bond along the glass edge (i.e. in glass beams). When loaded, the joining is sheared off in its longitudinal axis. To create such a connection, three general options were considered:

- direct joining by creating a rough glass surface (glass - UHPC),
- direct joining by using special adhesives (glass - adhesive - UHPC), or
- indirect joining by using additional anchoring elements (glass - adhesive - metal - UHPC).

Glued sand grains (type B)

By roughening glass with conventional methods (i.e. sandblasting), the surface receives a multitude of minimal defects. Under loading, stress peaks occur at these points, which reduce the tensile strength significantly [2]. Alternatively, the roughness can be achieved by gluing grains of sand on the surface with high strength adhesives. In this way, the fresh concrete can interlock on the sand surface providing a rigid shear bond.

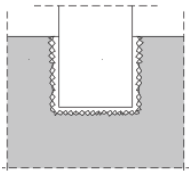

Figure 1: Interlocking of glued sand and UHPC

Indirect joining with H-shaped metal profiles (type A)

A different way to create a smooth joining is to glue the glass into manufactured metal profiles that are separately anchored in the concrete. This variant offers the advantage to combine well-known joining technologies (embedding steel into concrete, adhere glass to steel). Besides anchoring bare metal profiles, two methods were tested to anchor H-shaped metal profiles into the fresh UHPC: metal profile with drill holes and steel dowels (see Fig. 2 left), and metal profile with drill holes and concrete dowels (see Fig. 2 right).

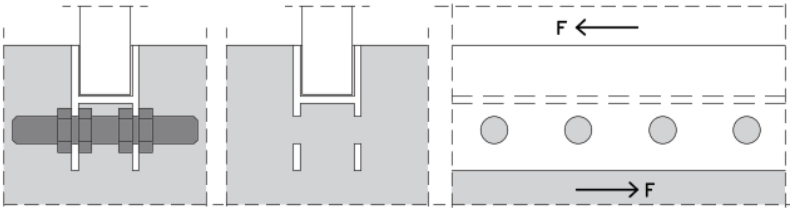

Figure 2: Indirect joining with metal profiles: steel dowels (left), concrete dowels (centre and right)

3 Experimental investigations

Test Specimens

The experiments were applied on indirect joining (type A) and direct joining (type B). The bond characteristic between anchored H-shaped metal profiles and UHPC was examined in preliminary tests on three different profile settings: unmachined (A0), with drill holes Ø 8 mm every 25 mm (A1), and with steel dowels Ø 8 mm every 25 mm (A2) (see Fig. 2). Furthermore, the bond between glass and H-shaped metal profiles was determined on two different adhesives: "3M DP 620" (A3), and "Huntsman Araldite 2047-1" (A4), which are different with regard to stiffness and strength, respectively.

Based on these results, a well-fitting bond configuration was identified for the push-through-tests. The configuration contained drill holes Ø 8 mm every 25 mm in the profile as well as the glue "Huntsman Araldite 2047-1" applied on the glass (A5, see Fig. 2 blue dashed line).

For the push-through-tests of type B, the bond conditions were improved by adhesive layers scattered with grains of sand: glue "3M DP 490", layer thickness 0.5 to 1 mm, sand with grain size 0/2 (B1, see fig. 1 black line), as well as glue "Huntsman Araldite 2047-1“, layer thickness 0.5 to 1 mm, sand with grain size 0/2 (B2, see Fig. 1 red dotted line).

Test set-up and results

The setup of the push-trough-test is shown in figure 4. During the tests, the applied force and the slip between UHPC and glass was measured. In addition, the deformation behaviour was observed visually. Fig. 3 shows the results of the tests.

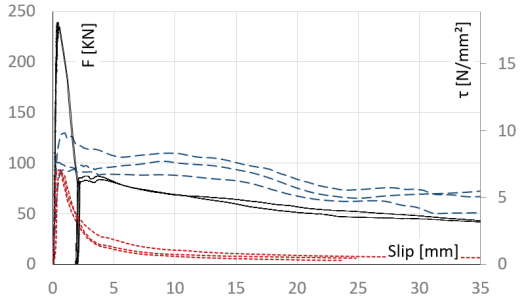

Figure 3: Force-Slip-Diagramme of types B1, B2 and A5

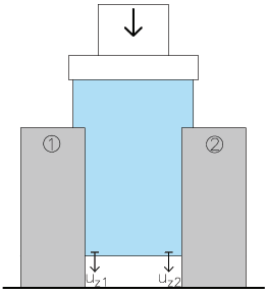

Figure 4: Setup of the push-through tests

While type B1 shows a very high load bearing capacity, type B2 reaches less than half of the maximum load. Both types express a very uncertain, non-ductile post peak behaviour. In contrast, type A5 achieves up to half of the maximum load of B1, but shows a very ductile post peak behaviour with a relatively high post peak load level at about 80% of the maximum.
Type A5 will be chosen for the construction of a composite beam of glass and UHPC.

4 Conclusion

Tests on different bond configurations led to the result, that a combination of drill holes Ø 8 mm every 25 mm in the anchored H-shaped metal profiles as well as the glue "Huntsman Araldite 2047-1" between glass and profile (A5) achieves an adequate load bearing capacity, as well as a very ductile post peak behaviour without any negative impact on the glass surface.

References

[1] Plóciennik, D.: Die Wirkungsweise von Glas-UHPC-Verbindungen - Theorie, Experiment, Bemessung, Dissertation, Technische Universität Graz, 2016.

[2] Freytag, B.: Die Glas-Beton-Verbundbauweise, Dissertation, Technische Universität Graz, 2002.

Innovative retrofitting and strengthening of reinforced concrete structures using Ultra-High Performance Shotcrete

Jörg Jungwirth[1]; Andrea Kustermann[2]; Christoph Dauberschmidt[2]; Andre Strotmann[1]; Toni Pollner[2]; Markus Schmidt[1]

1: Structural Engineering, University of Applied Sciences Munich (MUAS), Germany
2: Institute for Material and Building Research, Munich University of Applied Science (MUAS), Germany

1 Innovative Retrofitting and Strengthening of Reinforced Concrete Structures using Ultra-high Performance Shotcrete

In the sector of traffic infrastructure and building construction, the structures in Germany are typically up to 80 years old. Many of the structures are in damaged condition due to chloride attack and high loading. The established retrofitting methods -removing the chloride containing concrete and reprofiling- are usually associated with major intervention in the structure and thus they are expensive and time-consuming [1]. In addition, coating systems are usually not able to protect the structure from further damage over the rest of their expected lifetime.

The high-performance properties of UHPFRC are already used for retrofitting and strengthening. The properties of the material are ideal for protection against chloride ingress and for increasing the load-bearing capacity [2]. The advantages of UHPFRC as shotcrete are controllable fibre orientation, high compaction, good workability and superfluous of formworks. The combination of these already proven technologies –shotcrete and UHPFRC- is an innovative and highly efficient method for retrofitting and strengthening.

At Munich University of Applied Sciences, the research project titled "Retrofitting and strengthening of reinforced concrete structures by using UHPFRC shotcrete: Fields of Applications, Structural Design, Durability, Construction Technology" is conducted in order to investigate this innovative technology. The research work includes material technology and structural design as well as durability of retrofitted reinforced concrete structures using UHPFRC shotcrete. The project is realized in close cooperation with LafargeHolcim and Implenia Instandsetzung GmbH. The Paper provides first experience and results of the ongoing R&D project.

2 Investigations

As first experimental campaign investigations of UHPFRC spraying process, material properties and bond behaviour have been conducted.

Shotcreted UHFPRC specimens were analysed by means of magnetic resonance imaging (MRI) scans. This provided a plausible statement on load-bearing behaviour due to the internal steel fibre orientation. In addition, quantities of rebound material are determined and the spray shadow behind reinforcement layers is visually examined. The interface of the hardened composite is analysed by digital reflected light microscopy.

The material properties of the ultra-high performance shotcrete are assessed based on the guidelines for conventional shotcrete. Tests have been carried out to determine the modulus of elasticity and the stress-strain behaviour in compression and tension both axially and orthogonally to the applied spraying direction.

Furthermore, the adhesive bond to the existing concrete was examined. For this investigation, tensile bond tests and symmetric push-out tests were carried out for determining the adhesive tensile strength and the shear load bearing behaviour, respectively.

3 Selected Results

The UHPFRC is highly suitable for application as shotcrete. Spraying of the ultra-high performance concrete was realised in cooperation with the industrial partners LafargeHolcim and Implenia Instandsetzungs GmbH (see Figure 1). Due to the specific rheology of the ultra-high performance concrete, there are complex demands on the processing technology. The optimisation of the material and workability was a major aspect of the investigation.

Figure 1: UHPFRC spraying

Figure 2 and 3 exemplary show first results as a part of the experimental campaign: tensile and compressive stress-strain curves. First material tests have shown a compressive strength of about 130 MPa (tests on cylinders and cubes), tensile strength up to 6 MPa with strain hardening behaviour (axial tensile test) and a Young's modulus from 35 GPa to 40 GPa. Thus, the obtained UHPFRC concrete is highly suitable for strengthening and conform to UHPFRC requirements [2].

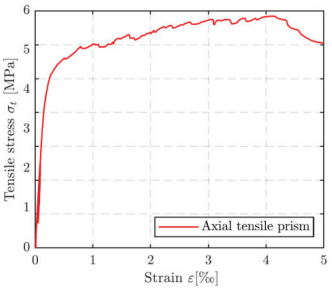

Figure 2: Tensile strength

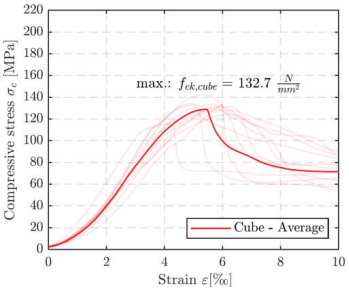

Figure 3: Compressive strength

4 Conclusions

The pumpability and sprayability has been proved by the test campaign. Application of the material as shotcrete is highly suitable.

The first testing of the UHPFRC shows excellent material properties and the feasibility of application with high-performance but conventional construction machinery.

The material properties correspond to the intended material behaviour. Based on the observed material properties, further investigations and optimisations regarding material technology will be carried out. A detailed consideration of the time-depending material properties will be investigated.

As next step in the research program, fields of application are investigated in cooperation with stakeholders and owners of damaged structures (e.g. building authorities). After this, investigation regarding structural design and durability will be carried out.

References

[1] Bundesanstalt für Straßenwesen (BASt), „Verstärkungen älterer Beton- und Spannbetonbrücken," 2016.

[2] R. Bornemann, M. Schmidt, E. Fehling und B. Middendorf, „UHPC Herstellung, Eigenschaften und Anwendungsmöglichkeiten," Beton- und Stahlbetonbau Heft 7, 2001.

List of Authors

Schriftenreihe Baustoffe und Massivbau

Structural Materials and Engineering Series

Heft 1: **Fehling, E. / Schmidt, M. / Teichmann, T. / Bunje, K. / Bornemann, R. / Middendorf, B. (2005)**
Entwicklung, Dauerhaftigkeit und Berechnung Ultra-Hochfester Betone (UHPC). Forschungsbericht, ISBN 3-89958-108-9, € 18,00

Heft 2: **Schmidt , M. / Fehling, E. (Hrsg.) (2003)**
Ultra-Hochfester Beton - Planung und Bau der ersten Brücke mit UHPC in Europa. Tagungsbeiträge zu den 3. Kasseler Baustoff- und Massivbau-tagen am 10. September 2003, ISBN 978-3-89958-518-6, € 18,00

Heft 3: **Schmidt, M. / Fehling, E. / Geisenhanslüke, C. (Hrsg.) (2004)**
Ultra High Performance Concrete (UHPC), ISBN 3-89958-086-9, € 79,00

Heft 4: **Bornemann, R. (2005)**
Untersuchungen zur Modellierung des Frisch- und Festbetonverhaltens erdfeuchter Betone, ISBN 3-89958-132-6, € 24,00

Heft 5: **Solyman, M. (2006)**
Classification of Recycled Sands and their Applications as Aggregates for Concrete and Bituminous Mixtures, ISBN 978-3-89958-218-5, € 24,00

Heft 6: **Tesch, V. (2007)**
Gefügeoptimierte Instandsetzungsmörtel auf Calciumsulfat-Basis für die Anwendung im Außenbereich, ISBN 978-3-89958-333-5, € 24,00

Heft 7: **Schmidt, M. (ed.) (2007)**
Ultra High Performance Concrete (UHPC). 10 Years of research and development at the University of Kassel - 10 Jahre Forschung und Ent-wicklung an der Universität Kassel, ISBN 978-3-89958-347-2, € 49,00

Heft 8: **Schmidt, M. (Hg.) (2007)**
Nanotechnologie im Bauwesen Nanooptimierte Hightech-Baustoffe. 9. Mai 2007, ISBN 978-3-89958-348-9, € 22,00

Heft 9: **Leutbecher, T. (2008)**
Rissbildung und Zugtragverhalten von mit Stabstahl und Fasern bewehrtem Ultrahochfesten Beton (UHPC), ISBN 978-3-89958-374-8, € 39,00

Heft 10: **Fehling, E. / Schmidt, M. / Stürwald, S. (eds.) (2008)**
Ultra High Performance Concrete (UHPC). Second International Symposium on Ultra High Performance Concrete, March 05-07, 2008, ISBN 978-3-89958-376-2, € 79,00

Heft 11: **Fehling, E. / Leutbecher, T. / Röder, F.-K. (2008)**
Zur Druck-Querzug-Festigkeit von Stahlbeton und stahlfaserverstärktem Stahlbeton in scheibenförmigen Bauteilen - Biaxial Compression-Tension-Strength of Reinforced Concrete and Reinforced Steel Fibre Concrete in Structural Panels, ISBN 978-3-89958-440-0, € 39,00

Heft 12: **Teichmann, T. (2008)**
Einfluss der Granulometrie und des Wassergehaltes auf die Festigkeit und Gefügedichtigkeit von Zementstein, ISBN 978-3-89958-441-7, € 24,00

Heft 13: **Geisenhanslüke, C. (2009)**
Einfluss der Granulometrie von Feinstoffen auf die Rheologie von Feinstoffleimen, Influence of the granulometry of fine particels on the rheology of pastes, ISBN 978-3-89958-706-7, € 24,00

Heft 14: **Nöldgen, M. (2010)**
Modellierung von ultrahochfestem Beton (UHPC) unter Impaktbelastung. Auslegung eines Hochhauskerns gegen Flugzeuganprall, ISBN 978-3-89958-862-0, € 29,00

Heft 15: **Eden, W. (2011)**
Einfluss der Verdichtung von Kalk-Sand-Rohmassen auf die Scherbenrohdichte von Kalksandsteinen, ISBN 978-3-86219-040-9, € 29,00

Heft 16: **Stephan, D. (2011)**
Nanomaterialien im Bauwesen. Stand der Technik, Herstellung, Anwendung und Zukunftsperspektiven, ISBN 978-3-86219-066-9, € 29,00

Heft 17: **Emami, A. D. (2011)**
Kleben von Naturfaserverbundwerkstoffen auf Mauerwerk zur nachträglichen Verstärkung erdbebengefährdeter Bauwerke – von der Werkstoffprüfung bis zur Anwendung, ISBN 978-3-89958-558-2, € 29,00

Heft 18: **Stürz, J. (2011)**
Ein empirischer Ansatz zur Beschreibung der Horizontaltragfähigkeit gemauerter Wandscheiben unter Berücksichtigung der Interaktion innerhalb der Gebäudestruktur ISBN 978-3-89958-559-9, € 29,00

Heft 19: **Schmidt, M. / Fehling, E. / Glotzbach, C. / Fröhlich, S. / Piotrowski, S. (eds.) (2012)**
Ultra-High Performance Concrete and Nanotechnology in Construction. Proceedings of Hipermat 2012. 3rd International Symposium on UHPC and Nanotechnology for High Performance Construction Materials, Kassel, March 7–9, 2012, ISBN 978-3-86219-236-6, € 79,00

Heft 20: **Schmidt, Cornelia (2012)**
Konstruktion und Wirtschaftlichkeit von Whitetopping aus Hochleistungsbeton für Fahrbahnen ISBN 978-3-86219-342-4, € 29,00

Heft 21: **Rafiee, Alireza (2012)**
Computer Modeling and Investigation on the Steel Corrosion in Cracked Ultra High Performance Concrete ISBN 978-3-86219-388-2, € 29,00

Heft 22: **Schmidt, M. / Fehling, E. / Fröhlich, S. / Thiemicke, J. (Hrsg.) (2014)**
Nachhaltiges Bauen mit Ultrahochfestem Beton. Ergebnisse des Schwerpunktprogrammes 1182 gefördert durch die Deutsche Forschungsgemeinschaft (DFG) ISBN 978-3-86219-480-3, € 79,00

Heft 23: **Röder, Friedrich Karl (2015)**
Kippstabilität von Stahlbeton- und Spannbetonträgern, 2. überarb. und aktualisierte Auflage ISBN 978-3-86219-934-1, € 49,00

Heft 24: **Ismail, Mohammed (2015)**
Behavior of UHPC Structural Members subjected to Pure Torsion ISBN 978-3-86219-952-5, € 39,00

Heft 25: **Thiemicke, Jenny (2015)**
Zum Querkrafttragverhalten von UHPC-Balken mit kombinierter Bewehrung aus Stahlfasern und Stabstahl ISBN 978-3-86219-962-4, € 49,00

Heft 26: **Mtani, Isabela Wilfred (2016)**
Salt Deterioration of Historic Mortars in Tropical Climate: Analysis and Characterisation. Case Studies from Tanzania ISBN 978-3-7376-0074-3, € 39,00

Heft 27: **Fehling, E. / Middendorf, B. / Thiemicke, J. (eds.) (2016)**
Ultra-High Performance Concrete and High Performance Construction Materials. Proceedings of HiPerMat 2016 4th International Symposium on Ultra-High Performance Concrete and High Performance Construction Materials Kassel, March 9-11, 2016 ISBN 978-3-7376-0094-1, € 49,00

Heft 28: **Otten, S. (2018)**
Synthetischer Zeolith als Anreger der Erhärtungsreaktionen zementartiger Bindemittel, ISBN: 978-3-7376-0418-5, € 39,00

Heft 29: **Chengula, D. H. (2018)**
Improving Cementitious Properties of Blended Pozzolan Based Materials for Construction of Low Cost Buildings in Mbeya Region, Tanzania, ISBN: 978-3-7376-0442-0, € 29,30

Heft 30: **Le, A. H. (2018)**
Behavior of Circular Steel Tube Confined UHPC and UHPFRC Columns under Axial Compression, ISBN: 978-3-7376-0496-3, € 49,00

Heft 31: **Simon, J. (2019)**
Granulometrische Anpassung von ZFSV zur Optimierung von Wurzelhemmung und thermischer Leitfähigkeit, ISBN: 978-3-7376-0808-4, € 39,00

ISBN 978-3-7376-0828-2